BUBBLE HYDRODYNAMICS IN GAS FLUIDIZED BEDS

by

KYM MARTIN IDE

B.E. (Hons.), ADELAIDE

A dissertation submitted in fulfilment of the requirements

for the degree of Master of Engineering Science

in The University of Adelaide

February, 1989

Department of Chemical Engineering

The University of Adelaide

Adelaide, S. A. 5001

Australia

To my mother

DECLARATION

This thesis contains no material which has been accepted for the award of any other degree or diploma in any University and, to the best of the author's knowledge and belief, the thesis contains no material previously published or written by another person, except where due reference is made in the text or where common knowledge is assumed.

The author consents to the thesis being made available for photocopying and loan if accepted for the award of the degree.

Kym M. Ide

PREFACE

I would like to thank the following people and organisations for their assistance in this work :

- Dr. Pradeep Agarwal, my supervisor, for his valuable guidance and constant encouragement throughout this work;

- The academic staff of The Chemical Engineering Department, in particular, Dr. Brian O'Neill and Prof. John Agnew;

- Particular thanks to David Atkinson for professional writing of the data collection software;

- The technical staff, Peter Kay for experimental apparatus construction, Bruce Ide ("Dad") for construction of the capacitance probes, Andrew Wright, Brian Mulcahy and Colin Tipper for assistance;

- The South Australian State Energy Research Advisory Committee for providing the financial assistance necessary to perform this investigation;

- Theo Sudomlak of the The Psychology Department for loan of the video camera;

- The Materials Engineering Department for loan of the video recorder and television;

- Rashid Muhammad, Lim K. S. and the other postgraduate students for fruitful discussions and help;

- My girlfriend, Mandy Furlan for support and compassion;

and - Most importantly, my mother, Elizabeth, Bill Richards and John, for the opportunity to come this far and for support, encouragement and patience.

TABLE OF CONTENTS

LIST OF FIGURES

LIST OF TABLES

ABSTRACT

Thorough knowledge of the hydrodynamic properties of gas fluidized beds is a prerequisite for complete mastery of fluidization as a process technology. Detailed analyses require prohibitively large quantities of computer time and effort. Only limited bubble size and velocity distribution data are available in the literature. Invariably, mean bubble properties are tabulated, reducing the quantity of data available for model fitting and calculation of bed performance. The aim of this investigation was to develop a technique capable of quick, simple and inexpensive measuring of the distribution of bubble sizes and velocities in a gas fluidized bed. An extensive tabulation of measured bubble characteristics is provided.

Tests were conducted in a 23 cm diameter gas fluidized bed. Construction in perspex enabled visual observation of the fluidization process. AB Glass ballotini served as the bed material with air as the fluidizing medium. A dual tipped capacitance probe was employed to measure the local variations in bed porosity. Unique computer software enabled the elimination of many complex hardware components previously employed in this type of study. All data collection and analysis was performed in real-time by the computer software.

Comparison of the collected data with a population balance model proposed by Agarwal (1986) was performed. The model predictions were in good agreement with the experimental bubble vertical dimensions but significant departures from the bubble rise velocities were noted. The median bubble characteristics derived from the experimental data and correlations were

contrasted with predicted average values. The average bubble characteristics were greater than the median values. A significant contribution from small bubbles may be neglected when an average characteristic is employed.

Figures detailing the distributions of bubble vertical dimensions and rise velocities are presented. As bed height increases the bubbles conglomerate towards the centre of the bed and as a consequence bubble size and rise velocity increase in the centre of the bed.

This investigation should be of great benefit to future studies linking bed hydrodynamics to fluidized bed performance and any study where high speed data acquisition is necessary given the improvement in the ease of measurement.

CHAPTER I

INTRODUCTION

In 1926 the first large-scale, commercially significant fluidized bed commenced smooth operation. The process, known as the Winkler gas generator, involved the gasification of powdered coal. By today's standards the Winkler gas generator may be considered inefficient because of its high oxygen consumption and its large carbon loss through entrainment.

The application of fluidized bed technology to commercial processes has grown phenomenally over the decades since the Winkler gas generator was state-of-the-art. Examples of present-day commercial applications are in the production of ethylene, alkyl chloride, phthalic anhydride and polypropylene. Processes using fluidized bed technology include fluid catalytic cracking, catalytic reforming and coking, coal gasification and liquefaction, calcination and nuclear fuel preparation.

Fluidized beds are unsurpassed in maximising both gas-solid contact and solids mixing. The dynamics of the bubbles, the mechanisms of bubble formation and growth, the spatial distribution of bubbles within the bed and the bubble-particle interactions play dominant roles in the extent of heat transfer, mass transfer and solid catalysed chemical reactions in a fluidized bed. A thorough knowledge of bubble dynamics is necessary for complete mastery of fluidization as a process technology. Despite industry's wide usage, the dynamics of fluidization is poorly characterised and as such modelling and design of fluidized beds is difficult.

Experimental techniques have therefore been applied to the study of bubble behaviour throughout the bed. Investigations of bubble properties and dynamics have been performed by many workers and their results are well represented amongst the voluminous literature dealing with fluidization.

Within the literature, studies may be found which present data which is, at least in part, contradictory. While measurements carried out in a two dimensional bed are of only limited interest, as in most commercial situations a three dimensional bed is employed.

Investigations carried out to characterise the bubble hydrodynamics in three dimensional gas-solid fluidized beds involve numerous measurements of local bubble velocity and size, as functions of fluidizing gas velocity and location in the bed. As pointed out by Yoshida et. al. (1978b), detailed analyses require almost prohibitively large amounts of computer time and effort. Figures showing the variations in local bubble velocity and local bubble size are limited within the literature. The quantity of data collected is almost invariably reduced by averaging the measured bubble velocity and size. An array of figures exhibiting the variation of local *mean* bubble velocity and local *mean* bubble size throughout the bed, with different fluidizing gas velocities, is the usual method of demonstrating the fluidized bed bubble hydrodynamics.

This in many ways diminishes the value of the data collected, as a lot of detail becomes "hidden" by the averaging process. It is probable that a significant amount of information could be derived from analysis of the distributions of local bubble rise velocity and local bubble size. Certainly a data base would be provided from which many descriptive parameters could be derived for comparison with fluidized bed models.

The first goal of this investigation was to develop a miniature capacitance probe linked to a high speed data acquisition system capable of collecting local measurements, with minimum disturbance to the state of fluidization. The probe response yields bubble pulse duration, number of bubbles detected by the probe per unit time and bubble rise time.

The second aim was to evaluate from the collected data those parameters which further characterise the local state of fluidization. These parameters include, bubble pierced length, bubble volume fraction, gas flow passing as bubbles and bubble rise velocity - all as local values.

Finally, figures fully representative of the collected data would be presented. Including, probability density functions and cumulative distributions of bubble vertical dimension and rise velocity for various superficial gas velocities, at many locations throughout the bed. A comparison with a population balance model for predicting bubble characteristics, as detailed by Agarwal (1985, 1986), would also be made. Also presented would be the variation of bubble frequency, volume fraction and gas flow throughout the bed.

CHAPTER II

LITERATURE REVIEW

2.1 Experimental Methods For Studying Gas-Solid Fluidized Beds

Investigators have applied a variety of techniques to obtain data representative of the bubble behaviour, solid-particle mixing and heat and mass transfer properties of gas-solid fluidized beds. A detailed review of experimental methods for studying gas-solid fluidized beds is presented in Cheremisinoff (1986). In this chapter a critique of the techniques for studying gas-solid fluidized beds, in particular bubble hydrodynamics, is presented. The methods reviewed include:

a) Photographic and X-Ray Techniques,

b) Light Transmission Techniques,

c) Pressure Fluctuations,

d) Electromagnetic and Acoustical Wave Transmission,

e) Thermal Techniques and

f) Electroresistivity Measurements.

a) Photographic and X-Ray Techniques:

Generally, photographic methods are restricted to the study of two-dimensional fluidized beds, or when wall-controlled phenomenon is of interest. A shortcoming of these methods are their inability to reproduce meaningful statistical properties of the bubble, as in most commercial situations a three-dimensional bed is employed.

Studies of two-dimensional beds have been conducted by Upson and Pyle (1973). These workers analysed, frame-by-frame, a cinephotography film to determine the frequency of bubble splitting as a function of bubble size, in an air-fluidized bed. Geldart (1970/71) measured the diameter and frequency of bubbles bursting at the surface of two-dimensional and three-dimensional gas-fluidized beds from a cine film record. Kunii and Levenspiel (1977) recorded bubbles rising in a two-dimensional gas-fluidized bed with a cine-camera, in order to study the effects of bed temperature on the bubble size and velocity. Backmixing phenomenon in a two-dimensional bed was studied by Fryer and Potter (1973). Data on eruption diameters were used in the evaluation of various backmixing models.

In commercial fluidized beds, where the application of photographic methods is severely limited, direct observation of bubble characteristics can be made using X-rays. Rowe and Partridge (1965), Rowe and Matsumo (1971), Rowe (1971), Hager and Thompson (1973) and Judd and Dixon (1978) have employed X-rays for measuring the size and shape of bubbles. Difficulties encountered with this technique include limited transmission through thick-walled vessels and poor resolution of individual bubbles under profuse bubbling conditions. Rowe and Masson (1980, 1981) used a combination of X-ray and cinephotography in a three-dimensional bed, to study the disturbance to bubbles caused by various probe types. They compared the bubble velocity and height as measured by each probe with that recorded on the cine or X-ray film. A quantitative analysis of the disturbance caused by each probe to the passage of the bubble was made.

Banholzer et. al. (1987) studied the time averaged flow pattern in a gas fluidized bed using X-ray computed tomography (CT). The CT technique has revolutionised medical imaging diagnostics (Maylotte et. al. 1982). The technique produces images taken as a two-dimensional slice through the object, rather than as a projection of a three-dimensional object onto a plane. A scan of the bed took nine seconds, thus events occurring in less than nine seconds were unresolved. Individual bubble motions could not be viewed, rather an average density over nine seconds was determined. (CT machines with millisecond capability do exist.) The CT technique is complementary to the X-ray method, the former emphasising spatial resolution, the latter stressing temporal resolution.

b) Light Transmission Techniques:

Light scattering and fibre optic probes have been successfully employed to measure local bubble size distributions. The local bubble size distribution is expressed by a representative bubble characteristic such as the radius.

The experimental detection of the bubble size using the light scattering technique, is based on the interaction between a horizontal light beam and the fluidized solids. When the fluidized solids are present within the beam, light is scattered with consequent attenuation. However, if only gas is present, no attenuation of the focused light occurs. The technique provides a local measurement of the number of bubbles passing the probe per unit time and the cumulative density function of the bubble size. The signal resolution is affected by bubble passage through the line of light transmission. Hence, measurement resolution is adversely effected when the detector and transmitter are far apart.

Many other workers including, Put et. al. (1973), Yasui and Johanson (1958), Kilkis et. al. (1973) Yoshida et. al. (1978a,b), Yong et. al. (1980), Valenzuela and Glicksman (1984) and Sung and Burgess (1987) have utilised light scattering.

Fibre optic probes provide in-situ localised measurements (Lockett and Safekourdi (1977), Coulaloglou et. al. (1976), Ohki and Shirai (1978), Burns and Roe Corp. (1982)). Simultaneous measurement of the bubble rise velocity, frequency and size are possible. Ohki et. al. (1977) and Ohki and Shirai (1978) used fibre optic probes to simultaneously measure local particle movement and bubble phenomenon. They found that the particle rise velocity was proportional to the local bubble velocity. Fibre optic probes have been widely employed for the measurement of solid particle velocities, Ishida et. al. (1980), Patrose and Caram (1982), Muramoto et. al. (1985).

Dutta and Wen (1979) described the procedure for the application of fibre optic probes for measuring bubble characteristics. The behaviour of bubbles in fluidized beds where differing fluidizing gases were employed in turn, was studied by Kai et. al. (1987). They used both a hot wire and fibre optic probe and made comparisons of the measurements collected from each. Yamazaki et. al. (1986) and Yang et. al. (1987) measured the distribution of the porosity of the emulsion-phase. Bubble properties from large particle fluidized beds were presented by Glicksman et. al. (1987). Berruti et. al. (1988) measured the residence time distribution of low density solids in a fluidized bed reactor of sand particles.

c) Pressure Fluctuations:

Transducers located along the height of a fluidized bed provide information on the dense bed behaviour and bed expansion. Several investigators have applied this technique to studying fluidization quality namely, Broadhurst and Becker (1976), Fan et. al. (1981, 1983) and Taylor

et. al. (1973). Chan et. al. (1987) utilised pressure probes to study the effect of increasing bed pressure on bubble characteristics. Bubble size was found to decrease with pressure while bubble frequency increased.

Drahos et. al. (1988) utilised a pressure probe to measure local pressure drop fluctuations in a freely bubbling fluidized bed, the fluctuations were used to characterise the axial stability of fluidized beds. The amplitude of local pressure drop fluctuations was found to be a linear function of gas velocity in the broad range of fluidizing gas temperatures used.

d) Electromagnetic and Acoustical Wave Transmission:

The basis of the gamma-ray detector technique is the interaction of the radiation with the detection device. Measurement of the number of interactions is indicative of the bubble frequency whilst measurement of the total effect of radiation can be related to bed voidage.

Gamma-ray detectors have been exploited successfully by Orcutt and Carpenter (1971) who applied gamma-ray transmission to detect the presence of bubbles and Weimer et. al. (1985), who employed gamma radiation to quantify the characteristics of bubbles. Weimer measured expanded bed height, dense phase voidage, bubble size and bubble frequency.

A microwave signal can be transmitted down onto the surface of the bed and the reflected signal is shifted in a frequency proportional to the bed surface velocity. Surface rise velocity will give an indication of the average bubble rise velocity, which in turn is proportional to the size of the bubbles present (Cheremisinoff and Cheremisinoff (1984), Kunii and Levenspiel (1977)). A serious disadvantage with this method is the restriction of the region of study to the upper portion of the bed. Therefore, deep beds pose a problem, as the surface behaviour need not reflect the true average bubble size.

In an operating system, a sonic wave is generated and directed into the flow, where it is scattered by particles. A second transducer picks up the scattered energy and the signal once analysed should be able to detect differences between regions of high and low solids concentration. Yosef et. al. (1975) applied a Doppler velocitimeter for measuring the gas bubble size distribution. Poor resolution between bubble sizes made it difficult to obtain meaningful quantitative data. Krautkramer and Krautkramer (1983) provide a detailed discussion on the application of ultrasonics.

e) Thermal Techniques:

Thermal and constant temperature anemometry techniques have so far been applied to indirectly detect bubbles in fluidized beds. Wen et. al. (1978) constructed a miniature probe comprised of a self-heating thermistor to sense the presence of bubbles. When in the emulsion, the probe's temperature decreases as the probe's heat transfer coefficient is significantly greater in the emulsion compared to the bubble-phase. Techniques for similar measurements are described by Hiraki et. al. (1968/69), Bernis et. al. (1973), Goosens and Hellinckx (1973), and Bashakov et. al. (1973).

f) Electroresistivity Measurements:

Measurable differences between air and a packed bed of solid granulates form the basis for this technique. Point measurements of conductivity, capacitance, resistance/impedance, or inductance are related to the local state of fluidization. For example, closely packed coke particles have a measurable resistance/impedance in the order of several hundred ohms, by contrast, the resistance of air is practically infinite. The resistance of the solids is a function of the packing arrangements of the particles. Thus, the response of an appropriately designed sensor located in the bed will be comprised of information on both the bubble-phase and local porosity fluctuations of the solids.

An analysis of these responses yields bubble pulse duration, number of bubbles striking the probe per unit time and local bubble rise velocity. From these parameters, pierced length of the bubble, local bubble volume fraction and local bubble gas flow can be derived.

Cairns and Prausnitz (1960) studied macroscopic mixing in a liquid fluidized bed. A salt solution was injected from a point source and electrical conductivity cells measured the time averaged and fluctuating salt concentrations at various points. The mixing data for the central portion of the bed yielded radial-eddy diffusivities plus scales and intensities of turbulence.

An electroresistivity probe measuring the mixing of two dissimilar coke particles was described by Hayakawa et. al. (1964). Data obtained was presented to illustrate its utility. Park et. al. (1969) employed an electroresistivity probe to measure the bubble characteristics in a bed of conducting particles. Figures indicating bubble frequency, volume fraction, average size, rise velocity and size distribution as a function of particle size, bed position and fluidizing velocity were presented.

Burgess and Calderbank (1975a) evaluated an electroresistivity probe with bubble-orientation signal processing capacity. Only bubbles central to the probe axis were accepted. Measurements of bubble velocities, size and shape were conducted. Experimental data was compared to that of Johnson (1970) and found to be consistent. In a further study, Burgess and Calderbank (1975b) employed an electroresistivity probe in a bed of carbon particles to measure the bubble rise velocity, distribution of bubble size and bed void fraction for one fluidizing gas velocity. Figures presented data at the centerline and one radial position for various heights in the bed. Bubble velocities were compared with the expression given by Nicklin (1962a, b) and were found to be in good agreement. Bubble shapes and sizes were similar to those observed by Rowe and Partridge (1965). It was concluded that emulsion-phase circulation had a marked effect on the bubble properties and gas flow in the bed.

The bubble parameters of a fluidized-bed gasifier were measured by Lowry and Barrett (1979) and (1980). The behaviour of gasifiers at elevated temperatures was studied. Matsui et. al. (1987) studied coal char gasification using an electroresistivity probe. The bubble size under gasification conditions was measured. This was then used in a modified bubbling bed model to predict char and CO_2 conversion.

Choi et. al. (1986,1988) utilised an electroresistivity probe to measure bubble parameters in a square gas fluidized bed, for comparison with a model for mean bubble sizes. It was concluded that the model represented the data on bubble size well.

Werther and Molerus (1973a) measured the parameters characterising the local state of fluidization in beds of arbitrary size with a capacitance probe. They noted that other workers' (Morse and Ballou (1951), Bakker (1958), Fukuda, Asaki and Kondo (1967), Kunii, Yoshida and Hiraki (1967) and Geldart and Kelsey (1972)) capacitance probes did not gain general acceptance due to the probe shape, which in many cases caused destruction of the rising bubbles rather than determination of the local state of fluidization. They developed a miniature probe which caused minimum disturbance.

A statistical analysis of the signal, yielded mean bubble pulse duration, number of bubbles striking the probe per unit time and local mean bubble rise velocity. From these parameters, local mean pierced length of the bubble, local bubble volume fraction and local bubble gas flow were derived.

An investigation of the spatial distribution of bubbles in gas fluidized beds of various sizes was undertaken by Werther and Molerus (1973b). A comparison of bubble-phase flow data was made with that of a study of flow profiles carried out by Whitehead et. al. (1970) and general agreement was obtained.

Werther (1974a) employed a capacitance probe to study the distribution of bubble pulse durations. A distribution of pierced lengths was deduced and this in turn was used to construct a local bubble size distribution by means of geometric probability theory. Data from various sized beds showed that the bubble size distribution could be approximated by a log-normal distribution.

The influence of bed diameter on the hydrodynamics of fluidized beds was studied (Werther (1974b)) by gathering parameters characterising the state of fluidization. The results showed that for laboratory scale fluid beds diameter had a strong influence on the bed hydrodynamics.

Werther (1976) predicted quantitative convective solids transport occurring in large diameter fluid beds on the basis of measured properties of the bubble-phase. Based on the fundamentals of Rowe et. al. (1971) an equation was derived from measurements of bubble development in large fluid beds (>1 m) which related solids transport in the bubble wakes to determinable parameters. Predictions of this relationship were found to be in good agreement with direct measurements of convective solids transport by Schmalfeld (1973) on pilot scale semi-cylindrical beds.

Bubble chain formation in large diameter fluidized beds was studied by Werther (1977, 1978a). A capacitance probe collected information for processing into local bubble size distributions and local average bubble shapes, he found evidence of the formation of bubble chains, i.e., the non-random rise of bubbles. He concluded that this phenomenon had a deleterious effect upon gas-solid contacting, as demonstrated by Askins et. al. (1951).

Lanneau (1960) investigated gas-solid contacting parameters in a fluidized bed using a capacitance probe. The parameters studied included : distribution of solids between the bubble and emulsion-phases, gas back-mixing and interchange between the bubble and emulsion-phases. A mathematical model was developed to describe the kinetics of first order irreversible chemical reactions in fluid beds. The results demonstrated the importance of fluidizing conditions on the efficiency and selectivity of chemical reactions in a fluidized bed.

Numerous workers have also employed capacitance probes for the study of gas-solid fluidization. Yoshida and Kunii (1968) used a capacitance probe to measure bubble frequency in a fluidized bed. From the bubble frequency the residence time distribution of the fluidizing gas was calculated. Experimental results were in good agreement with model predictions. Geldart and Kelsey (1972) described the procedure for calibration of a capacitance probe in a fluidized bed via the use of a cine-camera.

Haines et. al. (1972) utilised a combination of capacitance probe and radioisotope probe to measure bubble characteristics in a fluidized bed. These later supplemented a study of solids mixing. Tomita and Adachi (1973) measured bubble frequency and volume fraction in a fluidized bed using a capacitance probe. Data was presented for various fluidizing gas velocities, and bed locations.

A simulation model to predict the performance of a fluidized bed reactor was derived by Tone et. al. (1974) from the observed bubble behaviour. The results confirmed the applicability of the model for predicting the performance of a methylcyclohexane cracker. Otake et. al. (1975) measured the changes in the size and rise velocity of bubbles in a fluidized bed at elevated temperatures with a capacitance probe. The bubble frequency increased with rising temperature.

Homsy (1981) discussed the development of a capacitance probe to study bubble characteristics in a fluid bed. In addition, he detailed interest in the measurement of particle velocities or particle momentum via an optical fibre probe. An "oversized" capacitance probe to measure bed levels, density and "dynamics" in a high temperature fluidized bed reactor, with a view to industrial applications was developed by Fasching et. al. (1982). Yutani et. al. (1983a, 1983b, 1986) measured bubble frequency and its stochastic variation in a gas-solid fluidized bed. A stochastic model was proposed and appeared to predict the experimental data well.

Gunn and Al-Doori (1985) described the calibration of a capacitance probe in a two-dimensional fluid bed by means of a cine-camera. Jet instability and bubble frequency in a single orifice two-dimensional fluidized bed, with a capacitance probe was studied by Zhang et. al. (1987). A model which accounted for particle size, particle density, probe vertical location and jet flow rate predicted bubble frequency adequately. Hilligardt and Werther (1986) studied the bubble throughflow velocities and dense phase gas velocities in a freely bubbling three-dimensional bed, with the combination of a capacitance probe and a pressure probe. It was concluded that gas flow in and around bubbles exerted a significant influence on bubble growth. A coalescence model for bubble growth was proposed which included the influence of the measured parameters, i.e., bubble throughflow and dense phase gas velocities.

In characterising the bubble hydrodynamics in gas-solid fluidized beds workers have measured large quantities of local bubble velocity and size as functions of fluidizing gas velocity and location in the bed. Investigators usually reduced the quantity of data by averaging bubble velocity and size, and presenting the variation of local mean bubble velocity and local mean bubble size throughout the bed, with different fluidizing gas velocities. Figures showing the variations in local bubble velocity and local bubble size are in most cases very limited.

Table 2.1 Summary of Experimental Methods For Studying Gas-Solid Fluidized Beds

General Measurement Technique	Detailed Measurement Technique	Single Bubbles Counted	Distribution of Mean	Reference for Detailed Information
Photographic	Still Photography	Yes	No	Rowe, 1971
	Cine Photography	Yes	Yes (Size, shape, rise velocity)	Upson and Pyle, 1973 Geldart, 1970/71 Kunii and Levenspiel, 1977 Fryer and Potter, 1973
X-Ray	X-Ray detection	Yes	Yes (Size and shape)	Rowe and Partridge, 1965 Rowe and Matsumo, 1971 Rowe, 1971 Hager and Thompson, 1973 Judd and Dixon, 1978 Rowe and Masson, 1980, 1981
	X-Ray CT	No	No	Banholzer et. al., 1987
Optical	Light Obscuration	Yes	Yes (Size and rise velocity)	Put et. al., 1973 Yasui and Johanson, 1958 Kilkis et. al., 1973 Yoshida et. al., 1978a, b Yong et. al., 1980 Valenzuela and Glicksman, 1984 Sung and Burgess, 1987
	Fibre Optics	Yes	Yes (Size and rise velocity)	Ohki et. al., 1977 Ohki and Shirai, 1978 Ishida et. al., 1980 Patrose and Caram, 1982 Muramoto et. al., 1985 Dutta and Wen, 1979 Kai et. al., 1987 Yamazaki et. al., 1986 Yang et. al., 1987 Glicksman et. al., 1987 Berruti et. al., 1988

General Measurement Technique	Detailed Measurement Technique	Single Bubbles Counted	Distribution of Mean	Reference for Detailed Information
Pressure Fluctuation	Uses Pressure Difference Between Bubble and Emulsion -phases	Yes	Yes (Size and rise velocity)	Broadhurst and Becker, 1976 Fan et. al., 1981, 1983 Taylor et. al., 1973 Chan et. al., 1987 Drahos et. al., 1988
Electro-magnetic Waves	Gamma-Ray Transmission	Yes	No (Mean bed voidage)	Orcutt and Carpenter, 1971 Weimer et. al., 1985
	Microwaves	Slugging Beds	No (Mean bed voidage)	Cheremisinoff and Cheremisinoff, 1984 Kunii and Levenspiel, 1977
	Ultrasonics	Yes	No (Mean bed voidage)	Yosef et. al., 1975
Thermal Techniques	Thermister Probe	Yes	Yes (Rise velocity)	Wen et. al., 1978 Hiraki et. al., 1968/69 Bernis et. al., 1973 Goosens and Hellinckx, 1973 Bashakov et. al., 1973
Electro-resistivity Properties	Resistance Probe	Yes	Yes (Pierced length, bubble size, rise velocity)	Cairns and Prausnitz, 1960 Hayakawa et. al., 1964 Park et. al., 1969 Burgess and Calderbank, 1975a, b Lowry and Barrett, 1979 Matsui et. al., 1987 Choi et. al., 1986, 1988

General Measurement Technique	Detailed Measurement Technique	Single Bubbles Counted	Distribution of Mean	Reference for Detailed Information
	Capacitance Probe	Yes	Yes (Pierced length, bubble size, rise velocity)	Werther and Molerus, 1973a, b Morse and Ballou, 1951 Bakker, 1958 Fukuda et. al., 1967 Kunii et. al., 1967 Geldart and Kelsey, 1972 Werther, 1974a, b Werther, 1976 Werther, 1977 Werther, 1978a Lanneau, 1960 Yoshida and Kunii, 1968 Haines et. al., 1972 Tomita and Adachi, 1973 Tone et. al., 1974 Otake et. al., 1975 Homsy, 1981 Fasching et. al., 1982 Gunn and Al-Doori, 1985 Yutani et. al., 1983a, b, 1986 Zhang et. al., 1987 Hilligardt and Werther, 1986

CHAPTER III

EXPERIMENTAL SYSTEM

This chapter details the experimental system employed for collecting the bubble characteristics. Several unique aspects are examined and explained including an original method of data collection and processing.

3.1 Capacitance Probe Design Criteria

The attributes of a capacitance probe capable of detecting local non-steady variations of porosity, i.e. the bubble hydrodynamics, in gas fluidized beds, were detailed by Werther (1973a). The probe should:

a) disturb the state of fluidization as little as possible;

b) measure local variables;

c) detect rapid variations in porosity;

d) possess adequate mechanical strength;

e) be capable of relocation within the bed.

Based upon these criteria coupled with a detailed evaluation of previous capacitance probe designs, a preliminary probe was designed and fabricated for testing and appraisal. It lacked sufficient mechanical strength and consequently its response to porosity changes was ambiguous. A modified single tip design with increased strength was constructed and tested successfully. Results are summarized in Section 3.3. The same design guide-lines were employed in the construction of a double tipped capacitance probe. A photograph of the capacitance probes used in this study is presented in Figure 3.1.

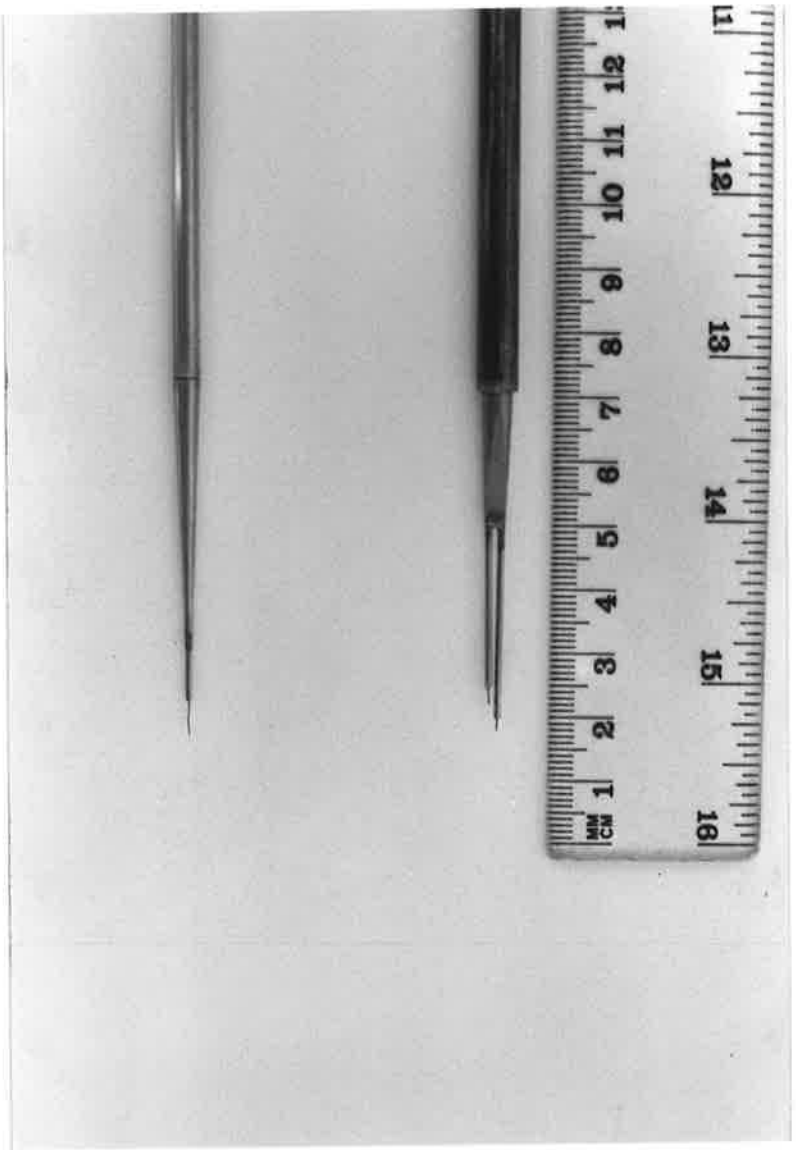

Figure 3.1 Detail of Capacitance Probes used in this study

3.2 Data Collection System

The probe forms part of a high frequency oscillator circuit. The temporal variations of the porosity at the capacitor cause a change in the capacitance resulting in a proportional d.c. voltage change. The protruding stainless-steel needle is one pole, whilst the enclosing stainless-steel tube forms the other pole of the capacitor. When the probe-contact is in the conducting particulate phase the circuit is closed, allowing current to flow. However, when the probe-contact is in a bubble (high capacitance phase) the circuit opens and current ceases flowing. The change in capacitance from bubble-phase to emulsion and back to bubble produces a voltage pulse which can be converted into digital form by a Analogue/Digital (A/D) converter and used by a digital computer for the calculation of bubble rise velocity and pierced length.

A schematic detailing the logic of the data collection system employed for use with the single and dual tipped capacitance probes is illustrated in Figure 3.2. Data collection systems of previous investigators were comprised mainly of hardware components. A novel approach was adopted in this study. Advanced software was written eliminating all of the complex and costly hardware previously employed. Probe signal amplification, filtering, and separation into bubble and emulsion-phase components all formed part of the data collection software. An integrated circuit (IC) driven by the data collection program supplied the input signal to the probe, rather than the previously used function generator or oscillator. The IC and other circuitry associated with the probe were placed in an aluminium circuit box located directly on top of the probe. This had not been done previously but was considered necessary to eliminate noise, as flexing of any electrical connections produces erroneous capacitance changes. The probe signal was received by an A/D interface which linked with an IBM-AT compatible computer. One of the computer motherboard slots held an A/D converter circuit board, which received the probe signal from the A/D interface.

The probe signal passed to the data collection program where the signal could be modified using a detailed options list (see Section 3.5) to obtain the desired separation of bubble and

emulsion-phase components. The modified signal was then displayed on the computer terminal and stored to hard disk, along with the raw data signal, for future analysis. The extensive use of computer software was a new and novel feature of this type of study. The need for expensive hardware was eliminated. Modifications in the data collection system were achieved simply and economically by rewriting the program code, rather than the purchase of new equipment. The program employed a menu system for interfacing with the user, providing logical and efficient operation. The collected and modified data was displayed in real-time allowing quick observation of changes made via the Process List functions. This permitted accurate discrimination of the bubble and emulsion-phase components. A large quantity of computer memory was required for data storage, as the volume of data collected became formidable. However, a "crunching and squeezing" program was employed to make the data more manageable. The ever diminishing cost of computer memory means that this is a minor irritant. A major advantage of this type of software is the envisaged application to any study where high speed data acquisition is essential.

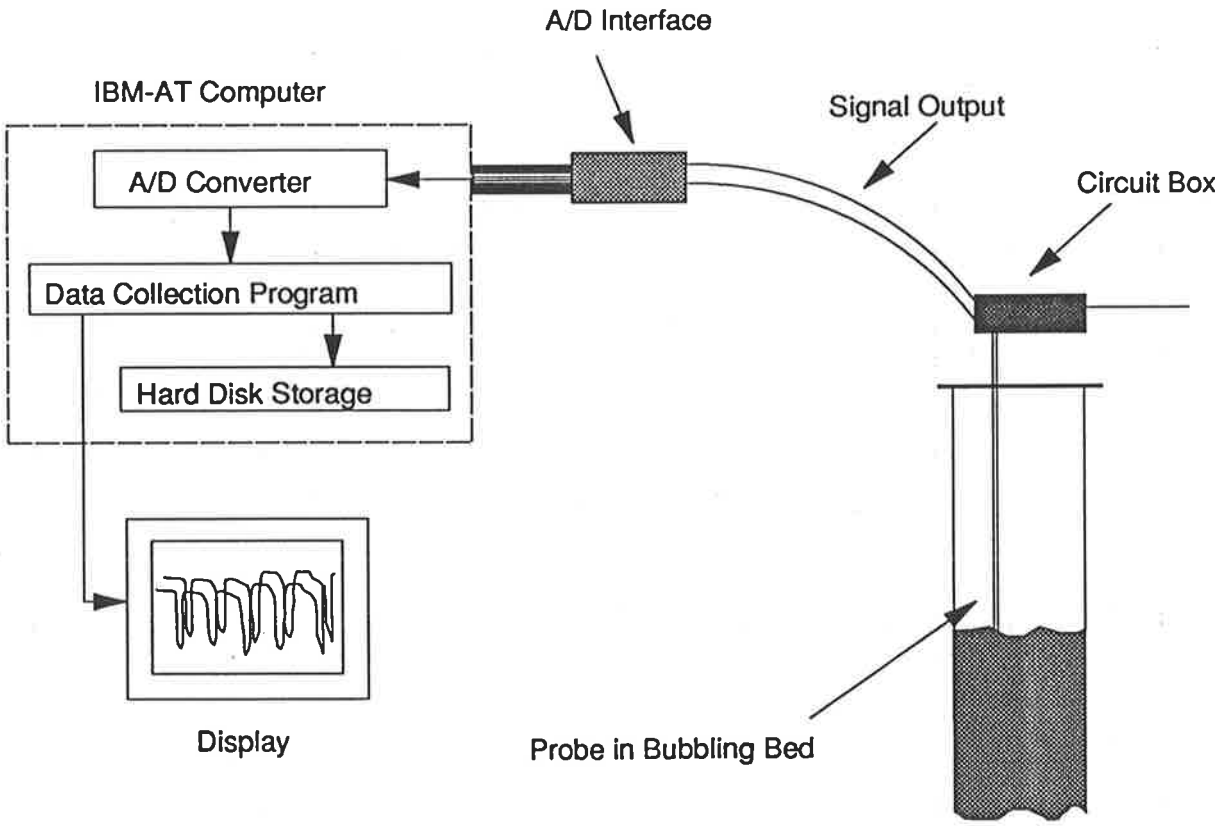

Figure 3.2 Data Collection System

3.3 Data Collection Program Calibration

3.3.1 Experimental System for Calibration

A single tipped capacitance probe was developed and employed to calibrate the data collection software. The probe was placed in a two dimensional gas fluidized bed with backlighting. A video camera and recorder were employed to film bubbles striking the probe tip. Included in the camera's frame of vision was a stopwatch and light emitting diode, which flashed at the instant the computer commenced data collection. Therefore, given the rate of data sampling by the computer, synchronisation of the video record and probe data collected by the computer was possible, over the duration of the experiment. Figure 3.3 outlines the experimental system used to calibrate the data collection program.

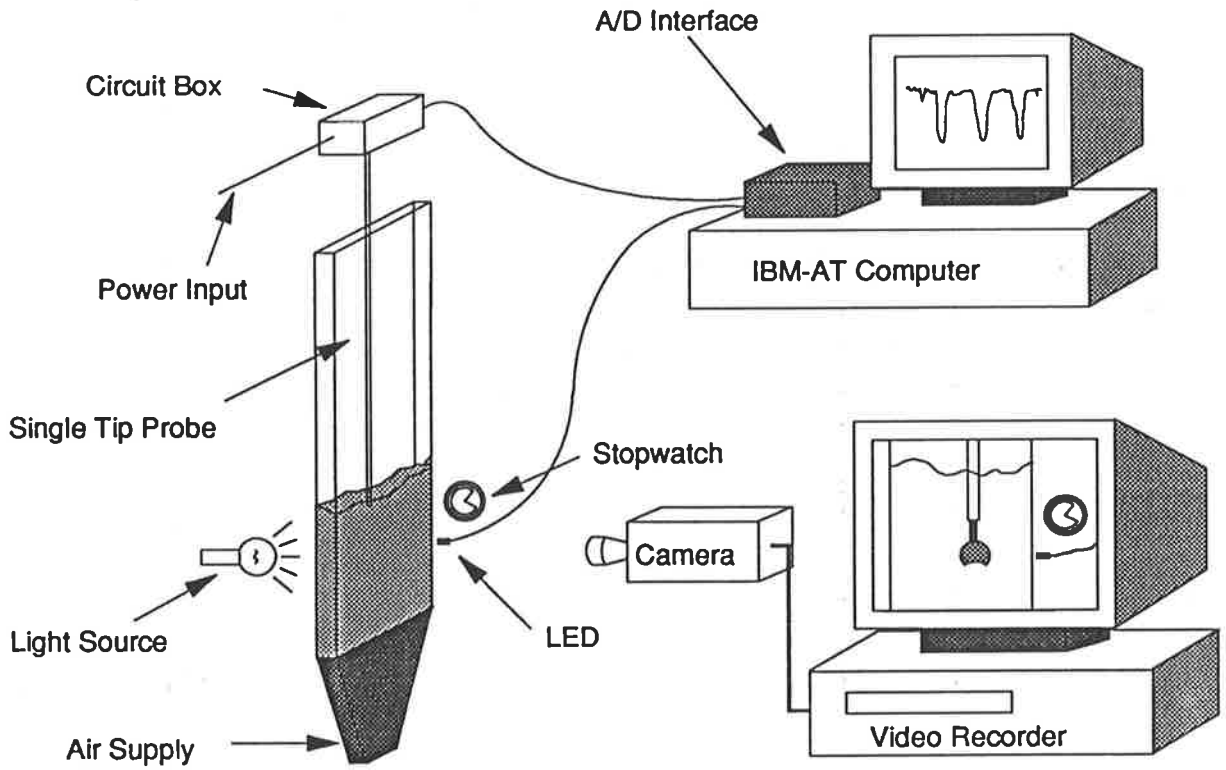

Figure 3.3 Experimental System for Data Collection Program Calibration

3.3.2 Signal Interpretation - Ideal Bubble

A schematic of the signal received from the probe when hit by an *ideal* rising bubble is illustrated in Figure 3.4.

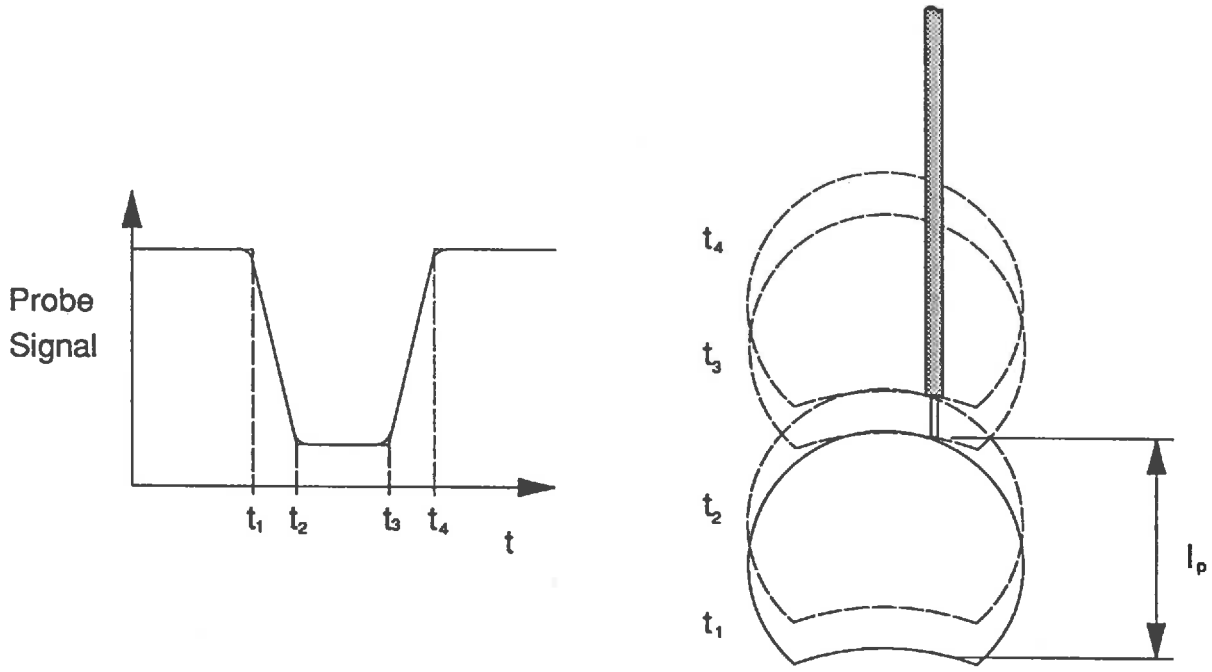

Figure 3.4 Probe Signal when Single Tip Probe hit by an ideal rising bubble

Prior to time t_1, the probe is located entirely in the emulsion-phase, the probe signal is at its maximum (emulsion-phase) level. At t_1 the roof of the bubble strikes the probe needle, subsequently the probe signal decreases. The roof of the bubble impinges upon the enclosing metal tube at t_2 and the probe signal falls to its minimum (bubble-phase) value. The probe is now located entirely in the bubble-phase. The bubble floor strikes the probe needle at t_3, the probe signal increases until t_4 when the metal tube is struck by the bubble floor. The probe signal returns to the maximum level.

3.3.3 Signal Interpretation - Real Bubble

In the case of real bubbles, the situation is more complex. For a rising real bubble, the recorded probe output is influenced by any emulsion-phase porosity variations, experienced by the probe. This emulsion-phase signal must be identified and removed before the bubble data can be utilised to derive the fundamental bubble hydrodynamics.

A typical probe output as recorded from the single tipped capacitance probe operating over one second is shown in Figure 3.5. The equivalent section of the video record was determined by observation of the flashing LED and the time record as displayed on the stopwatch, in comparison with the rate of data collection. Once the equivalent section of video record was found, slow motion and freeze-frame replay of the video film allowed pinpointing the position of the bubble's leading and trailing edges relative to the probe needle and enclosing tube at any instant.

Figure 3.6 shows the synchronised computer record. Clear identification of the passage of the bubbles relative to the probe tip was possible. Deviations caused by bubbles and emulsion-phase porosity variations were easily separated into their respective sections on the computer record. Some one hundred bubbles were identified from the video record, thus providing the necessary reliability of the probe and allowing calibration of the data collection program. Having identified the presence and position of bubbles on the computer record the calibrated software provides details of bubble pierced length, rise velocity and additional information on the bubble hydrodynamics in conjunction with the dual tipped capacitance probe.

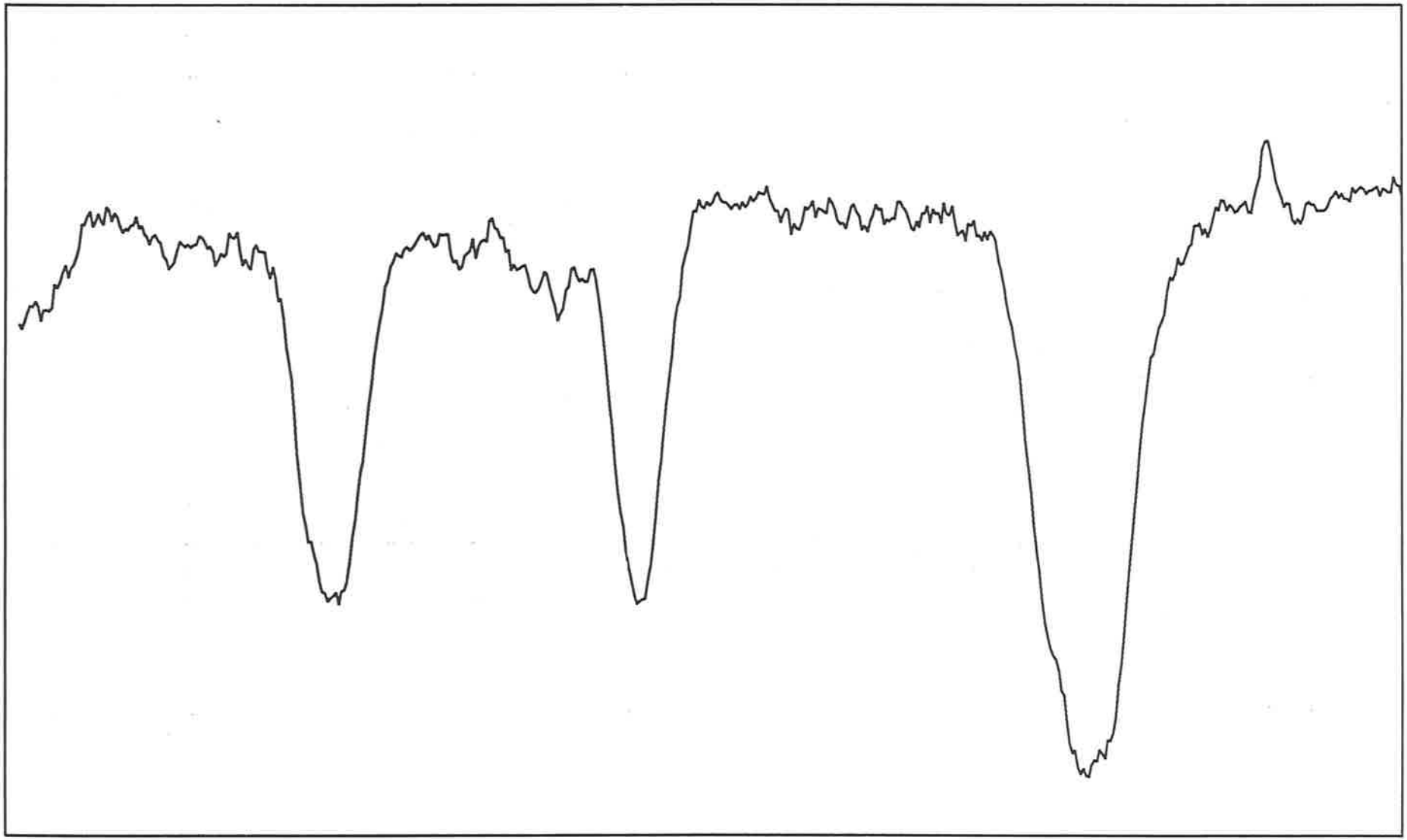

Figure 3.5 Output from Single Tip Capacitance Probe

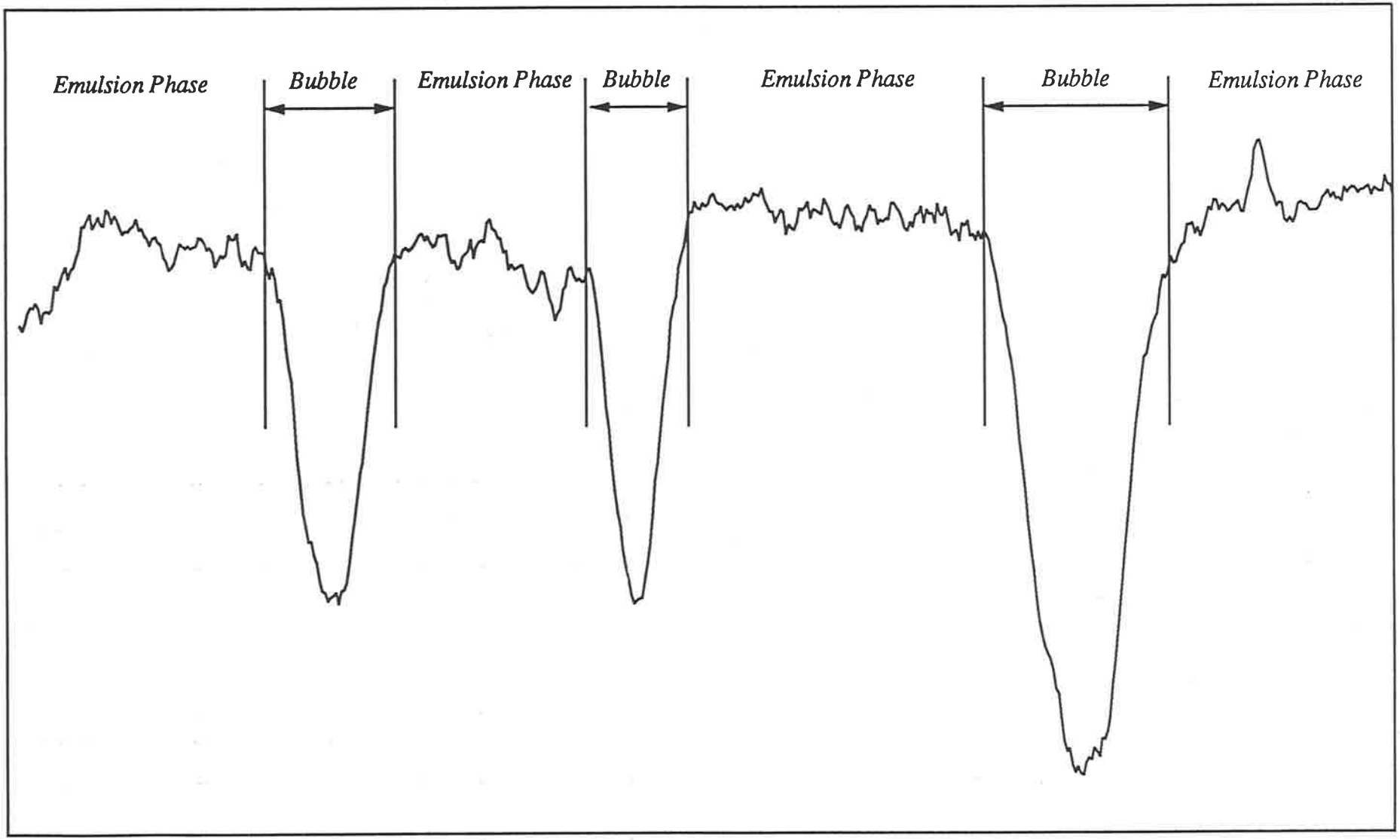

Figure 3.6 Calibrated Output from Single Tip Capacitance Probe

3.4 Dual Tip Capacitance Probe

This probe was constructed entirely of stainless steel. It was designed to measure bubble hydrodynamics at any point in the bed. Total probe length was 800 mm. The probe wires and enclosing metal tubes were inserted within a 6.3 mm diameter tube, so that buffeting by the bubbles did not cause longitudinal bending of the probe. Spacers held the probe wires in place and kept them separate, over the entire tube length. The probe and circuit box containing associated circuitry are sketched in Figure 3.7.

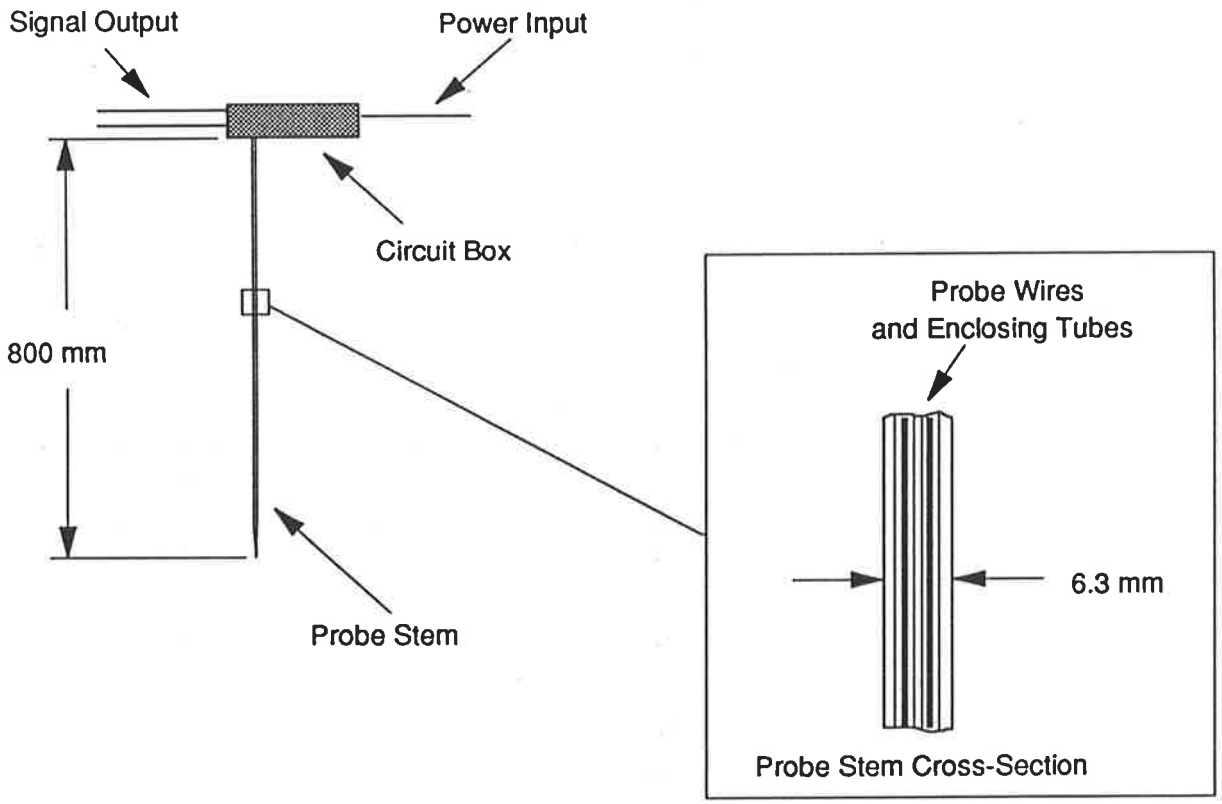

Figure 3.7 Dual Capacitance Probe

The dimensions of the dual capacitance probe tip are shown in Figure 3.8.

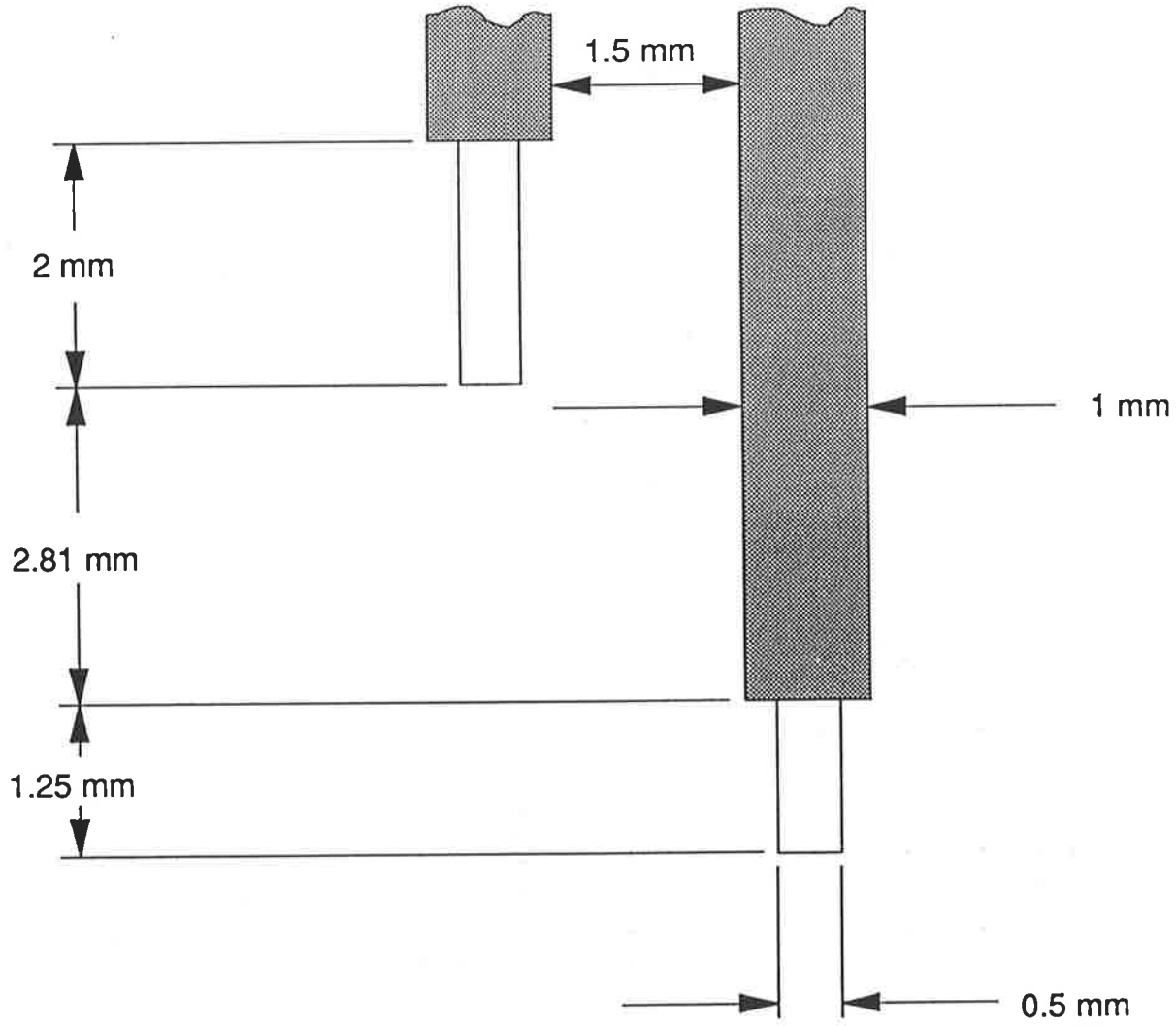

Figure 3.8 Dual Capacitance Probe Tip Dimensions

3.5 Data Analysis

The data collection software was written in TURBO PASCAL and was highly comprehensive. Upon receipt of the probe signal, the collection program performed a real-time analysis which converted the raw probe output data into a modified form and displayed the results on the terminal screen. The modifications performed on the raw data were assigned by the operator from a choice of menus. Five menus were available and each of these contained a process list which could be tailored for specific purposes. Figure 3.9 is a digitised image of the data collection program graphics, captured from the terminal display, while the program was running. In the bordered area, which is the terminal display area for the collected probe data, the process list of the fifth menu is presented. The modifications performed on a sample of raw data and a summary of their consequences are presented in Table 3.1.

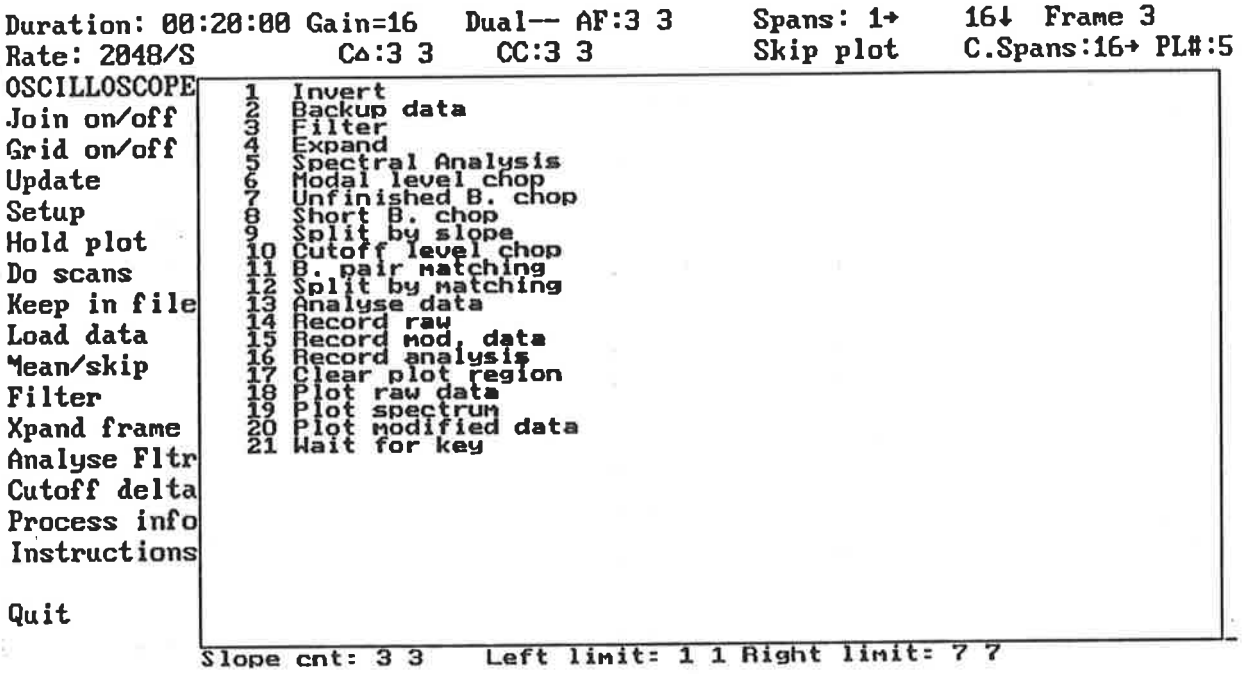

Figure 3.9 Process List choices of Data Collection Program

Table 3.1 Summary of Data Collection Program Process List

Process Number	Process	Function
1	Invert	Inverts probe signal.
2	Backup Data	Stores Raw probe output to RAM.
3	Filter	Filters probe output signal.
4	Expand	Expands collected data to fill terminal display area.
5	Spectrum Analysis	Calculates the concentration of the probe data horizontally and sets a Modal Level.
6	Modal Level Chop	From the Spectrum Analysis all data above the Modal Level set to the Modal Level.
7	Unfinished Bubble Chop	Any bubbles not completely recorded, e.g. data collection ceases as a bubble is being recorded, are set to the Modal Level.
8	Short Bubble Chop	Any "spikes" in the recorded data are set to the Modal Level.
9	Split By Slope	The collected record is split where a slope change, as specified by the user, in the data is found. The point at which the split is set is stored for later use.
10	Cut-off Level Chop	A cut-off level, as set by the user, defines those deviations from the emulsion-phase porosity fluctuations that are regarded as bubbles. All data outside points split by slope and above cut-off level are regarded as emulsion-phase porosity variations and are set to the Modal Level.
11	Bubble Pair Matching	A search is conducted across both data channels to pair the recorded bubbles, as each bubble recorded by one probe must also be recorded by the other in order to calculate the bubble rise velocity.
12	Split By Matching	Searches inside that part of the record designated as bubbles, in both channels, for any unmatched bubbles and sets them to the Modal Level.
13	Analyse	Calculates the pierced length, rise velocity and number of bubbles recorded, from the modified data.
14	Record Raw	Raw Data stored on hard disk.
15	Record Modified Data	Modified Data, that is, data processed by the user chosen Process List and separated into bubble and emulsion-phases, stored on hard disk.
16	Record Analysis	Calculated bubble pierced lengths, rise velocities and number stored on hard disk.
17	Clear Plot Area	The terminal display area is cleared.
18	Plot Raw Data	Raw Data plotted on terminal display area.
19	Plot Spectrum	Spectral Analysis plotted on terminal display area.
20	Plot Modified Data	Modified Data plotted on terminal display area.
21	Wait For Key	Pause

Figures 3.10(a) - (c) detail a variety of the features of the data collection process list as performed on a single channel of data, sampled over one second (c.f. Figure 3.5). In Figure 3.10(a) the Modal Level as calculated by the Spectral Analysis can be seen. This level is computed by counting the data points appearing at each horizontal level in the record, the horizontal level with the most data occurrences defines the Modal Level. The bubble Cut-off Level is set by the user to provide a threshold and thence to denote those peaks that the program must recognize as bubbles. All peaks passing below this line are regarded by the program as bubble peaks and remain in the modified data.

Bubble peaks in the data are more defined than porosity variations. From a consideration of the changing slope of the data record, determination of the bubble's leading and trailing edges is straight forward. Figure 3.10(b) shows the Split By Slope modification. The program splits the data record at points where the magnitude of the slope changes by an amount specified by the operator. The split points are set to the Modal Level and are recorded for future use.

Those segments of the data record which lie between the recorded Split By Slope points and possess a peak passing below the Cut-off Level are designated as bubbles. The sections of the data record which lie outside these points are regarded as emulsion-phase porosity variations and are set to the Modal Level. Figure 3.10(c) illustrates the modified data in its final form. The bubble and emulsion-phases are separated for analysis. Analysis consists of calculating the difference between the recorded bubble finish time and start time (the bubble pierced time, t_b) and in the case of a dual channel data record the difference between the bubble start times for the same bubble as recorded in each channel (the bubble rise time, t_r).

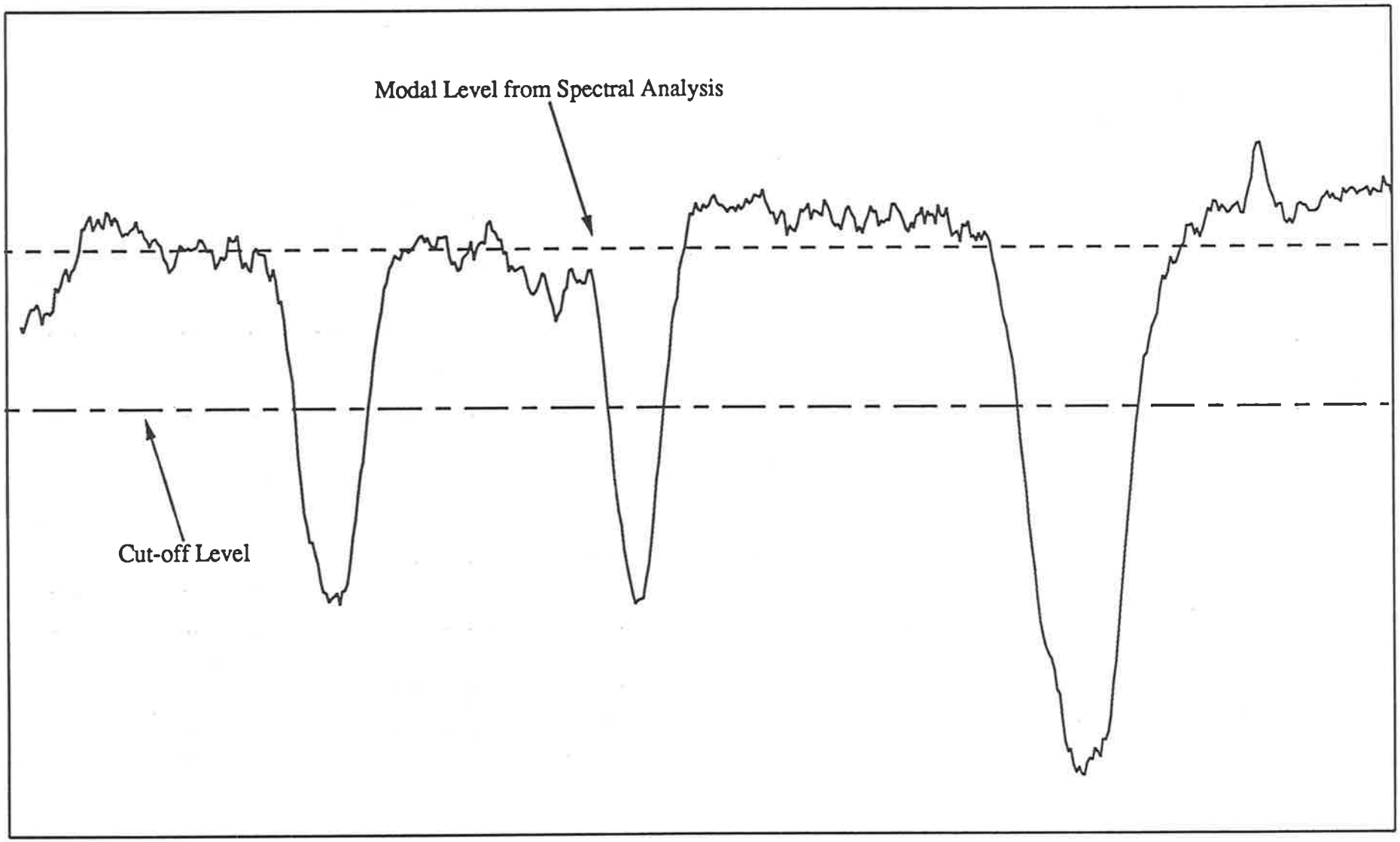

Figure 3.10(a) Probe Data Modification with Process List

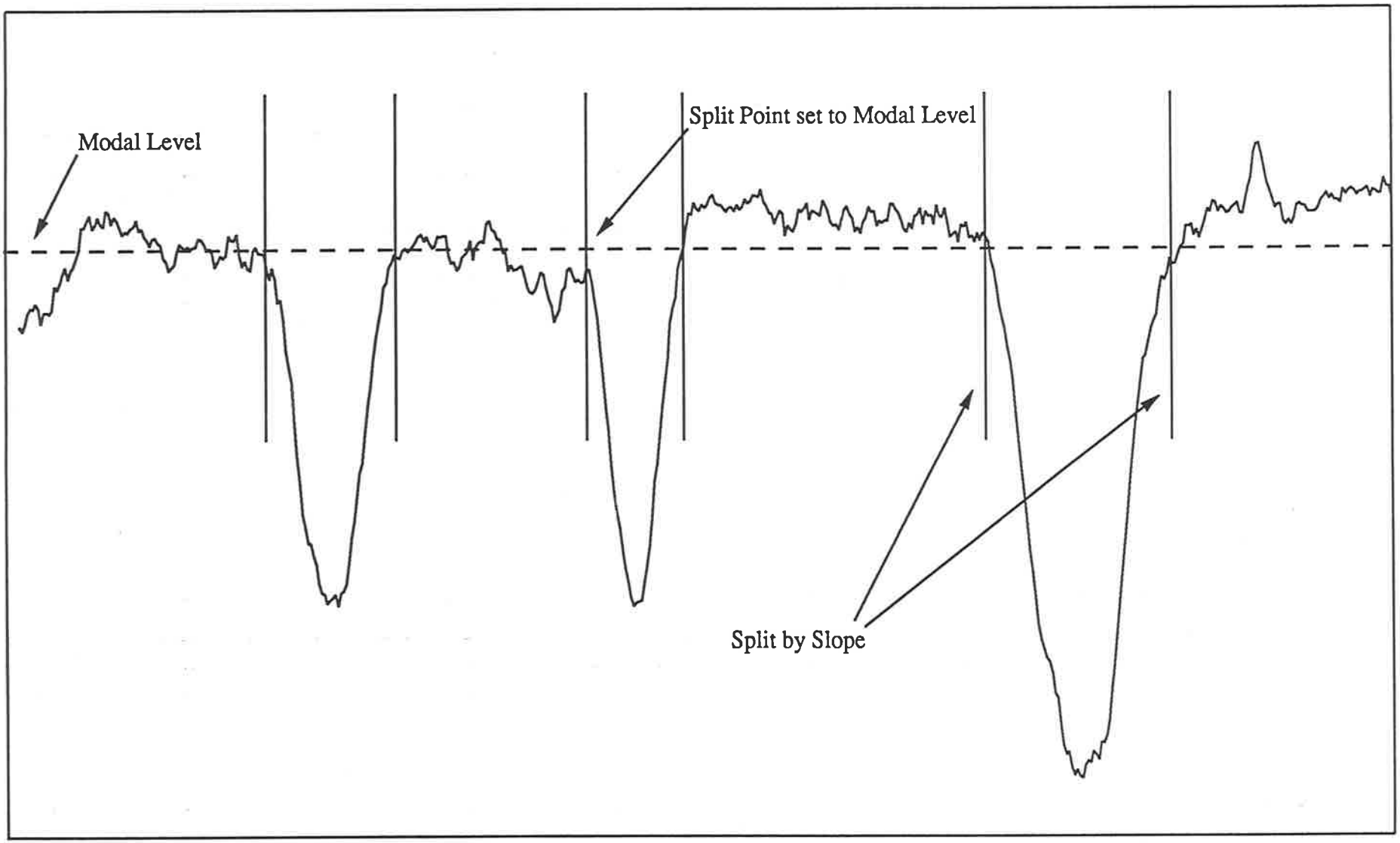

Figure 3.10(b) Probe Data Modification with Process List

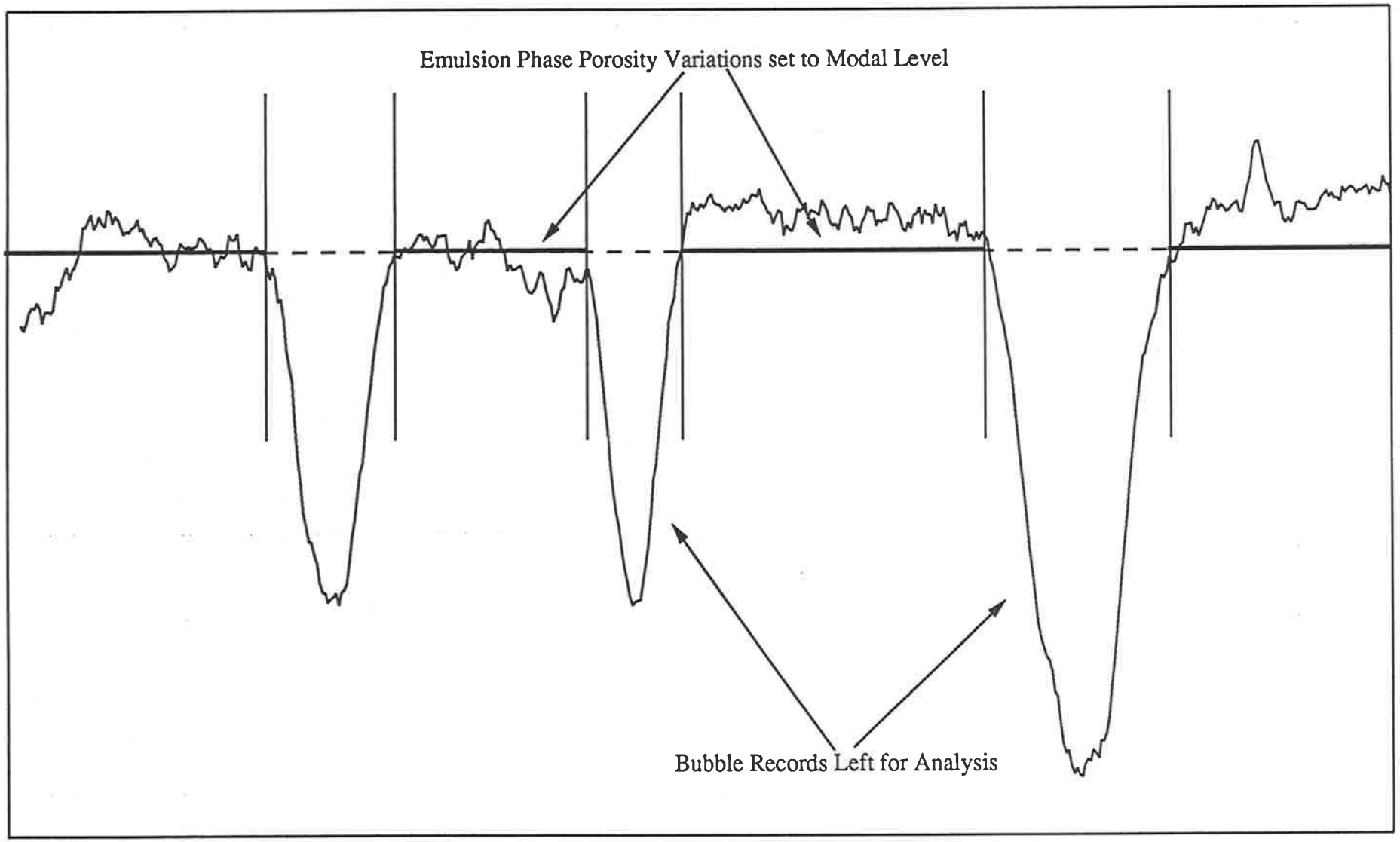

Figure 3.10(c) Probe Data Modification with Process List

The signal received from the dual capacitance probe in response to the rise of a single bubble, once modified, is shown in Figure 3.11.

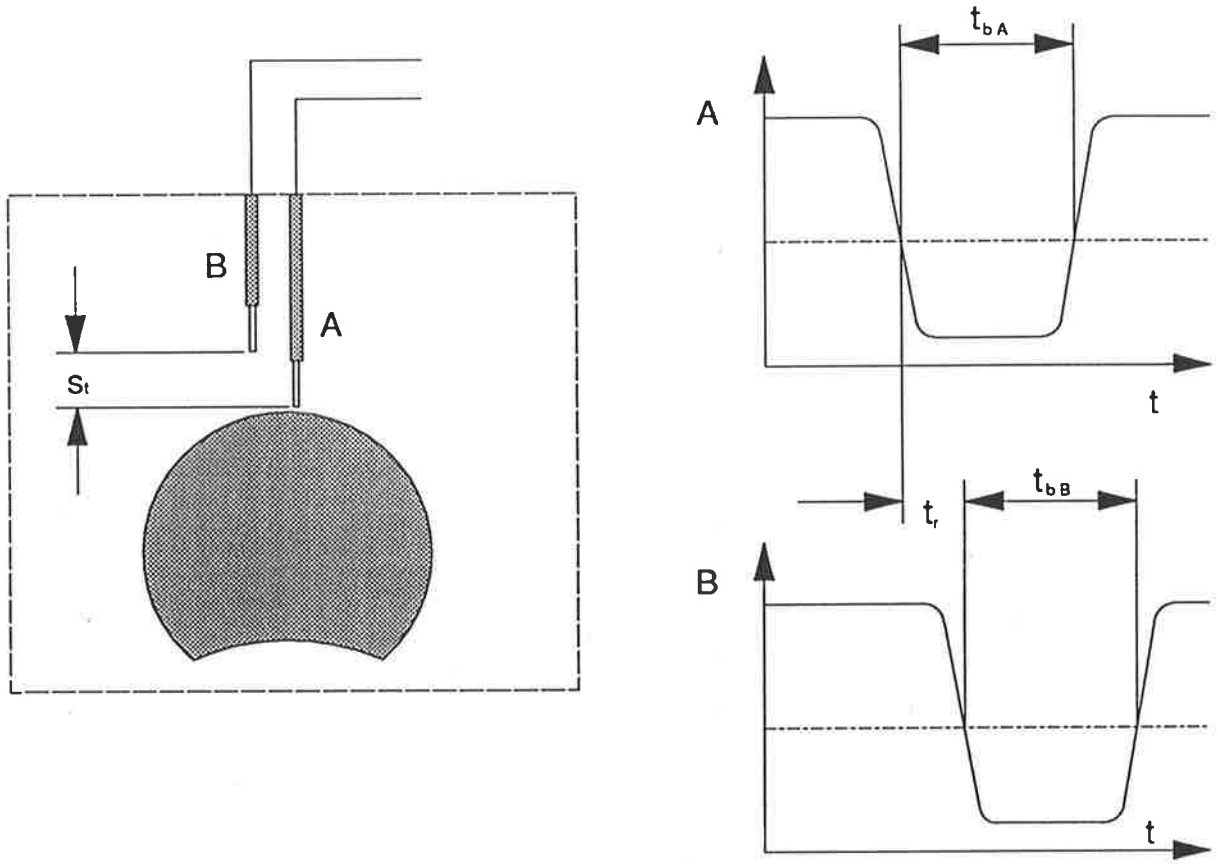

Figure 3.11 Modified Probe Signal when Dual Tip Probe hit by rising bubble

From the modified dual signal the single bubble rise velocity and pierced length can be calculated from the bubble pierced time and bubble rise time as follows :

The rise velocity of a single bubble can be expressed as:

$$u_{br} = \frac{S_t}{t_r} \qquad \ldots(3.1)$$

Calculation of the pierced length of the bubble can be expressed as:

$$l_p = u_{br} \cdot t_{bA} \qquad \ldots(3.2)$$

or

$$l_p = u_{br} \cdot t_{bB} \qquad \ldots(3.3)$$

3.6 Experimental Apparatus

The gas fluidized bed system used in the experiment is illustrated in Figure 3.12. The column was constructed of perspex thereby enabling visual observation of both the state of fluidization and uniformity of gas distribution. The bed column was 800 mm high and had an inside diameter of 230 mm. Compressed air served as the fluidizing gas. It entered the bed through a 300 mm high calming section, filled with 5 mm diameter glass beads. This ensured the absence of channelling and enhanced the uniformity of gas distribution across the distributor. A sintered-bronze porous plate was employed as the distributor. The flow of fluidizing gas was monitored by a 47 A rotameter. Figure 3.13 shows the dimensions of the experimental system.

The bed was filled to a height of 360 mm with glass ballotini (size range: AB -210 μm to +297 μm; ρ=2470 kg m^{-3}). Minimum fluidization velocity of the ballotini beads was 6.43 cm/s (see Figure 3.14).

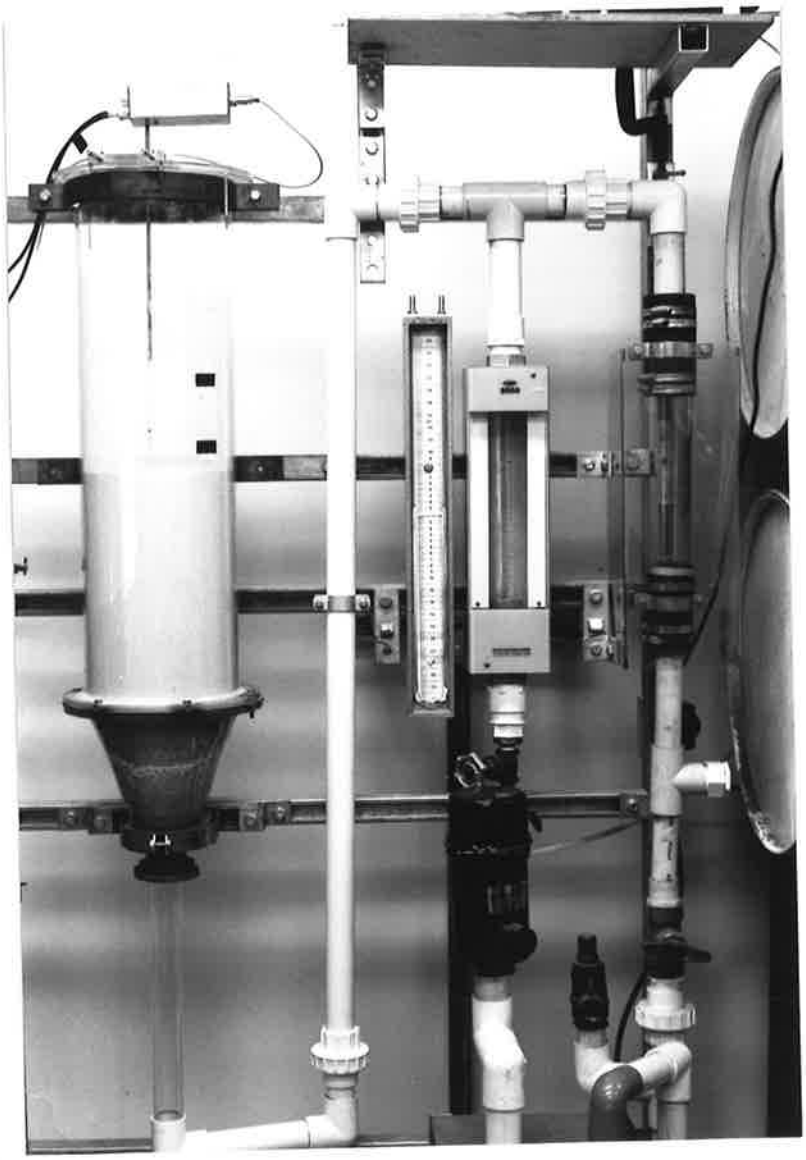

Figure 3.12 Experimental System

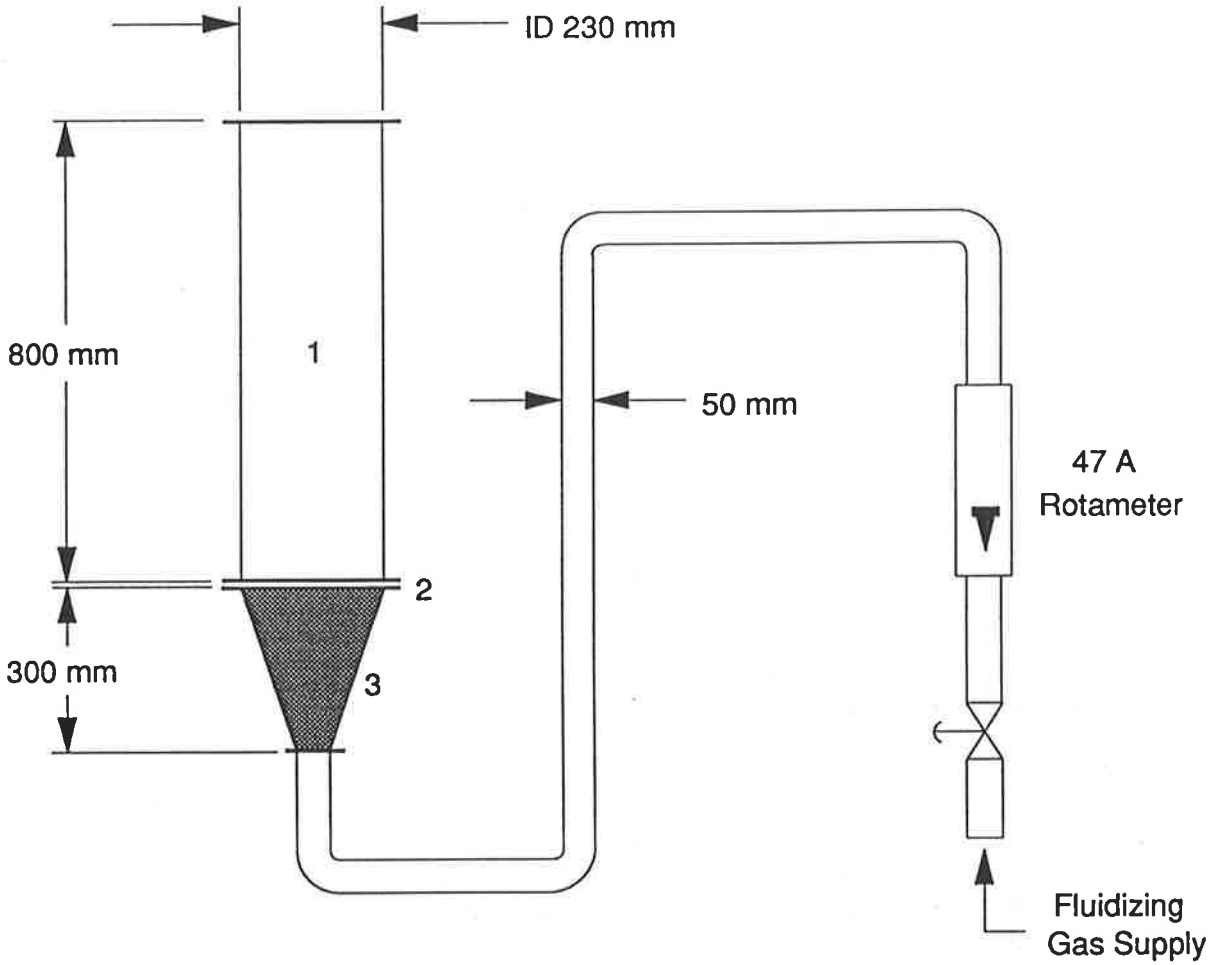

1: Fluidized Section
2: Distributor Plate
3: Calming Section

Figure 3.13 Experimental System Dimensions

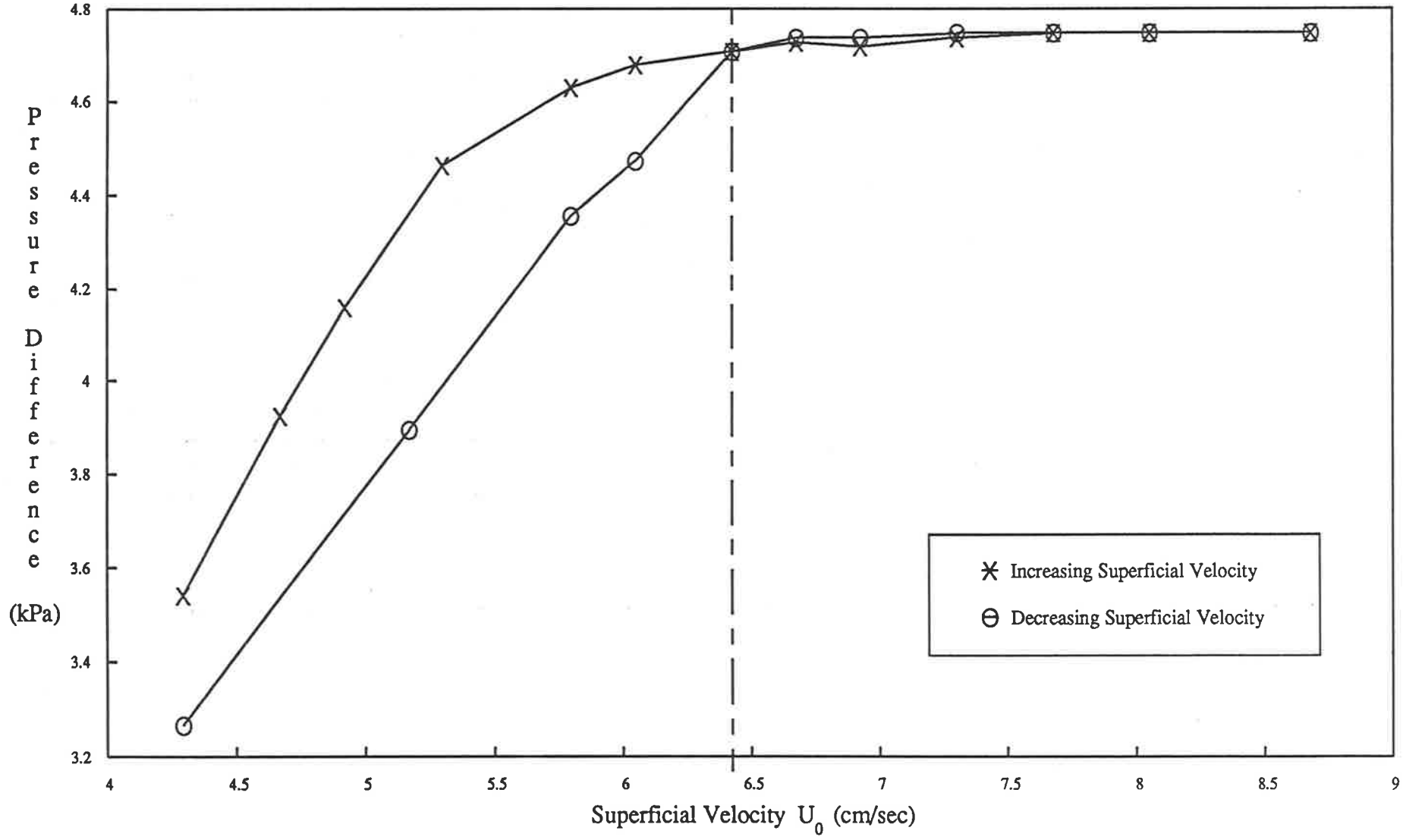

Figure 3.14 Calculation of Minimum Fluidization Velocity of AB Glass Beads

3.7 Experimental Procedure

It was envisaged that the bubble hydrodynamics throughout the bed would be recorded. To achieve this, it was necessary to position the probe at many points throughout the bed. The bed was divided equally into eight radii over which the probe could be manoeuvred. In the first instance, it was assumed that the fluidized bed exhibited similar bubble hydrodynamics at symmetrical radii throughout the bed. Experiments were, therefore, conducted at various heights for only one of the possible radial positions. The validity of this assumption was checked by repeating experiments at other radii from that used in the experiment. The probe tip was positioned by use of accurate measuring instruments. The tip was positioned according to the ratio of probe tip height in the bed to unexpanded solids height (l/L) and the ratio of probe tip radial position to bed radius (r/R). Values chosen were 0.0, 0.1, 0.2, 0.3, 0.4, - 0.9. Radius 1 was used in the experiment. Figure 3.15 shows the layout of probe positions used.

At each probe position in the bed five superficial gas velocities were employed 7.52, 8.75, 10.03, 11.39 and 12.64 cm/s. Or, expressed as the ratio of u_o/u_{mf} 1.17, 1.36, 1.56, 1.77, 1.97 and 2.17. An experimental run consisted of positioning the probe and recording data at each superficial velocity over a period of approximately 15 minutes.

Experiments were also conducted to test the reproducibility of data samples. The probe was located at several positions used in the original experimental runs, i.e. various heights throughout radius 1. Experiments were repeated at all previously employed superficial gas velocities but the time over which the data sample was recorded was extended to 60 minutes or in some cases 120 minutes. Also, the probe was located at various heights in other radial positions, e.g. radii 3, 5 and 7, to test the symmetry assumption of the bubble hydrodynamics.

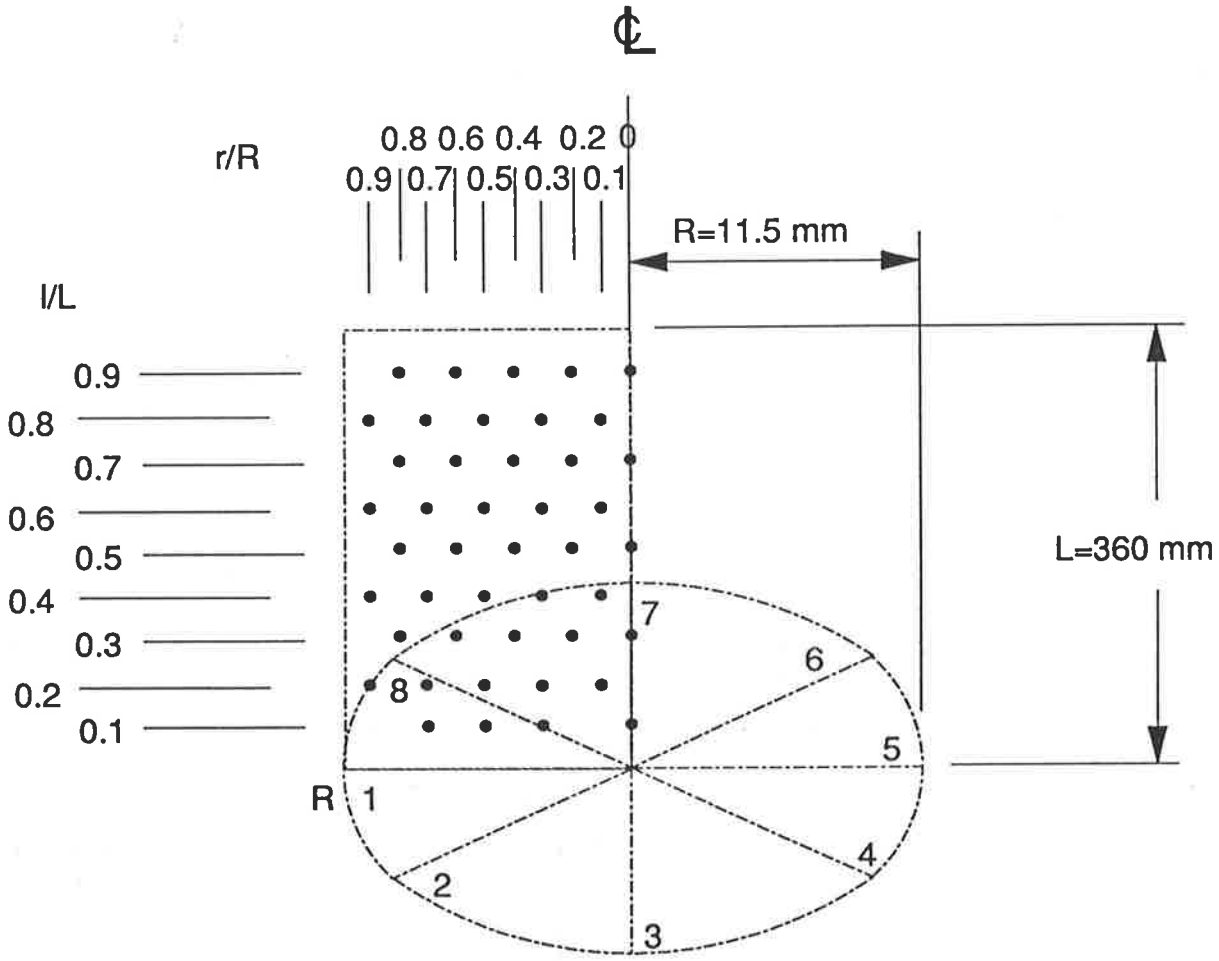

Figure 3.15 Layout of Probe Positions

CHAPTER IV

COMPARISON OF EXPERIMENTAL DATA WITH BUBBLE HYDRODYNAMIC MODEL

This chapter presents a comparison of the population balance model for bubble characteristics proposed by Agarwal (1985, 1986) and the experimental data collected in this study. A complete comparison was prohibitive in light of the quantity of data collected. An adequate comparison was made of bubble vertical dimension and rise velocity distributions, at various heights, radial positions and fluidizing velocities.

4.1 Bubble Characteristic Model

The modelling of various fluidized bed phenomena would be greatly facilitated by the availability of analytical expressions for describing the bubble characteristics. It has been recognised that the coalescence and growth of the bubble swarms rising from the distributor give rise to lateral as well as vertical distributions of bubble properties. Agarwal (1986) detailed the population balance approach for obtaining these distributions. The coalescence kernel was assumed to depend on the velocity as well as the location of the bubble in the bed. The effect of finite bubble size at the distributor was taken into account. The model equations include the constraining effect of the bed diameter which results in radial position dependent distributions of bubble sizes.

4.1.1 Bubble Characteristic Model Equations

A program was written to predict the bubble characteristics in a gas fluidized bed (See Appendix B). The equation for the probability density function of the bubble diameter was given by Agarwal (1986) as :

$$f(d_{br}) = \frac{1}{2}\left[\frac{\Gamma(m+1)}{\Gamma(m-1)}\right]^{\frac{m+1}{2}} \frac{x^{m+1}\exp\left[-\left[\frac{\Gamma(m+1)}{\Gamma(m-1)}\right]^{\frac{1}{2}}\frac{x}{\bar{y}}\right]}{\bar{y}^{m+2}\sqrt{d_{br}}\,[\Gamma(m+1)-\gamma(m+1,a)]} \qquad \ldots(4.1)$$

where
$$\bar{y} = (\sqrt{d_{br}} - \sqrt{d_{bo}}) \qquad \ldots(4.2)$$

$$a = \left[\frac{\Gamma(m+1)}{\Gamma(m-1)}\right]^{\frac{1}{2}} \frac{x}{\sqrt{D_t(1-r/R)} - \sqrt{d_{bo}}} \qquad \ldots(4.3)$$

$$x = \left(\bar{d}_b' - \frac{d_{bo}}{m}\right)^{\frac{1}{2}} - \left(\frac{m-1}{m} d_{bo}\right)^{\frac{1}{2}} \qquad \ldots(4.4)$$

and
$$\bar{d}_b' = d_{bo} + \frac{k}{11.13m} l^s \sqrt{d_{bo}} + \left(\frac{k}{22.26}\right)^2 \frac{l^{2s}}{m(m-1)} \qquad \ldots(4.5)$$

The Gamma function is defined as :

$$\Gamma(m+1) = \int_0^{\infty} p^m \exp(-p)\, dp \qquad \ldots(4.6)$$

and the incomplete Gamma function is defined as :

$$\gamma(m+1,a) = \Gamma(m+1)\left[1 - \exp(-a)\left(\sum_{i=0}^{m} \frac{a^i}{i!}\right)\right] \qquad \ldots(4.7)$$

The expression for the cumulative distribution of the bubble diameter was given as :

$$F(d_{br}) = \frac{\Gamma(m+1) - \gamma(m+1,b)}{\Gamma(m+1) - \gamma(m+1,a)} \qquad \ldots(4.8)$$

where $$b = \left[\frac{\Gamma(m+1)}{\Gamma(m-1)}\right]^{\frac{1}{2}} \frac{x}{\sqrt{d_{br}} - \sqrt{d_{bo}}} \quad \ldots(4.9)$$

The equation for the average bubble diameter was given as :

$$\overline{d}_{br} = x^2 \frac{\Gamma(m+1)}{\Gamma(m-1)} \frac{\Gamma(m-1) - \gamma(m-1, a)}{\Gamma(m+1) - \gamma(m+1, a)}$$

$$+ 2x\sqrt{d_{bo}} \left[\frac{\Gamma(m+1)}{\Gamma(m-1)}\right]^{\frac{1}{2}} \frac{\Gamma(m) - \gamma(m, a)}{\Gamma(m+1) - \gamma(m+1, a)} + d_{bo} \quad \ldots(4.10)$$

From the expression proposed by Miwa et. al. (1972) and fundamental considerations an equation was derived for predicting the diameter of a bubble formed at a porous plate distributor:

$$d_{bo} = 0.00376 \left[u_o - (1 + 2\varepsilon_b) u_{mf}\right]^2 \quad \ldots(4.11)$$

where $$\varepsilon_b = \frac{u_o - u_{mf}}{u_o - u_{mf} + 22.26\sqrt{d_{bo}} + 2u_{mf}} \quad \ldots(4.12)$$

Following the derivation presented by Agarwal (1985), the equation for the probability density function of the bubble rise velocity was obtained as :

$$f(u_{br}) = \frac{m^{m+1} (\overline{u}' - u_{bo})^{m+1} \exp\left[-\frac{m(\overline{u}' - u_{bo})}{(u_{br} - u_{bo})}\right]}{(u_{br} - u_{bo})^{m+2} \left[\Gamma(m+1) - \gamma(m+1, a')\right]} \quad \ldots(4.13)$$

where $$a' = \frac{m(\overline{u}' - u_{bo})}{u_{b\max} - u_{bo}} \quad \ldots(4.14)$$

$$u_{b\max} = u_o - u_{mf} + 22.26\sqrt{d_{b\max}} \qquad \ldots(4.15)$$

$$d_{b\max} = D_t(1 - r/R) \qquad \ldots(4.16)$$

$$\overline{u}' = \overline{u} + u_{bo} \qquad \ldots(4.17)$$

$$\overline{u} = \frac{k}{m} l^s \qquad \ldots(4.18)$$

and

$$u_{bo} = u_o - u_{mf} + 22.26\sqrt{d_{bo}} \qquad \ldots(4.19)$$

The cumulative distribution of the bubble rise velocity was derived as :

$$F(u_{br}) = \frac{\Gamma(m+1) - \gamma(m+1, b')}{\Gamma(m+1) - \gamma(m+1, a')} \qquad \ldots(4.20)$$

where

$$b' = \left[\frac{m(\overline{u}' - u_{bo})}{u_{br} - u_{bo}}\right] \qquad \ldots(4.21)$$

4.1.2 Bubble Characteristic Model Parameters

The model presented by Agarwal (1986) contains three adjustable parameters k, m and s, which have no fundamental significance. These parameters were varied in order to understand the effect the adjustment of each had on the predicted bubble characteristic distributions. After observing the modifications in the predicted bubble characteristic distributions, it was considered that, in the first instance, the criteria for the choice of k, m and s should be to match the position of the peak in the experimental data. Values of k, m and s were chosen for the comparison of the model with the experimental data. Time constraints did not permit detailed statistical fitting. Figures 4.1 to 4.6 show the effect of varying each parameter in turn. The distributions drawn with a solid line represent those predictions made using the values of k, m and s chosen for use in the comparison.

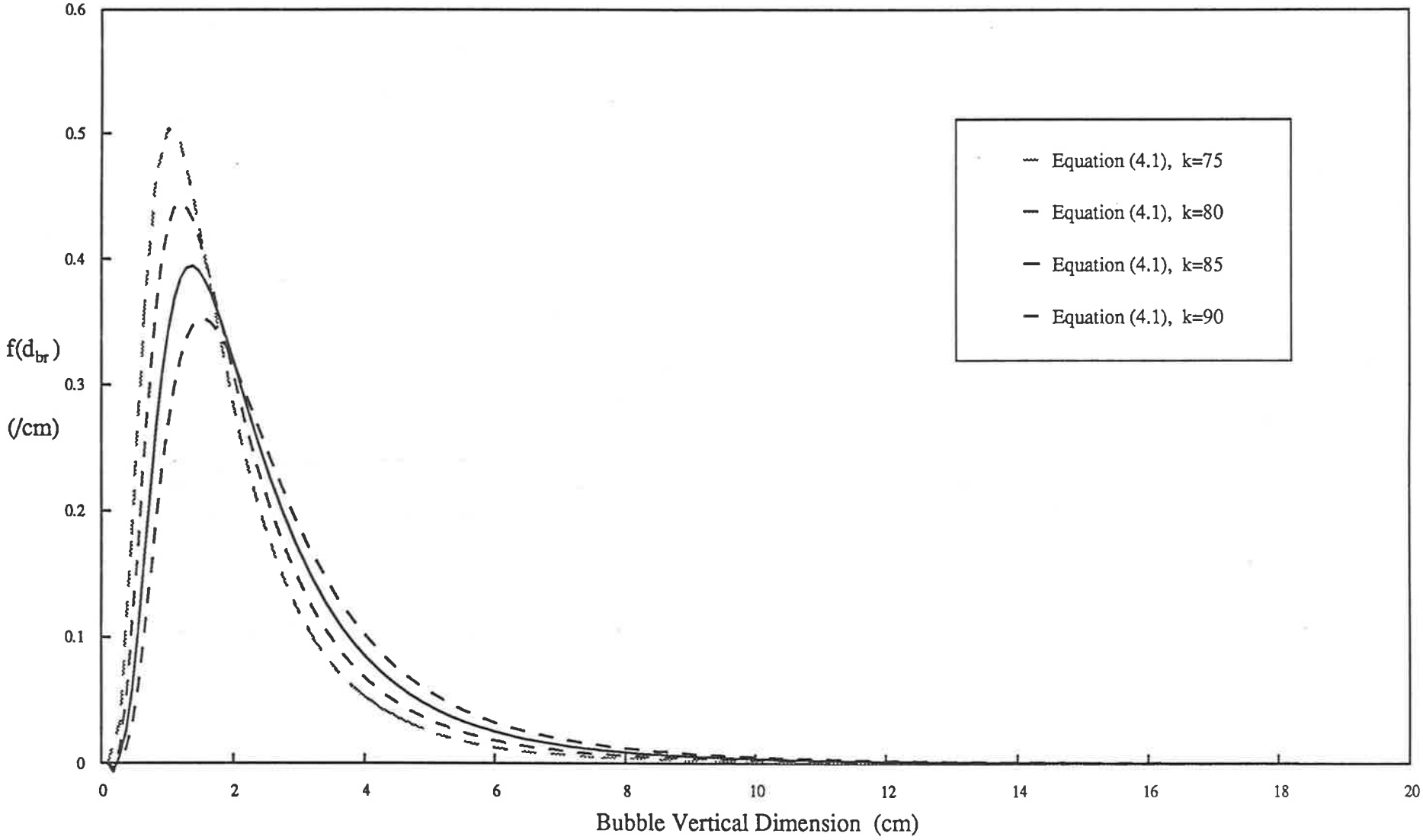

Figure 4.1 Effect of Varying k on $f(d_{br})$

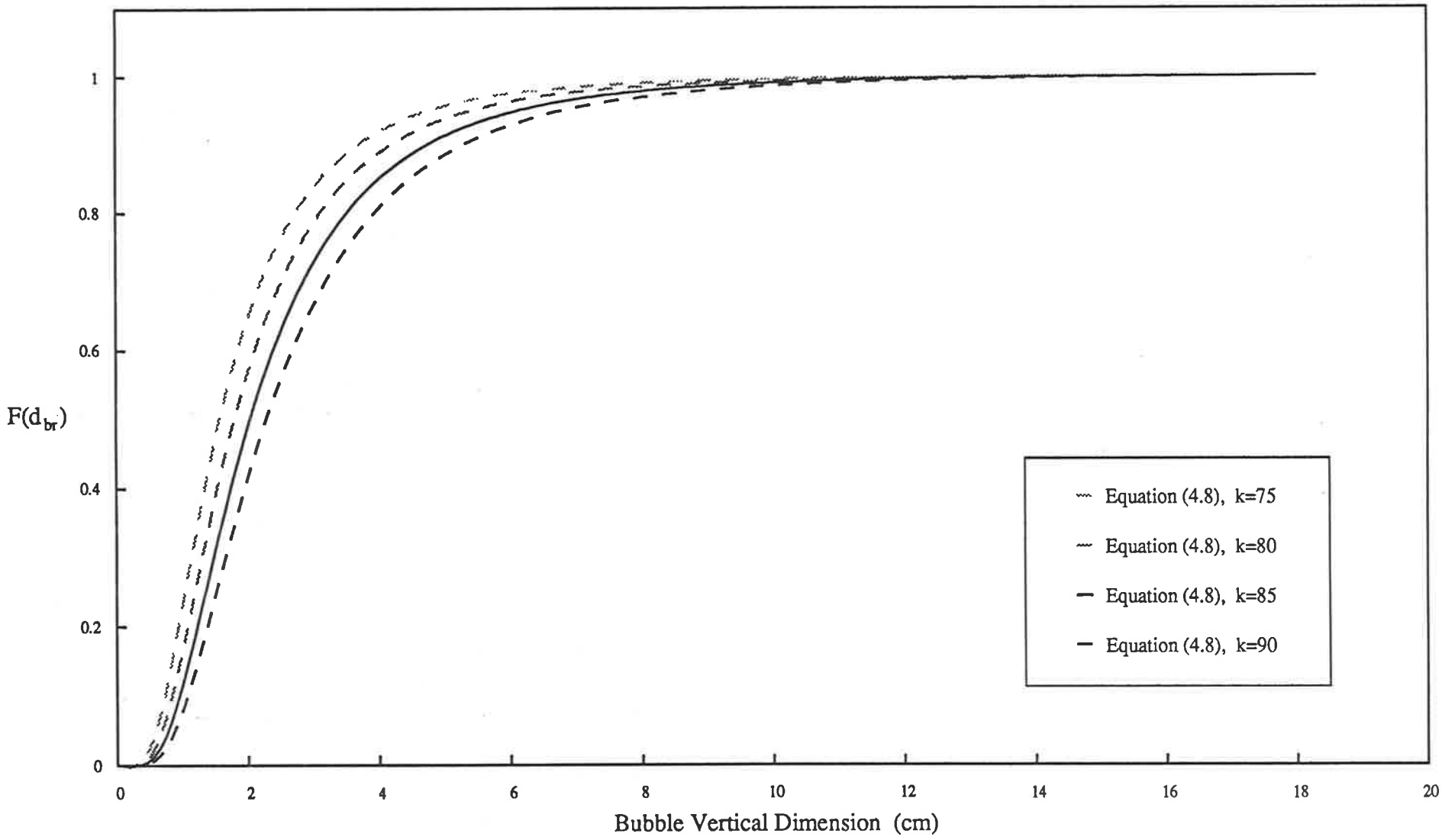

Figure 4.2 Effect of Varying k on $F(d_{br})$

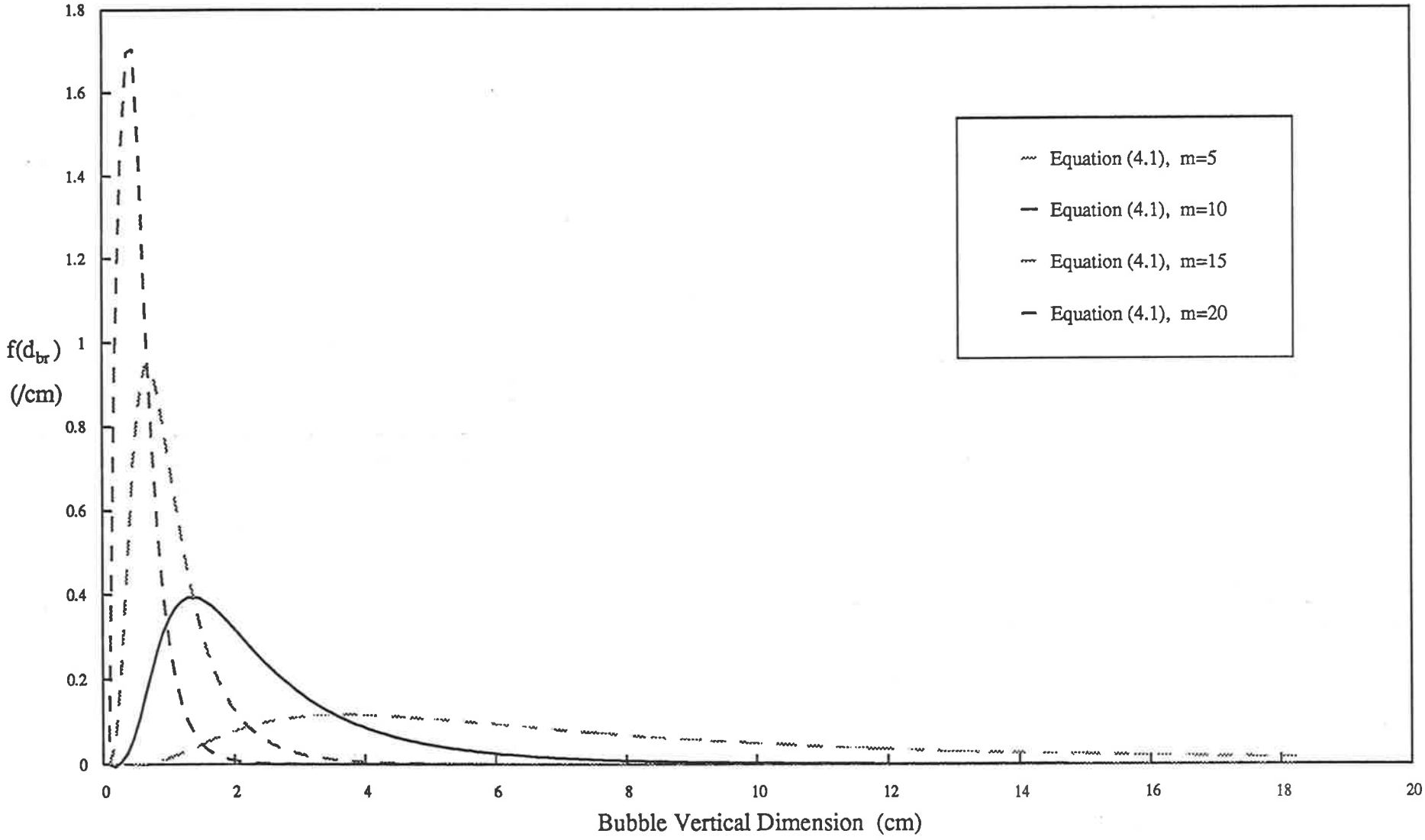

Figure 4.3 Effect of Varying m on $f(d_{br})$

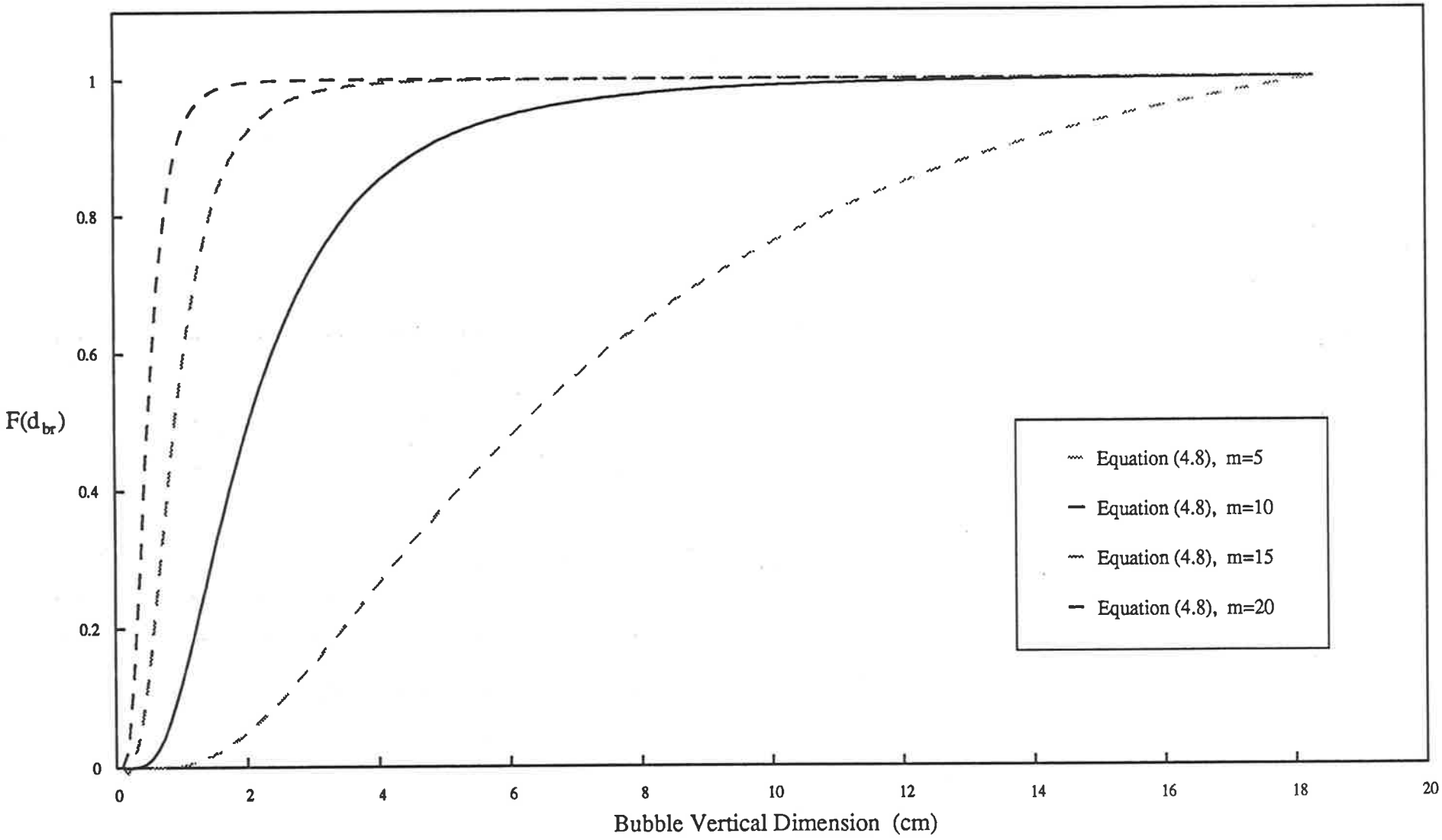

Figure 4.4 Effect of Varying m on $F(d_{br})$

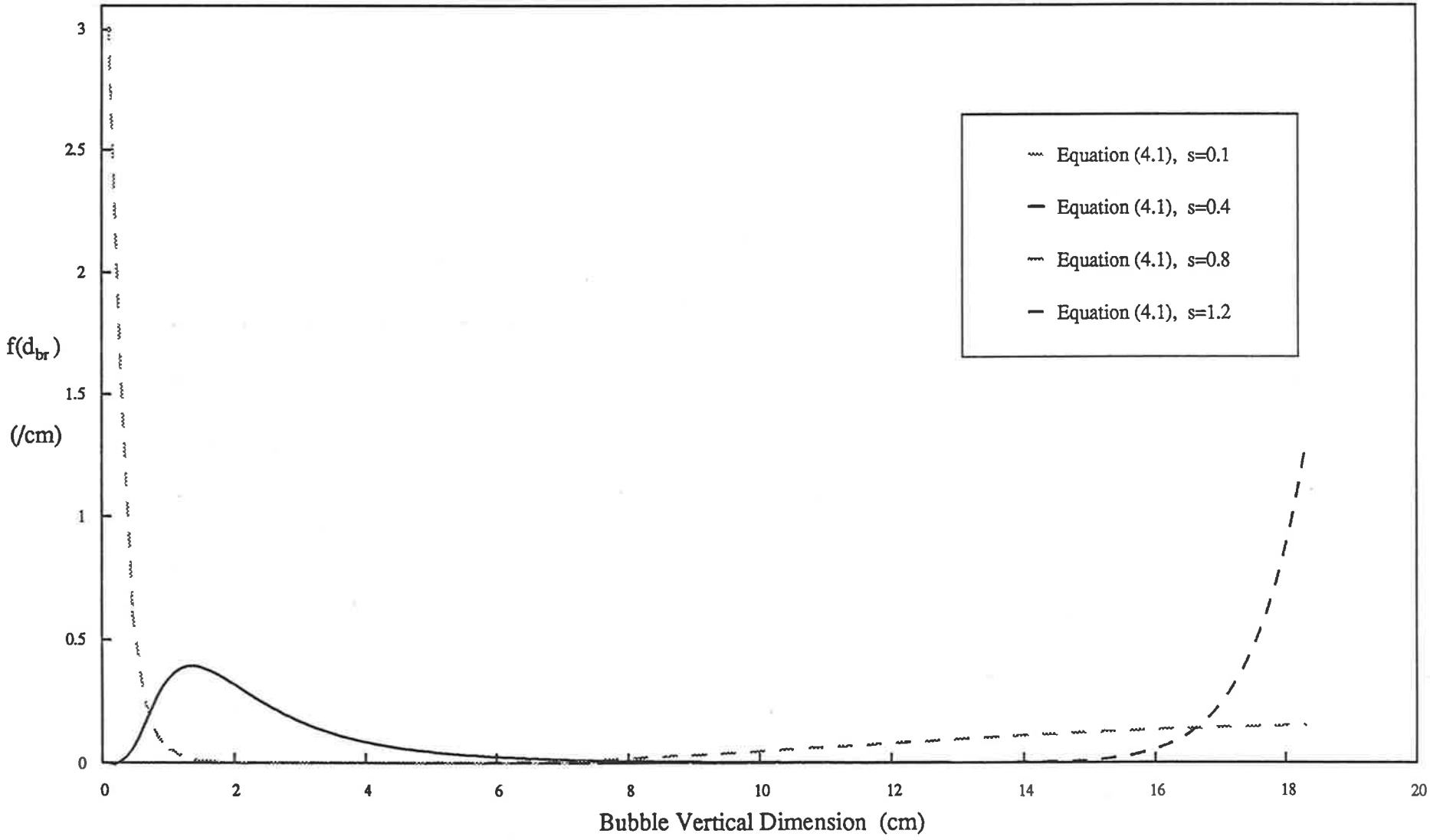

Figure 4.5 Effect of Varying s on $f(d_{br})$

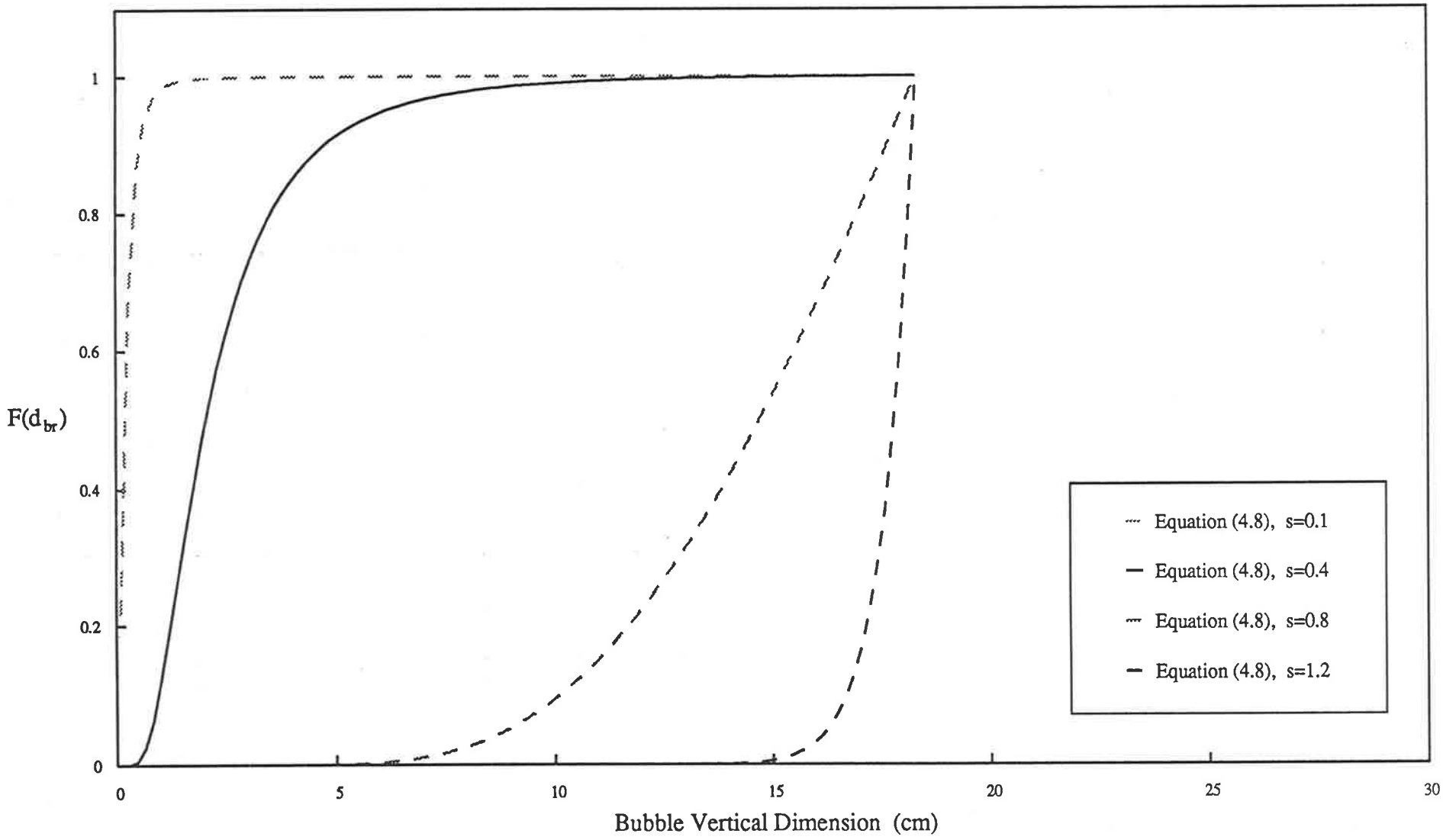

Figure 4.6 Effect of Varying s on $F(d_{br})$

4.2 Processing the Experimental Data

4.2.1 Local Bubble Rise Velocity and Pierced Length

As previously explained, the data collection software separates the raw probe output into bubble phase and emulsion phase porosity variations. The rise time (t_r) and pierced time (t_b) of the bubbles present in the modified data are stored on hard disk. This information must be recovered and converted into a form which is suitable for further processing into the rise velocity and pierced length of the bubbles. Once recovered and converted into ASCII format the bubble rise times and pierced times appear as in Table 4.1.

Table 4.1 Bubble Analysis as stored by Data Collection Program

Channel	Bubble	Column 1	Column 2	Column 3	Column 4	Column 5	Column 6
1	1	1119	1220	1180	1075	101	5
	2	3132	3194	3166	3092	62	15
	3	3345	3418	3377	3272	73	86
2	1	1075	1196	1175	1119	121	-5
	2	3092	3164	3151	3132	72	-15
	3	3272	3350	3291	3345	78	-86

The data was stored chronologically as a position in the modified data record, according to the rate of data collection. For example, Table 4.1 shows three bubble events, recorded by each channel sequentially to the hard disk. Column 1 contains those positions identified as the start of a bubble. Column 2 records the end of the bubble, Column 3 the minimum point in the bubble peak.

Column 4 records the start of the bubble in the other channel. The bubble start position indicated in Column 1 of Channel 1, i.e. the bordered position, matches with the bordered position in Column 4 of Channel 2, thus these two records refer to the same bubble as recorded by each channel. Column 5 contains the bubble pierced time, which is the difference between the end and start positions of the bubble (Column 2 -Column 1). Column 6 contains the bubble rise time, which is the difference between the minimum points of the identical bubble as recorded by both channels, in Column 3.

Software was developed (coded in TURBO PASCAL) to read the recorded information from the hard disk and convert it into the required bubble characteristics (See Appendix B). The program calculated the individual bubble rise velocity and pierced length as well as mean ensemble bubble characteristics, such as the average bubble rise velocity, average pierced length, the bubble frequency and volume fraction.

The bubble pierced time was recorded by both channels from each probe tip, as can be seen in Table 4.1 Column 5. Thus, two measurements were available for conversion to the bubble pierced length. Ideally the pierced times were identical, however, some inconsistency in the pierced times recorded by each channel occurred due to the horizontal and vertical separation of the probe tips. Lateral movement of the bubble, bubble splitting and coalescence all had a marked effect. The conversion program was designed to calculate the mean value of pierced time for each individual bubble from the two recorded pierced times. The mean pierced times approached the ideal more closely, as can be seen in Figure 4.7, where the average pierced times for one hundred bubbles are presented.

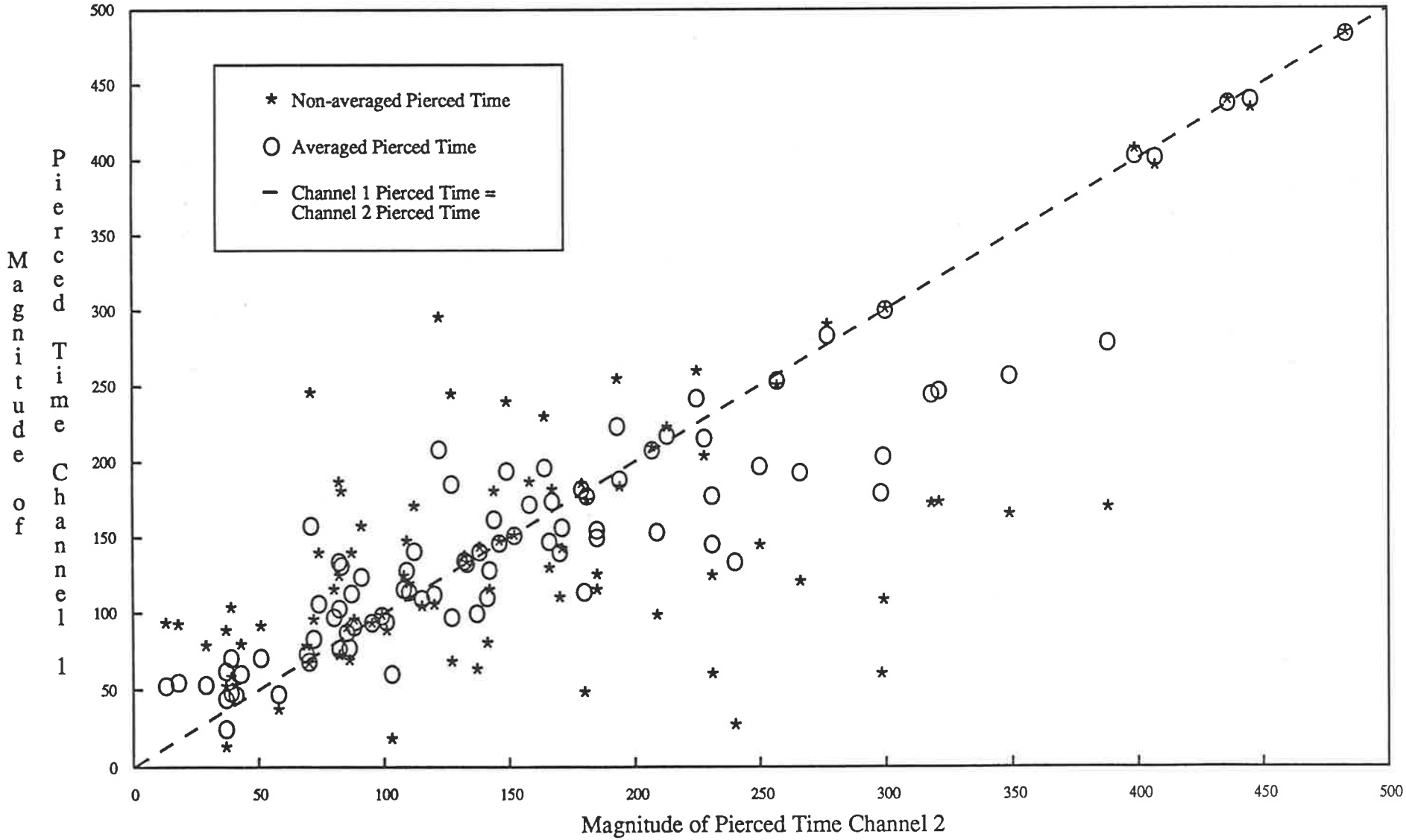

Figure 4.7 Averaged and Non-Averaged Bubble Pierced Times

4.2.2 Local Bubble Size Distribution

The ideal bubble sketched in Figure 3.4 is seldom encountered in a real fluidized bed. Over a period of time bubbles of quite different sizes and shapes will pass through a given horizontal control surface containing the probe as one of its points. Information about the size distribution of such an array of bubbles will provide a valuable insight into the bed hydrodynamics.

Werther (1974a) presented a method of deducing the local bubble size distribution by means of geometric probability theory, from the number density distribution of bubble pierced lengths. A comparison was made with particle size analysis. In the first instance, the array of particles are classified according to a dispersion characteristic, in sieve analysis, for example, the mesh width. Subsequently, by means of an appropriate model, it is possible to deduce a distribution of geometric equivalent dimensions. The distribution of geometric equivalent dimensions provides a measure of the size distribution of the particle array under investigation, as obtained from the measured distribution of the dispersion characteristic.

In the case of bubble size analysis the pierced length is adopted as the dispersion characteristic. A classification of the pierced length is the first step in analysing the bubble array. The pierced length is not uniquely related to the bubble size, there exists merely a correspondence between the distribution of pierced lengths and bubble sizes. The real array of bubbles is replaced by a model array consisting of geometrically equivalent elements in order to derive this correspondence. An ellipsoid is employed as the model bubble equivalent shape. It is characterised by a horizontal and vertical dimension (diameter or size), d_h and d_v respectively, as displayed in Figure 4.8.

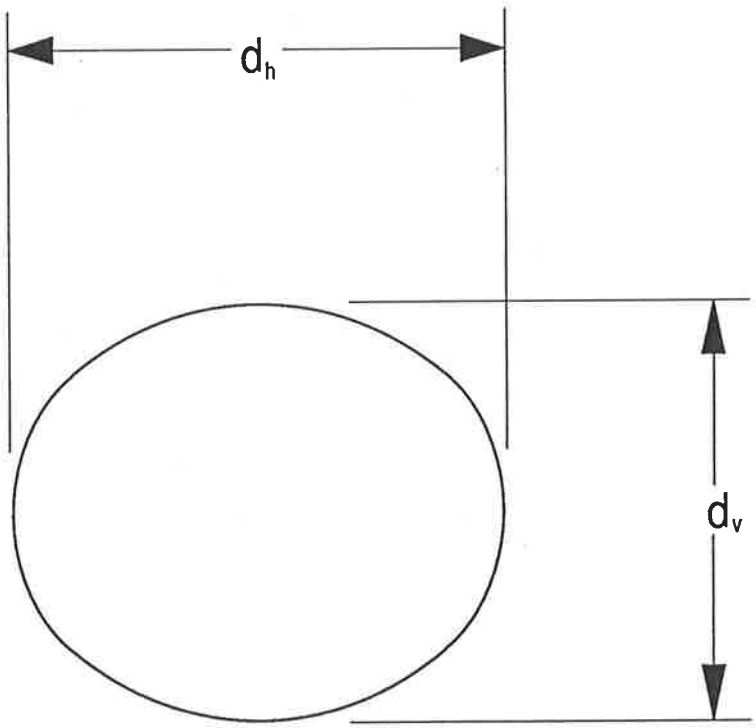

Figure 4.8 Characteristic Bubble Dimensions

An expression for the evaluation of the cumulative bubble size distribution from the number density distribution of pierced lengths was proposed by Werther :

$$F(d_v) = 1 - \left[\frac{g(l_p)}{g(d_{v\,min})}\right]\left[\frac{d_{v\,min}}{l_p}\right] \qquad \ldots(4.22)$$

where

$$d_{v\,min} \le l_p \le d_{v\,max}$$

The conversion program written included a subroutine for calculating the number density distribution of the bubble pierced length and the transformation of this distribution to the cumulative distribution of the equivalent bubble vertical dimension. To convert the cumulative distribution of the bubble vertical dimension, or bubble size, to the probability density function

of the bubble size, was a simple exercise. The difference between the magnitude of successive intervals was divided by the interval size to obtain the probability density function of the bubble vertical dimension.

The number density distribution of the bubble pierced lengths as calculated from the experimental data is a discrete distribution. Therefore some intervals in the pierced length distribution may contain many bubbles, while previous and subsequent intervals may contain very few. This fact was manifested when each of the intervals were transformed into intervals in the cumulative distribution of the bubble size, using Equation (4.22). For an interval containing few bubbles the product $\left[\frac{g(l_p)}{g(d_{v\min})}\right]\cdot\left[\frac{d_{v\min}}{l_p}\right]$ was low, thus $F(d_v) \to 1$. If the next interval contained more bubbles the product was higher and $F(d_v) \to 0$. Thus, the definition in Equation (4.22) produced a "dip" in the cumulative distribution. The difference between the interval with many bubbles and the previous interval containing a few was negative. Hence, the interval took a negative value when presented in the probability density function of the bubble size, the occurrence of this can be seen in various plots of probability density functions of bubble size.

A possible solution was to group the bubble pierced lengths into fewer intervals, of greater magnitude. This had the effect of conglomerating intervals with a few bubbles with those containing many, thus a more continuous distribution was obtained. However, two intervals containing many bubbles may also be grouped together, hence, less information is retained from the original data. While some negative values were present in the probability density functions of the bubble size, an interval of 0.4 cm was found to maximise the retention of original data. The negative values should be regarded as relics of the method of obtaining the bubble size distribution.

4.3 Comparison of Experimental Data with Bubble Hydrodynamic Model

Figures 4.9 to 4.18 provide a comparison of the experimental bubble vertical dimension and that predicted by the model as a function of radial position, height and fluidizing velocity. The model prediction of the probability density function appears more reliable in the upper half of the fluidized bed. Moving down the bed, the position of the peak in the model prediction deviates from the peak in the experimental data. The model under predicts the peak in the experimental data at the top of the bed and over predicts it near the distributor. The prediction of the cumulative distribution of the bubble vertical diameter is reasonably reliable. However, the vertical diameter is under predicted near the top of the bed and over predicted near the bottom, in similar fashion to the probability density functions.

A comparison of the experimental bubble rise velocity with the model predictions (Equations 4.13 and 4.20) is presented in Figures 4.19 to 4.28. In all instances, the experimental bubble rise velocities are evenly distributed between the maximum and minimum possible. The predicted velocities depart significantly from the experimental data.

Figures 4.29 to 4.33 provide sketches of the variation in the local bubble rise velocity with the corresponding local bubble pierced length. The graph includes a well known correlation for the local bubble rise velocity. The expression for the velocity of a bubble rising in a fluidized bed was first proposed by Davidson and Harrison (1963) as :

$$u_{br} = u_o - u_{mf} + u_{b\infty} \qquad \ldots(4.23)$$

where

$$u_{b\infty} = 22.26\sqrt{d_{br}} \qquad \ldots(4.24)$$

In general, the correlation passes through the middle of the experimental data. It must be remembered that the correlated values of the local bubble rise velocities are calculated from the

experimental values of the local bubble pierced lengths and not the local bubble diameters, as the correlation calls for. There is a considerable range of values for the bubble rise velocity. Some scatter is attributable to the displacement of the bubble centre line from the probe axis. The pierced length of a bubble rising quickly off centre from the probe axis, will be misinterpreted. Its pierced length will be underpredicted. The predominant influence causing the measured velocity to differ is the proximity of one bubble to another. As previous workers have shown (Harrison and Leung (1962)), when two bubbles are rising in close vertical proximity, the trailing bubble is affected by the leading bubble and has a substantially higher velocity. Figure 4.34 presents data as collected by Glicksman et. al. (1987). The variation of the experimental data as compared to the correlated single bubble rise velocity for an isolated bubble (Equation (4.24)) can be seen. The error bars represent the departure of the data from the bubble rise velocity calculated from Equation (4.23). The data behaves in much the same way as that presented in this work.

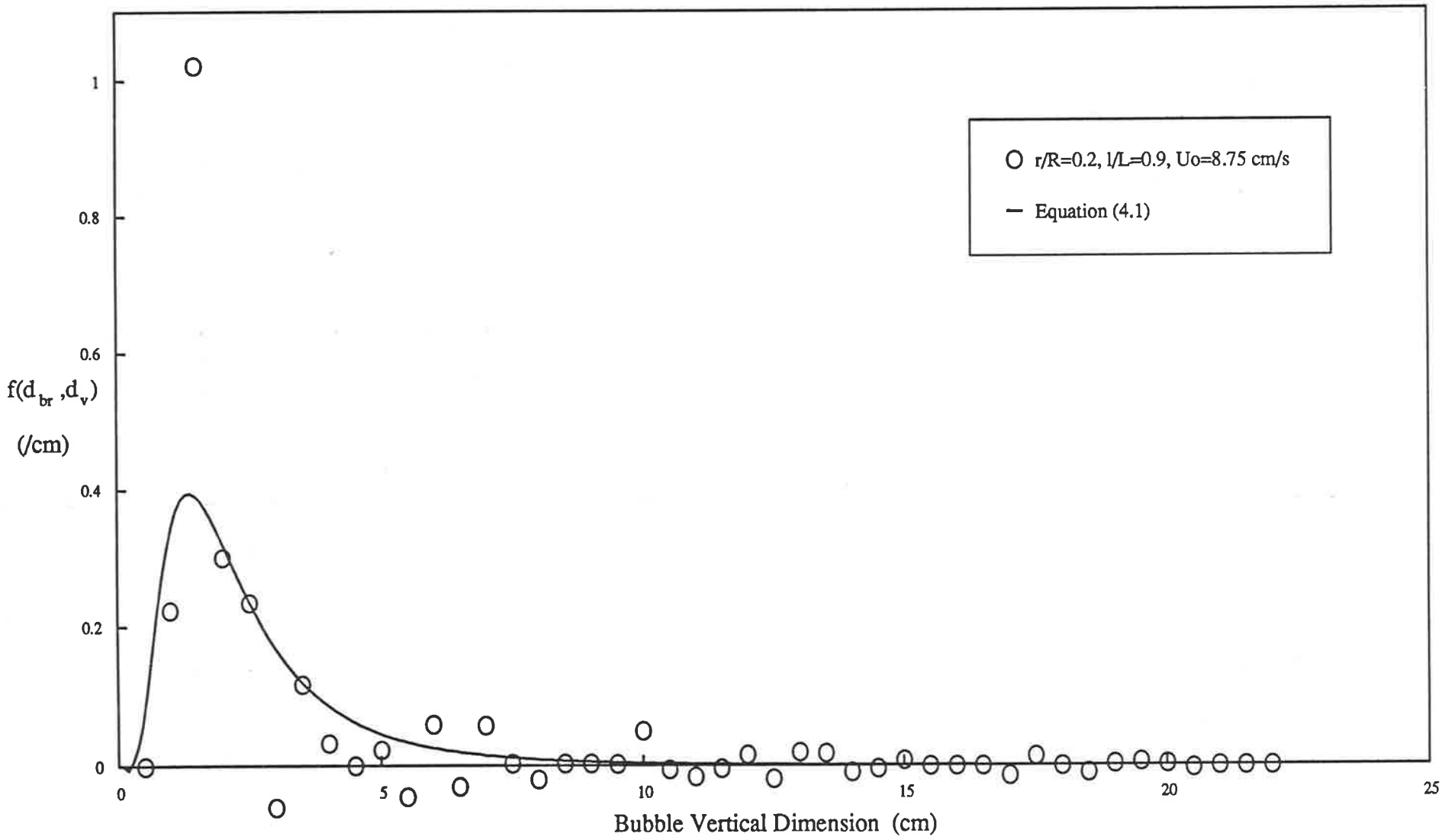

Figure 4.9 Probability Density Function of Bubble Vertical Dimension

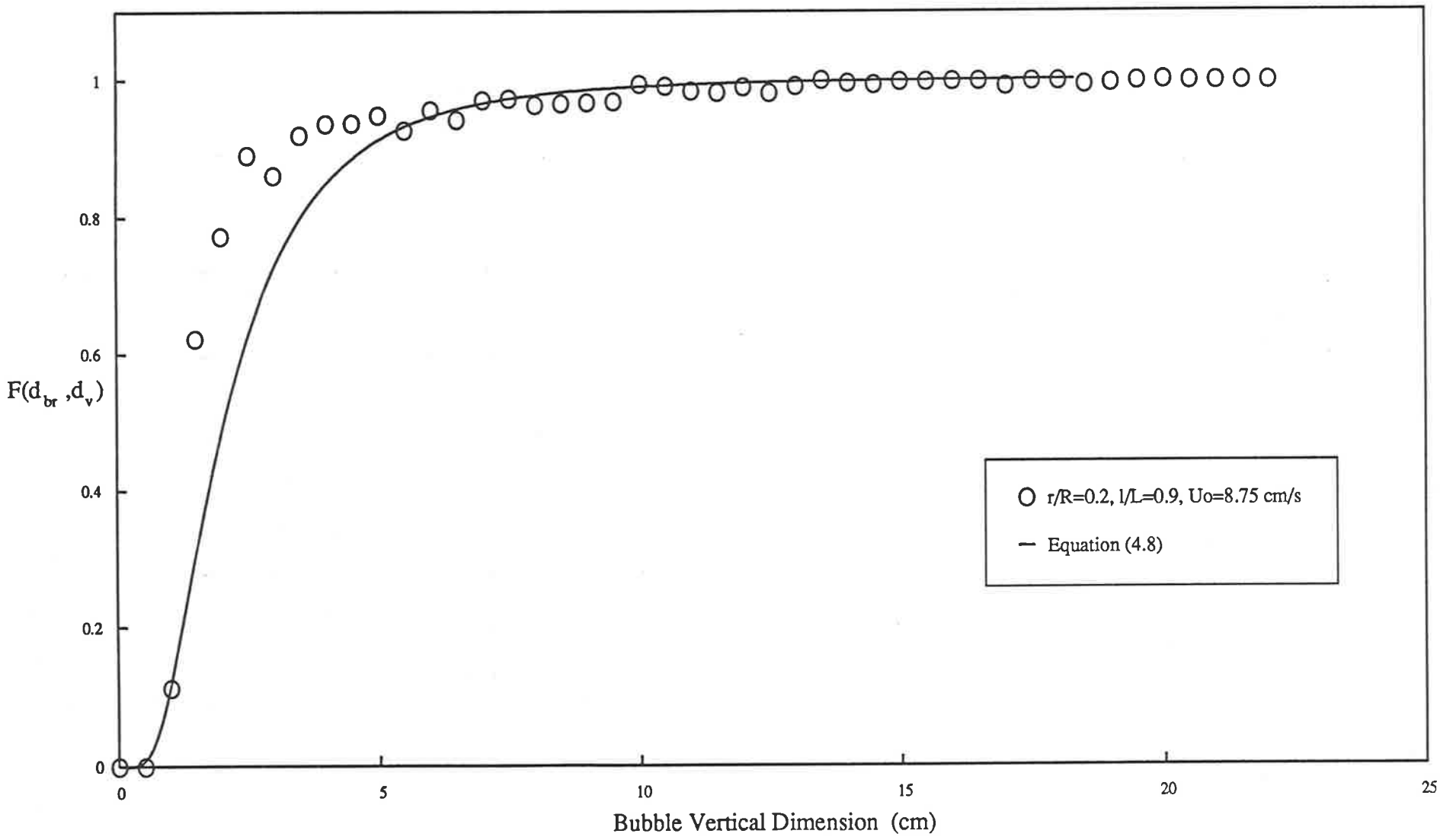

Figure 4.10 Cumulative Distribution of Bubble Vertical Dimension

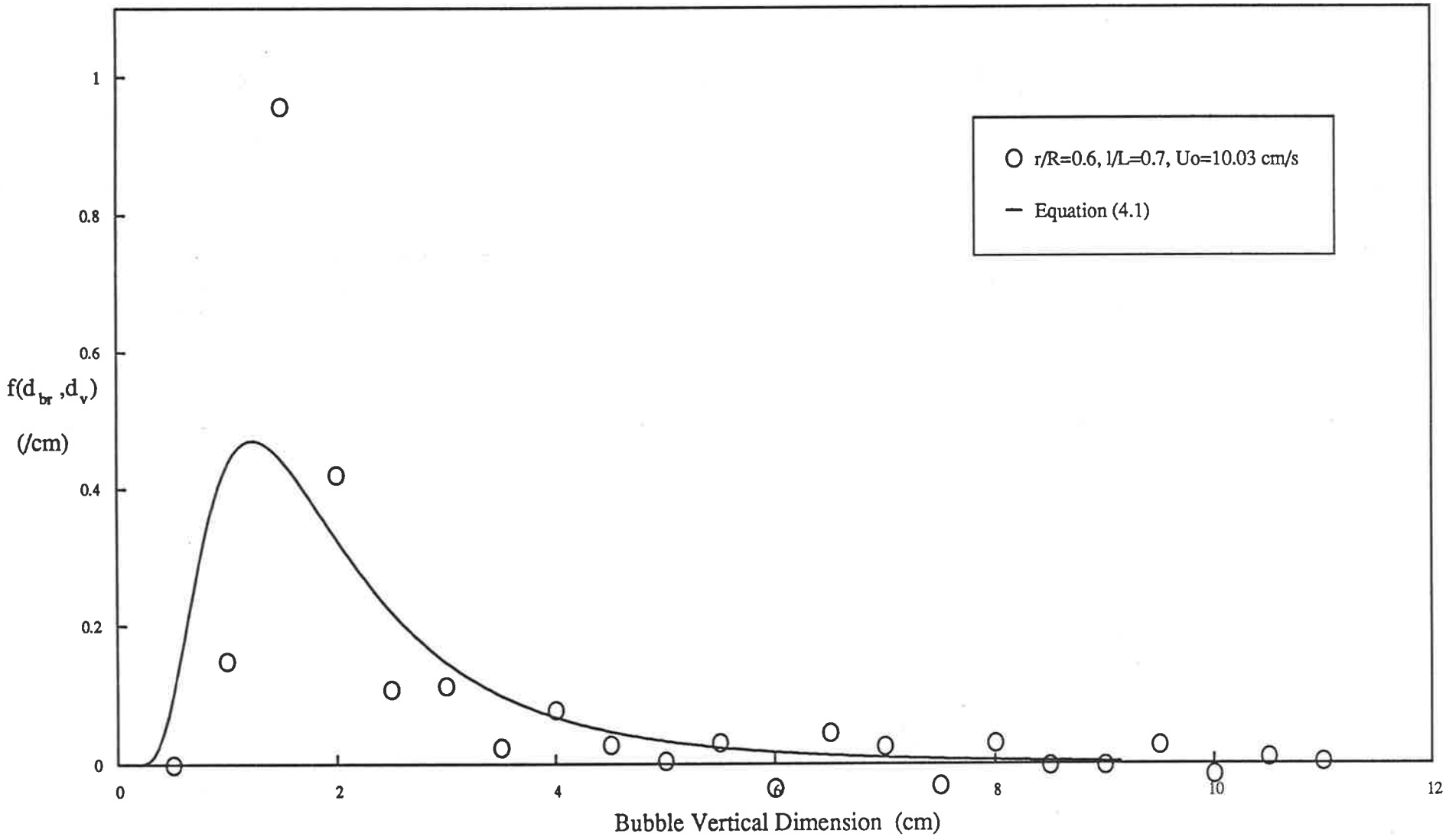

Figure 4.11 Probability Density Function of Bubble Vertical Dimension

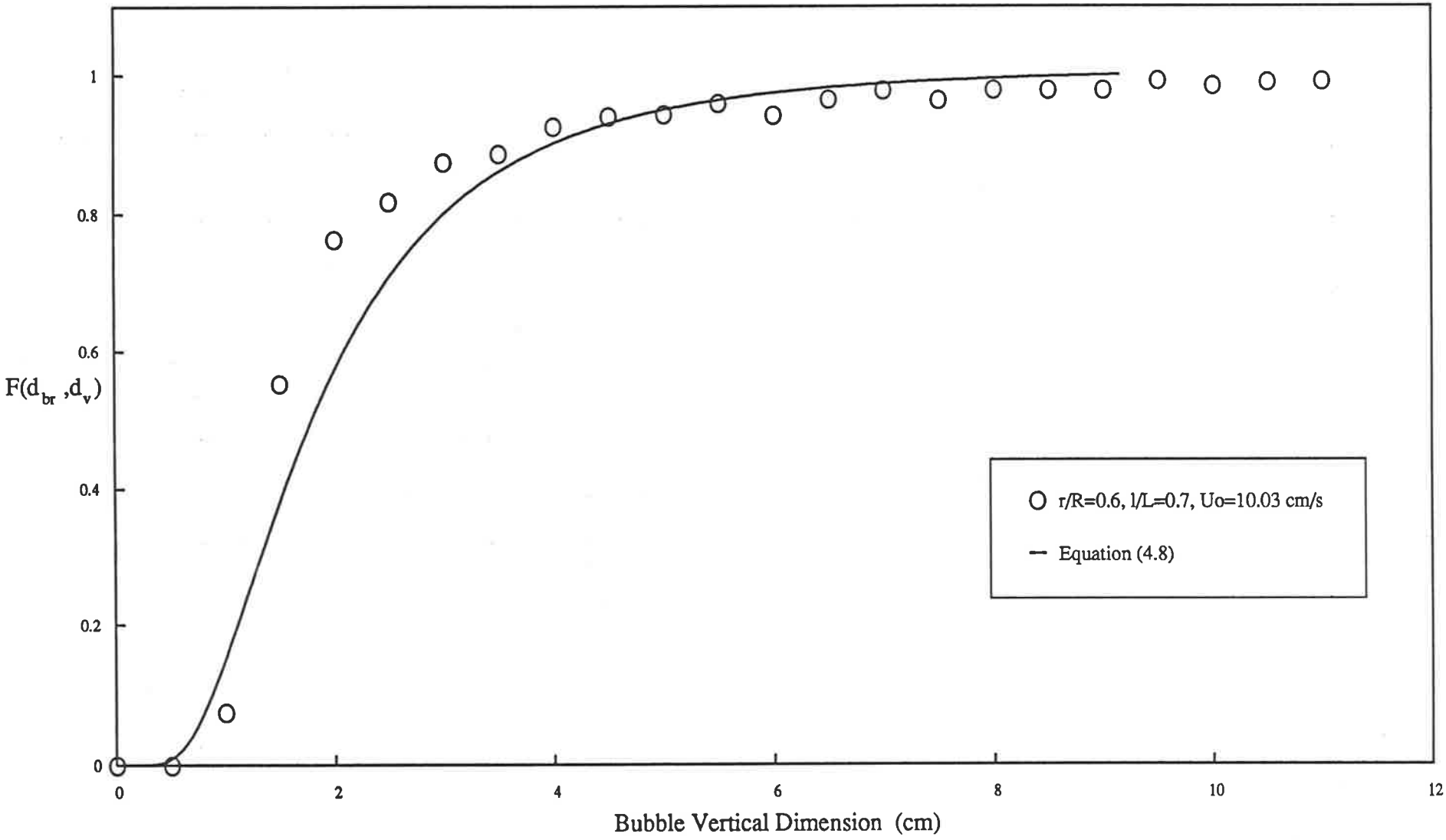

Figure 4.12 Cumulative Distribution of Bubble Vertical Dimension

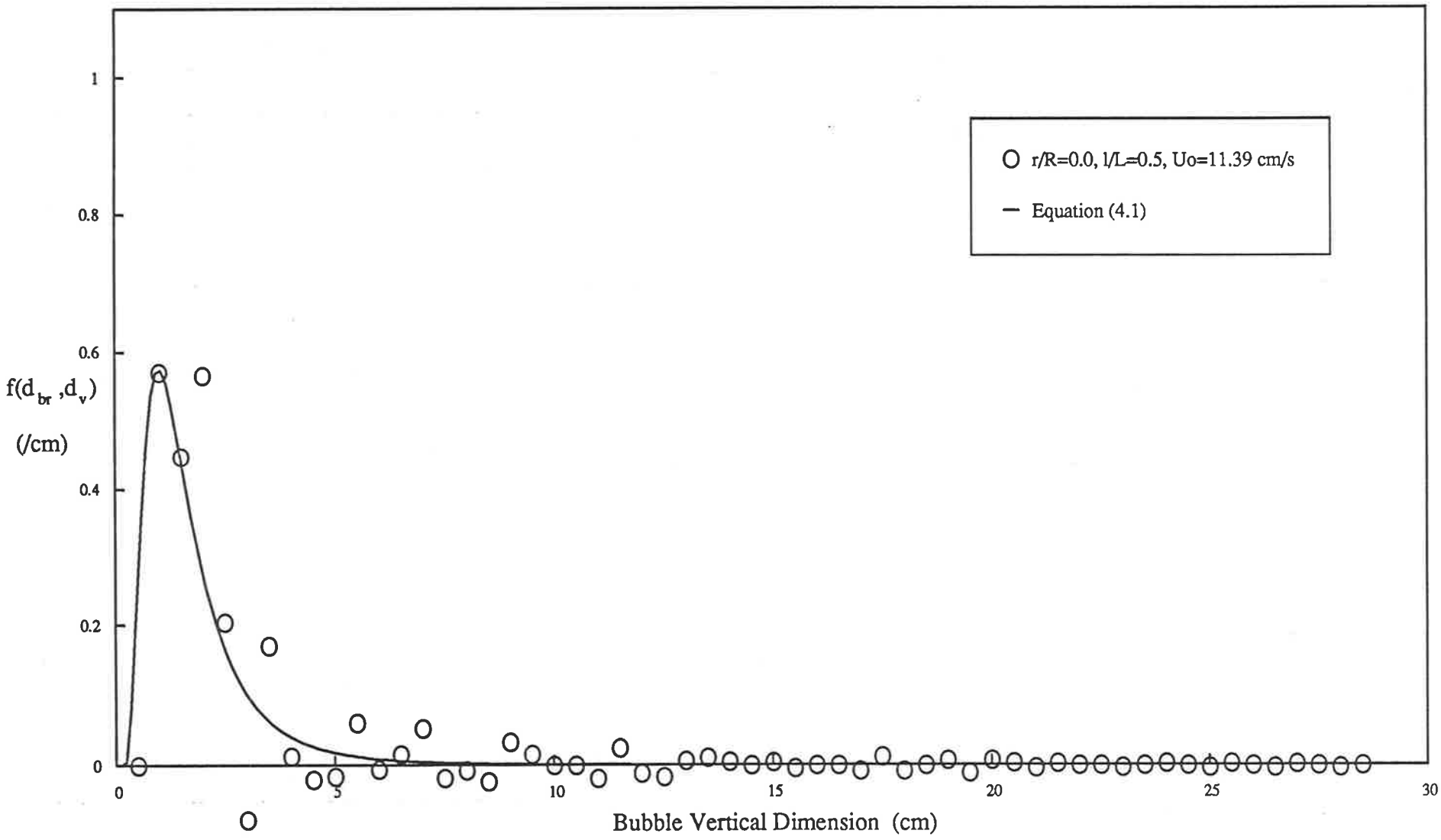

Figure 4.13 Probability Density Function of Bubble Vertical Dimension

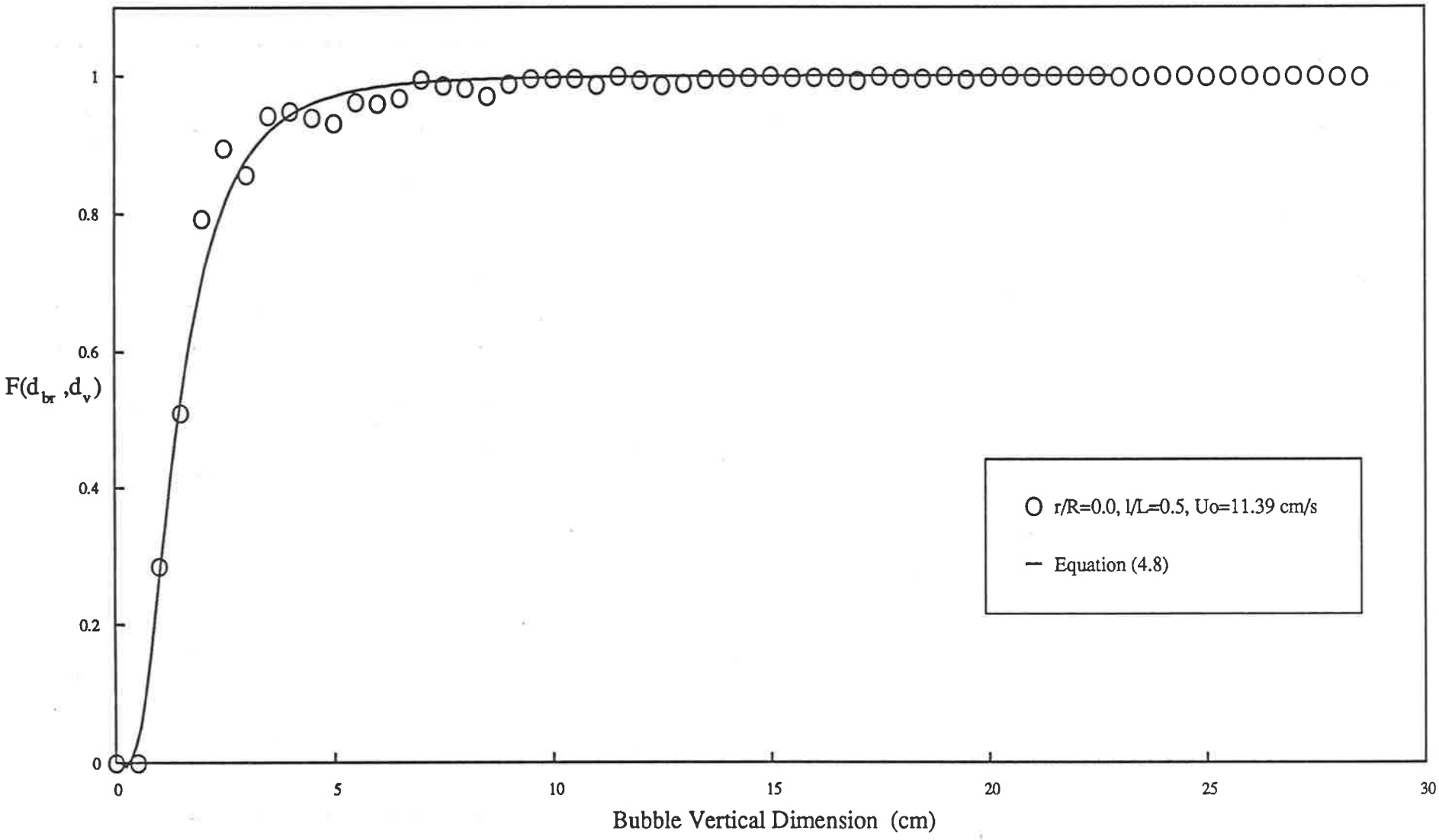

Figure 4.14 Cumulative Distribution of Bubble Vertical Dimension

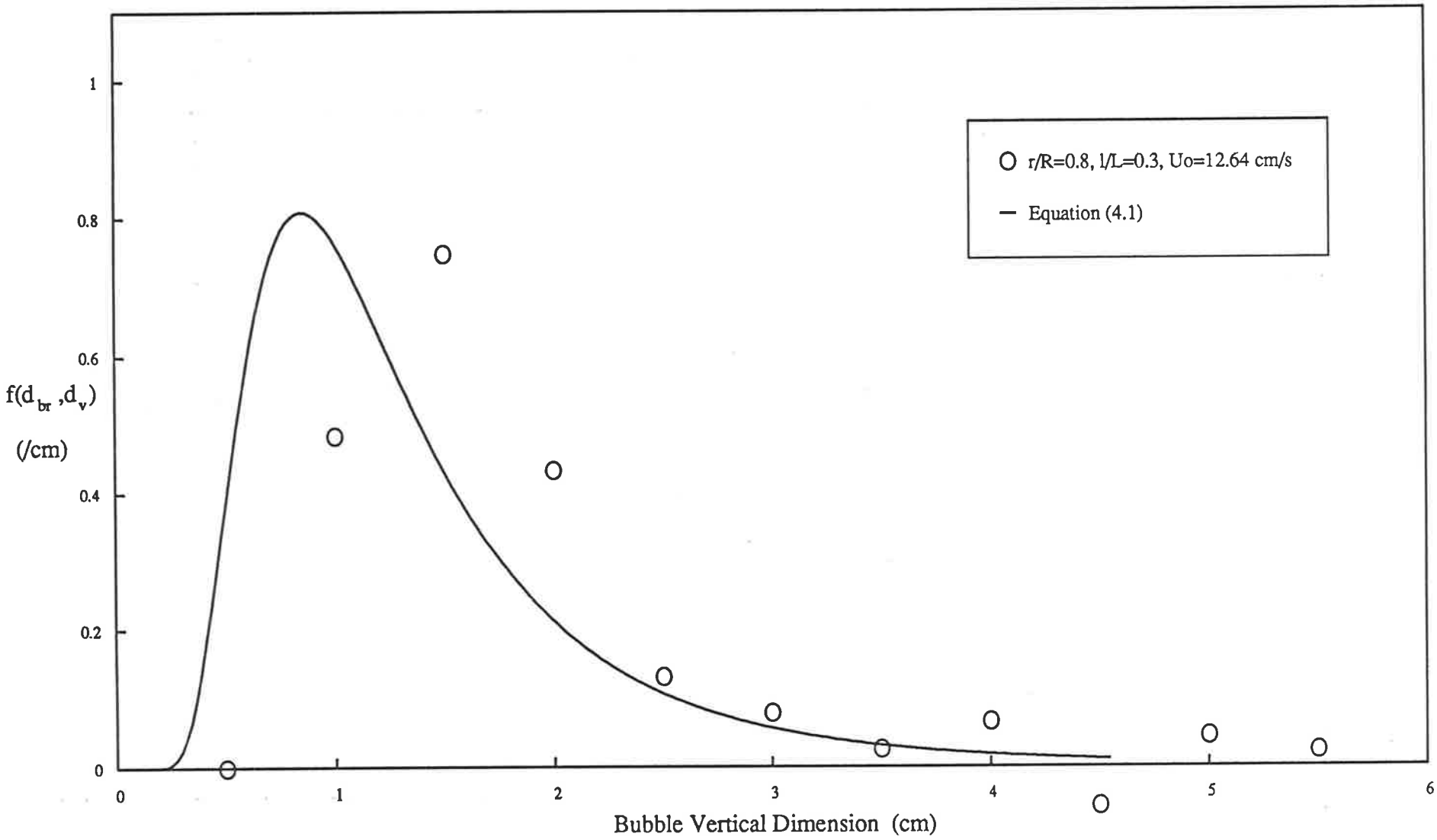

Figure 4.15 Probability Density Function of Bubble Vertical Dimension

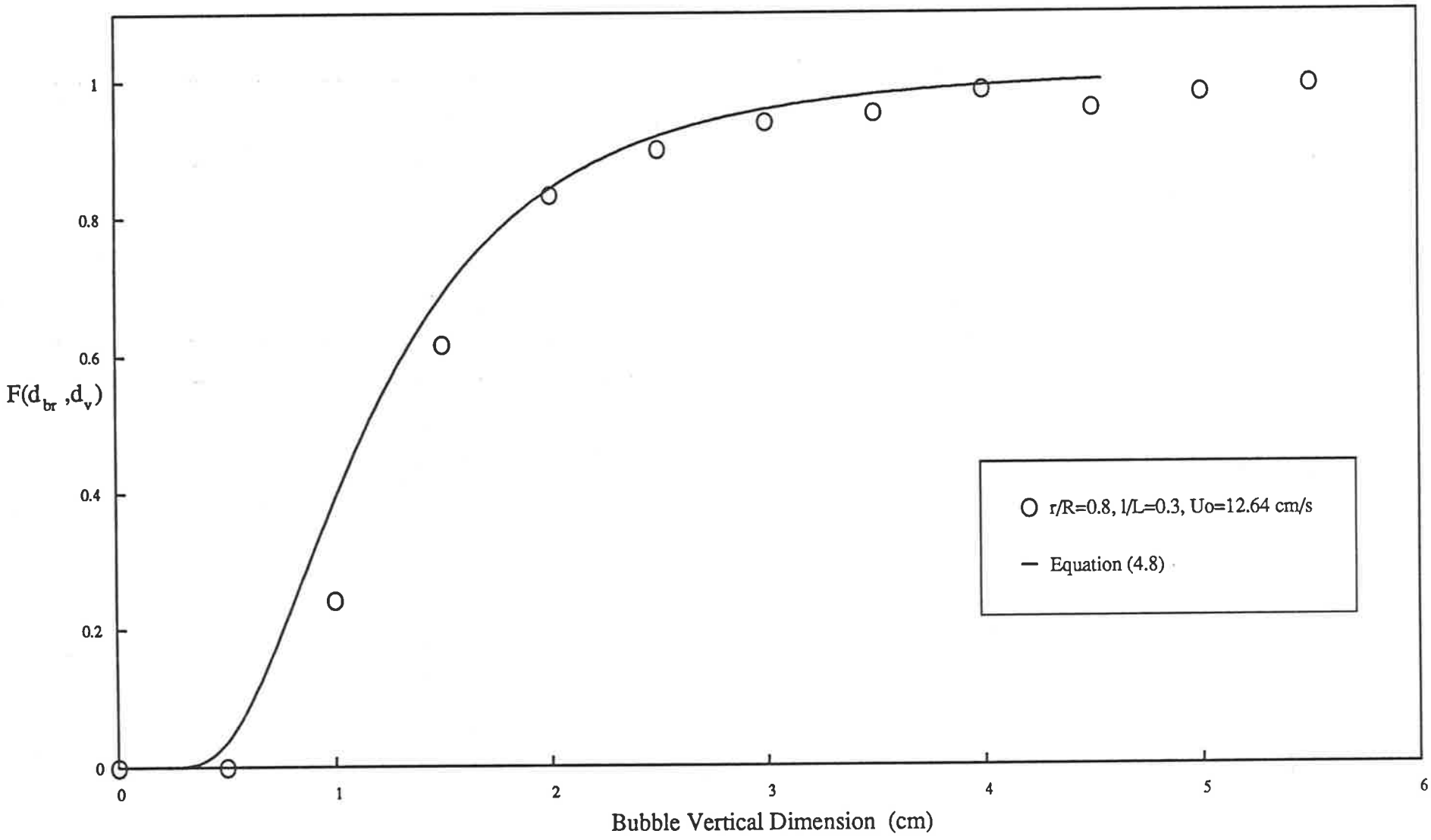

Figure 4.16 Cumulative Distribution of Bubble Vertical Dimension

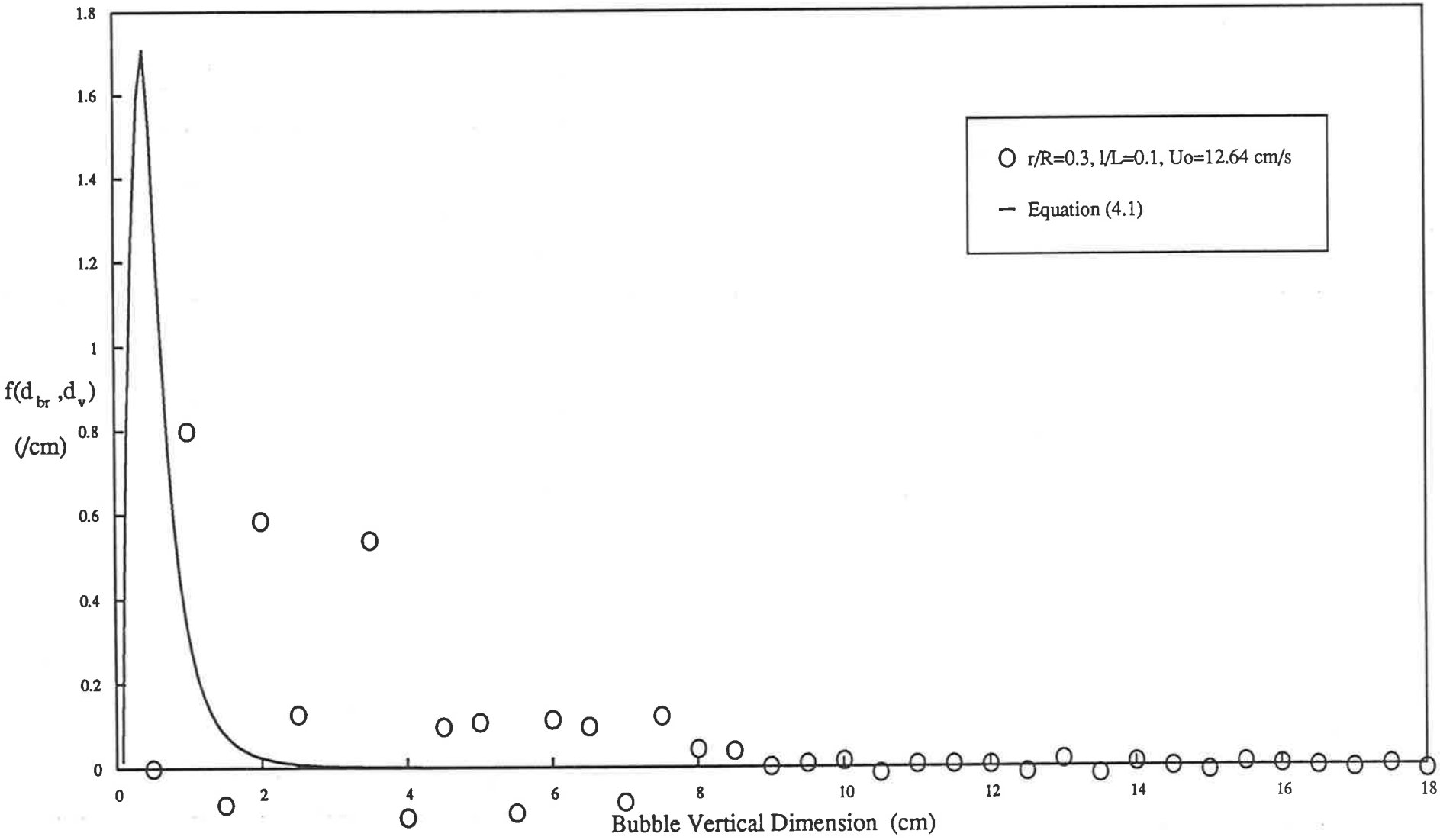

Figure 4.17 Probability Density Function of Bubble Vertical Dimension

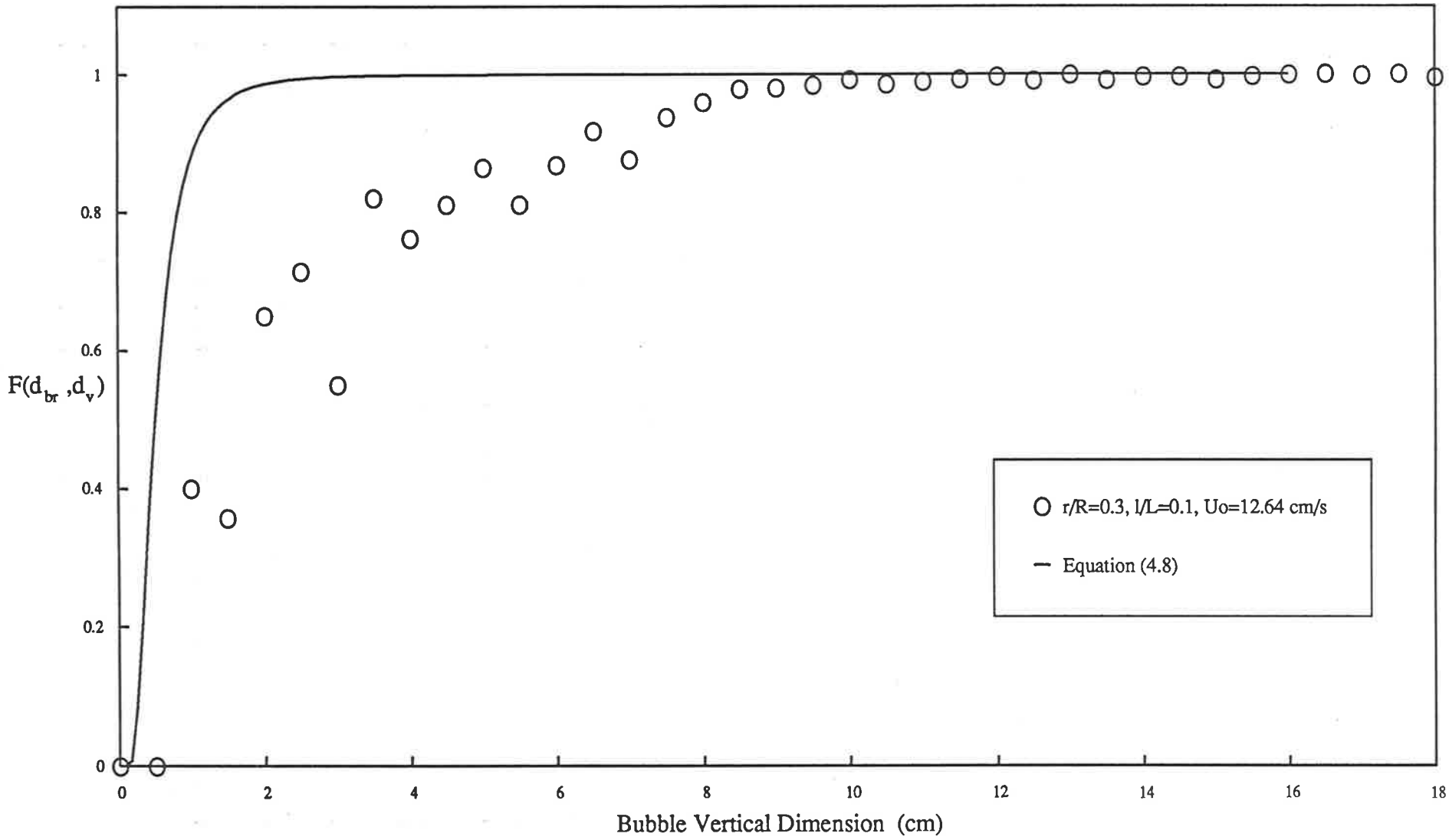

Figure 4.18 Cumulative Distribution of Bubble Vertical Dimension

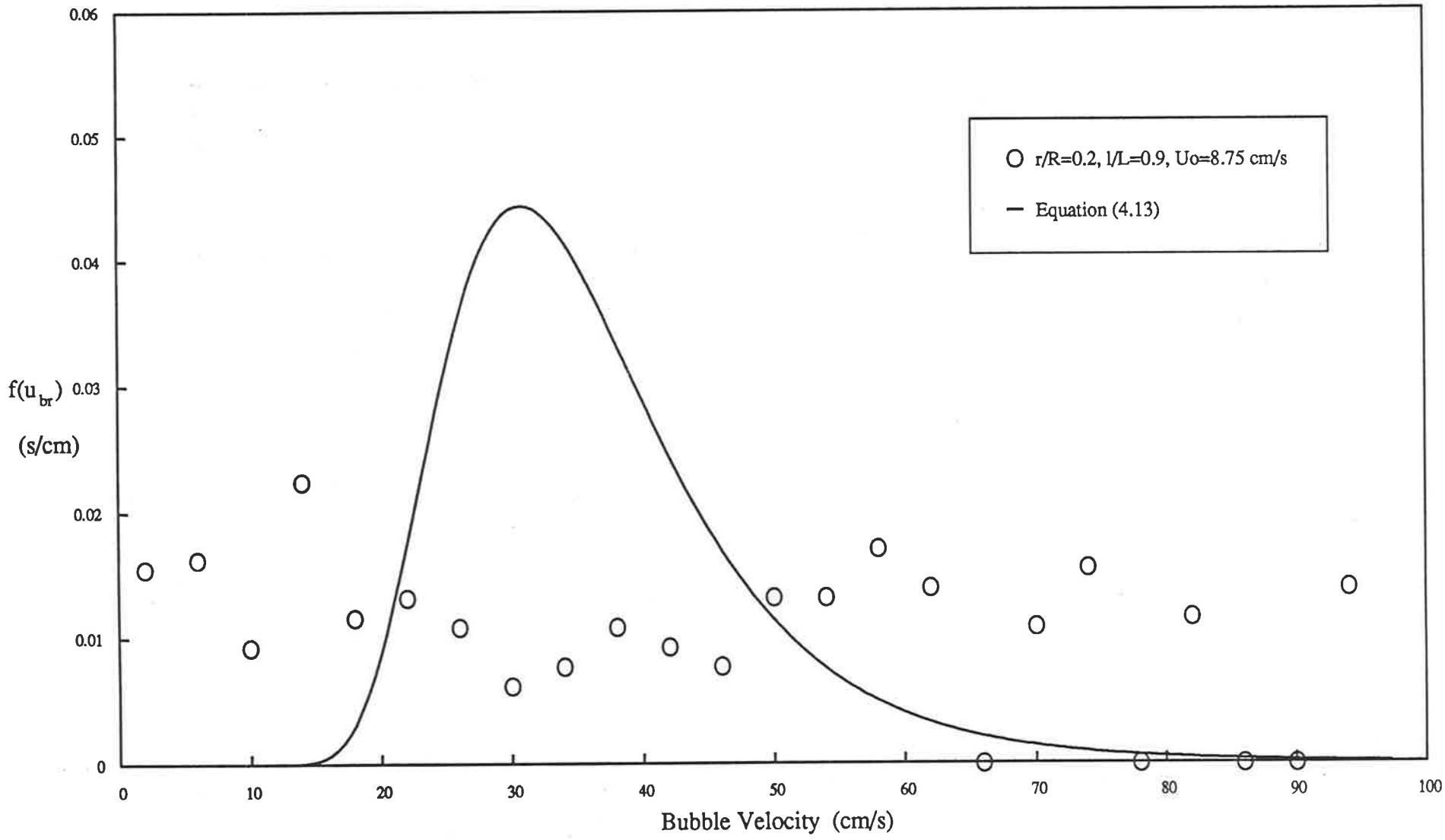

Figure 4.19 Probability Density Function of Bubble Velocity

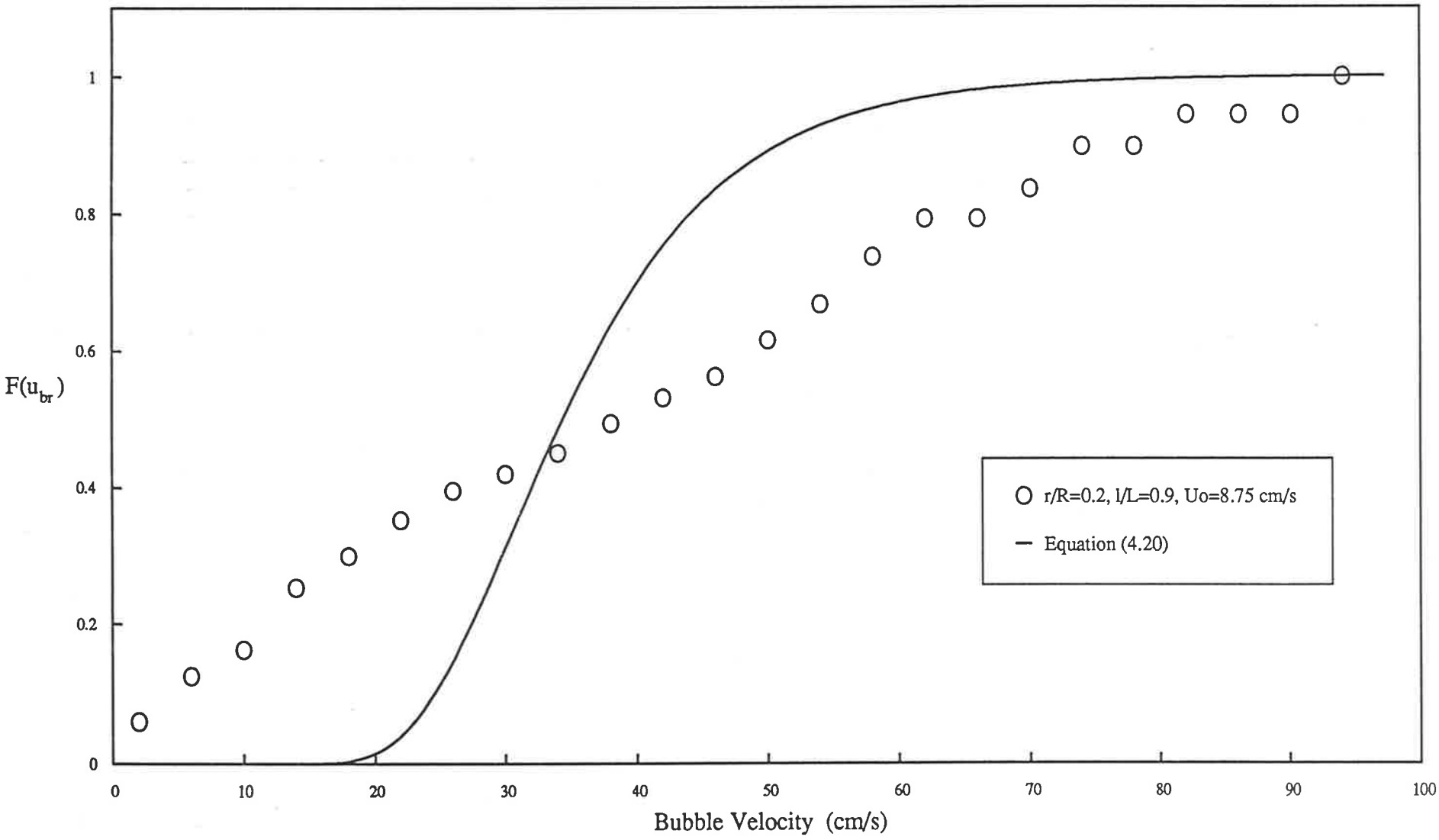

Figure 4.20 Cumulative Distribution of Bubble Velocity

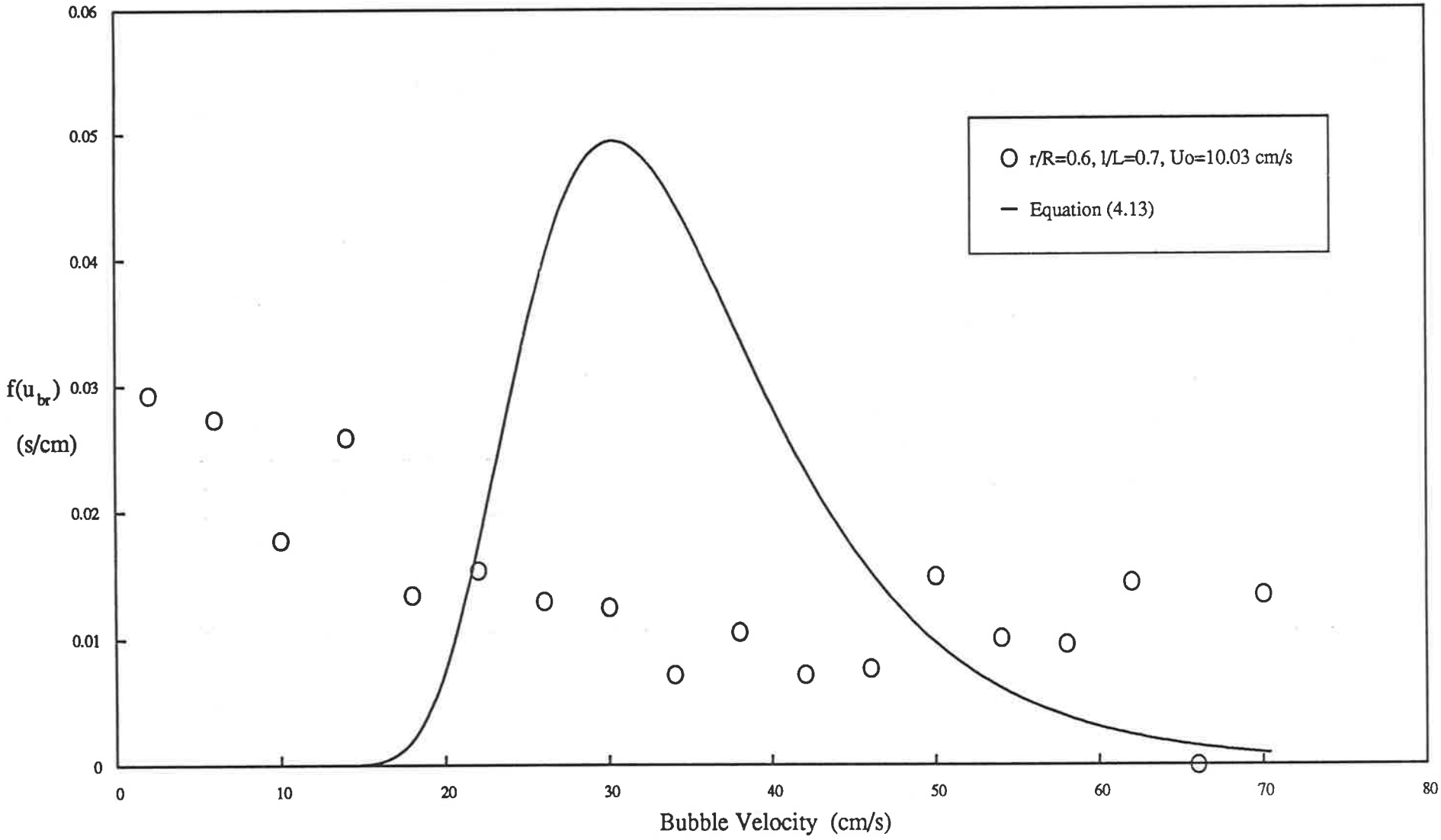

Figure 4.21 Probability Density Function of Bubble Velocity

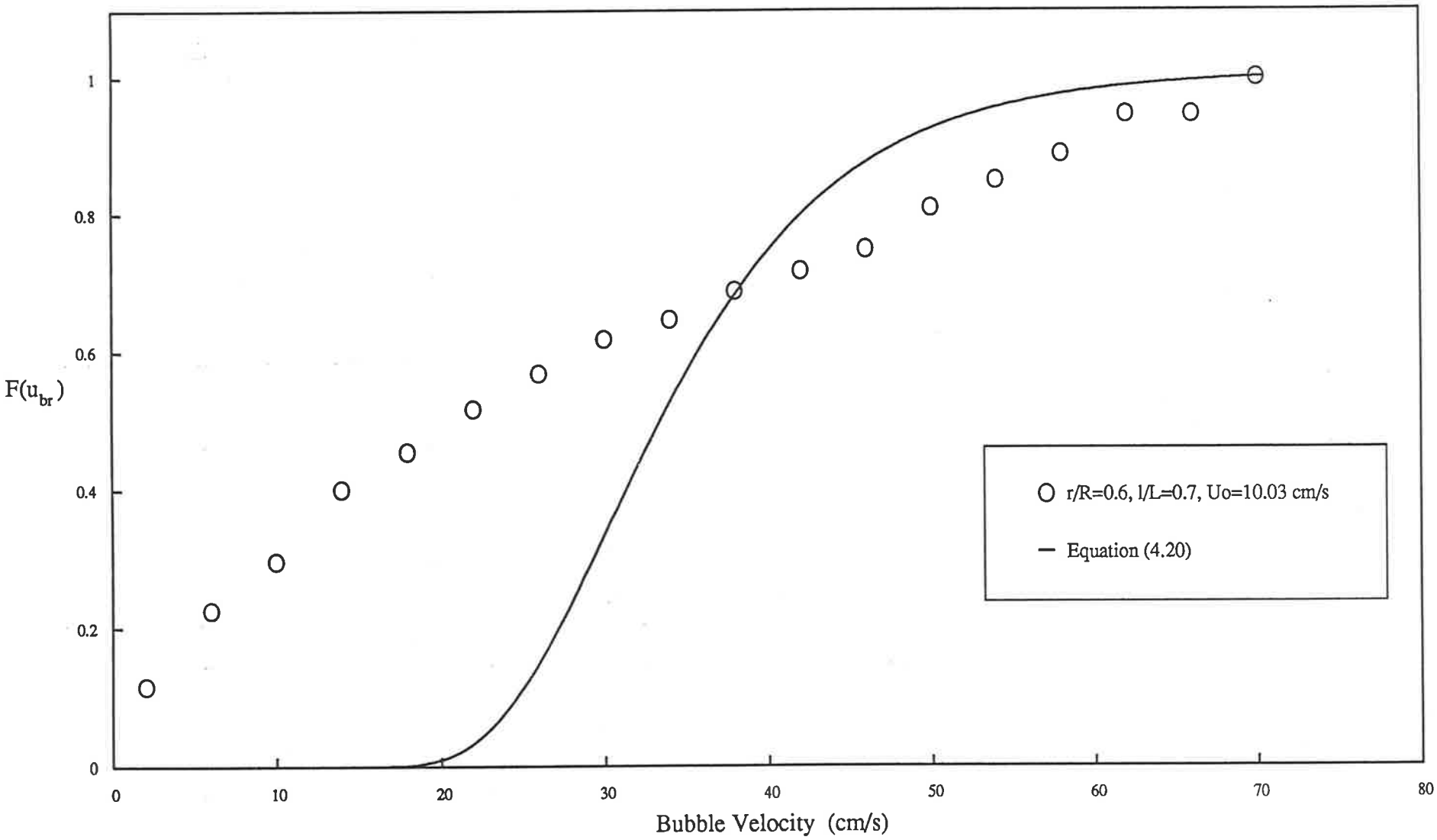

Figure 4.22 Cumulative Distribution of Bubble Velocity

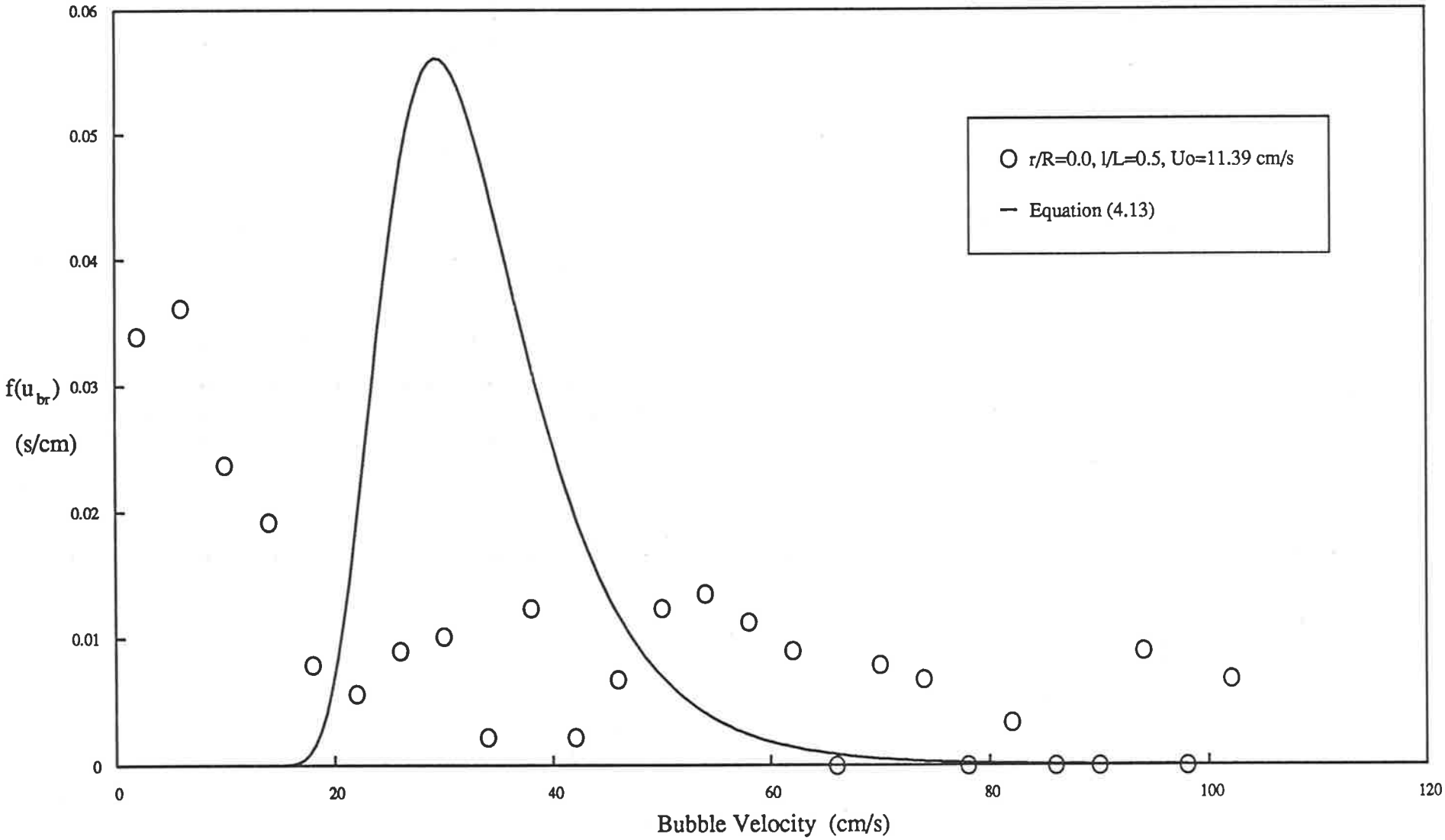

Figure 4.23 Probability Density Function of Bubble Velocity

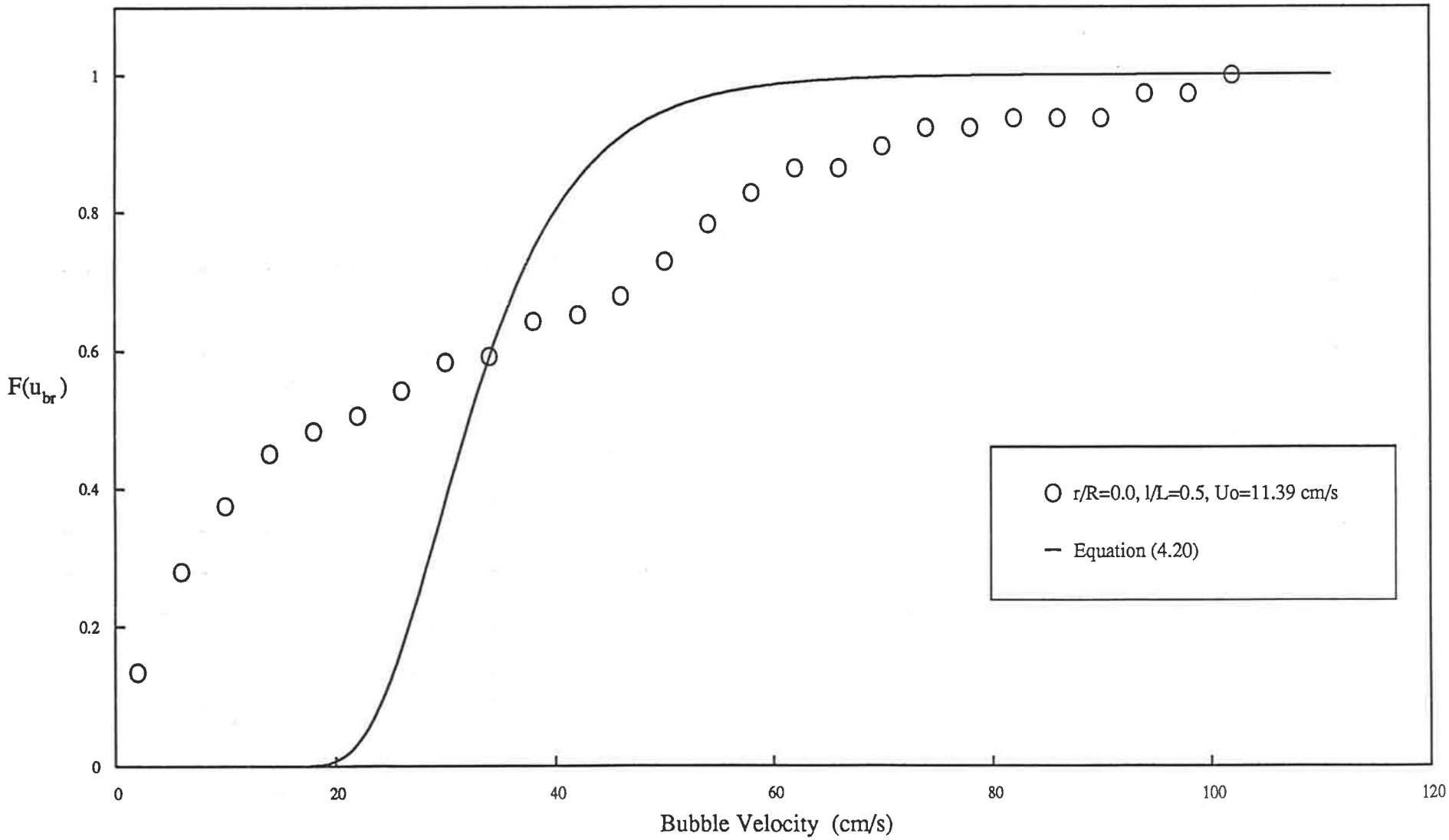

Figure 4.24 Cumulative Distribution of Bubble Velocity

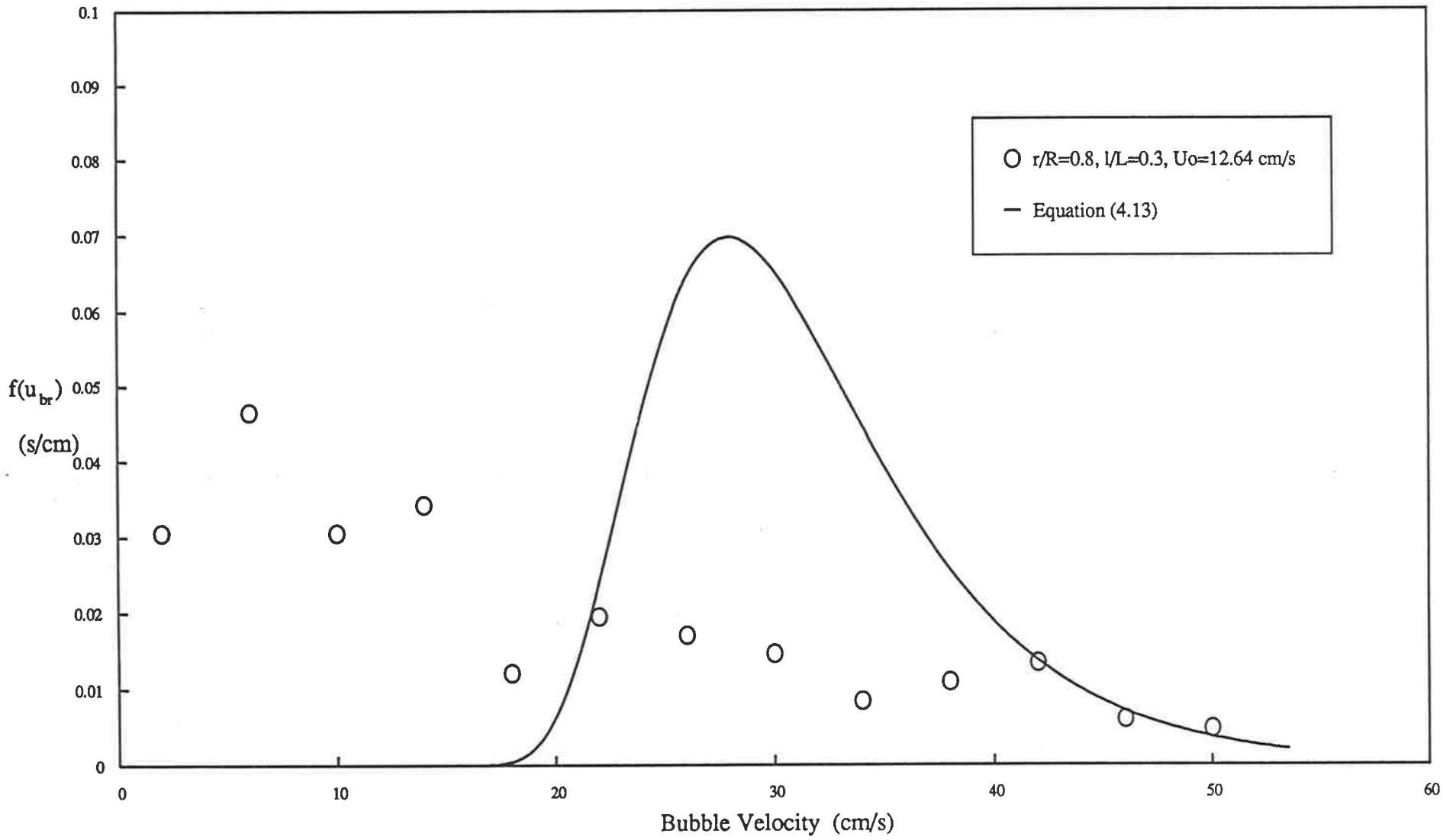

Figure 4.25 Probability Density Function of Bubble Velocity

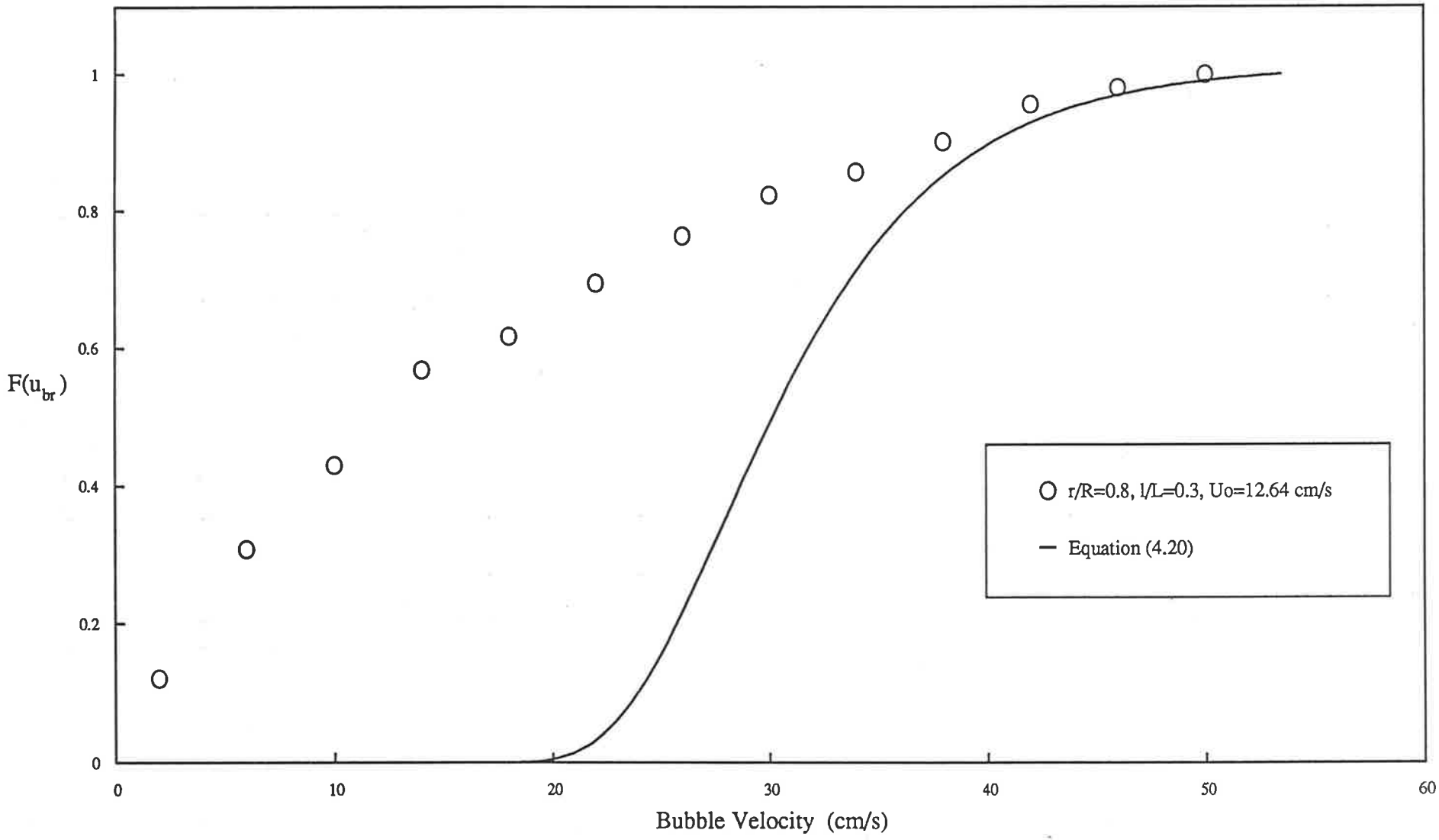

Figure 4.26 Cumulative Distribution of Bubble Velocity

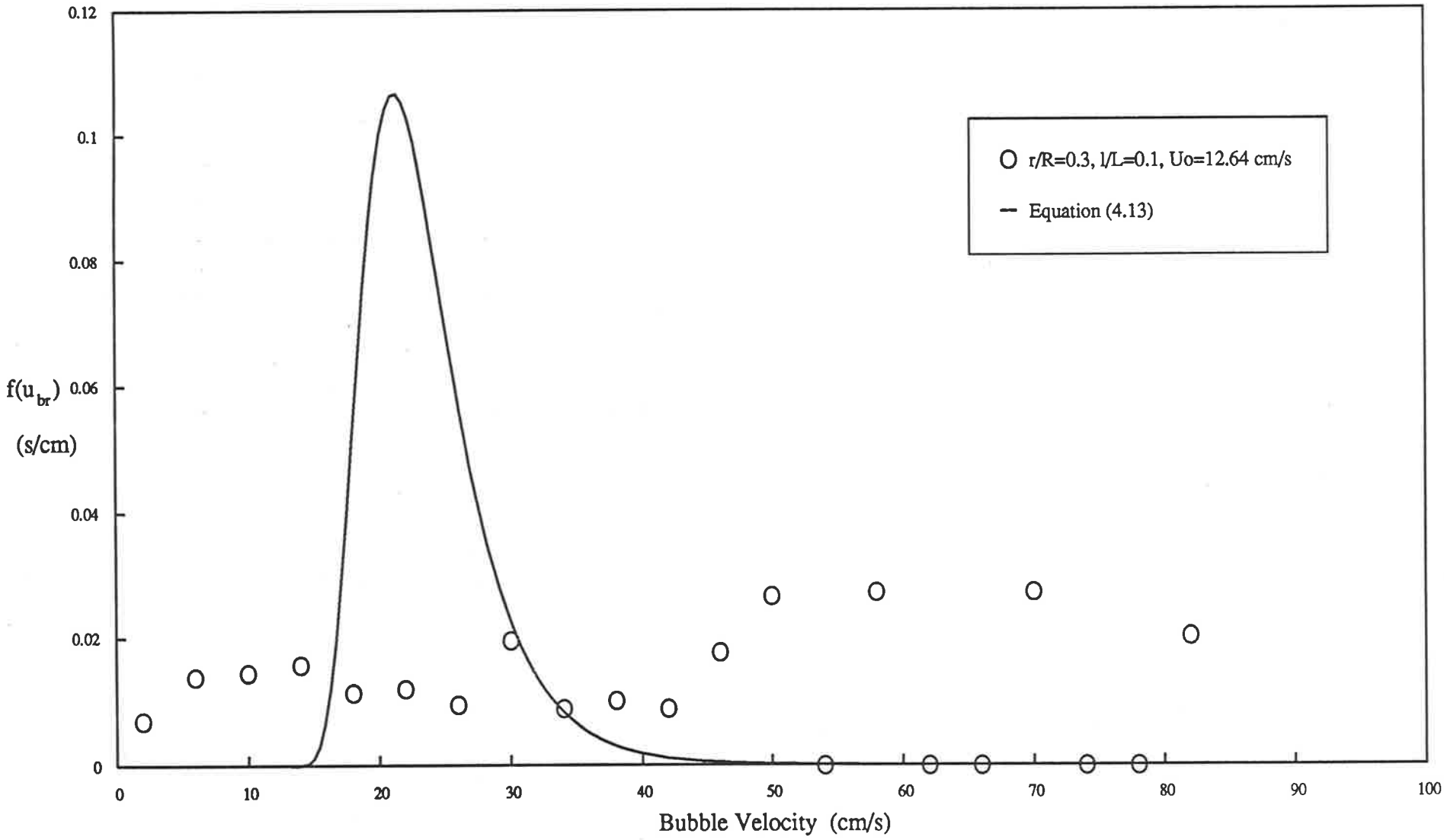

Figure 4.27 Probability Density Function of Bubble Velocity

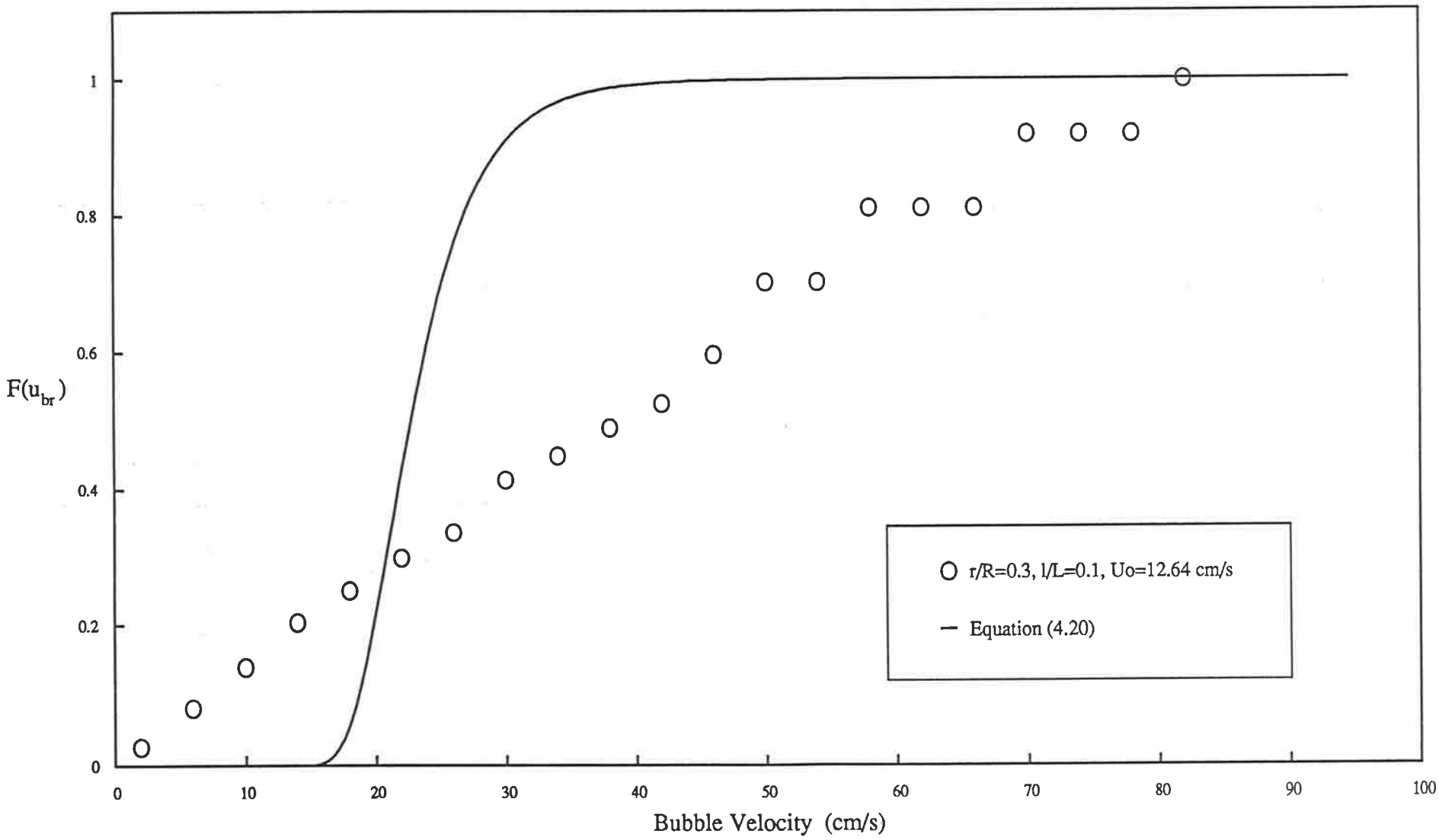

Figure 4.28 Cumulative Distribution of Bubble Velocity

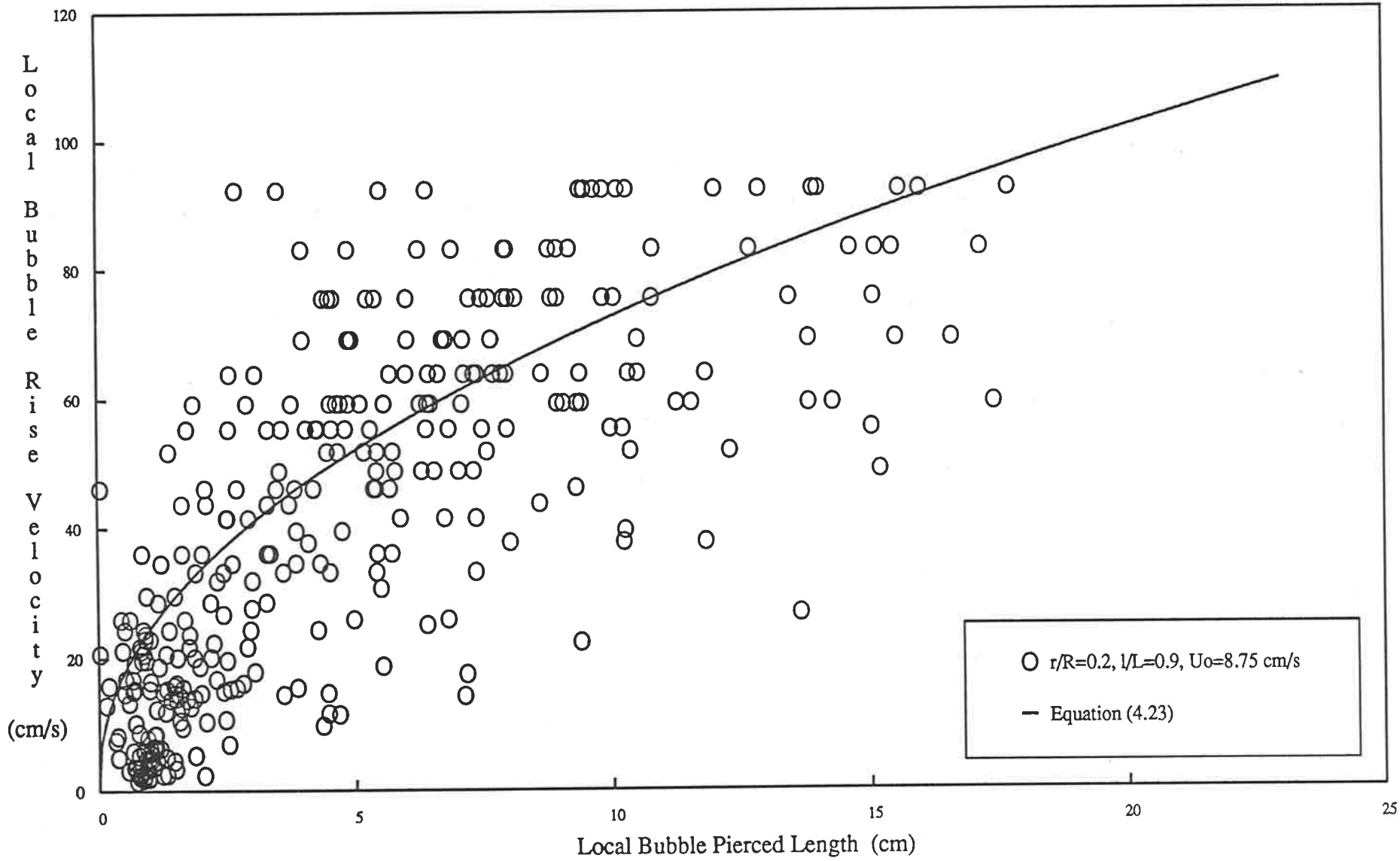

Figure 4.29 Variation of Local Bubble Rise Velocity with Pierced Length

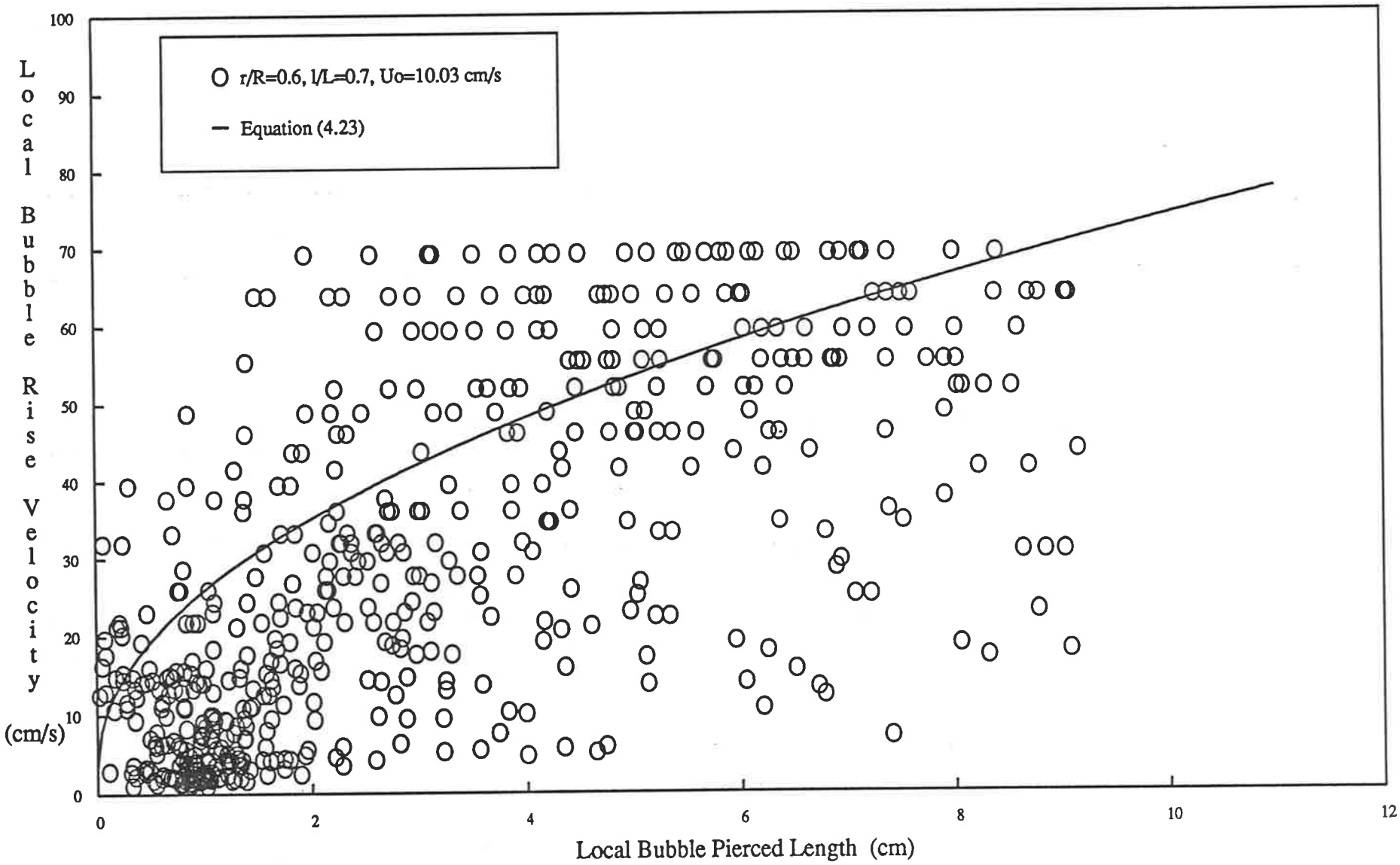

Figure 4.30 Variation of Local Bubble Rise Velocity with Pierced Length

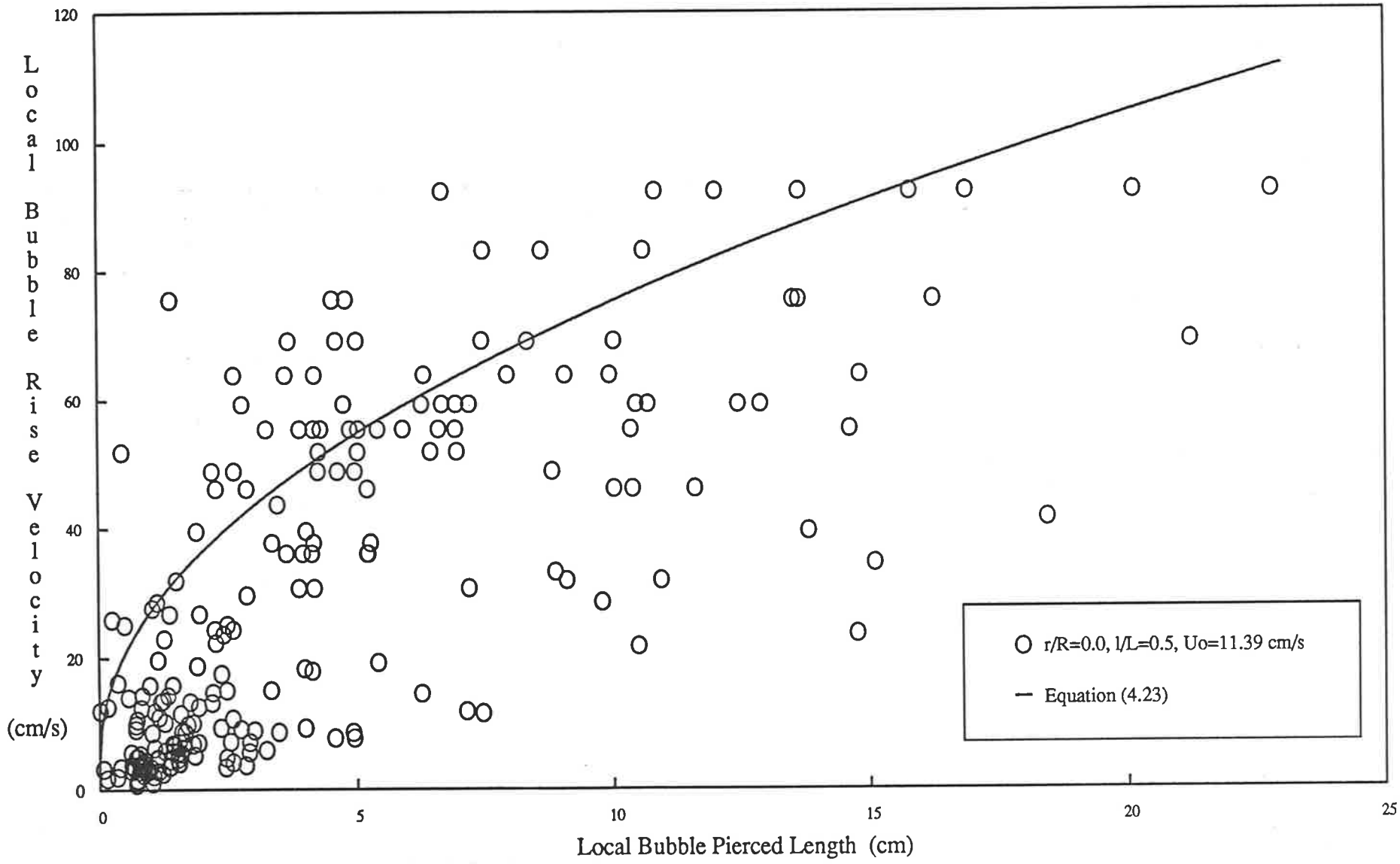

Figure 4.31 Variation of Local Bubble Rise Velocity with Pierced Length

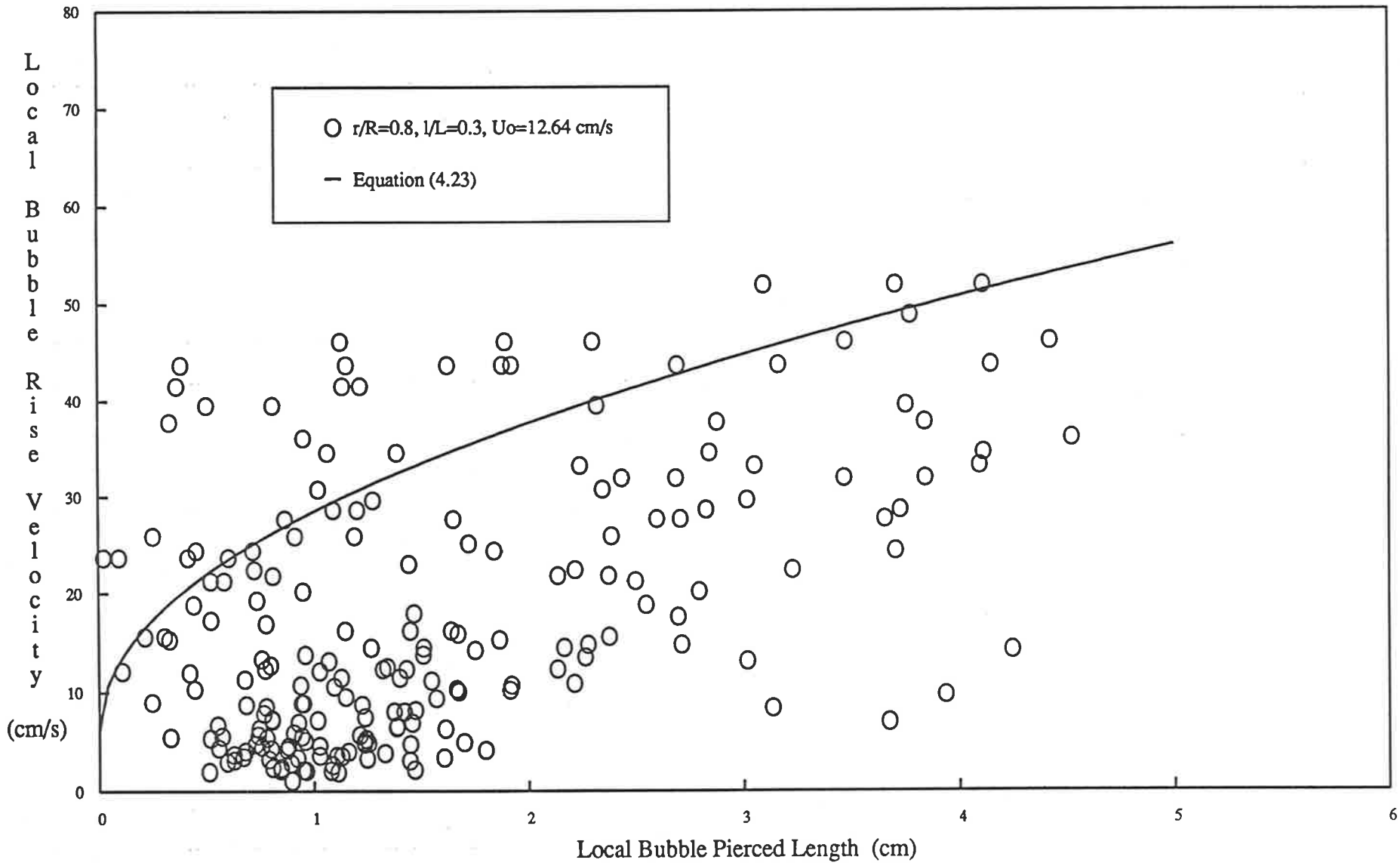

Figure 4.32 Variation of Local Bubble Rise Velocity with Pierced Length

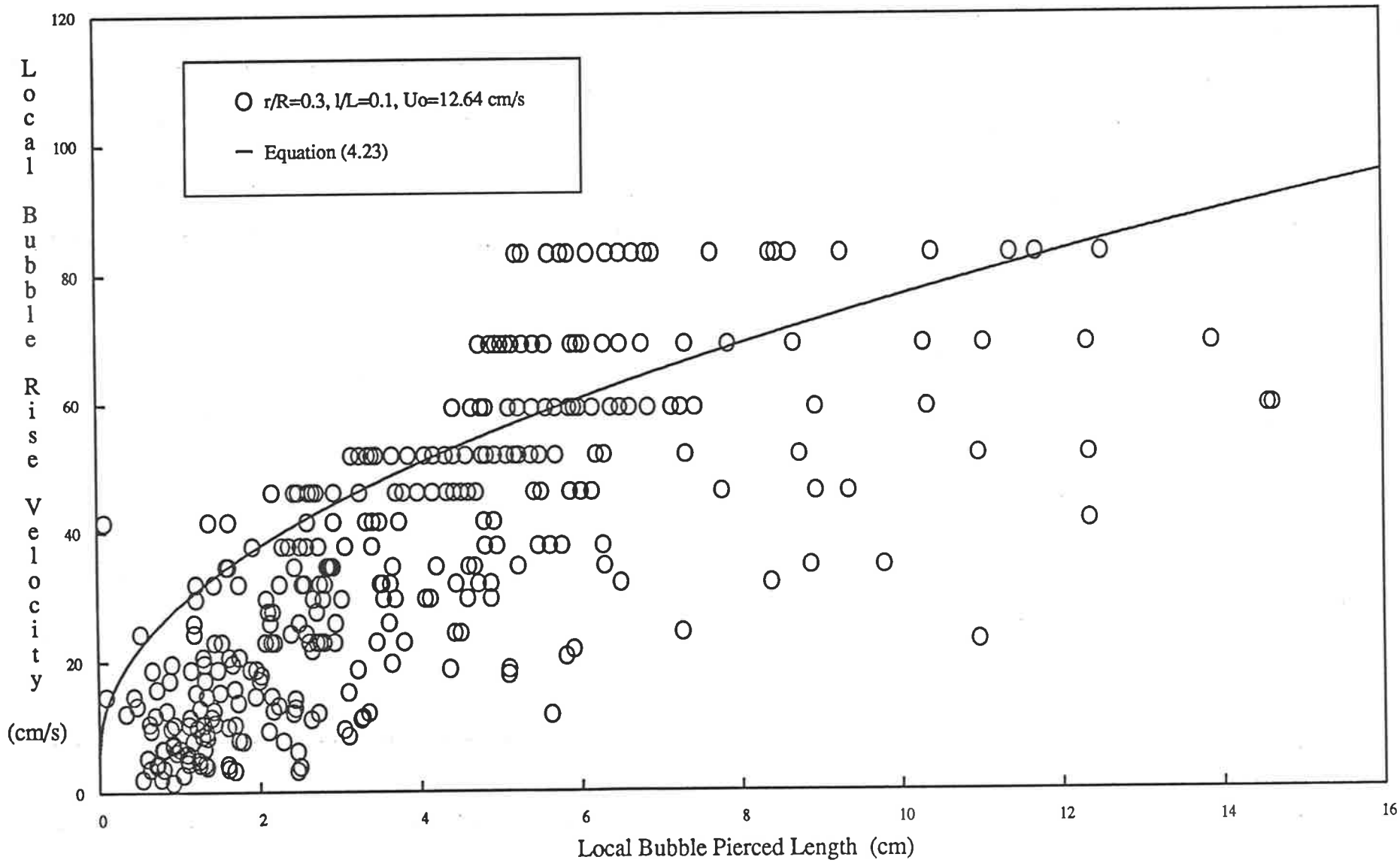

Figure 4.33 Variation of Local Bubble Rise Velocity with Pierced Length

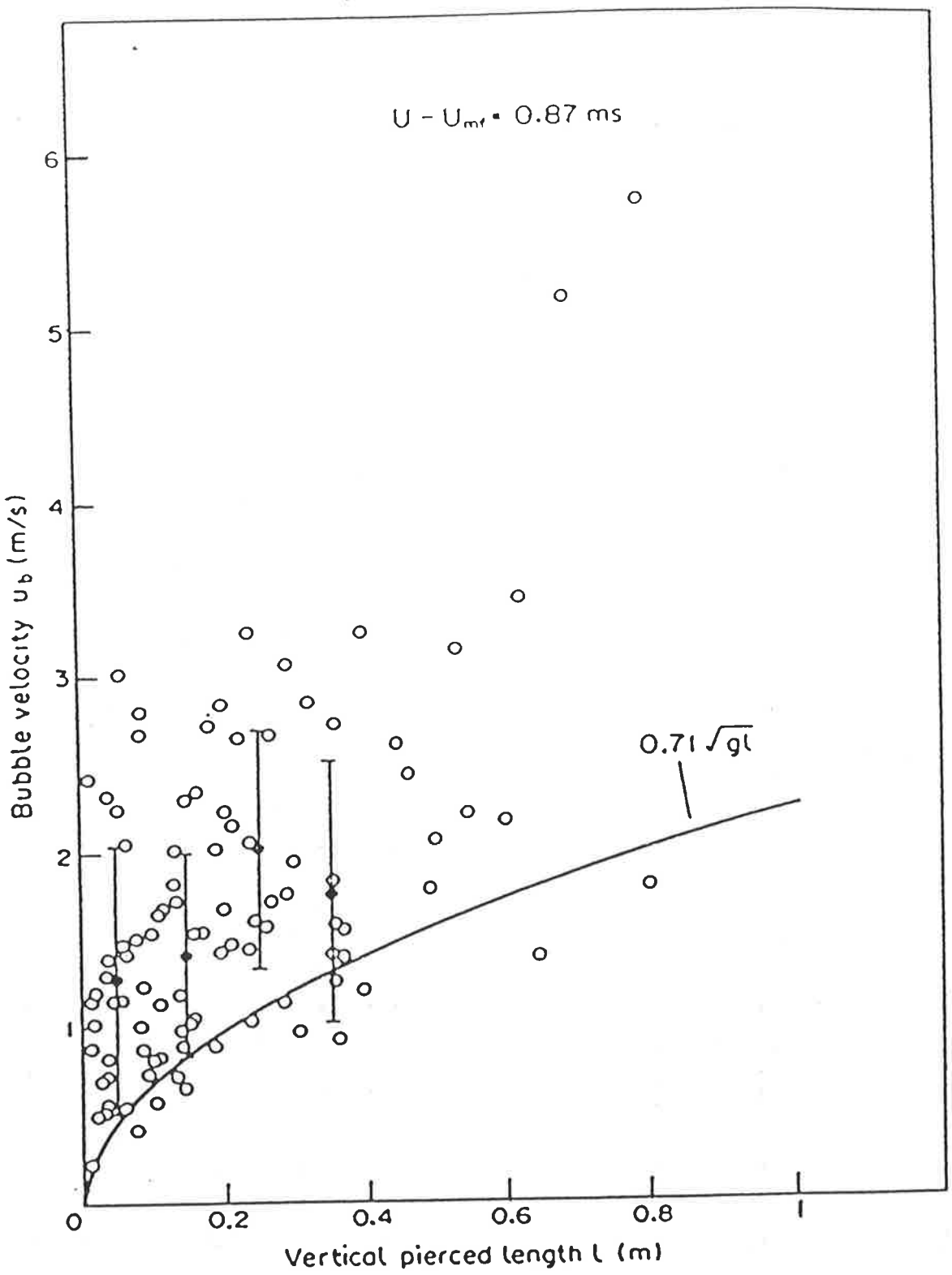

Figure 4.34 Bubble Rise Velocity vs Pierced Length from Glicksman et. al. (1987) U=1.45 m/s

A correlation was proposed by Werther (1978b) to predict the size of bubbles in gas fluidized beds :

$$d_{br} = 0.853\,[1 + 0.272\,(u_o - u_{mf})]^{\frac{1}{3}} \cdot [1 + 0.0684\,(l + l' - d_{bo})]^{1.21} \qquad \ldots(4.25)$$

where

$$l' - d_{bo} \cong 0$$

When performing calculations designed to provide an insight into the nature and quality of fluidization, it is normal to employ average bed characteristics. However, other bubble characteristics may convey more meaning. Table 4.2 presents a comparison of bubble characteristics as derived from the experimental data and correlations.

Table 4.2 Comparison of Bubble Characteristics

r/R	l/L	u_o (cm/s)	$d_{v,\exp}\|_{F(d_v)=0.5}$ (cm)	$d_{br,th}\|_{F(d_{br})=0.5}$ (cm)	$\overline{d}_{br}\|_{Equ(4.10)}$ (cm)	$d_{br}\|_{Equ(4.25)}$ (cm)
0.2	0.9	8.75	1.2	1.66	2.6548	4.098
0.6	0.7	10.03	1.5	1.79	2.214	3.577
0.0	0.5	11.39	0.58	0.58	1.905	2.977
0.8	0.3	12.64	1.34	1.16	1.3695	2.307
0.3	0.1	12.64	1.68	0.52	0.6863	1.540
			$u_{br,\exp}\|_{F(u_{br})=0.5}$ (cm/s)	$u_{br,th}\|_{F(u_{br})=0.5}$ (cm/s)	$\overline{u}_{br}\|_{Equ(4.23)}$ (cm/s)	$u_{br}\|_{Equ(4.23)}$ (cm/s)
0.2	0.9	8.75	38.0	33.9	38.60	47.4
0.6	0.7	10.03	21.4	33.9	36.72	45.7
0.0	0.5	11.39	22.1	32.1	35.68	43.4
0.8	0.3	12.64	12.1	30.0	32.26	40.0
0.3	0.1	12.64	38.7	22.6	24.65	33.8

There is no direct relationship between the average bubble characteristics and the 50% undersize characteristics and hence a quantitative comparison is not possible. However, both types of bubble characteristics can be used in calculations of fluidized bed performance and as such a qualitative comparison can be made.

In general, the average bubble characteristics are greater than the corresponding 50% undersize (or median) characteristics taken from the cumulative distribution figures presented. For example, the average bubble diameter calculated from Equation (4.10) and the bubble size predicted by Equation (4.25) at r/R=0.2 and l/L=0.9 are significantly greater than the median bubble vertical dimension and median bubble diameter taken from Figure 4.10.

When an average bubble characteristic is employed in fluidized bed performance calculations an associated standard deviation is almost never quoted. Clearly, the mean bubble characteristic alone may be insufficient to adequately characterise the fluidization process. A few large, fast bubbles may dominate many smaller, slower bubbles present in an array of bubbles. Consequent overprediction of mean bubble diameter and rise velocity is possible. There may exist a significant effect due to the presence of the smaller bubbles which is underestimated.

In summary, a knowledge of the distributor type, superficial gas velocity and minimum fluidization velocity can be used to predict values of the bubble size and velocity at the distributor. These may be regarded as the minimum values of these quantities. If the medians of the bubble size and velocity distributions at various positions in the bed are specified, a qualitative estimate of the maximum bubble sizes and velocities of the array of bubbles can then be made. Providing a greater perception of the fluidization process. Of course knowledge of the actual distribution provides the maximum information.

CHAPTER V

EXPERIMENTAL RESULTS

This chapter details the results collected in this study. Figures are presented which illustrate the Cumulative Distributions and Probability Density Functions (PDF) of the bubble vertical dimension and bubble rise velocity. Experiments conducted to test the reproducibility of the data are presented, as well as figures illustrating overall bed characteristics.

5.1 Distribution of Bubble Vertical Dimension

A comprehensive study of the distribution of bubble vertical dimensions was undertaken. The probe positions employed are illustrated in Figure 3.15. Figures 5.1 to 5.44 present distributions of the bubble vertical dimensions measured in this study. Inspection of the figures yields the distribution of bubble vertical dimensions, at numerous points in the bed for various fluidizing gas velocities. As l/L increases, the bubbles conglomerate and increase in size towards the centre of the bed.

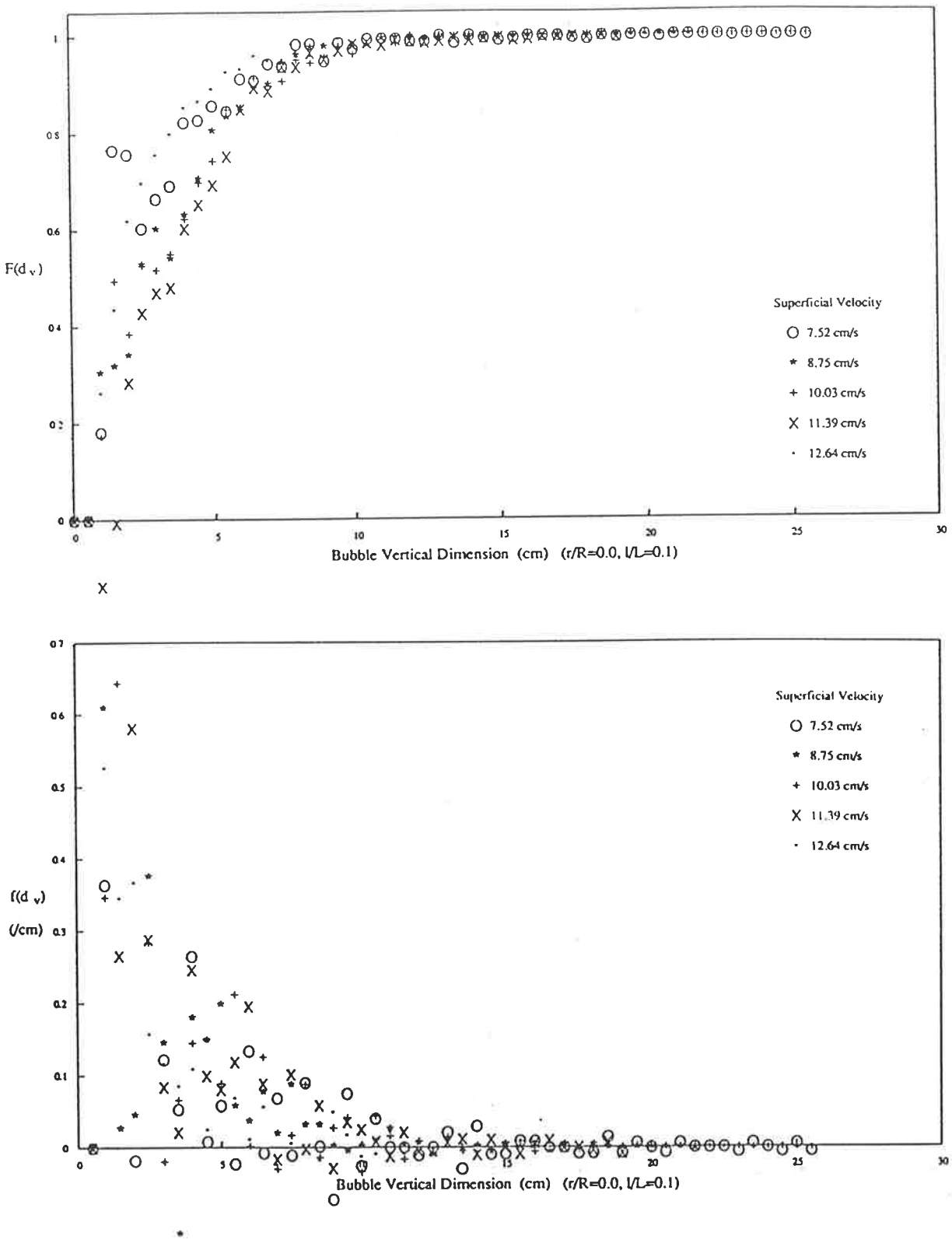

Figure 5.1 Cumulative Distribution and PDF of Bubble Vertical Dimension

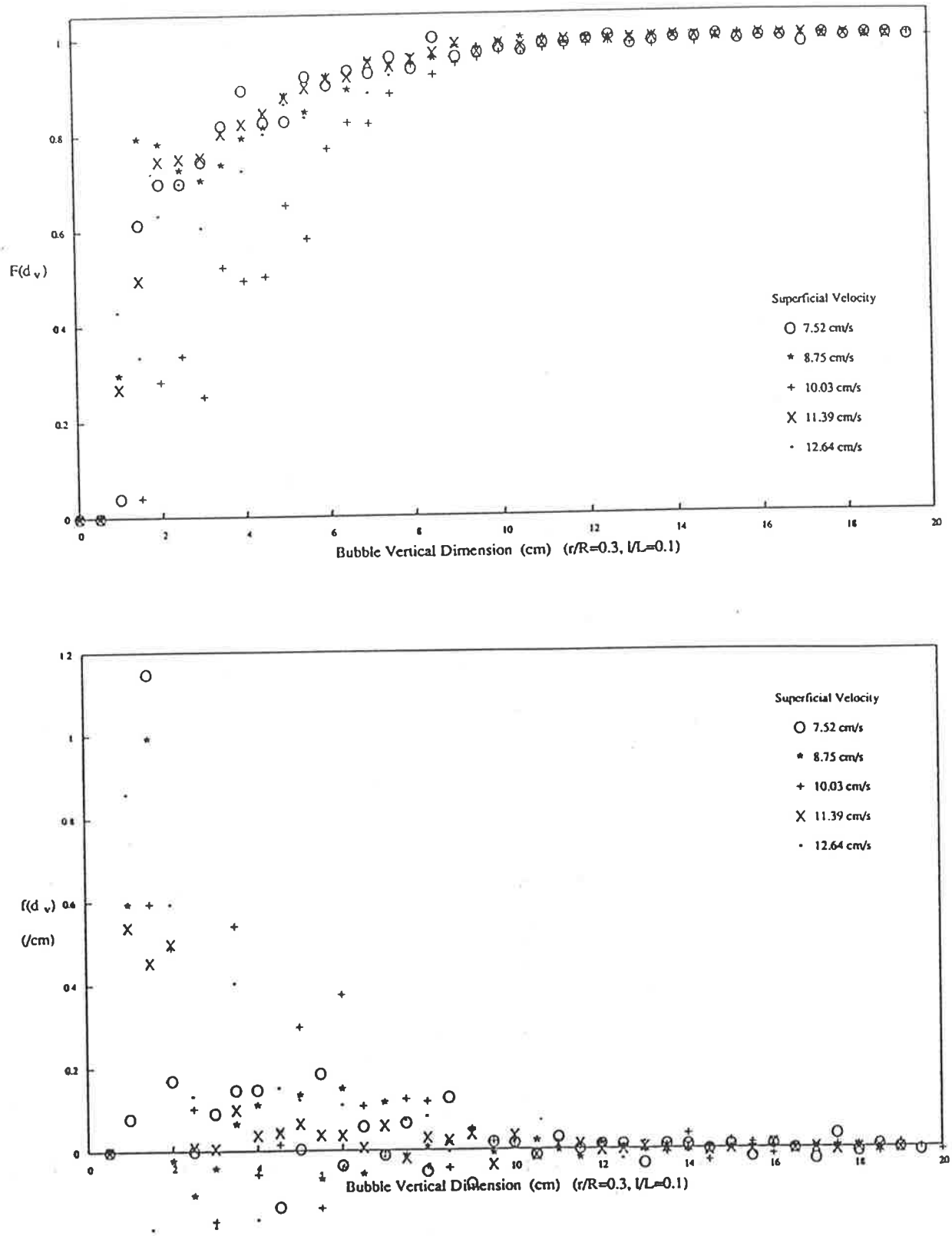

Figure 5.2 Cumulative Distribution and PDF of Bubble Vertical Dimension

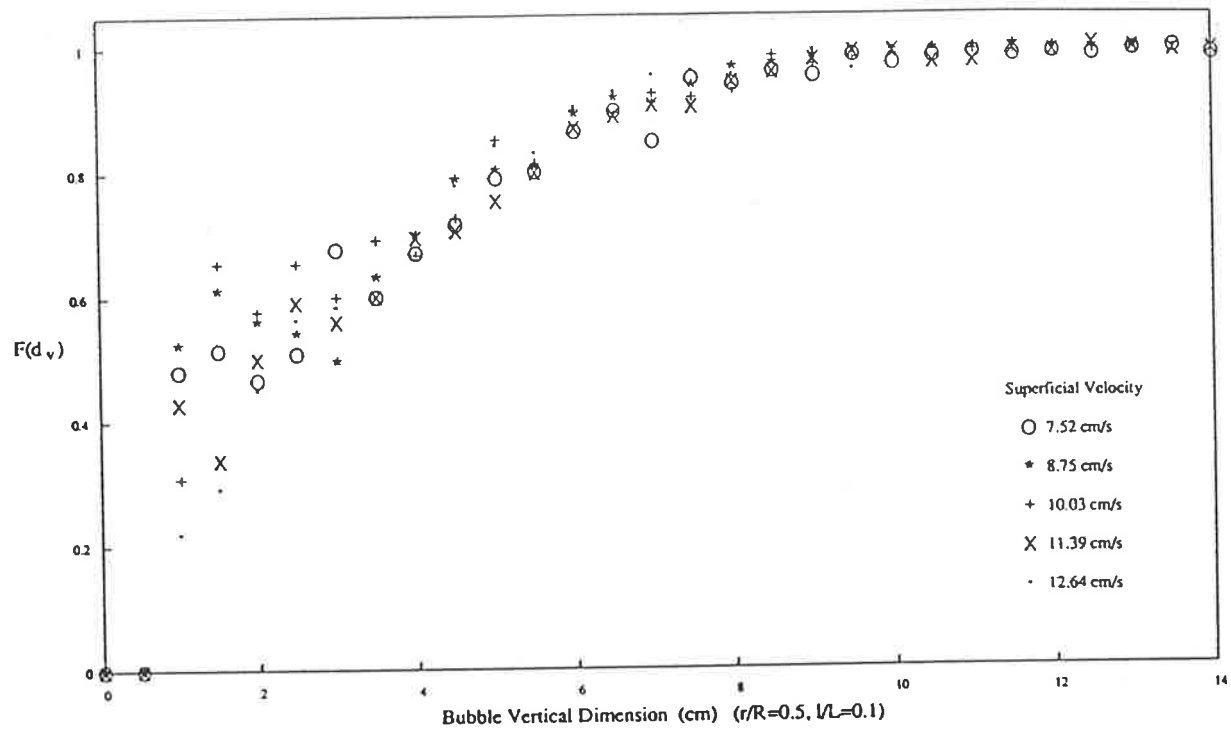

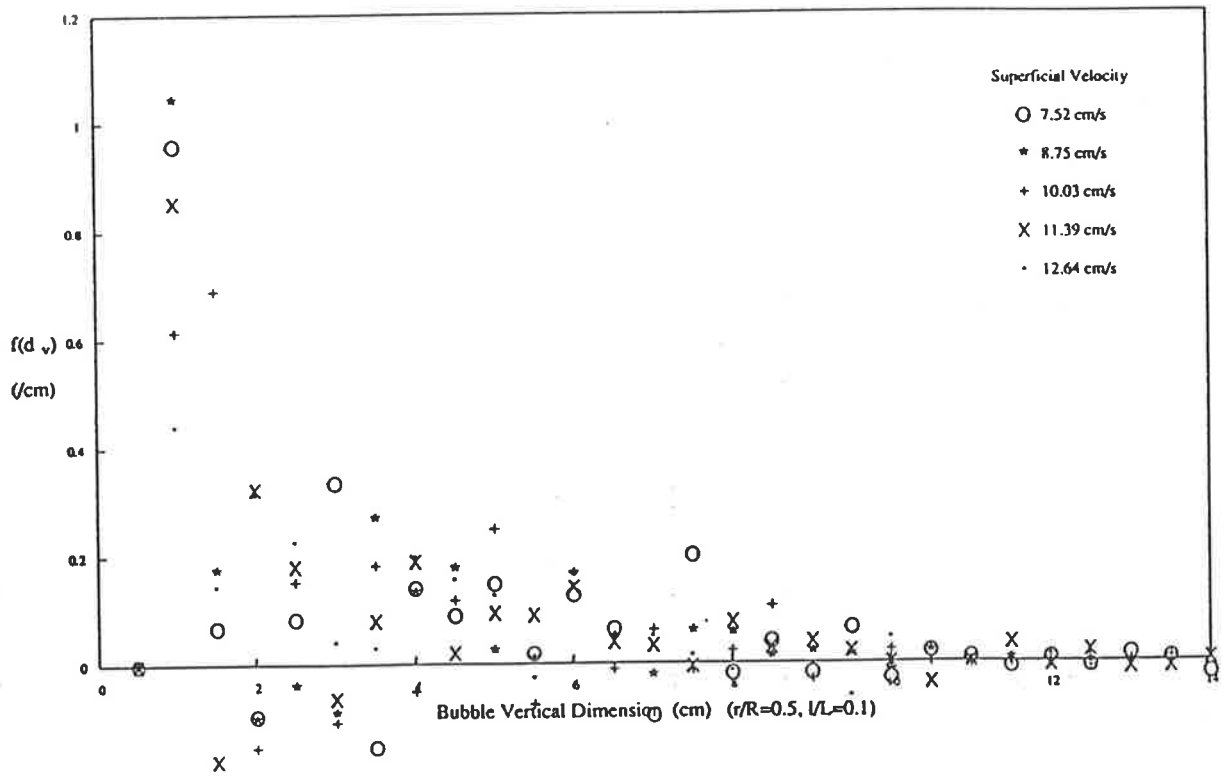

Figure 5.3 Cumulative Distribution and PDF of Bubble Vertical Dimension

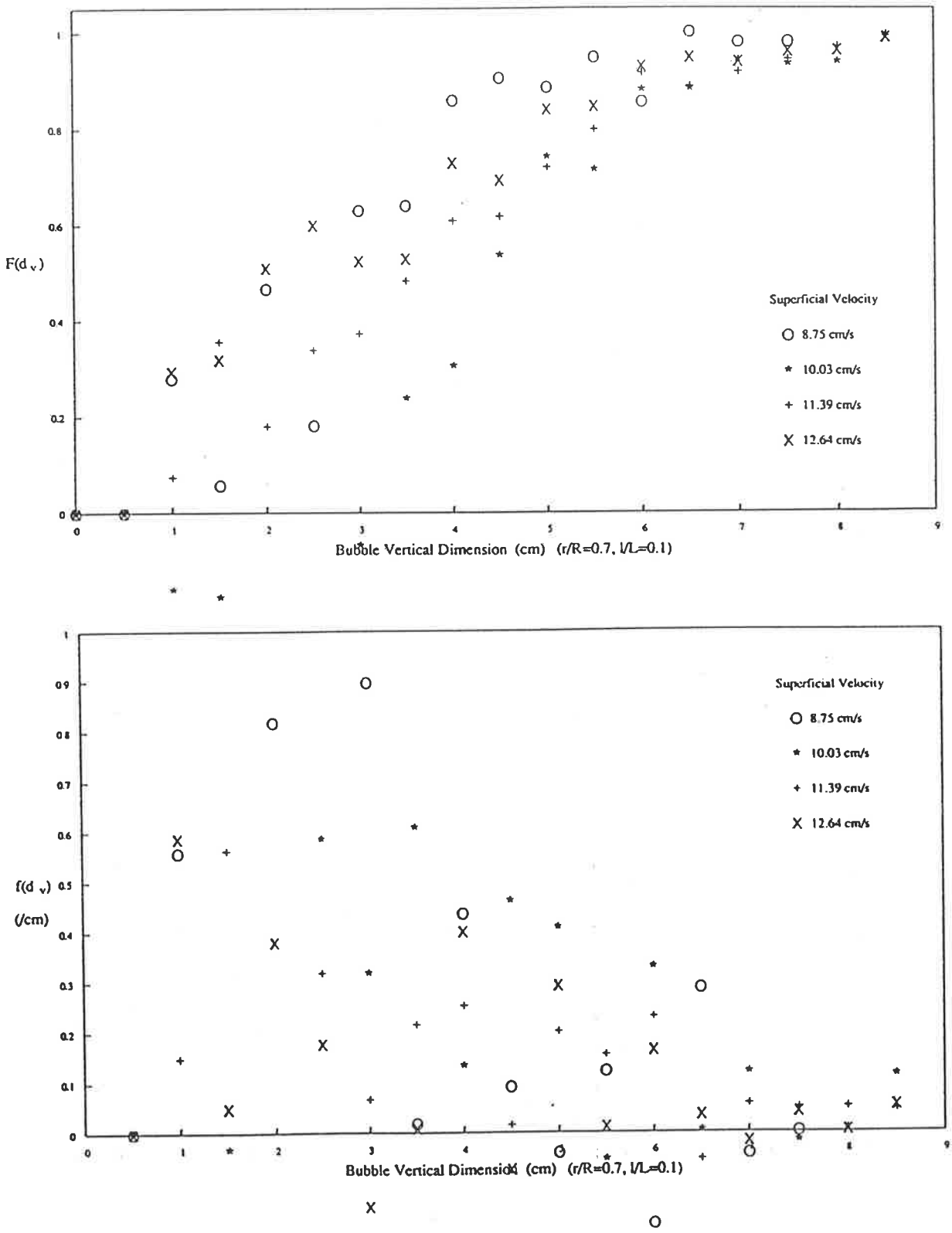

Figure 5.4 Cumulative Distribution and PDF of Bubble Vertical Dimension

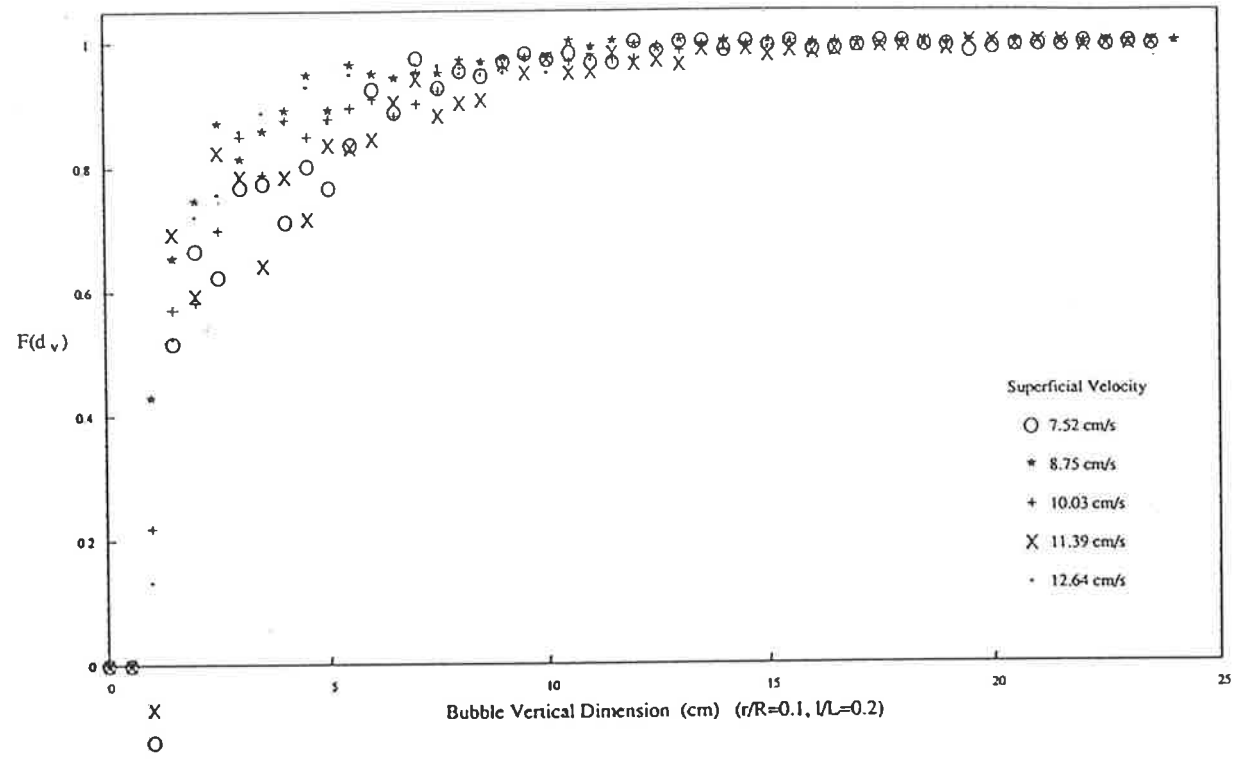

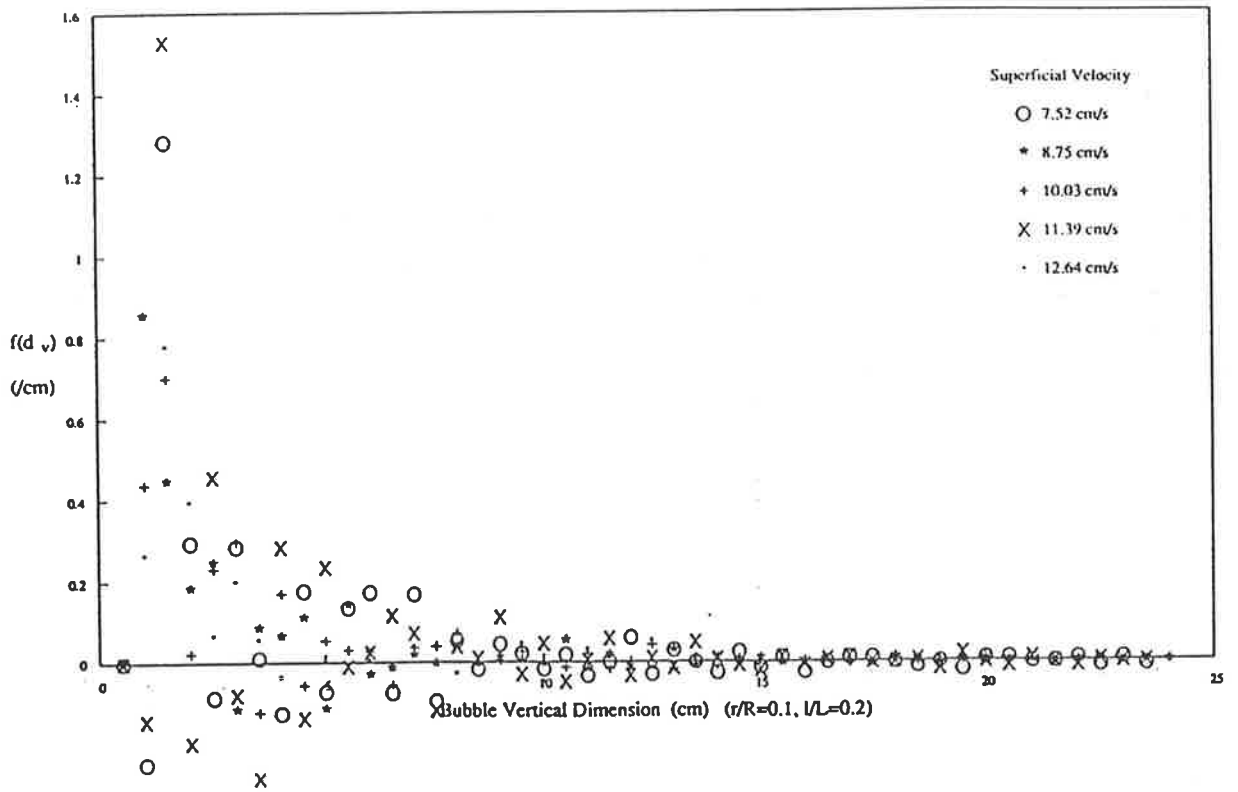

Figure 5.5 Cumulative Distribution and PDF of Bubble Vertical Dimension

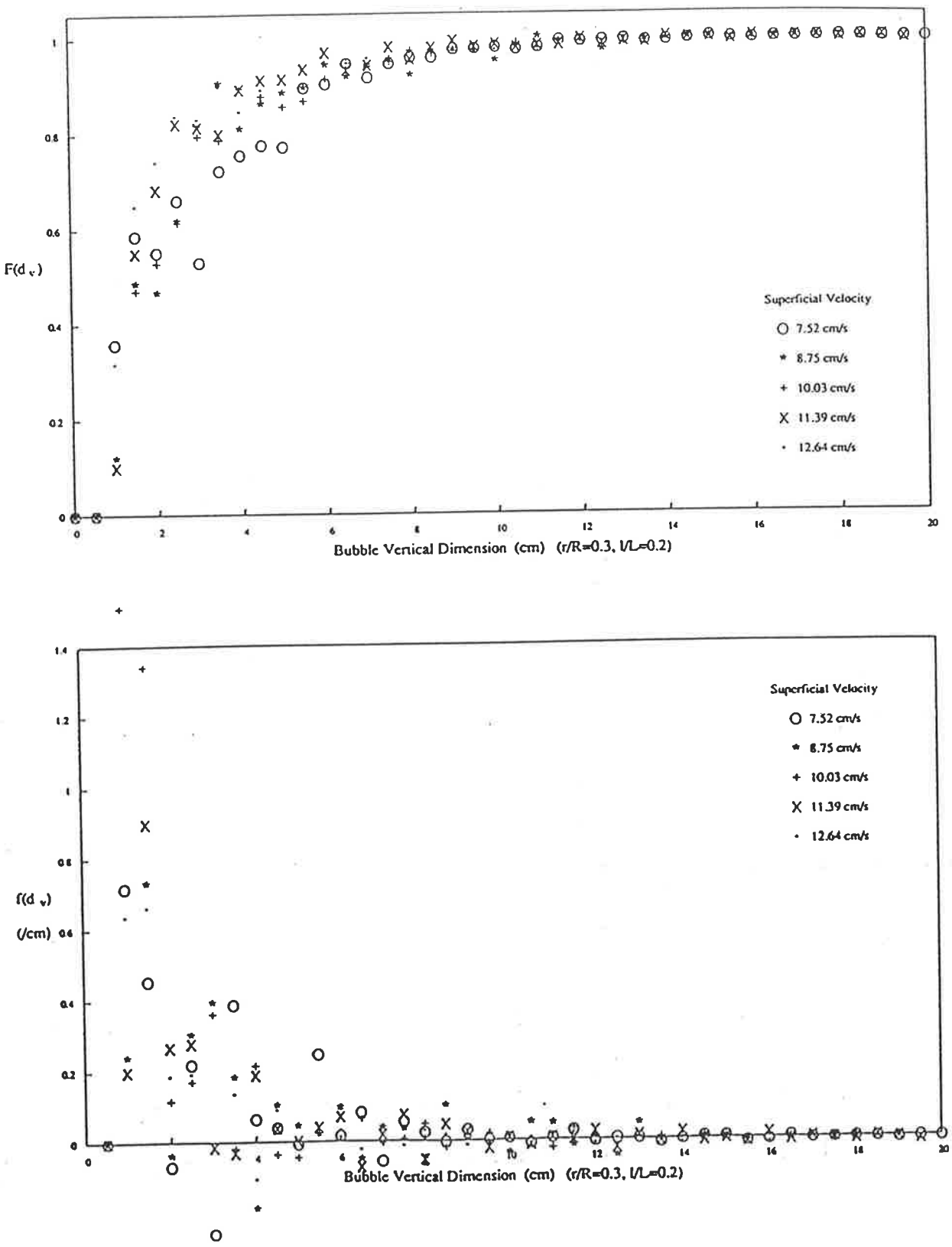

Figure 5.6 Cumulative Distribution and PDF of Bubble Vertical Dimension

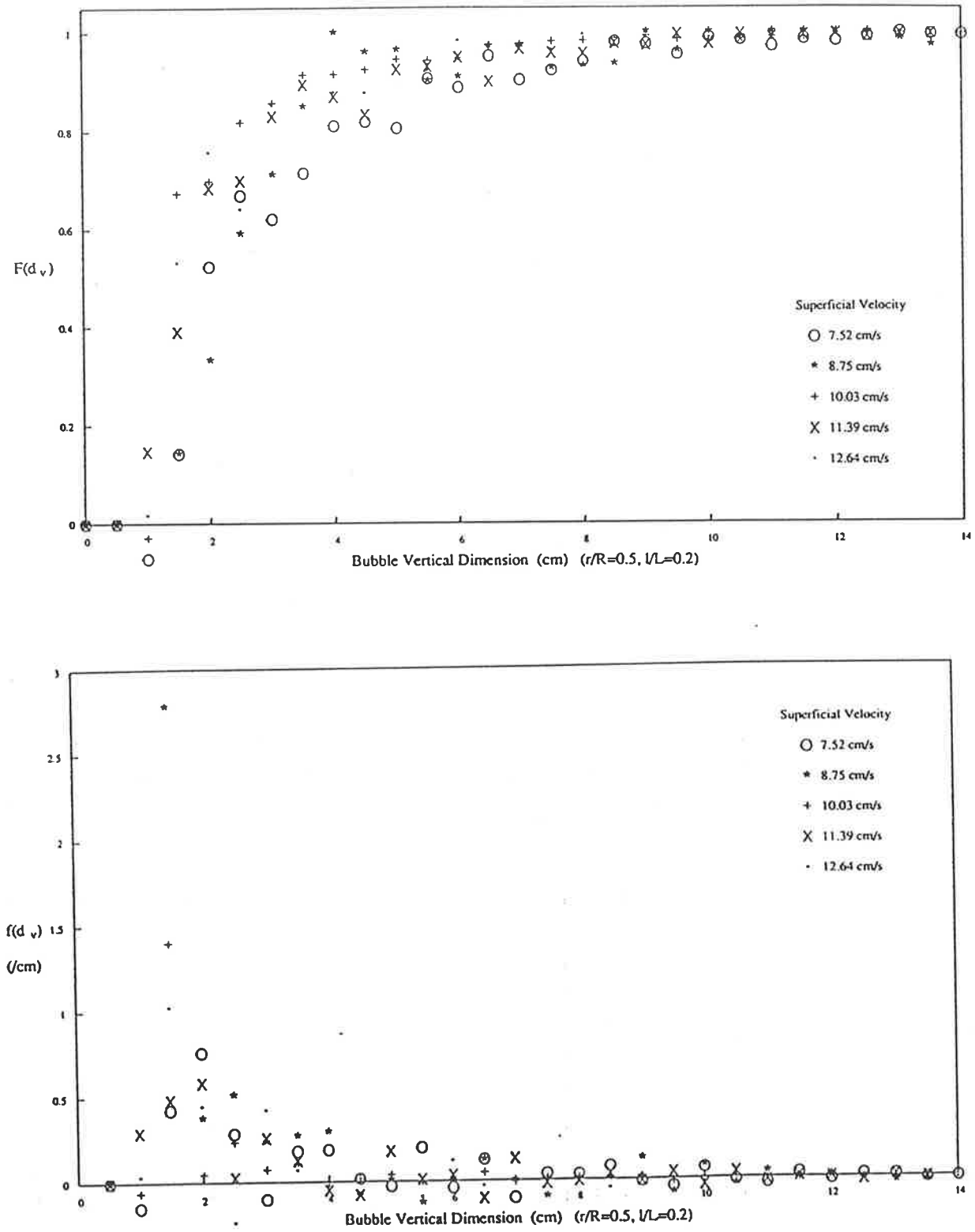

Figure 5.7 Cumulative Distribution and PDF of Bubble Vertical Dimension

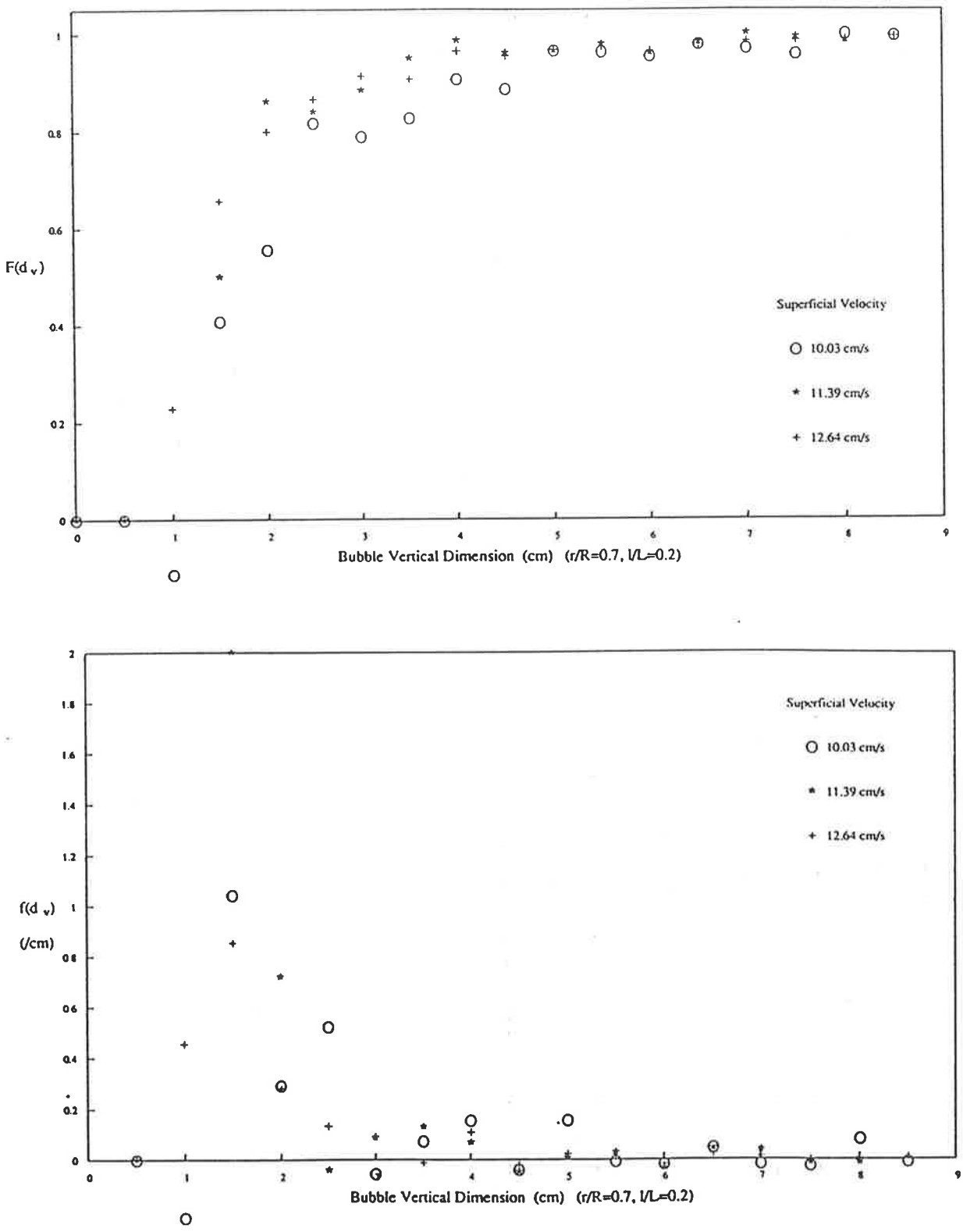

Figure 5.8 Cumulative Distribution and PDF of Bubble Vertical Dimension

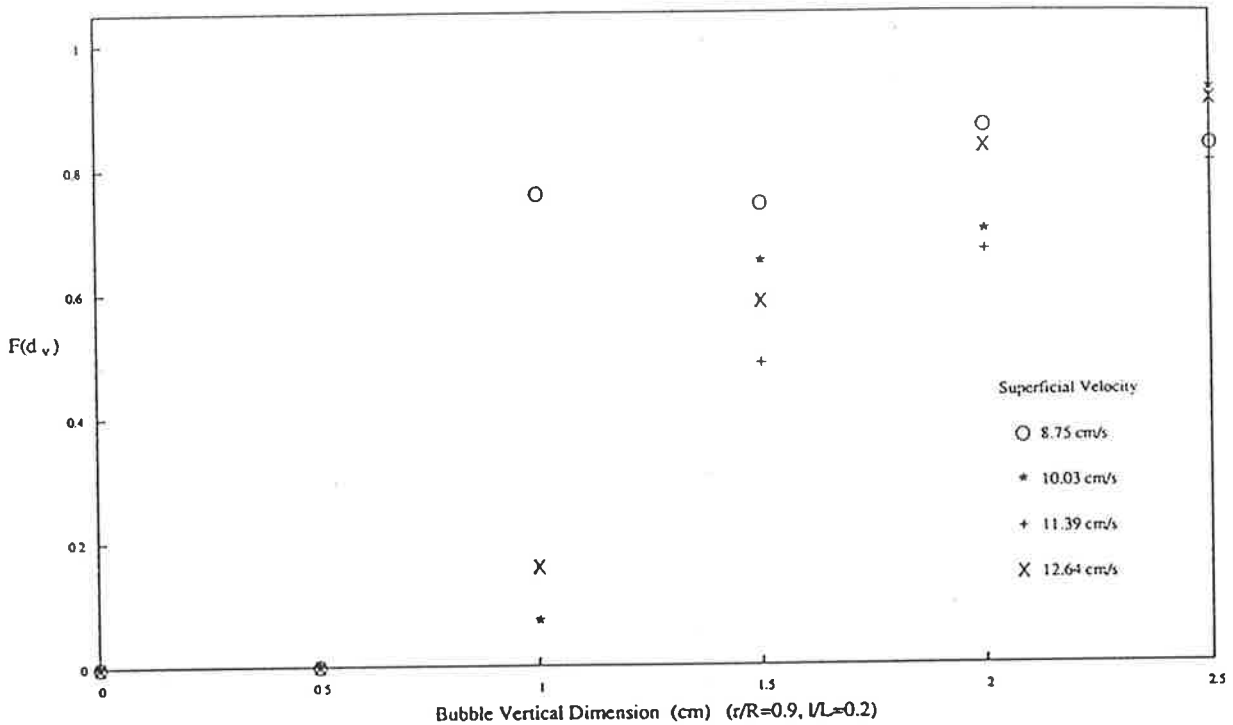

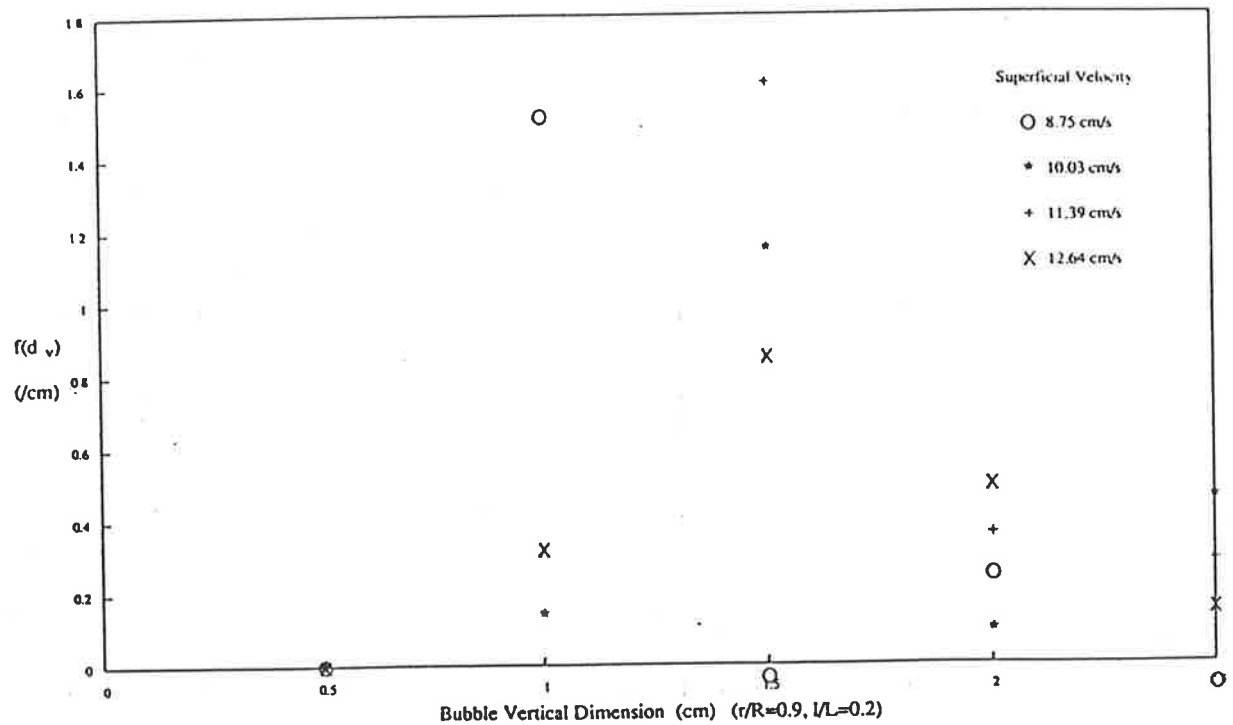

Figure 5.9 Cumulative Distribution and PDF of Bubble Vertical Dimension

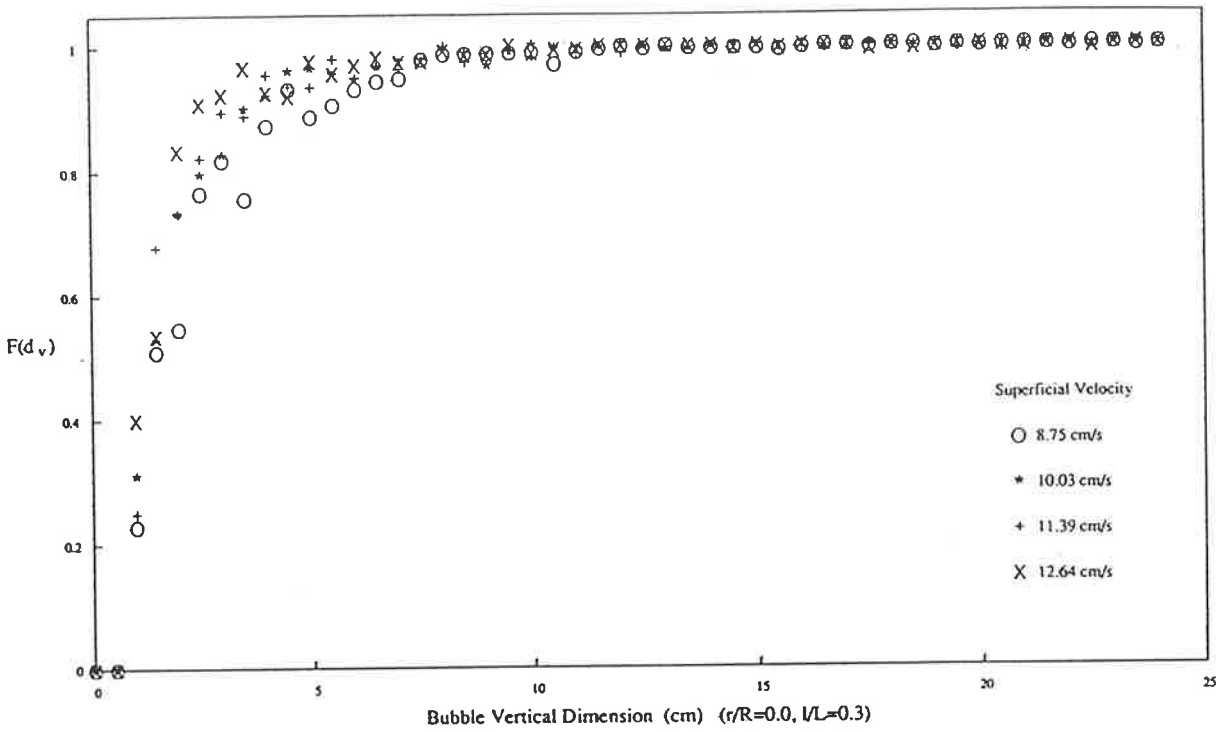

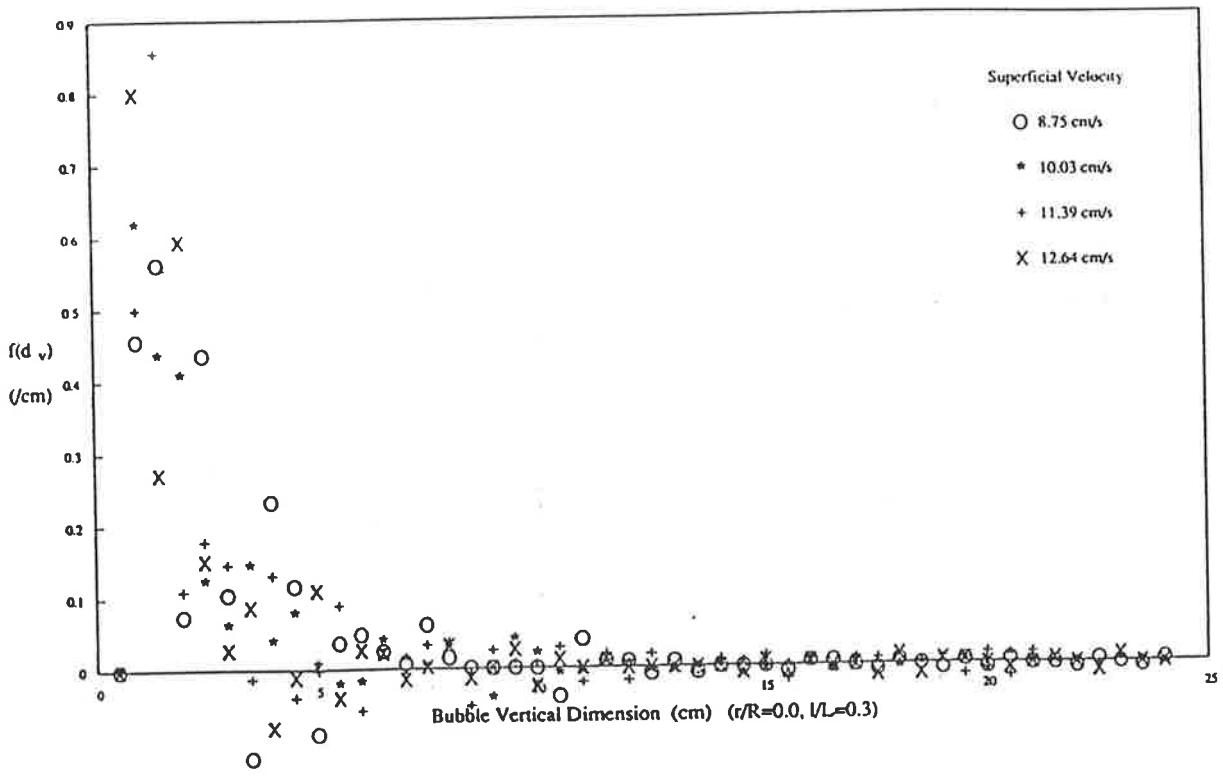

Figure 5.10 Cumulative Distribution and PDF of Bubble Vertical Dimension

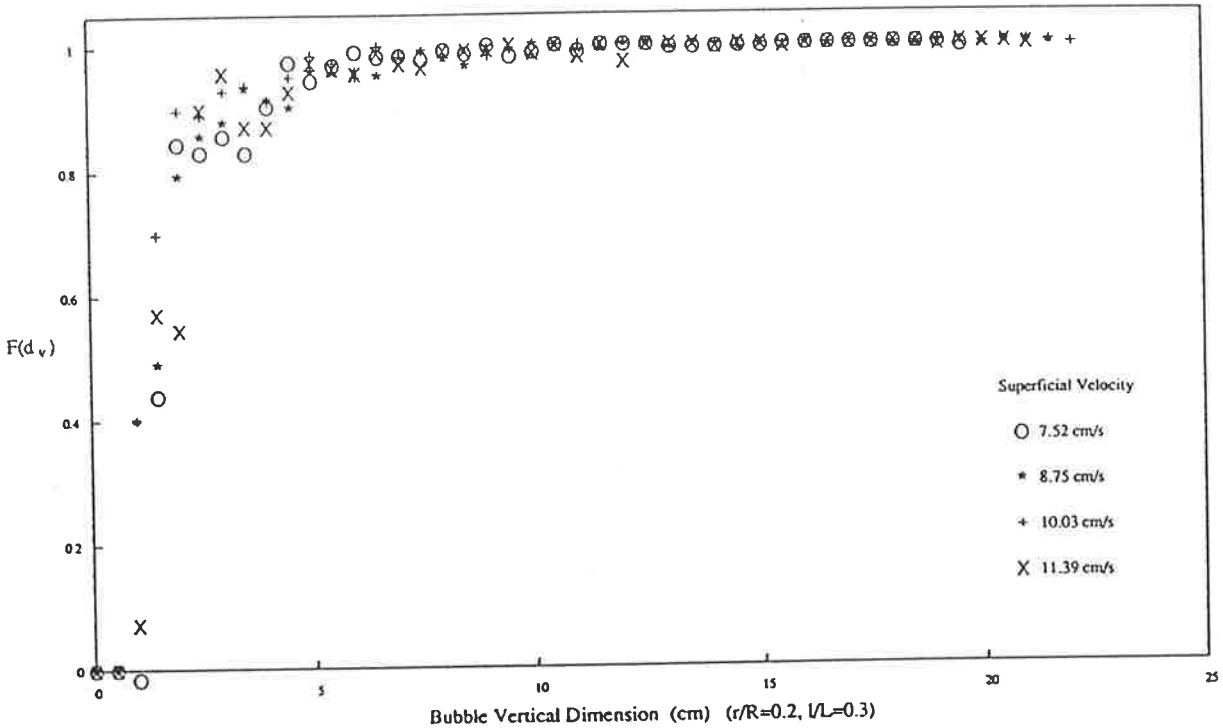

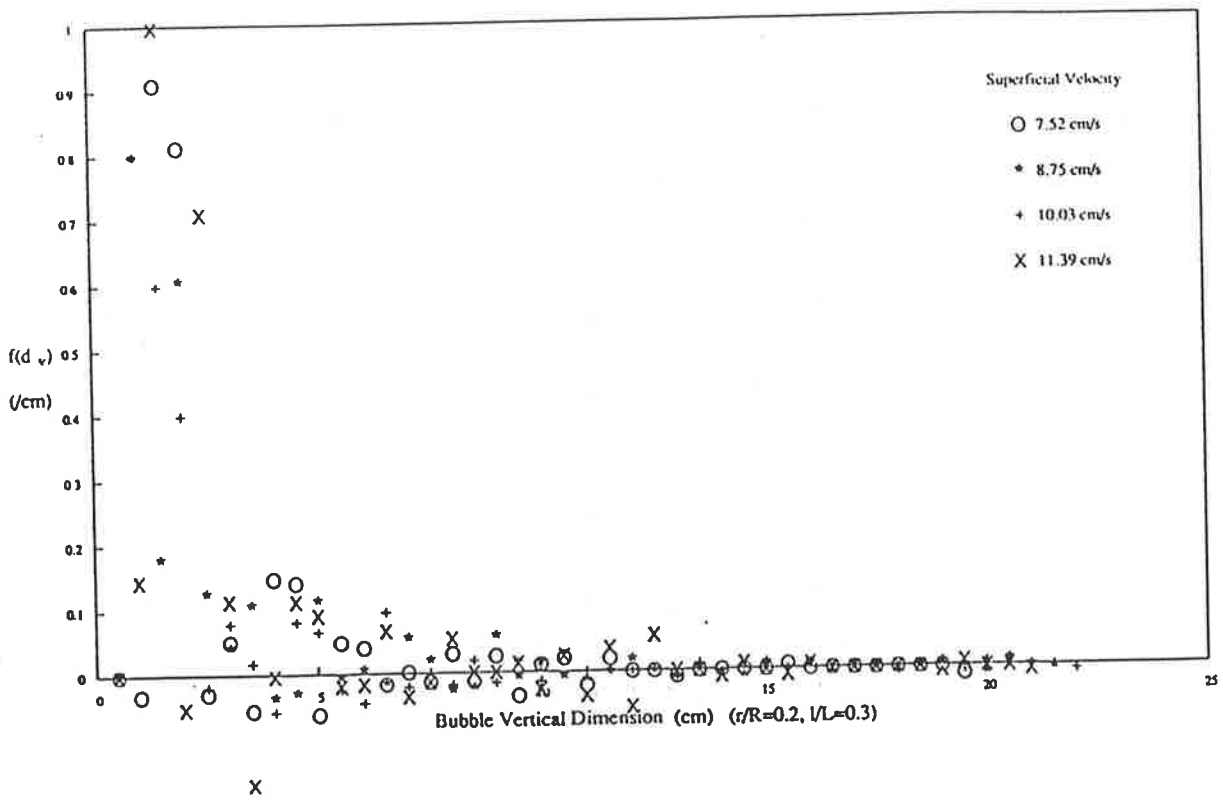

Figure 5.11 Cumulative Distribution and PDF of Bubble Vertical Dimension

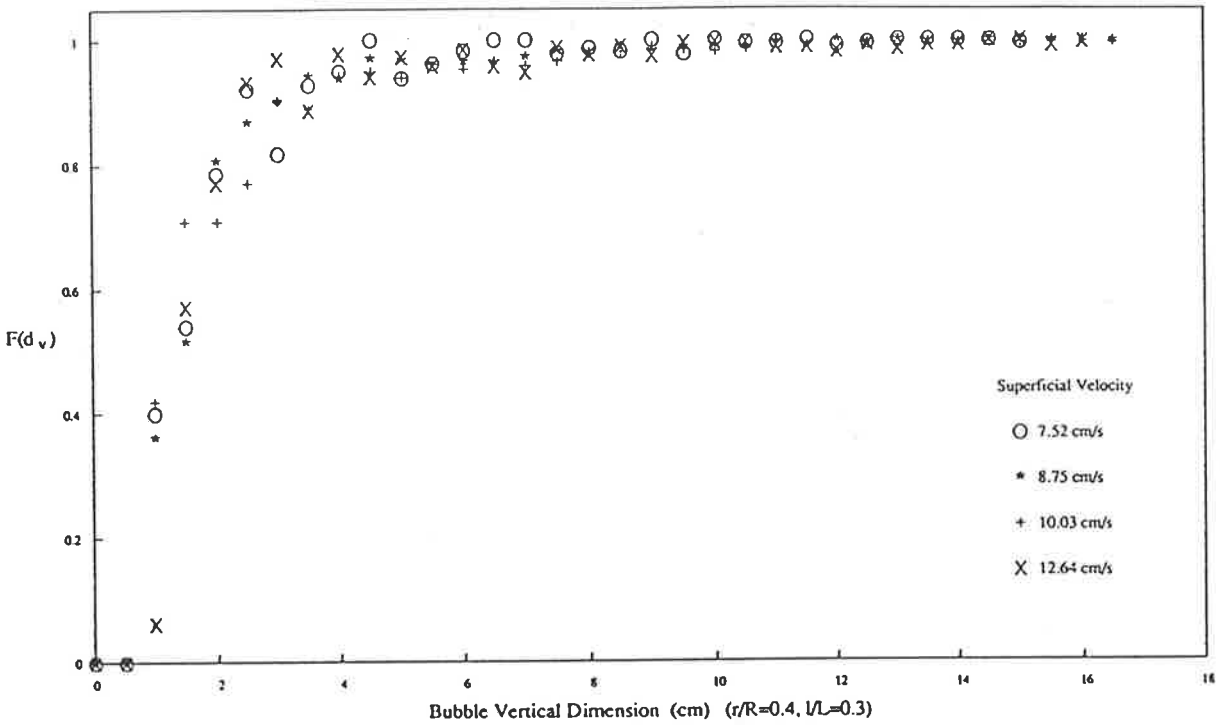

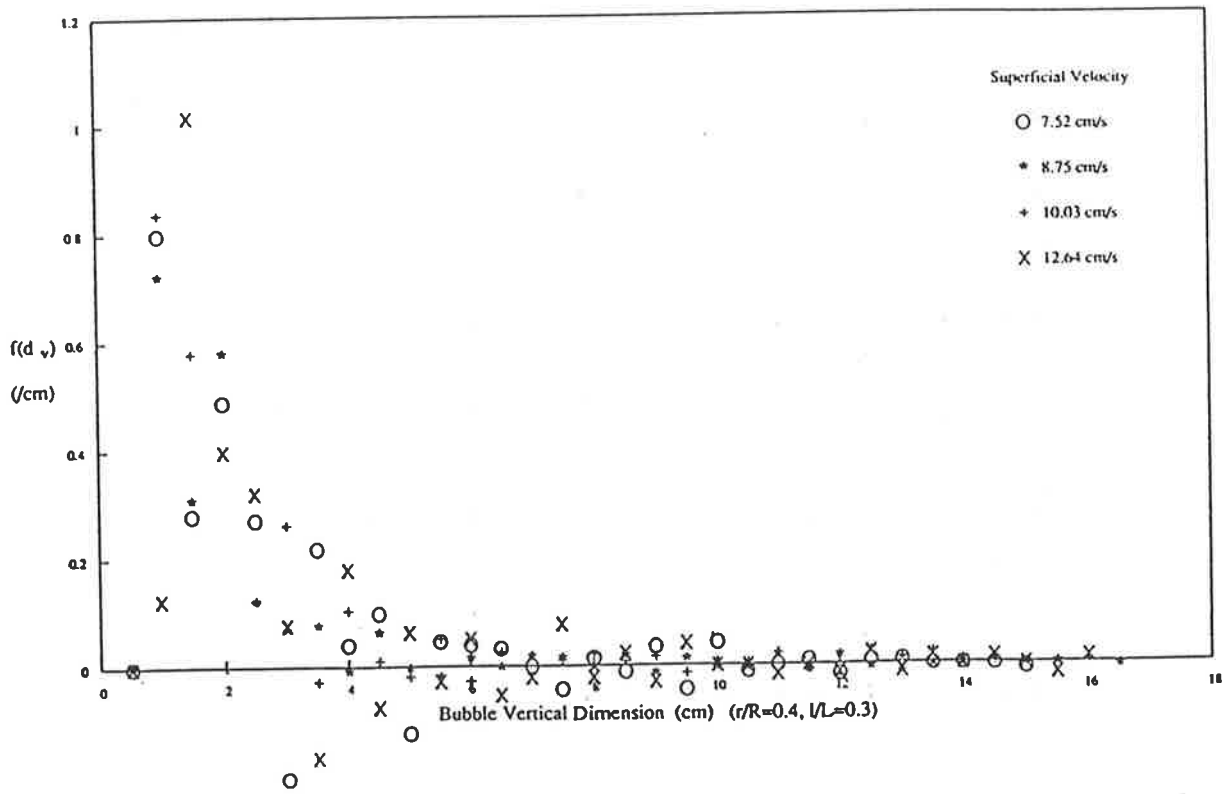

Figure 5.12 Cumulative Distribution and PDF of Bubble Vertical Dimension

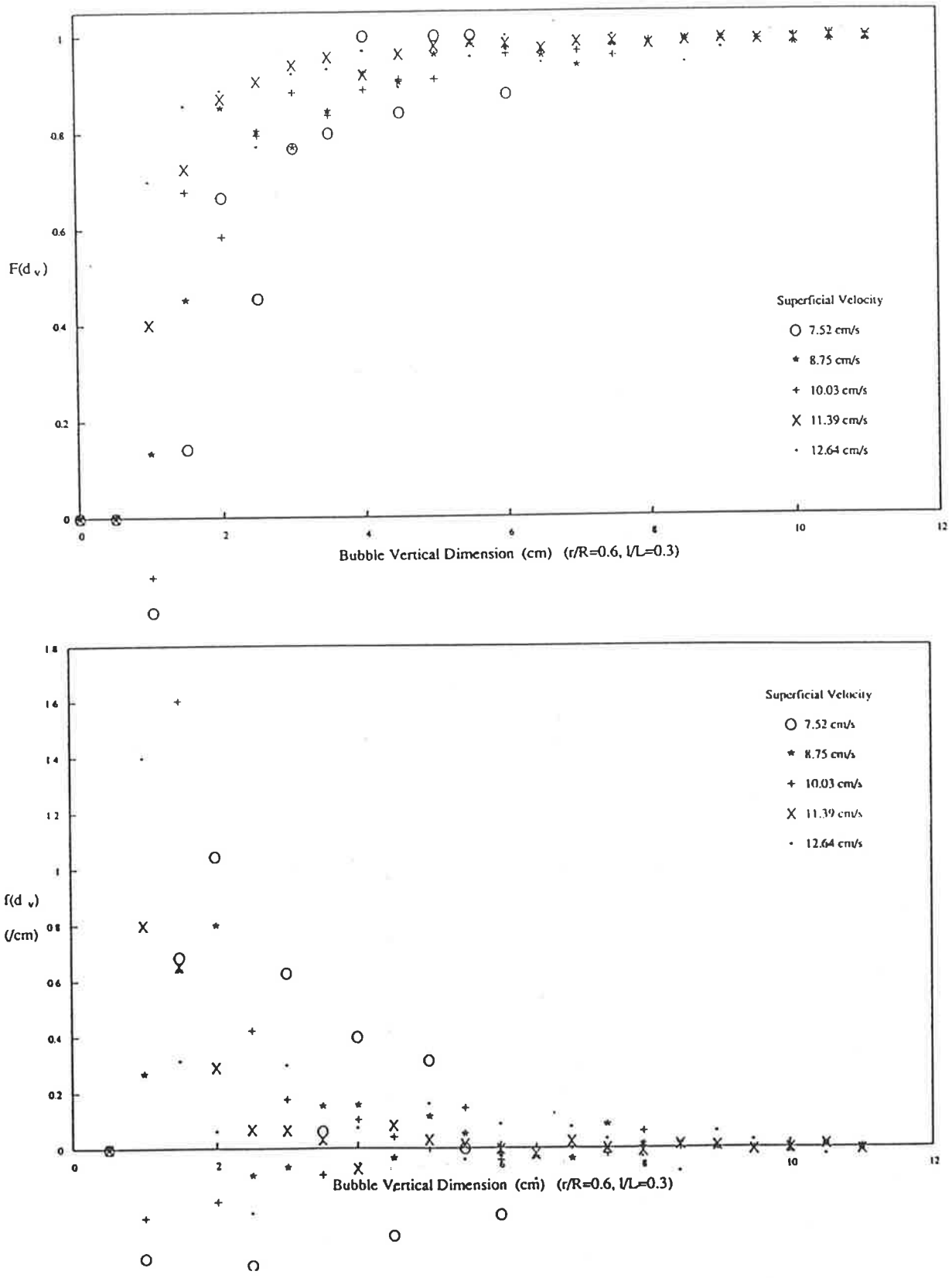

Figure 5.13 Cumulative Distribution and PDF of Bubble Vertical Dimension

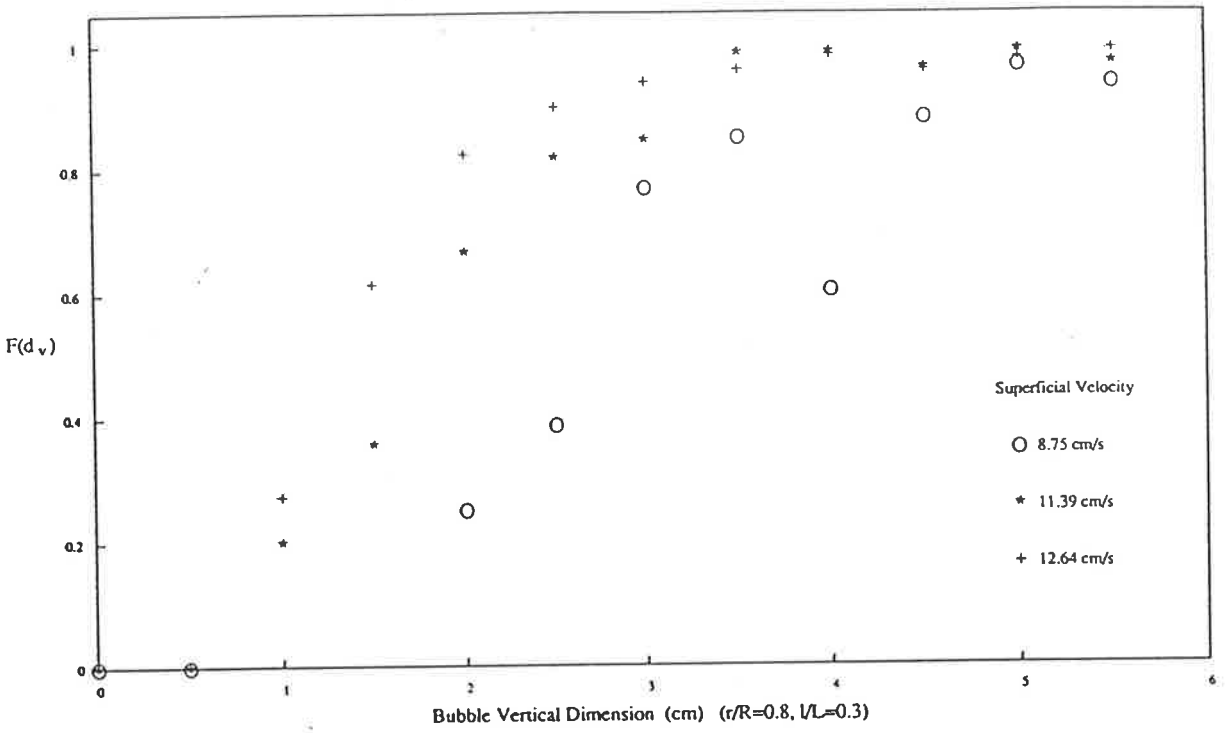

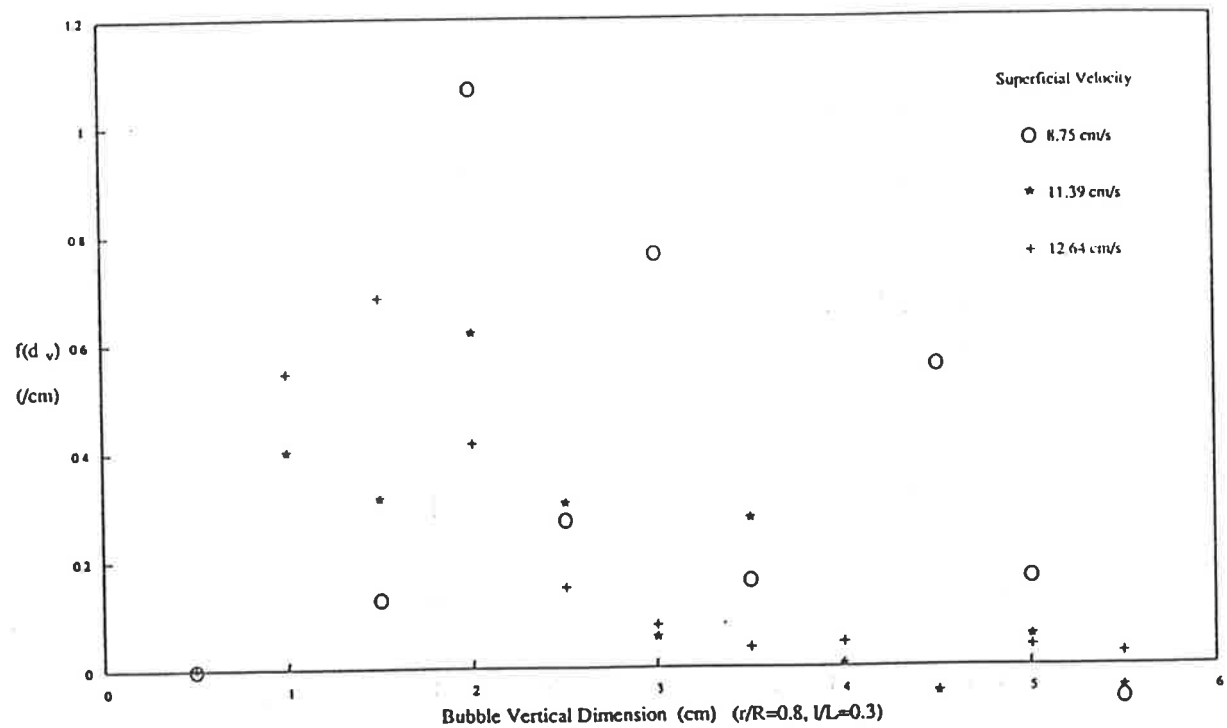

Figure 5.14 Cumulative Distribution and PDF of Bubble Vertical Dimension

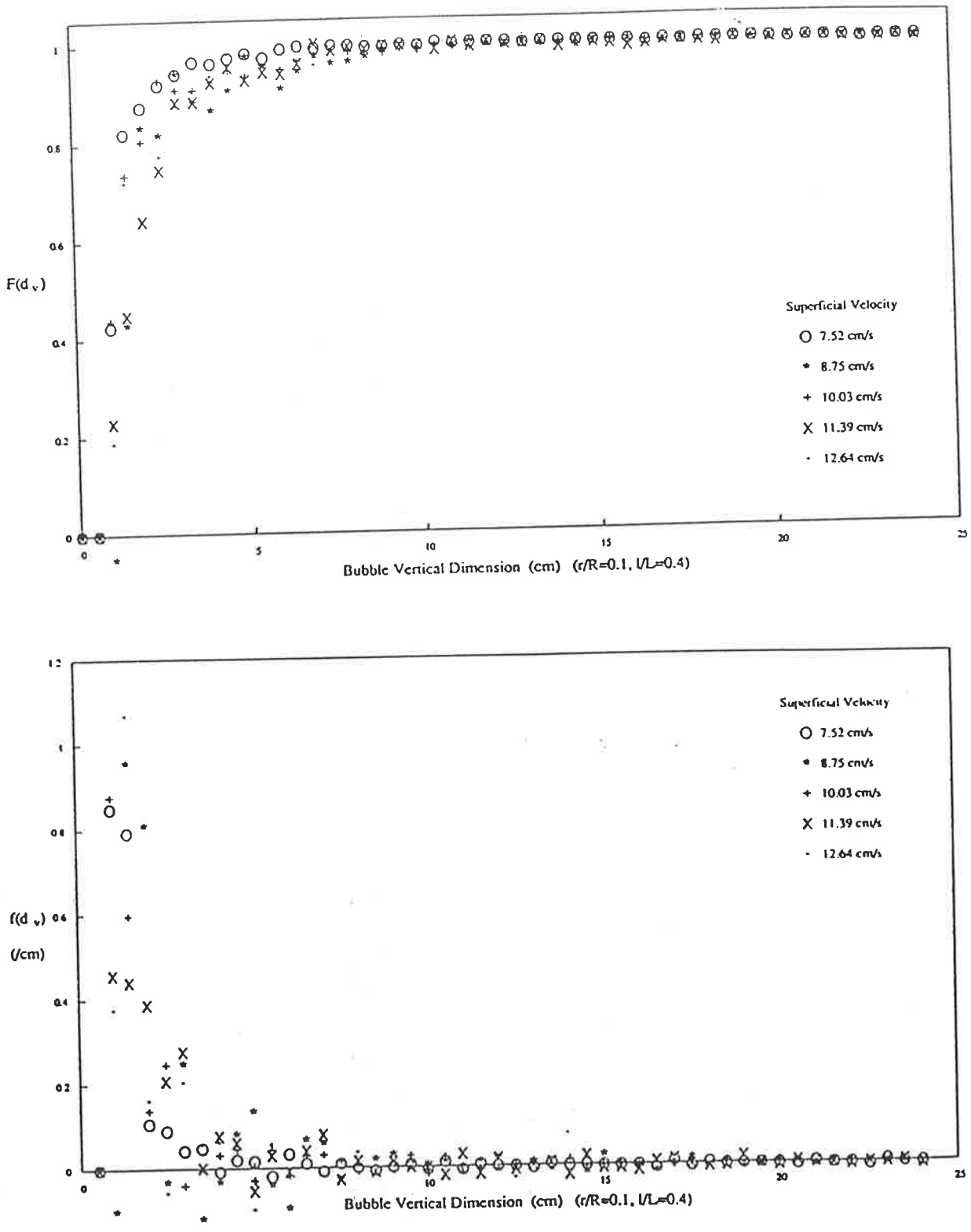

Figure 5.15 Cumulative Distribution and PDF of Bubble Vertical Dimension

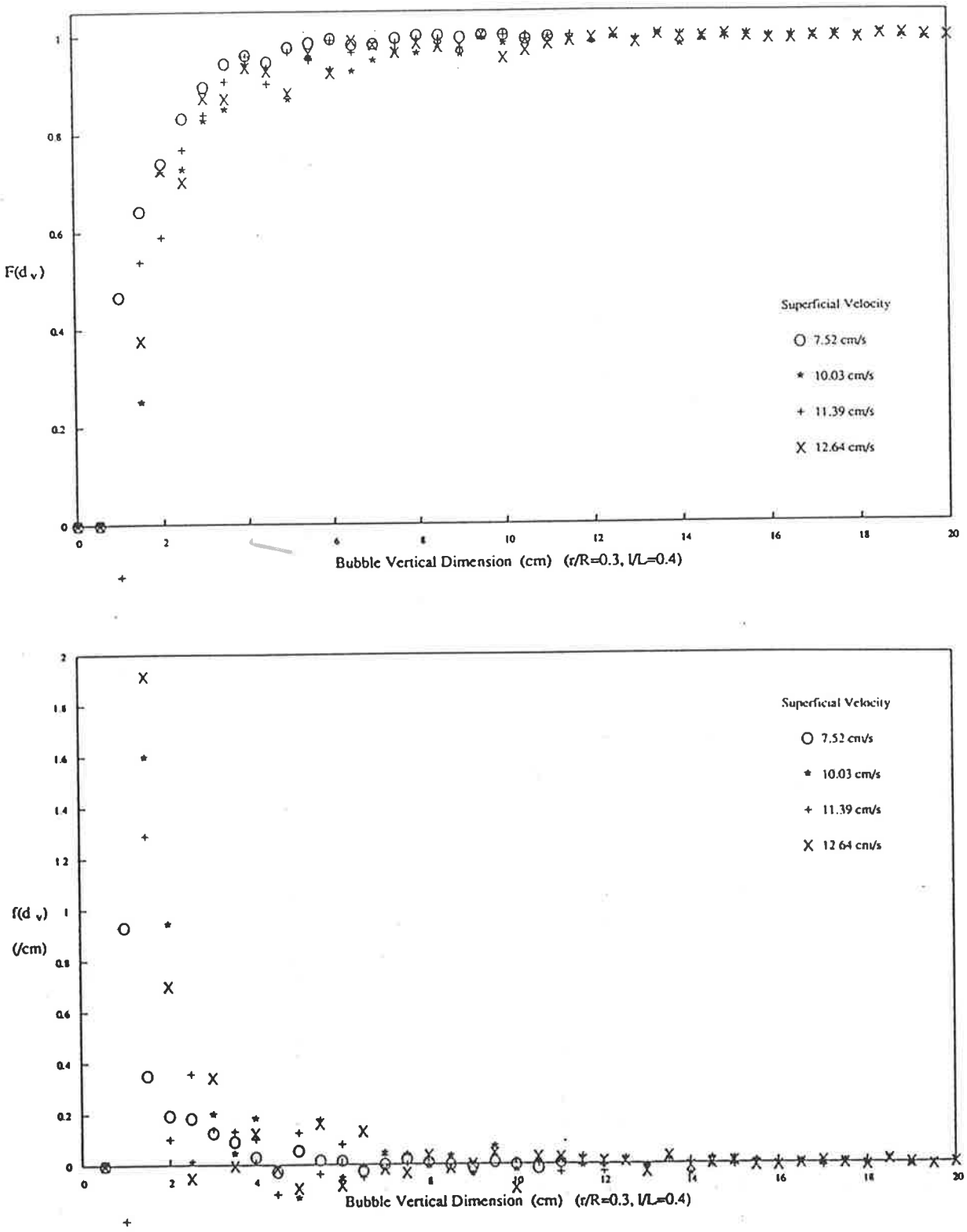

Figure 5.16 Cumulative Distribution and PDF of Bubble Vertical Dimension

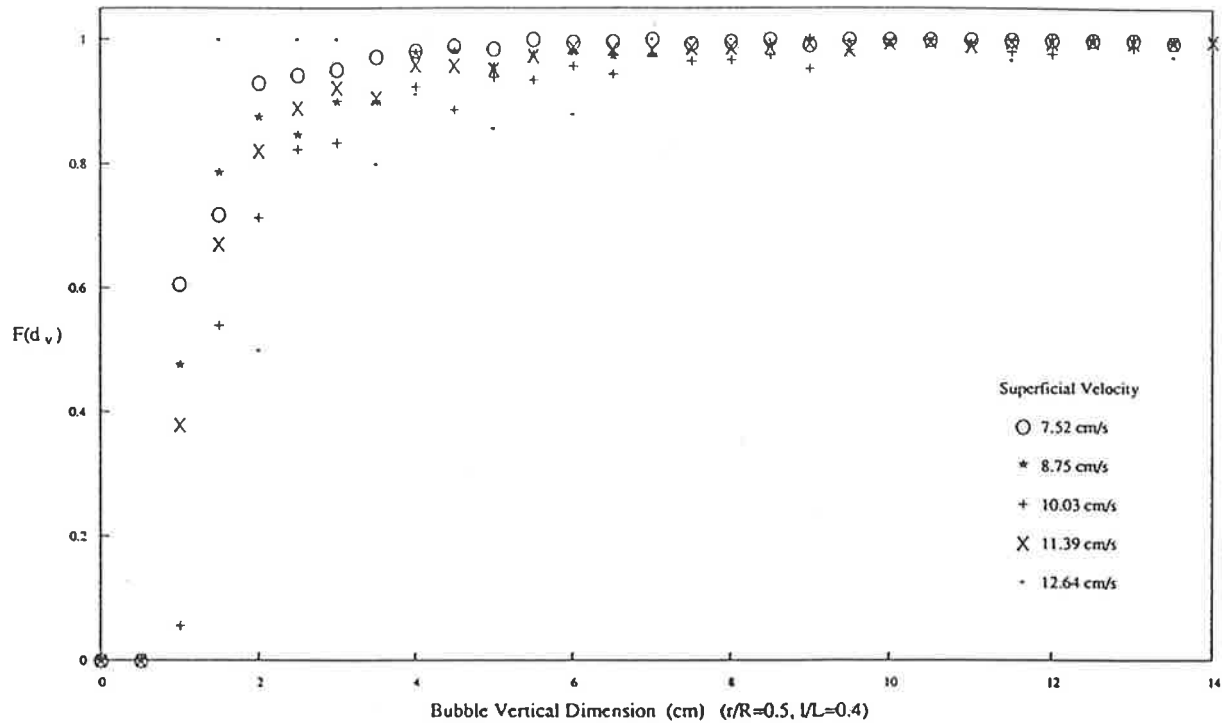

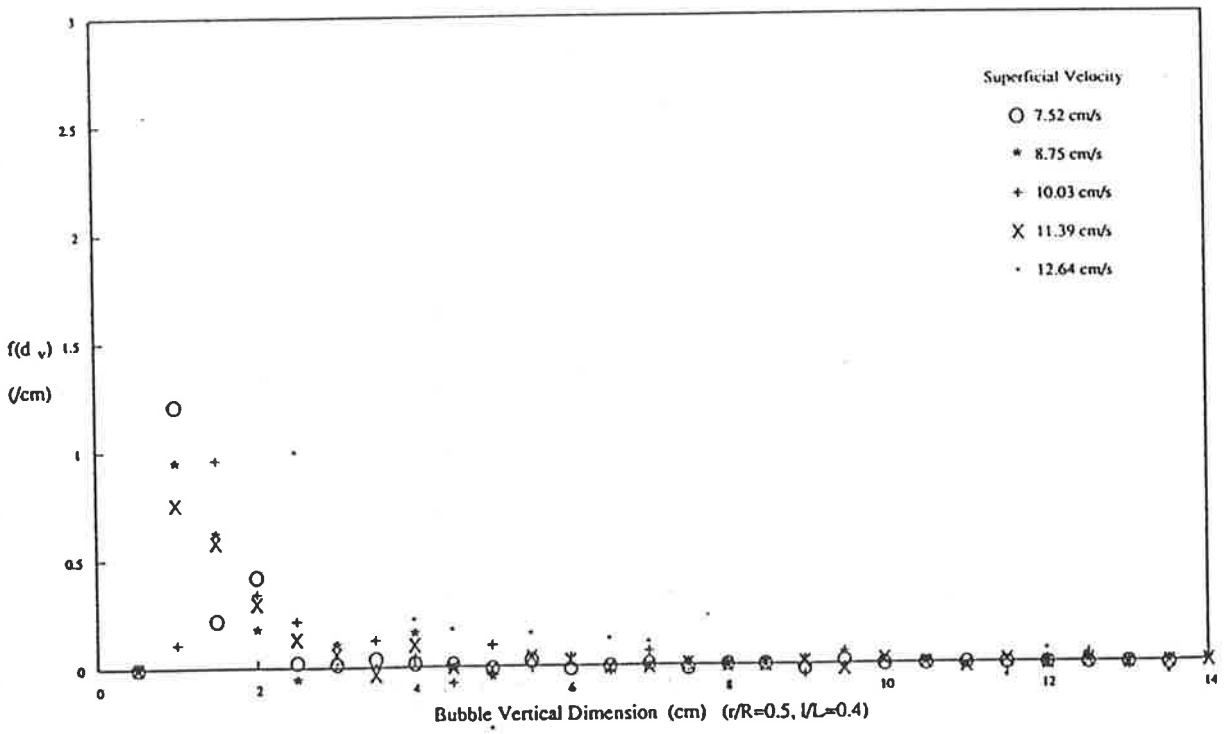

Figure 5.17 Cumulative Distribution and PDF of Bubble Vertical Dimension

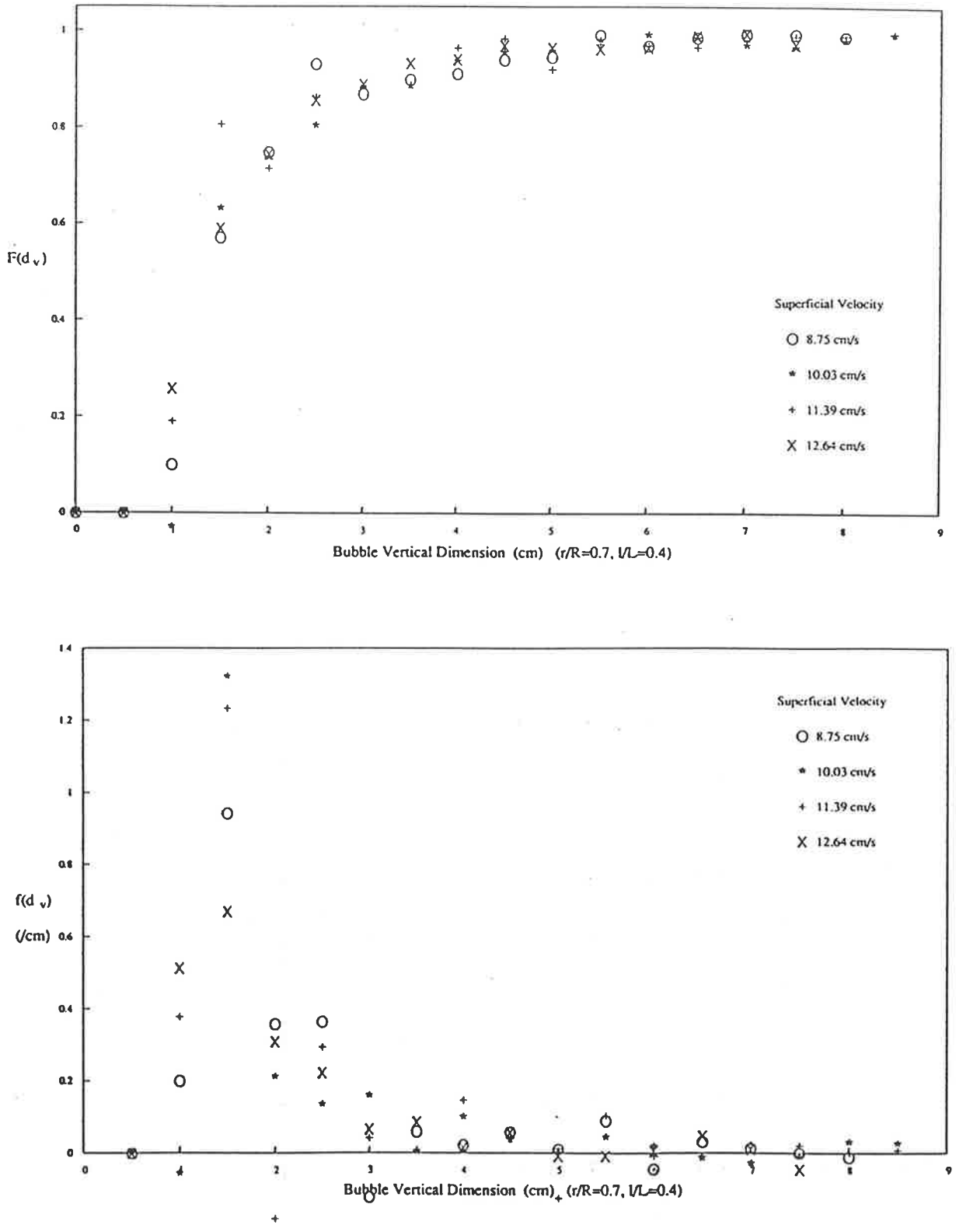

Figure 5.18 Cumulative Distribution and PDF of Bubble Vertical Dimension

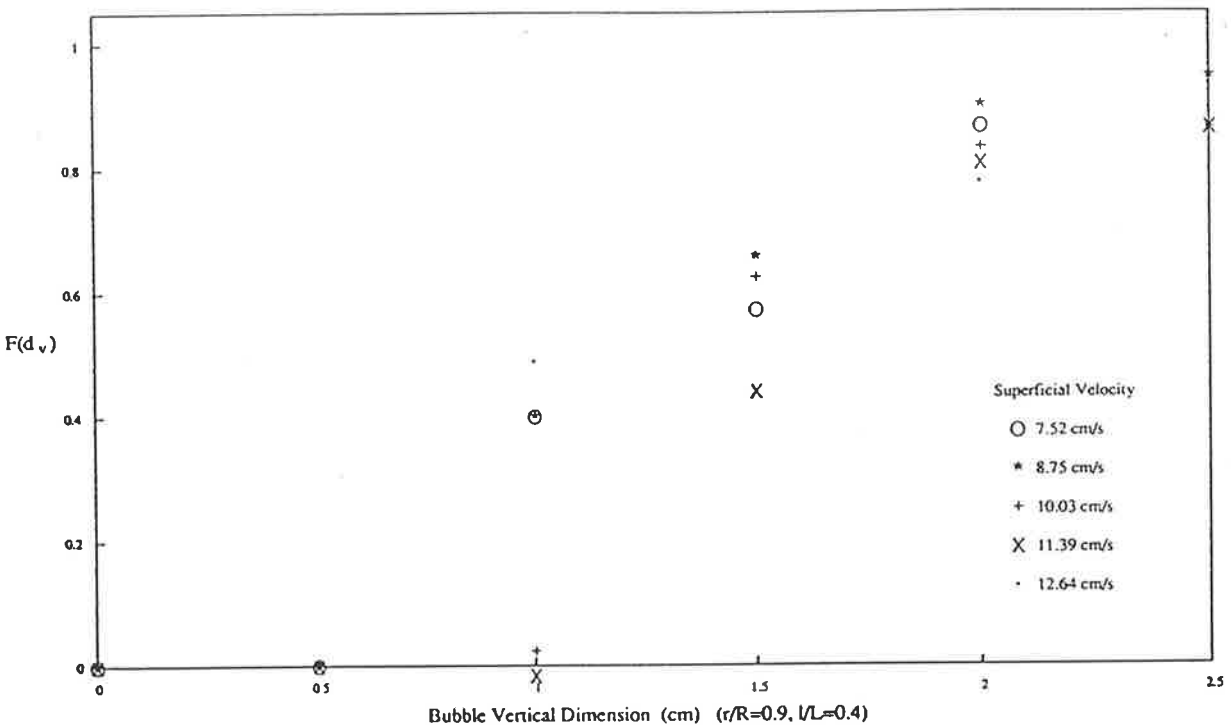

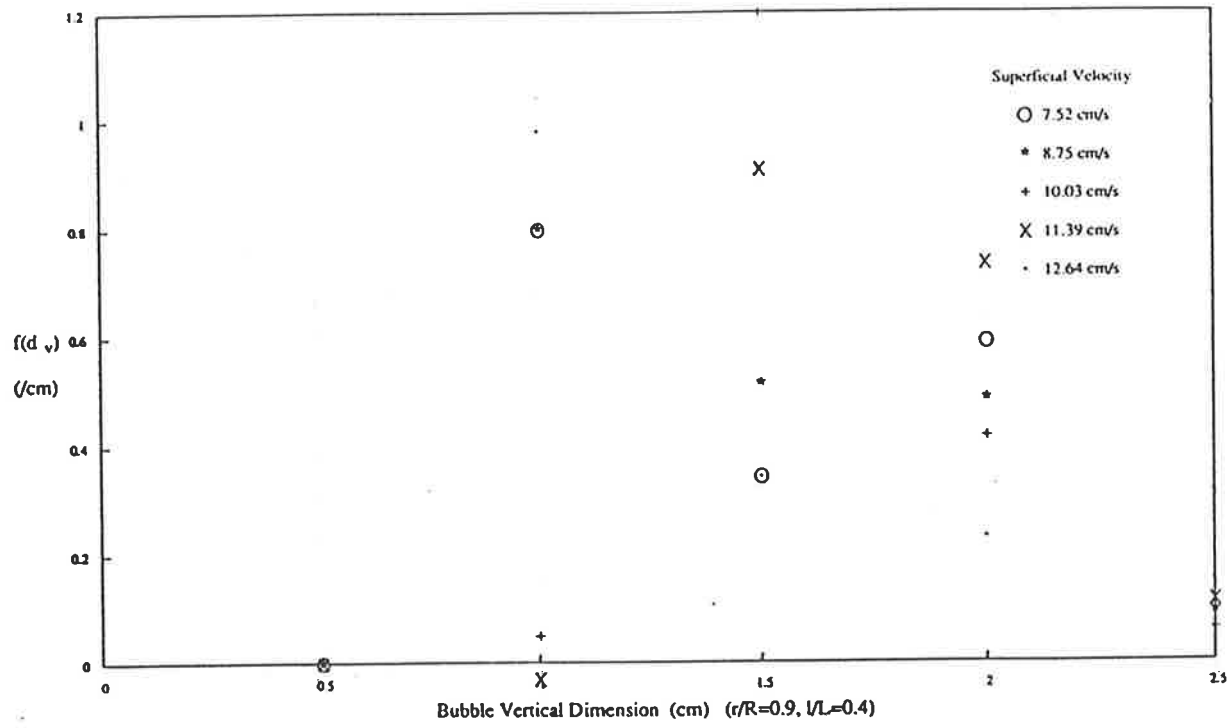

Figure 5.19 Cumulative Distribution and PDF of Bubble Vertical Dimension

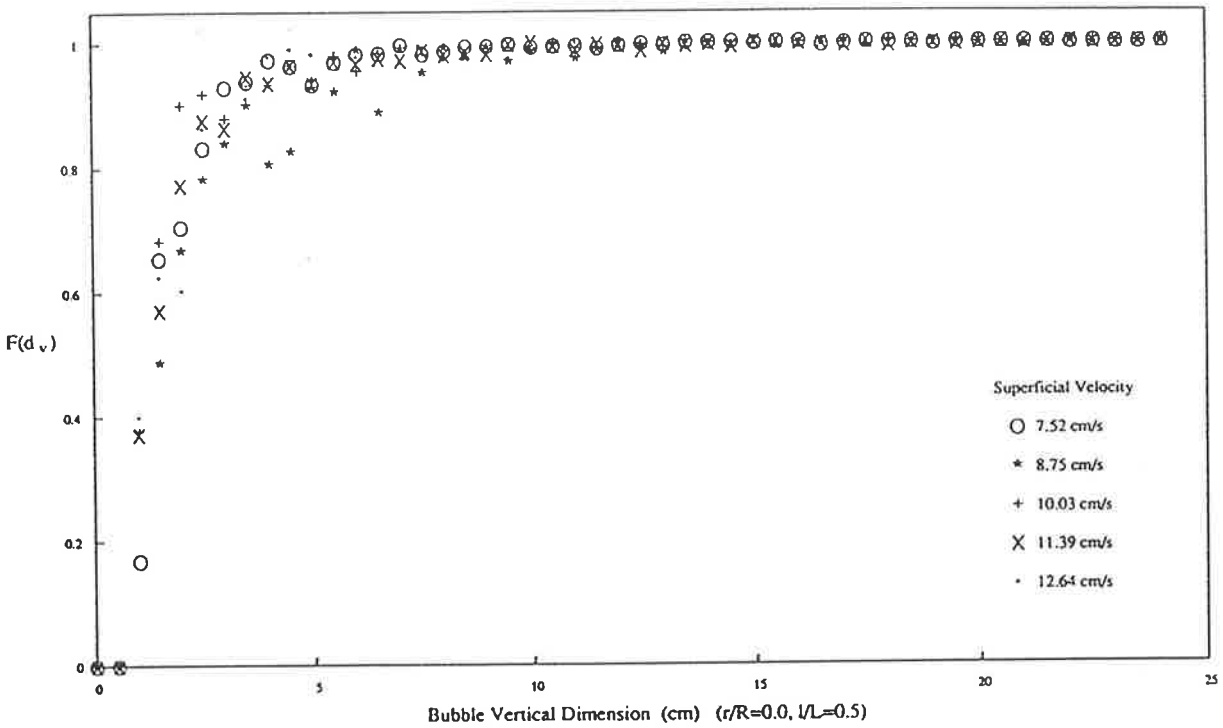

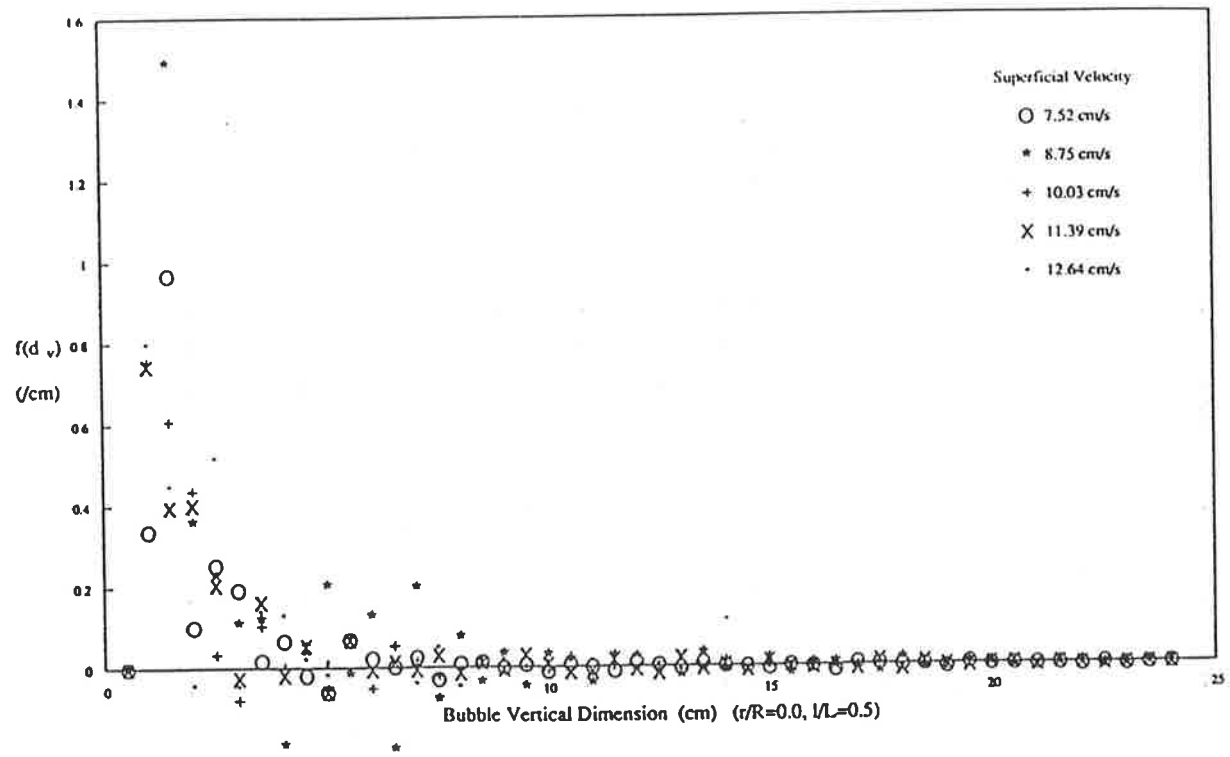

Figure 5.20 Cumulative Distribution and PDF of Bubble Vertical Dimension

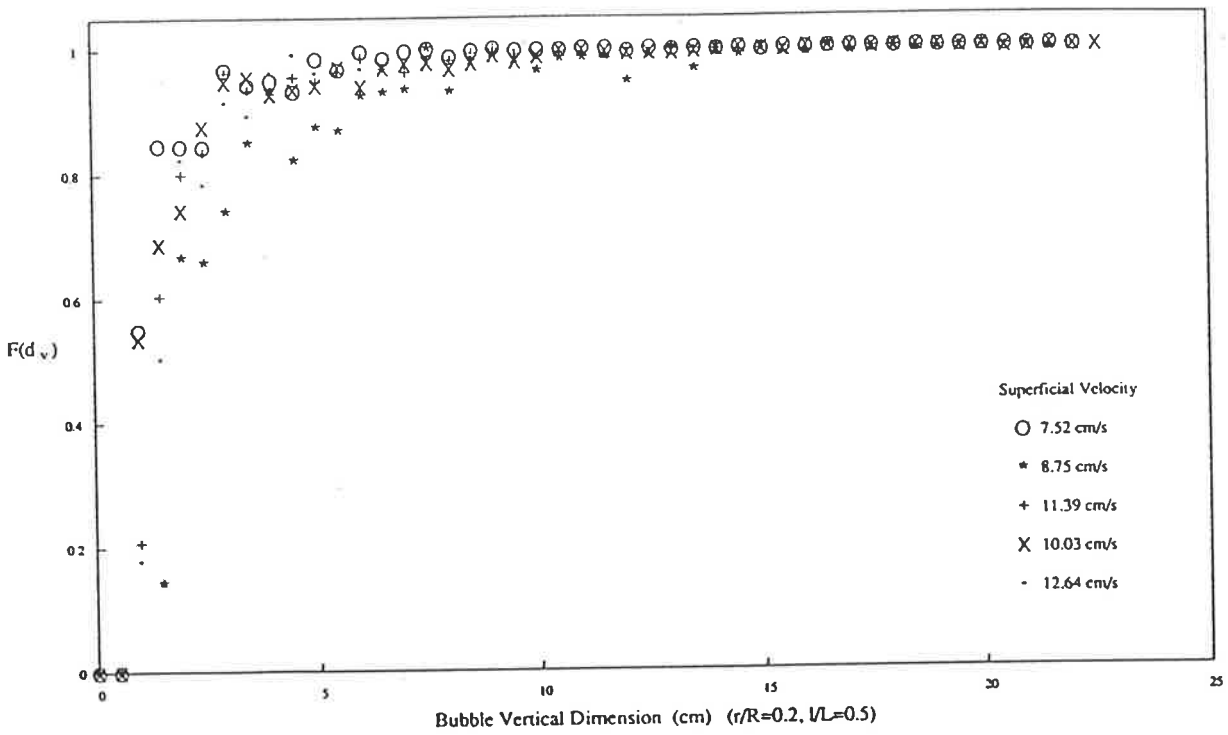

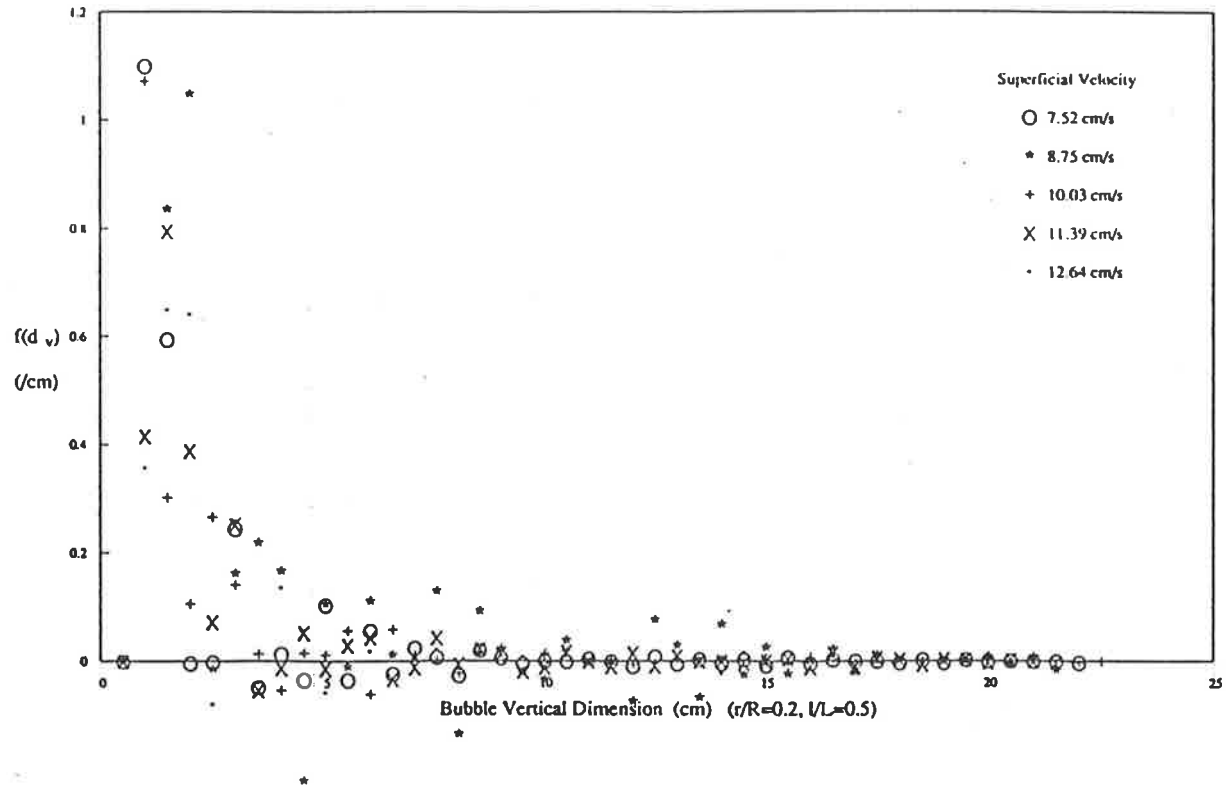

Figure 5.21 Cumulative Distribution and PDF of Bubble Vertical Dimension

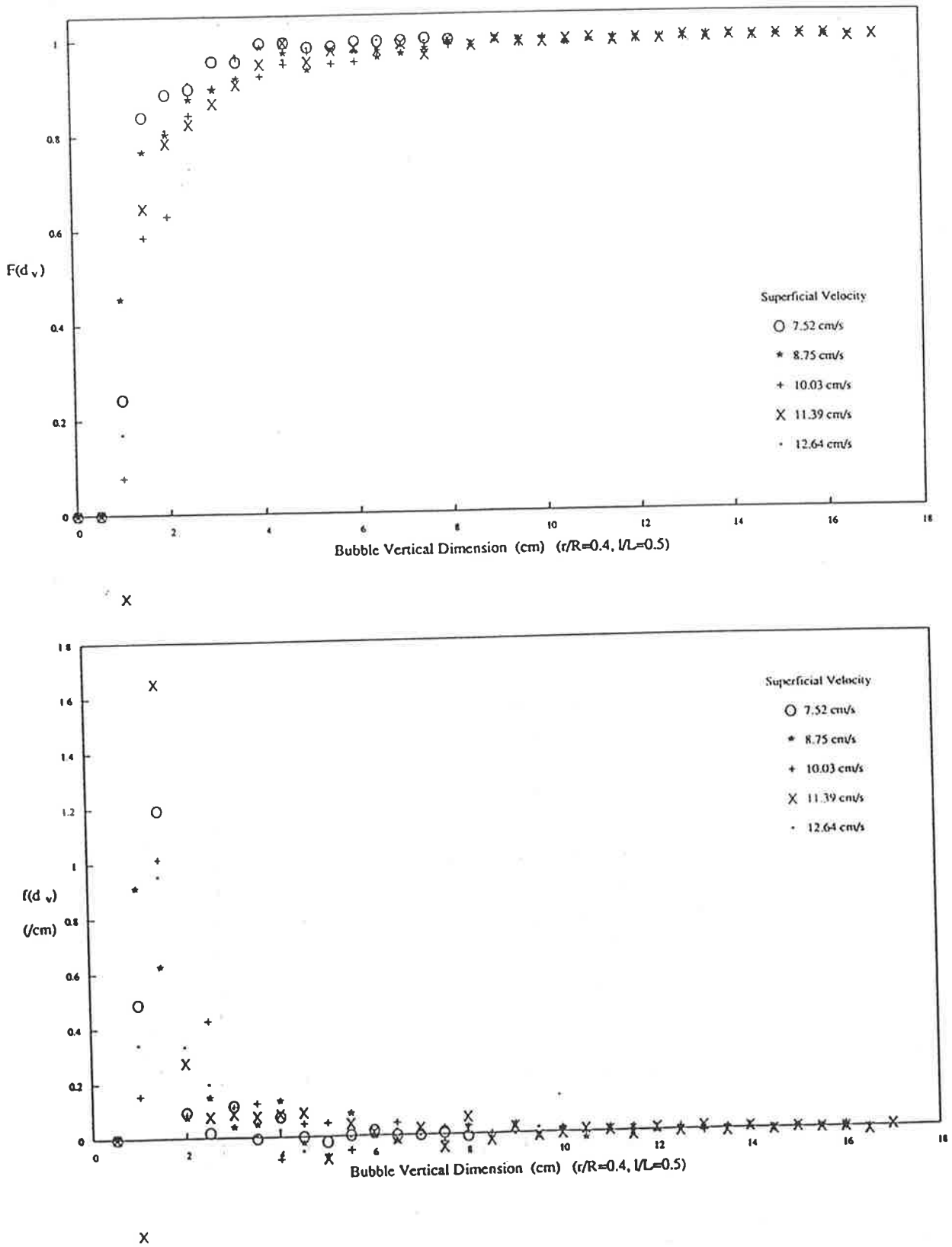

Figure 5.22 Cumulative Distribution and PDF of Bubble Vertical Dimension

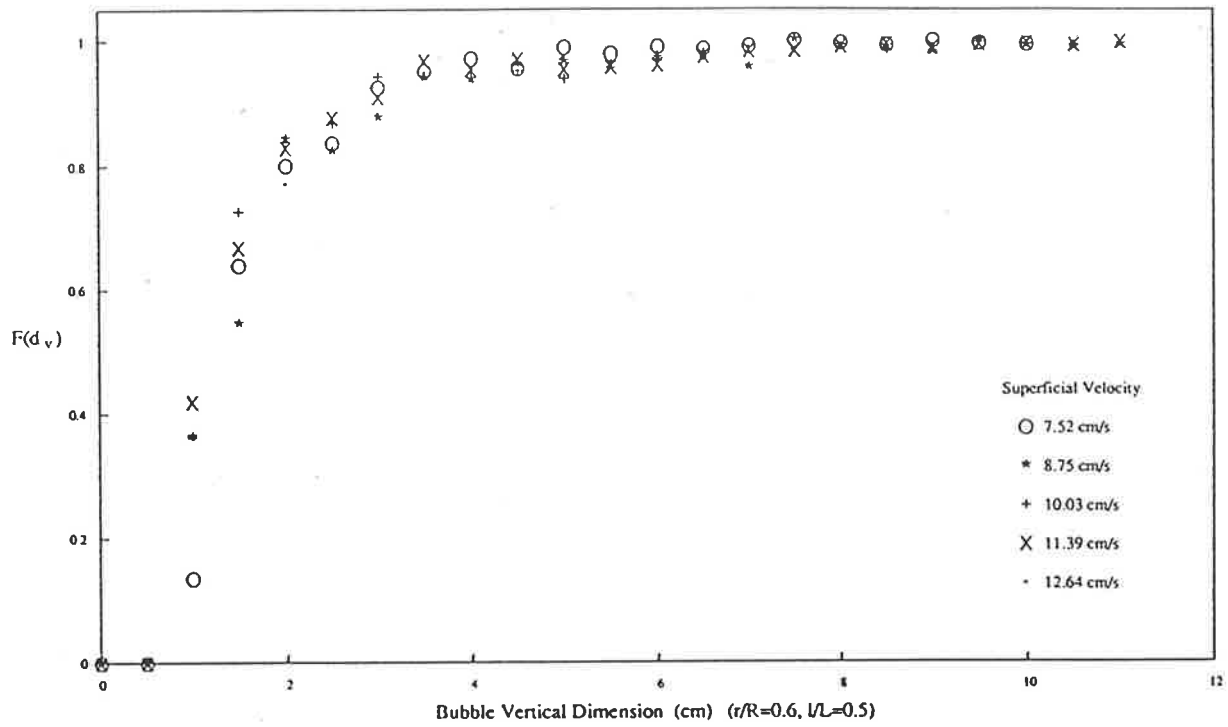

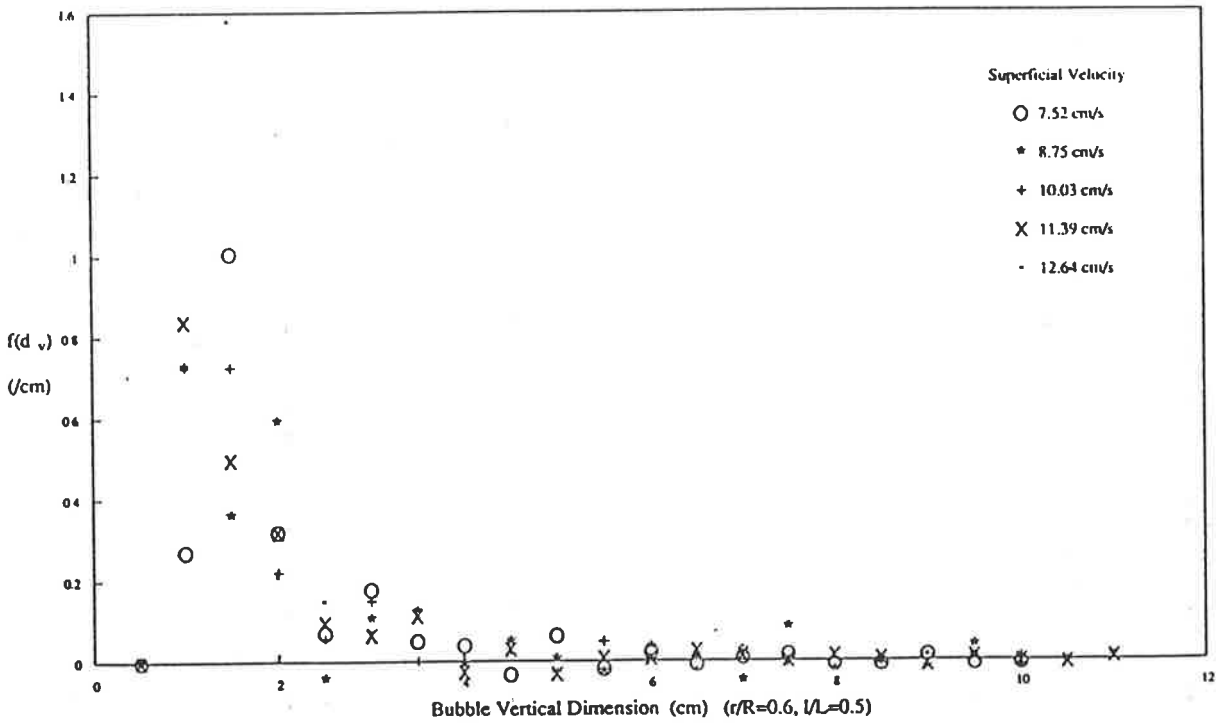

Figure 5.23 Cumulative Distribution and PDF of Bubble Vertical Dimension

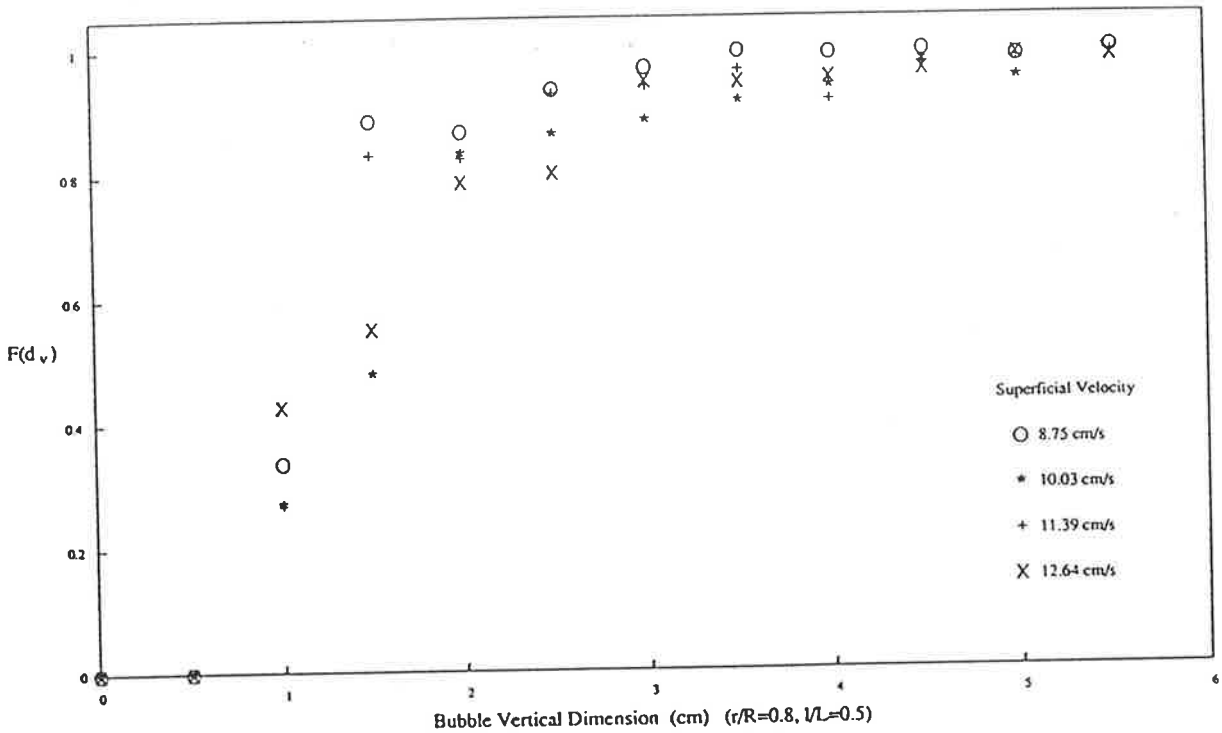

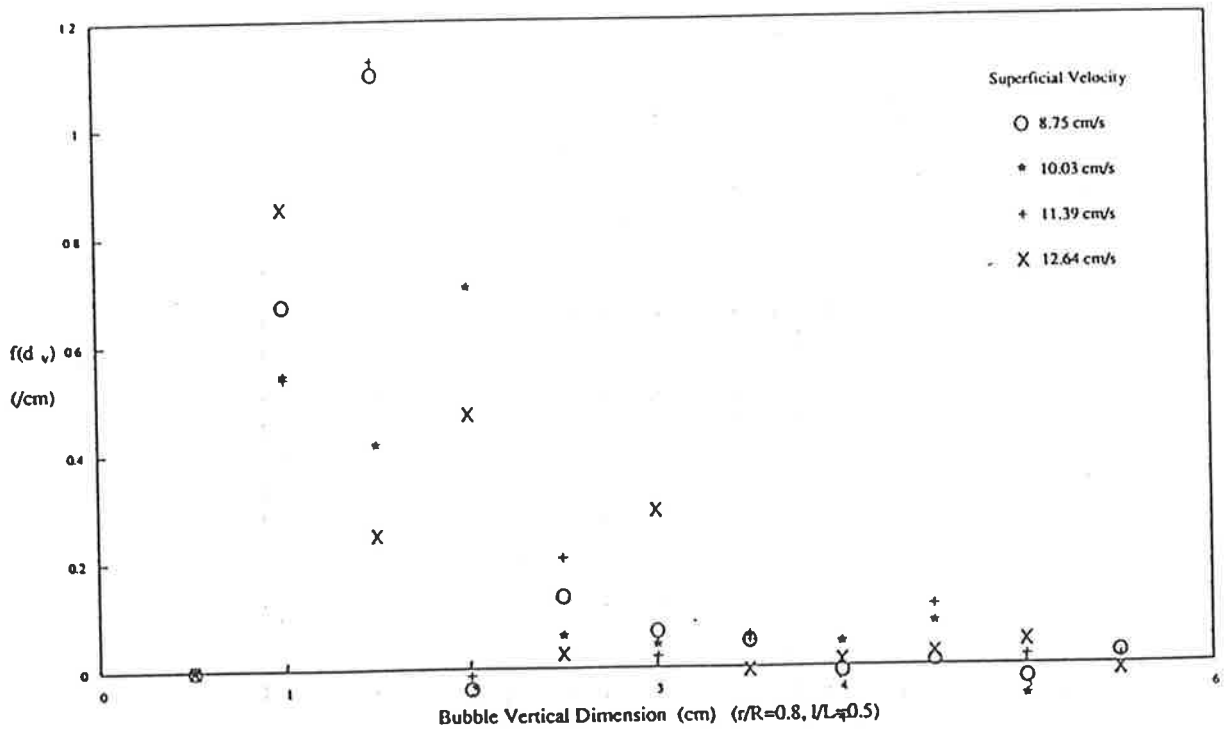

Figure 5.24 Cumulative Distribution and PDF of Bubble Vertical Dimension

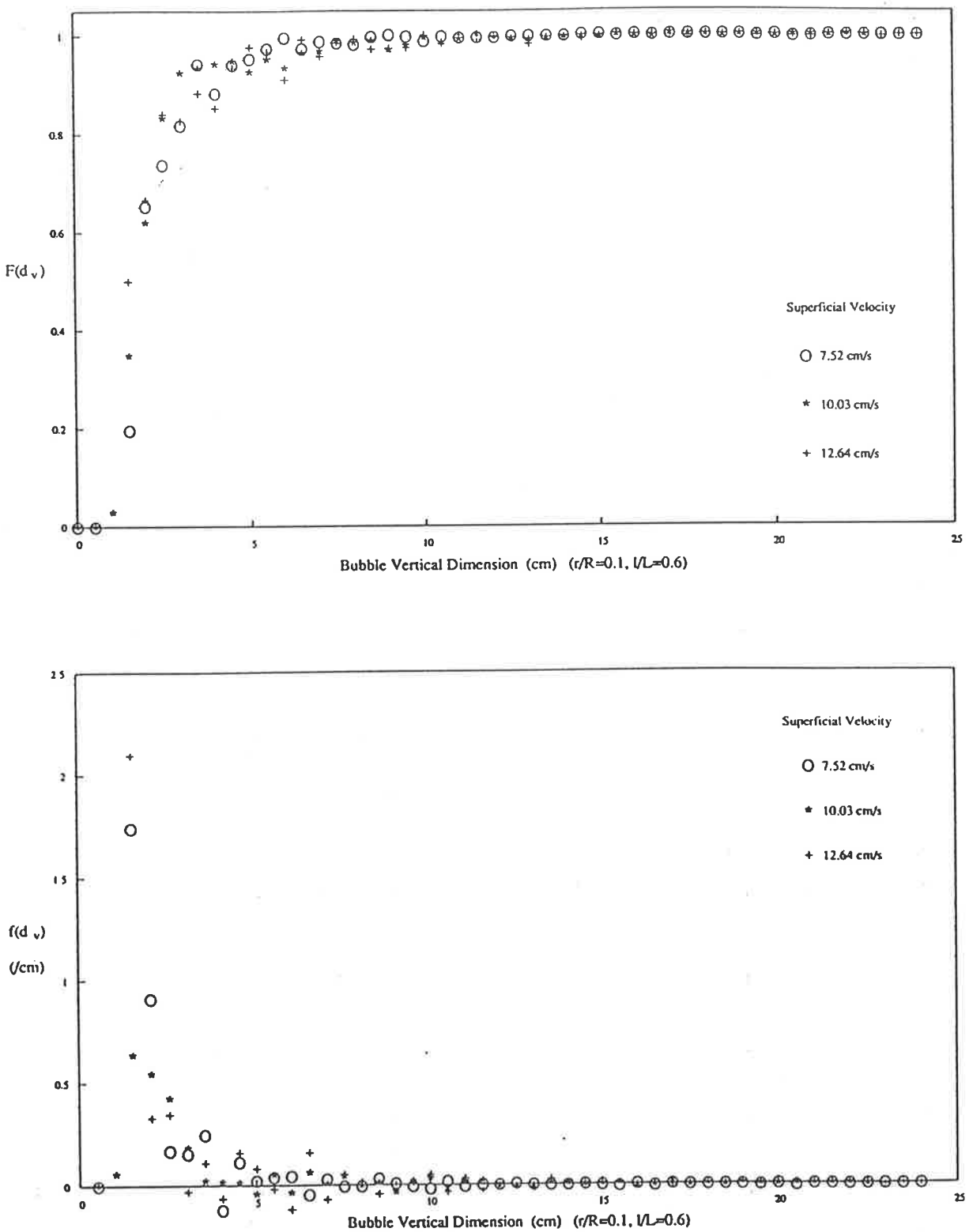

Figure 5.25 Cumulative Distribution and PDF of Bubble Vertical Dimension

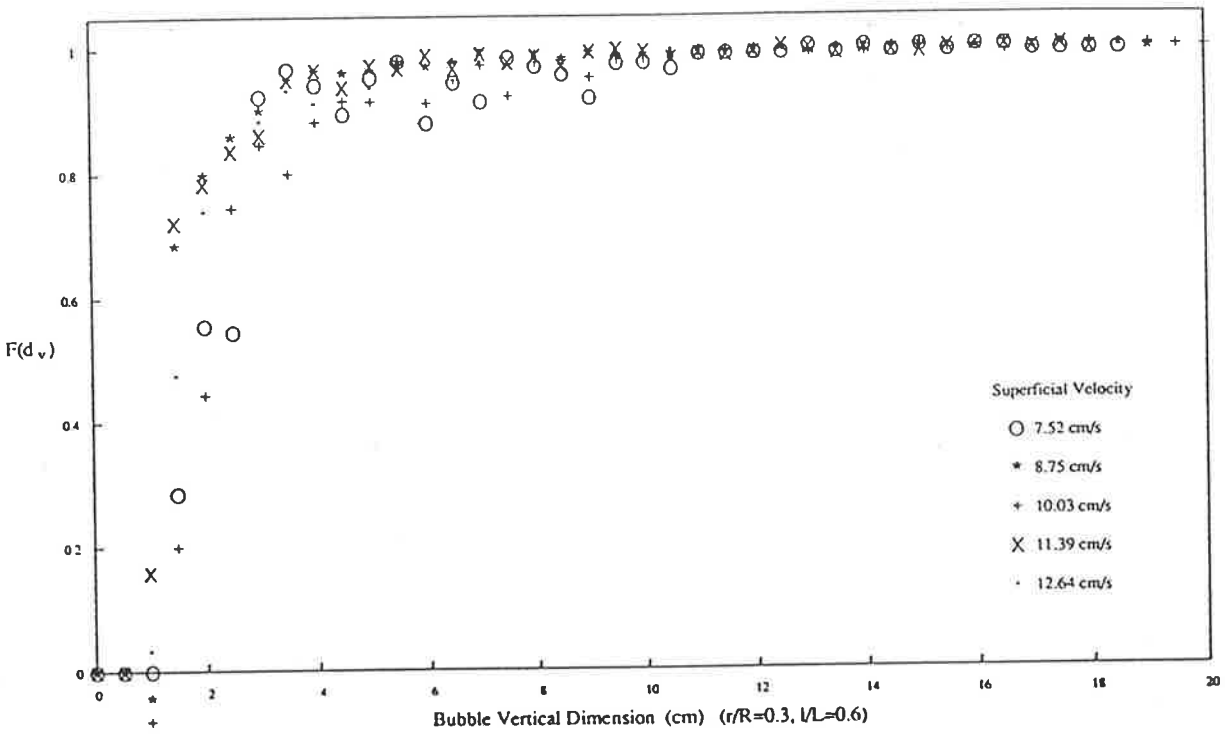

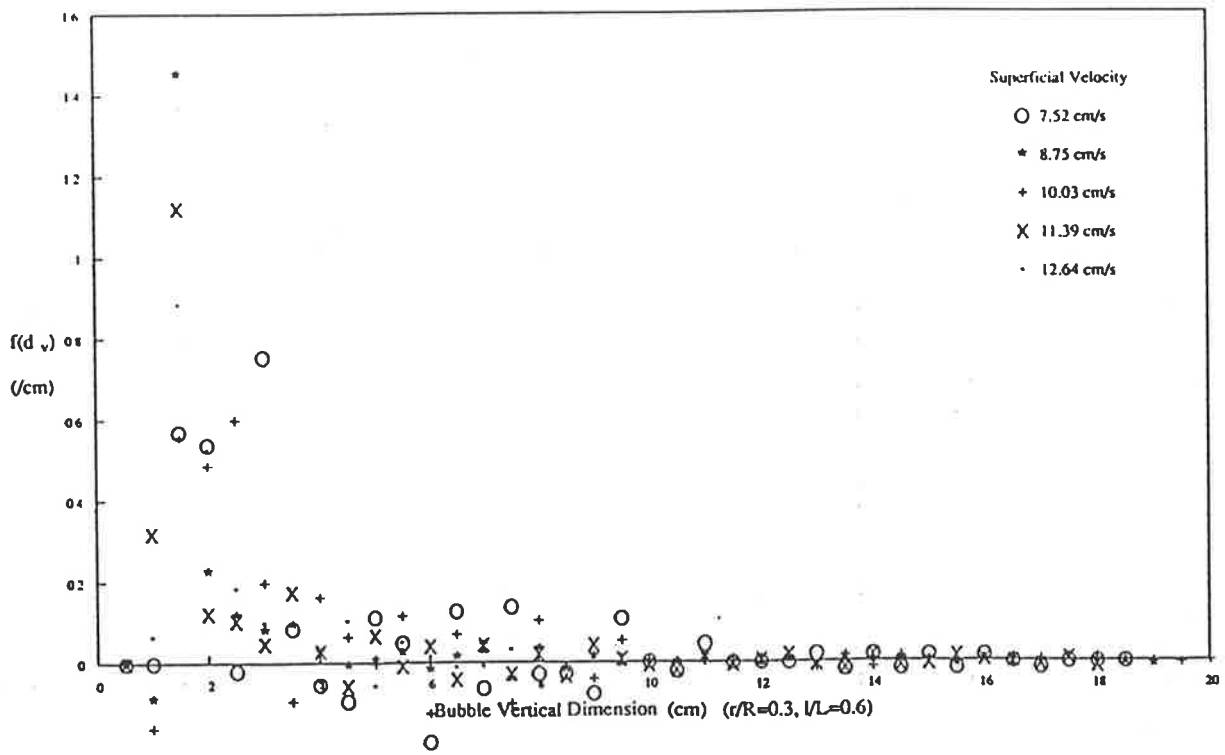

Figure 5.26 Cumulative Distribution and PDF of Bubble Vertical Dimension

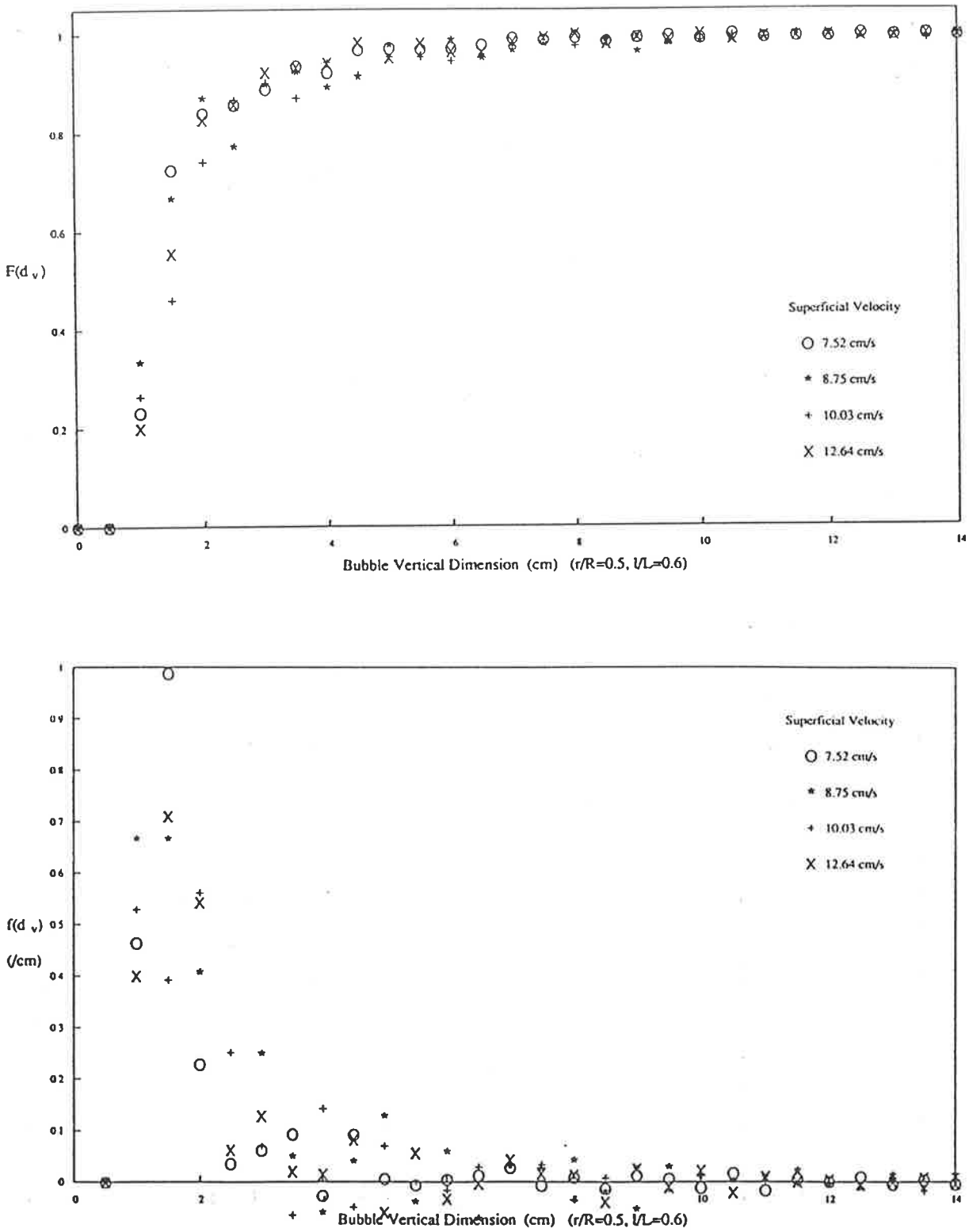

Figure 5.27 Cumulative Distribution and PDF of Bubble Vertical Dimension

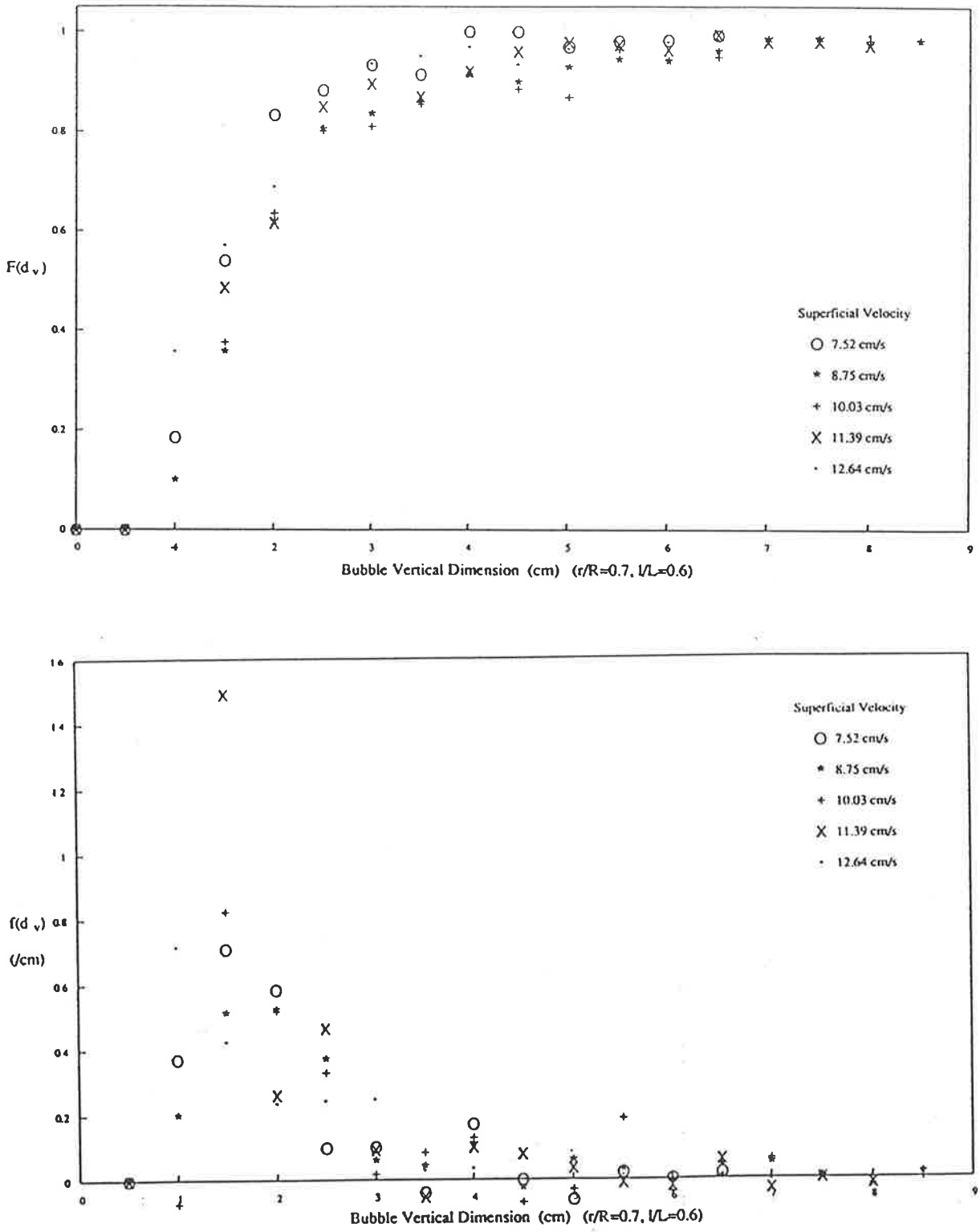

Figure 5.28 Cumulative Distribution and PDF of Bubble Vertical Dimension

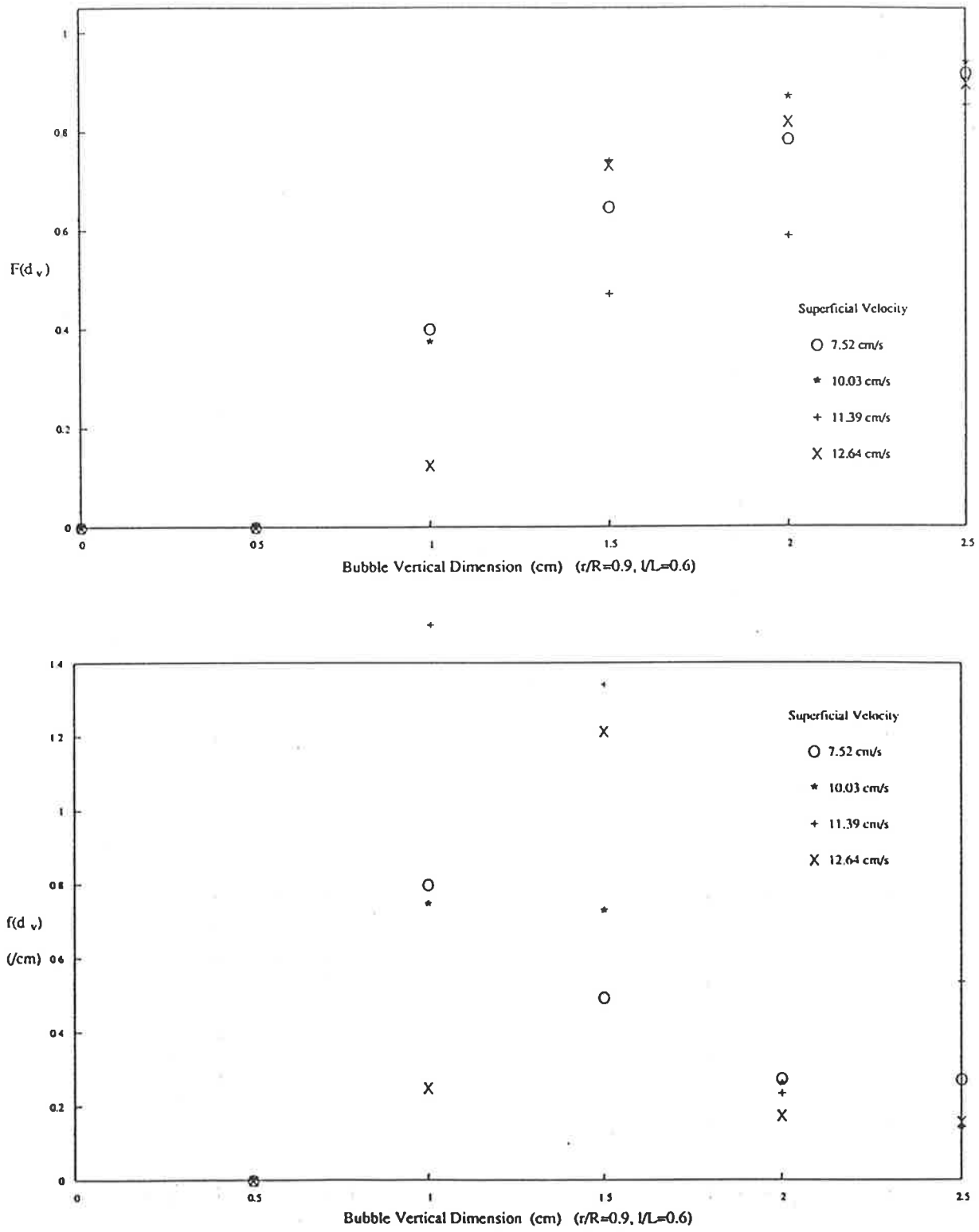

Figure 5.29 Cumulative Distribution and PDF of Bubble Vertical Dimension

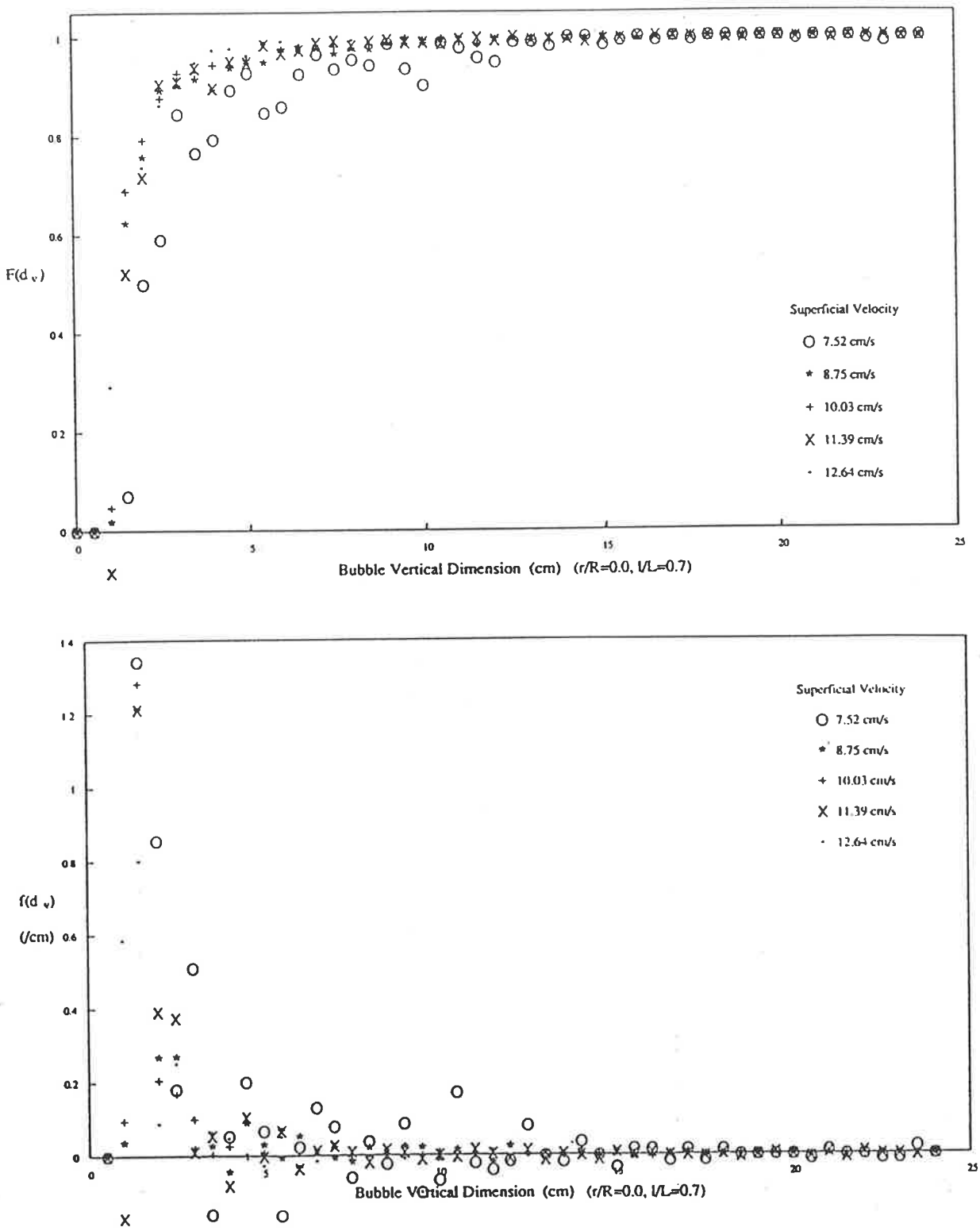

Figure 5.30 Cumulative Distribution and PDF of Bubble Vertical Dimension

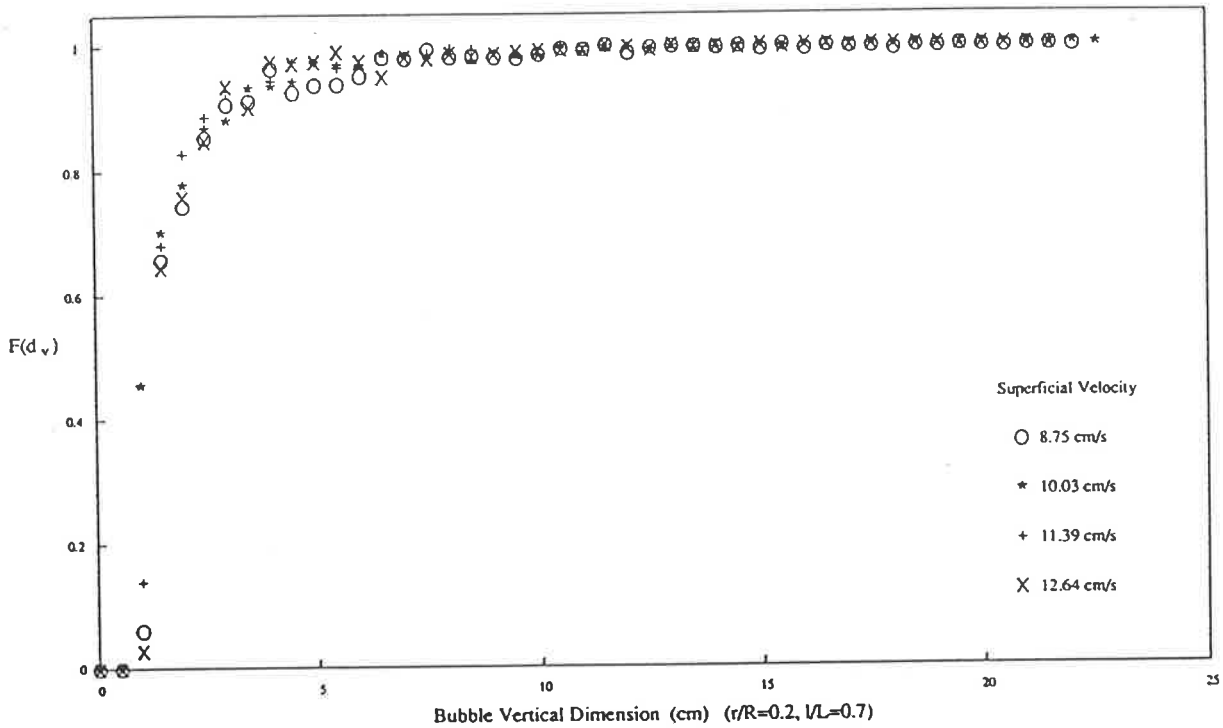

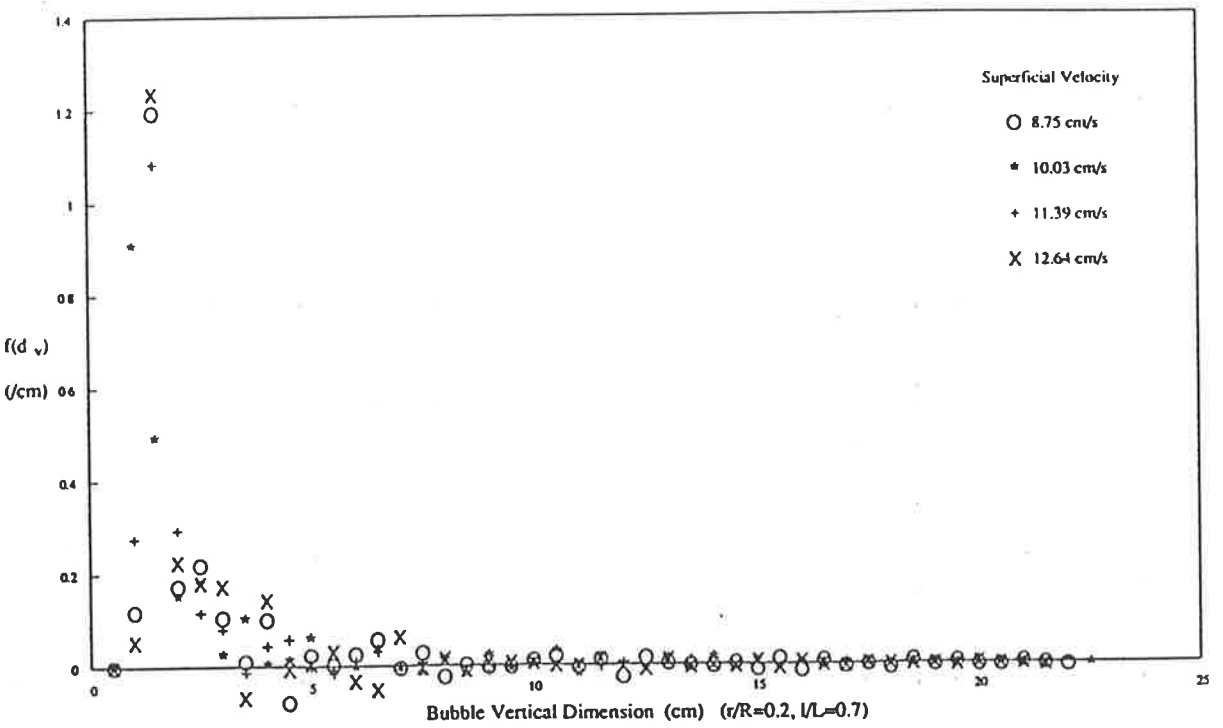

Figure 5.31 Cumulative Distribution and PDF of Bubble Vertical Dimension

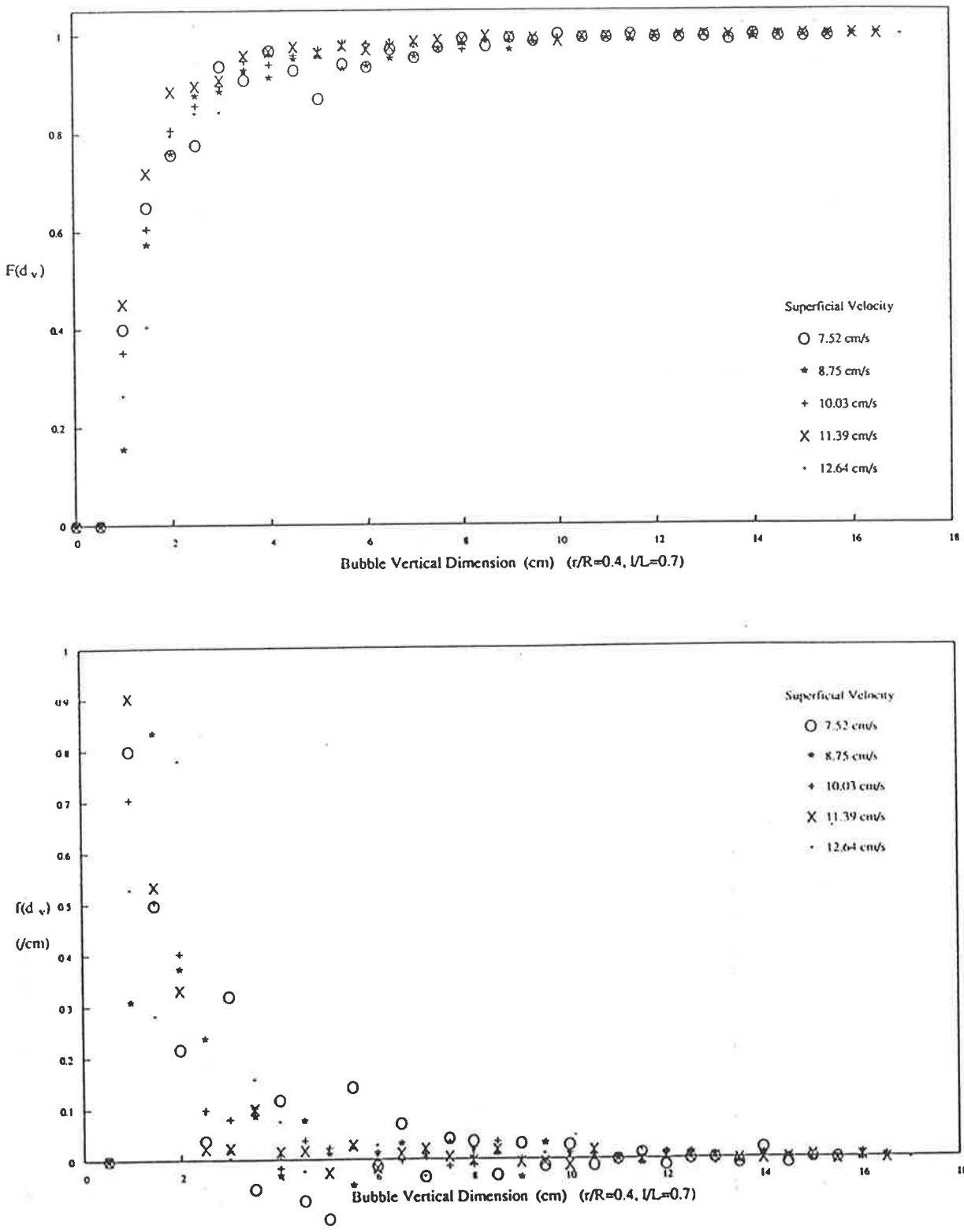

Figure 5.32 Cumulative Distribution and PDF of Bubble Vertical Dimension

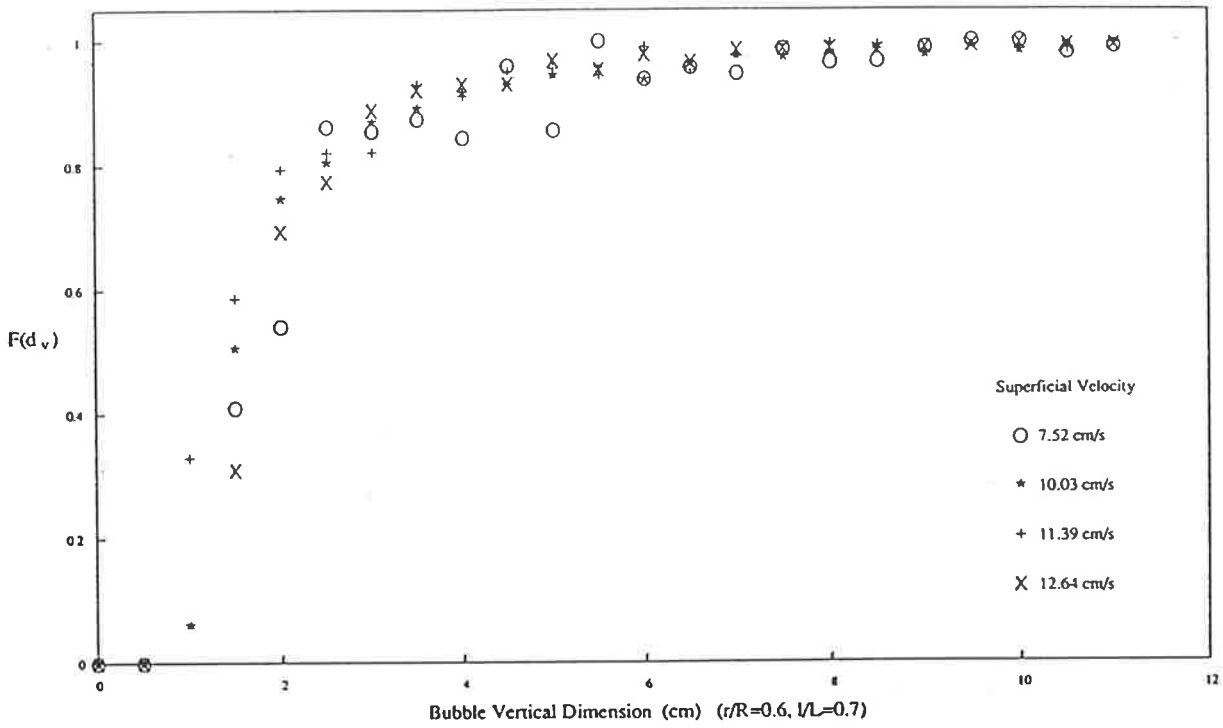

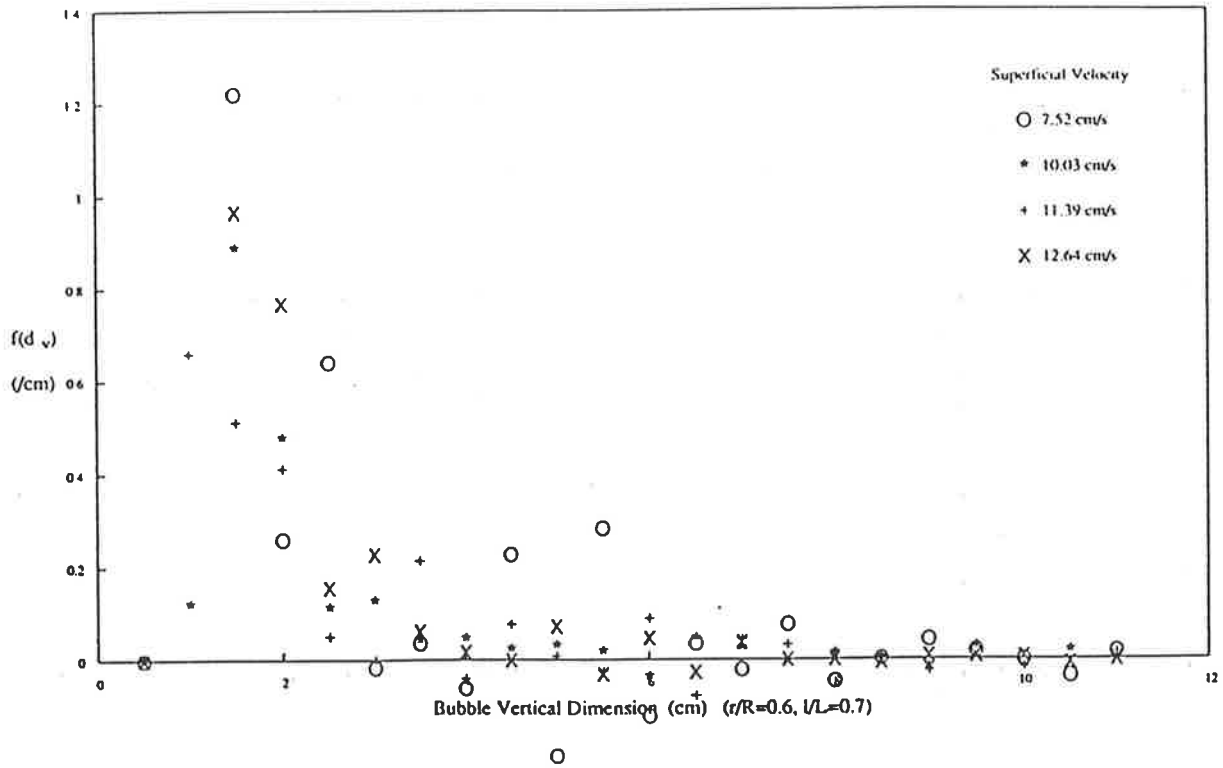

Figure 5.33 Cumulative Distribution and PDF of Bubble Vertical Dimension

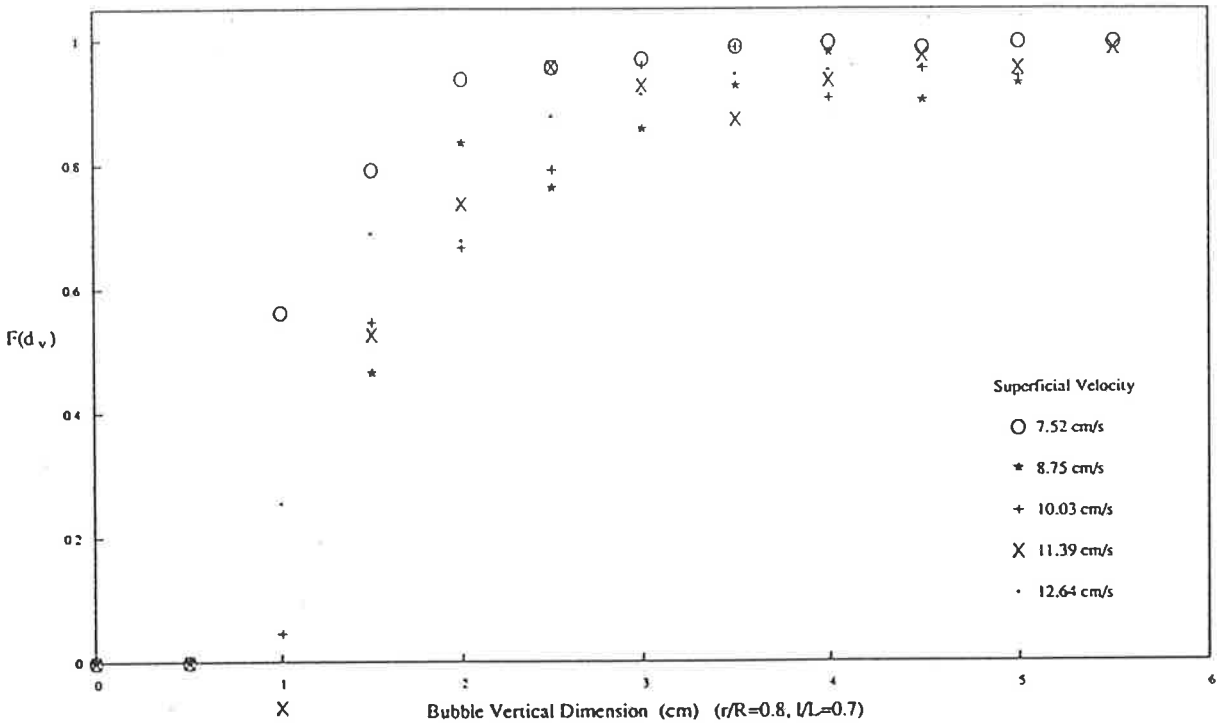

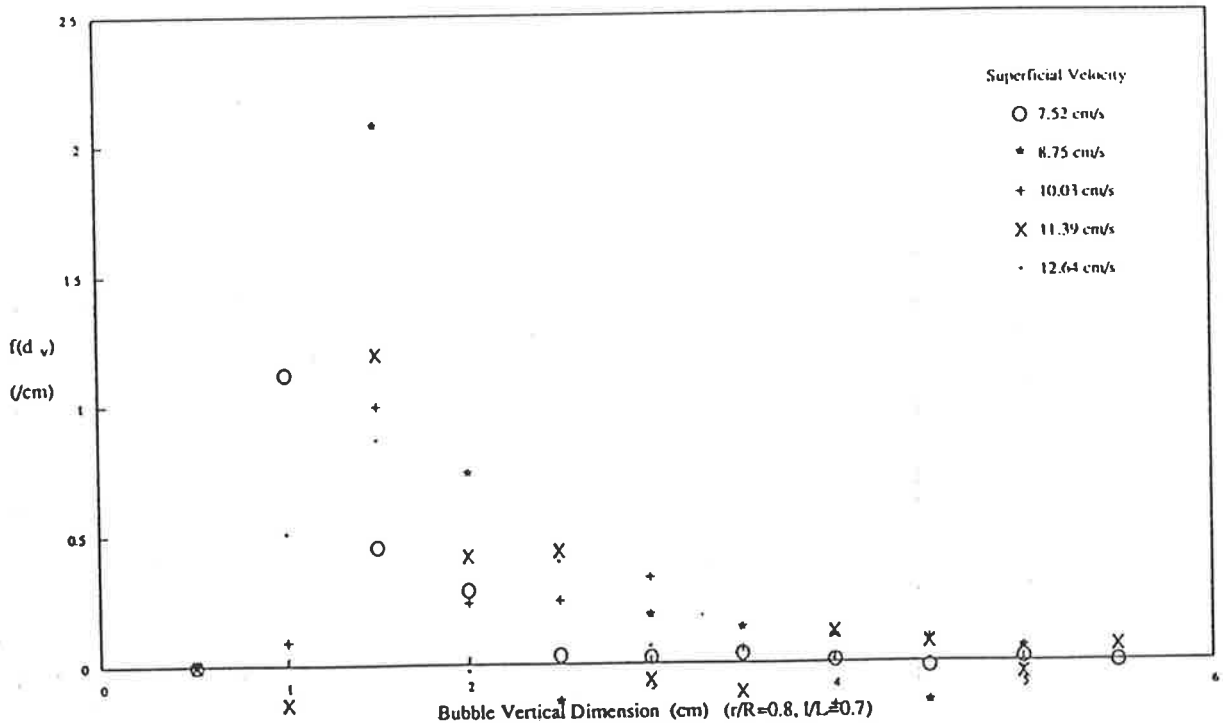

Figure 5.34 Cumulative Distribution and PDF of Bubble Vertical Dimension

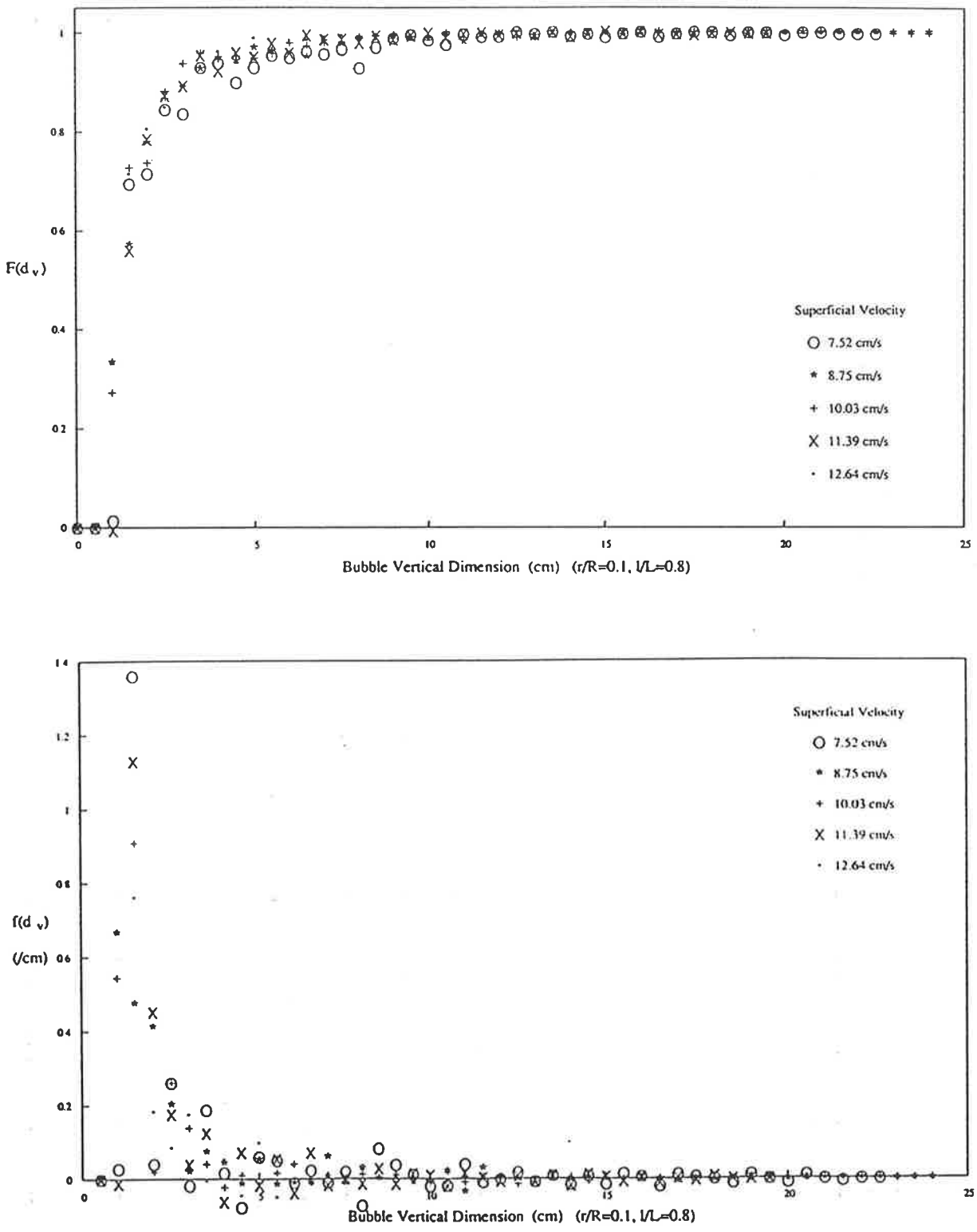

Figure 5.35 Cumulative Distribution and PDF of Bubble Vertical Dimension

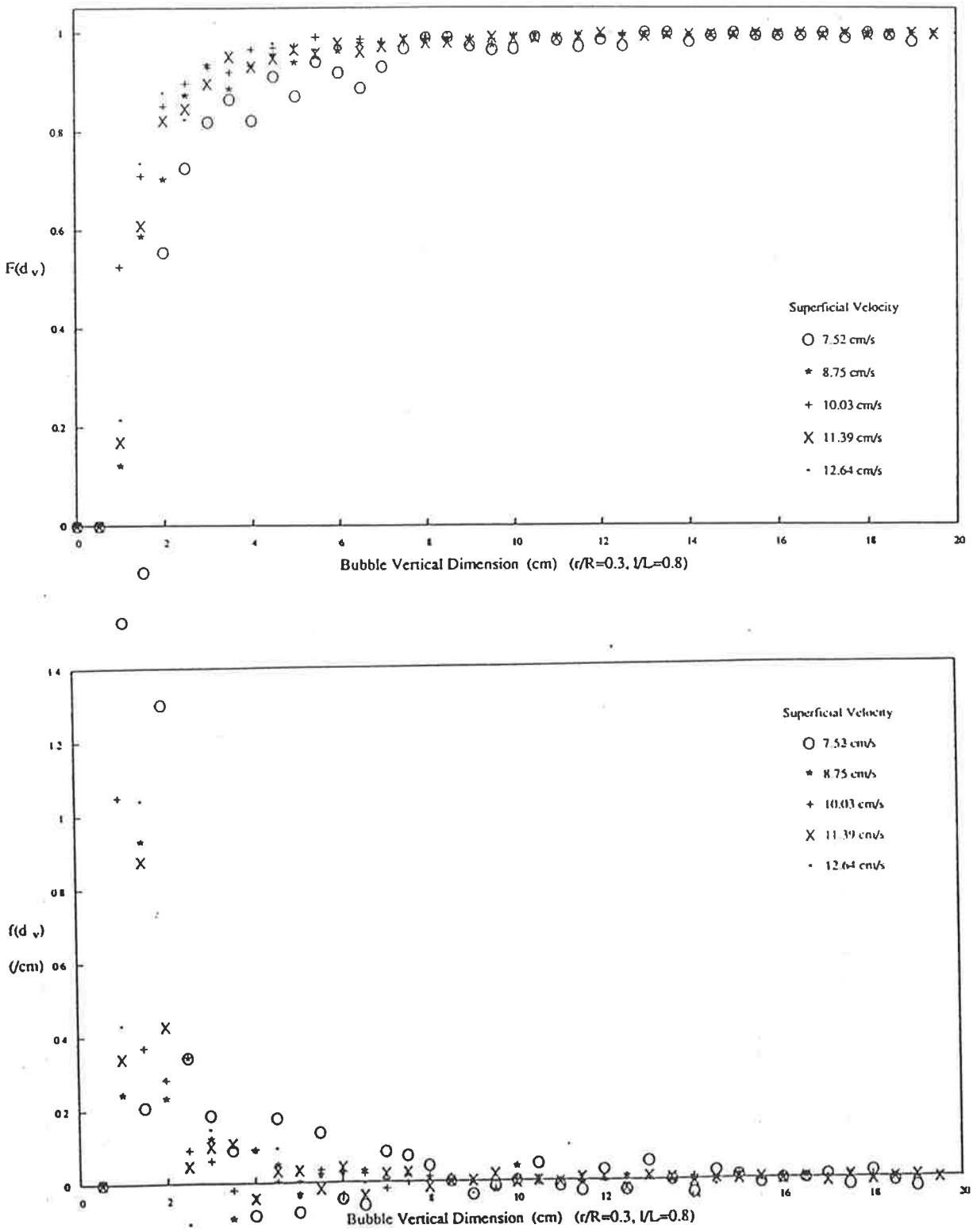

Figure 5.36 Cumulative Distribution and PDF of Bubble Vertical Dimension

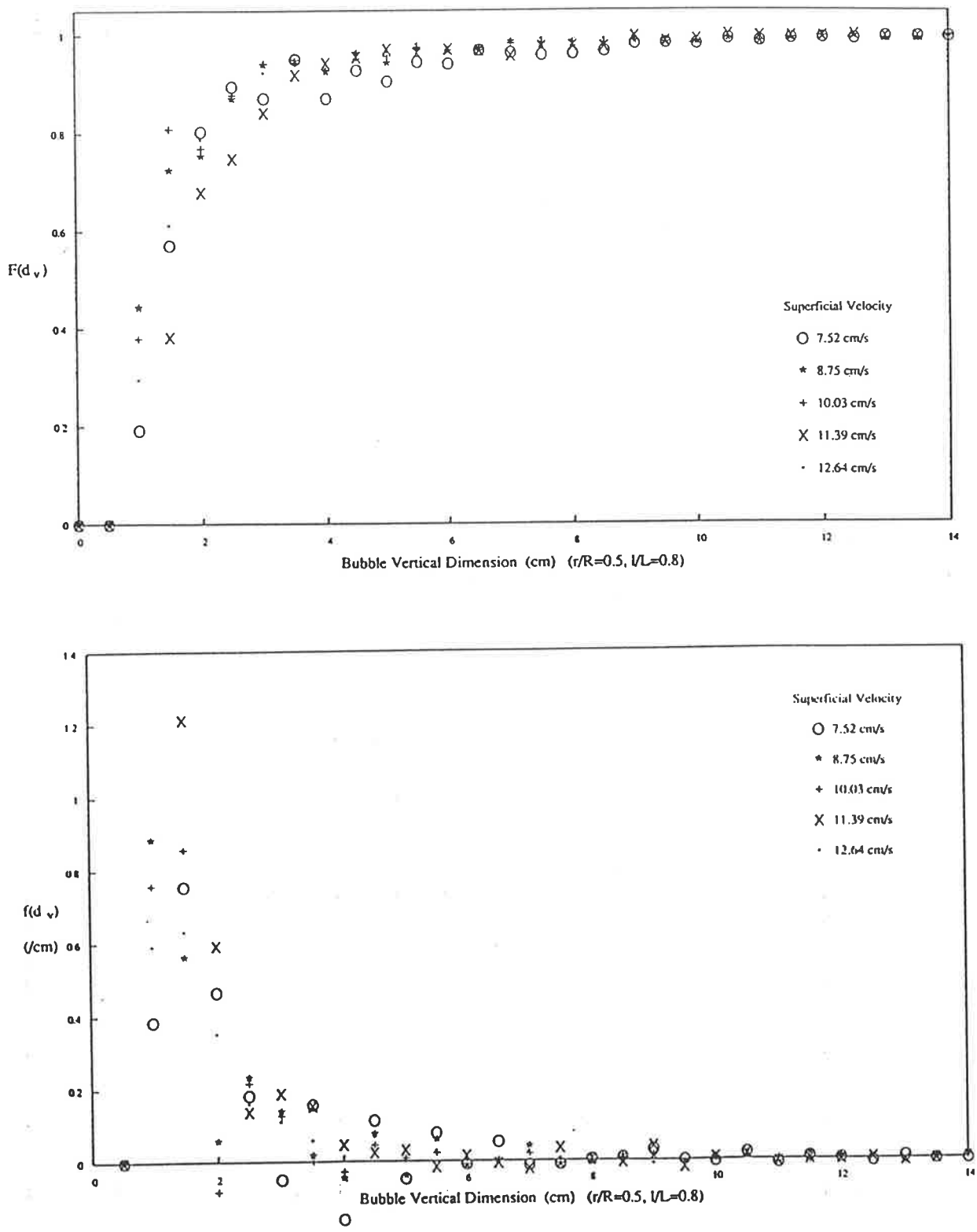

Figure 5.37 Cumulative Distribution and PDF of Bubble Vertical Dimension

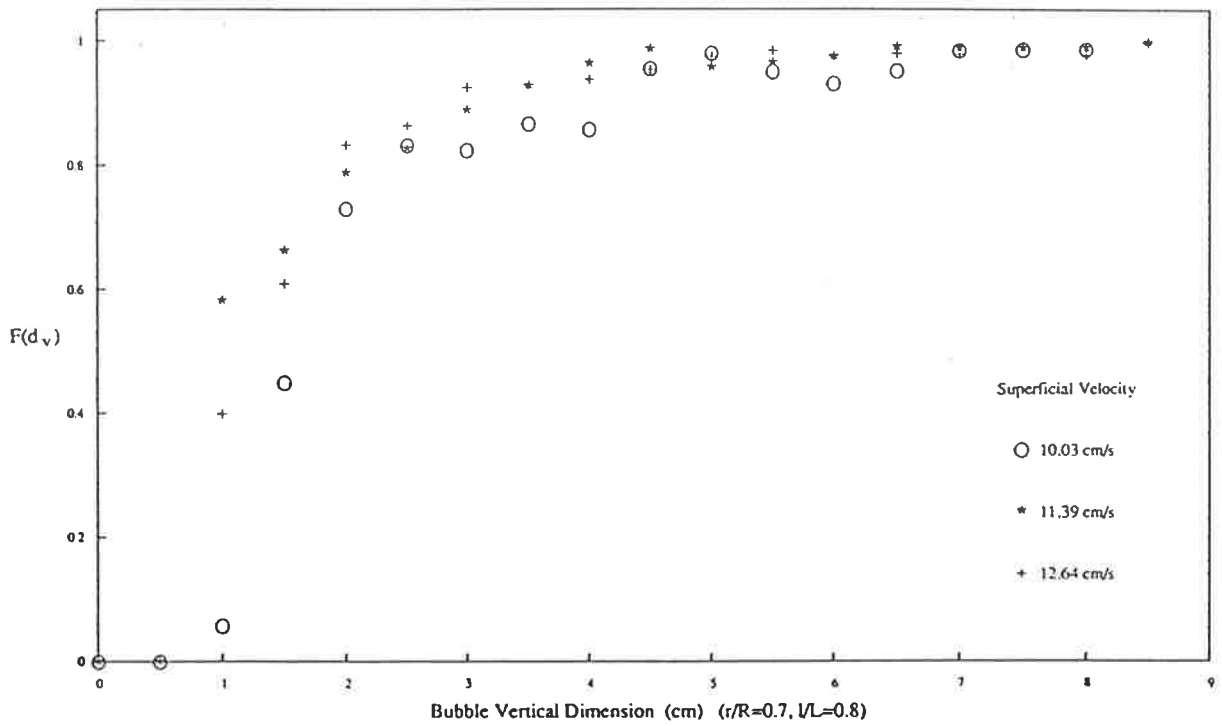

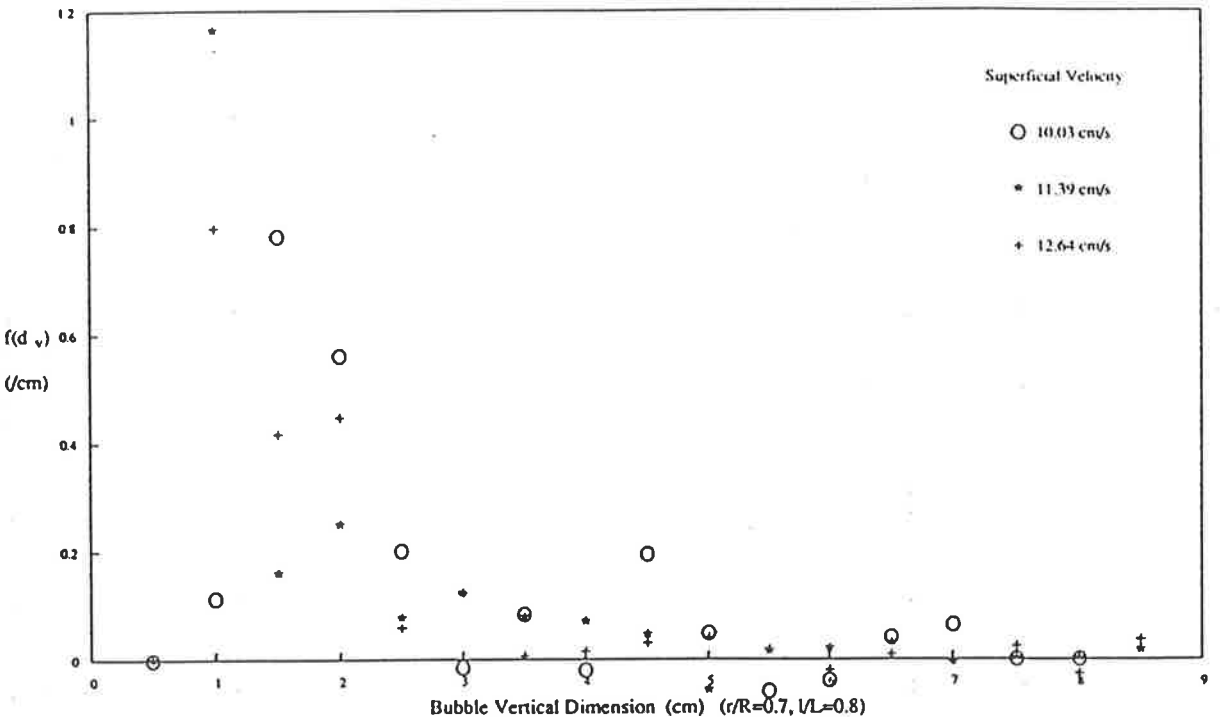

Figure 5.38 Cumulative Distribution and PDF of Bubble Vertical Dimension

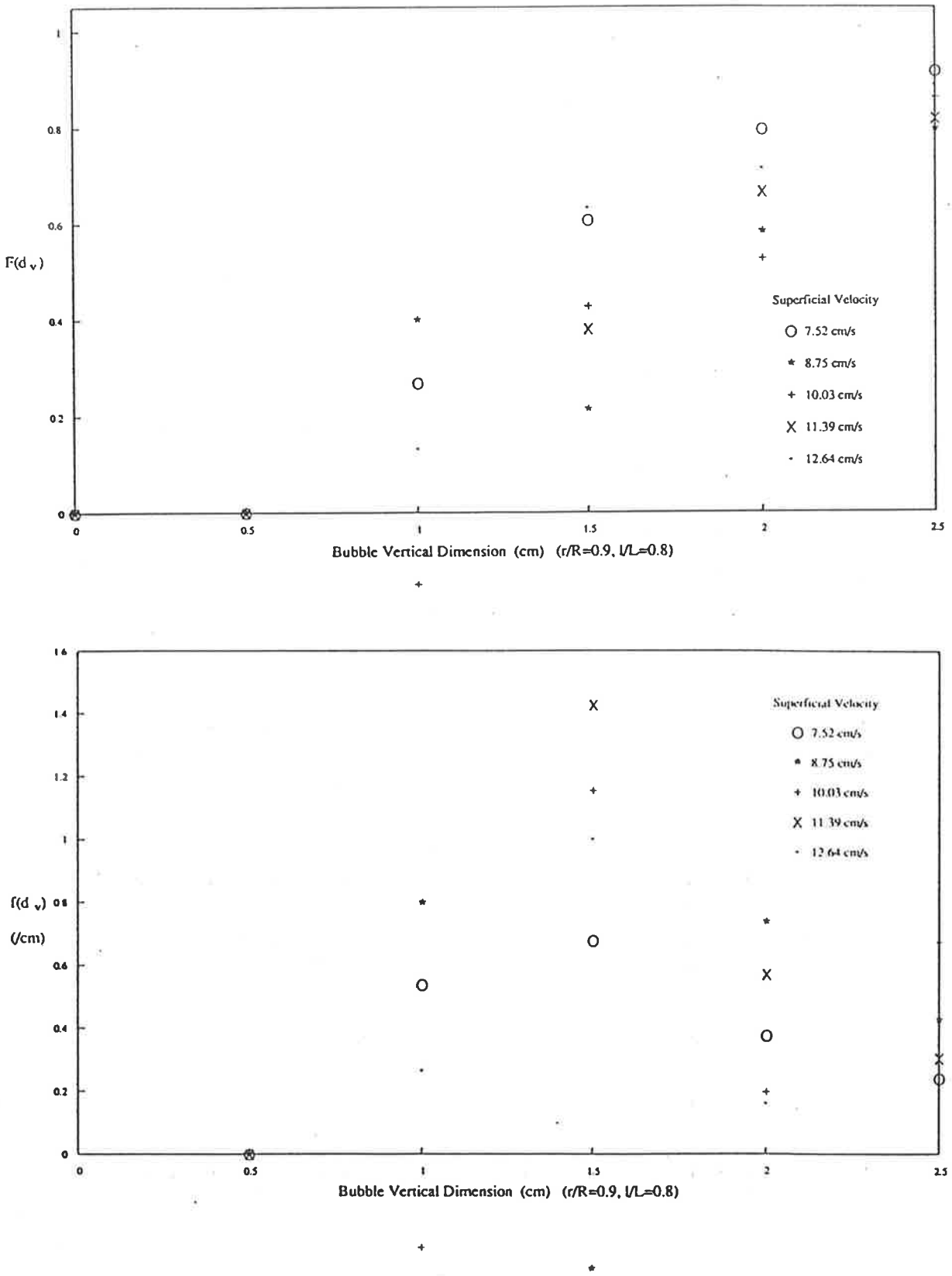

Figure 5.39 Cumulative Distribution and PDF of Bubble Vertical Dimension

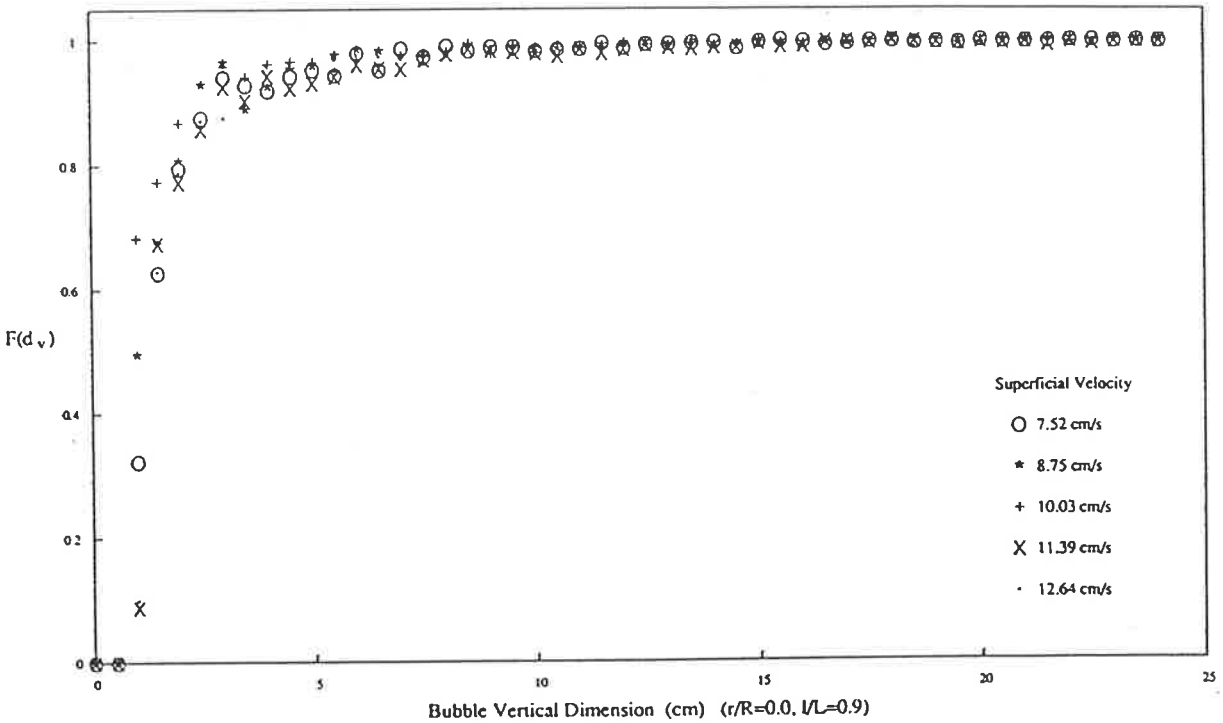

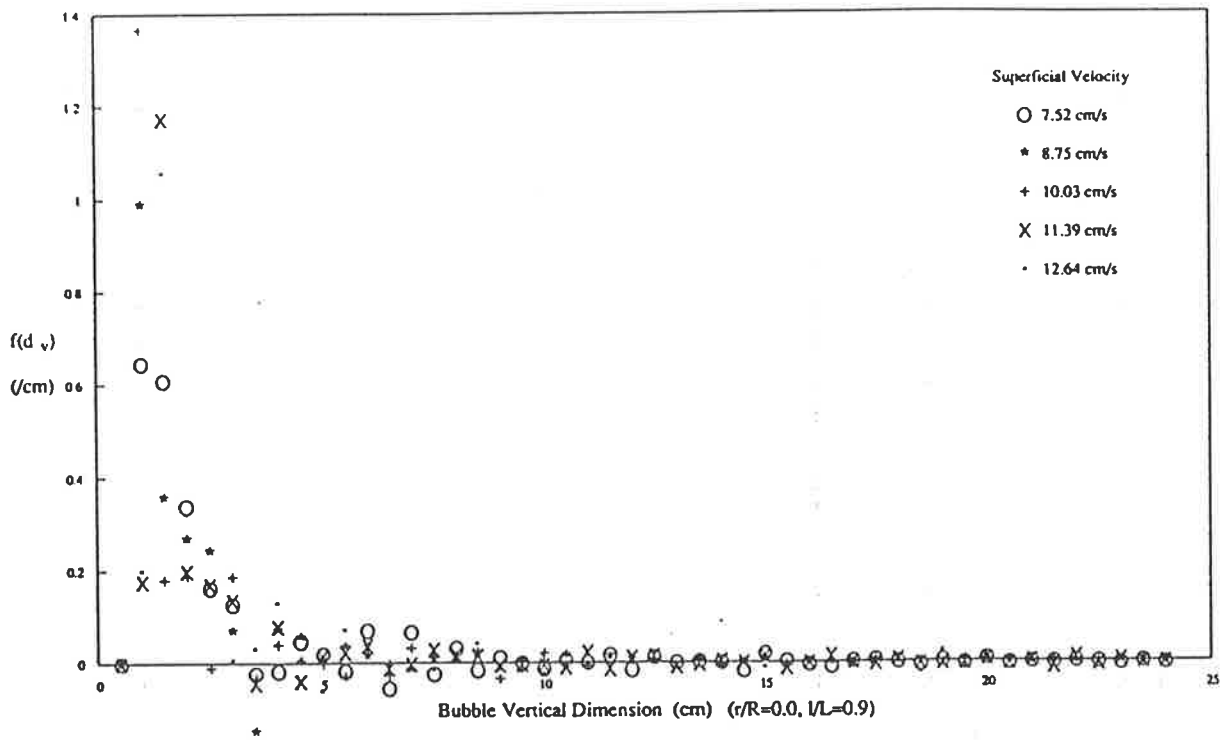

Figure 5.40 Cumulative Distribution and PDF of Bubble Vertical Dimension

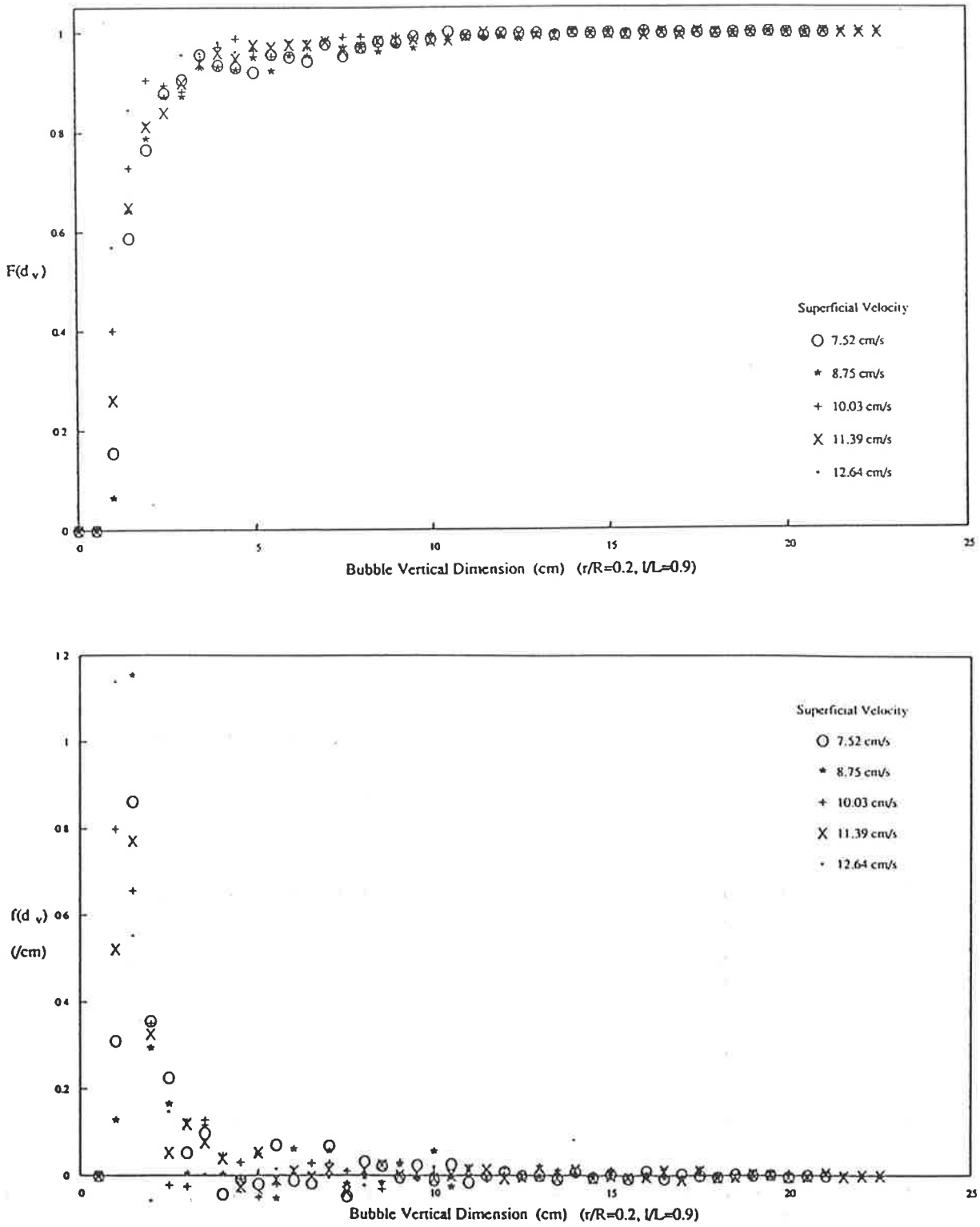

Figure 5.41 Cumulative Distribution and PDF of Bubble Vertical Dimension

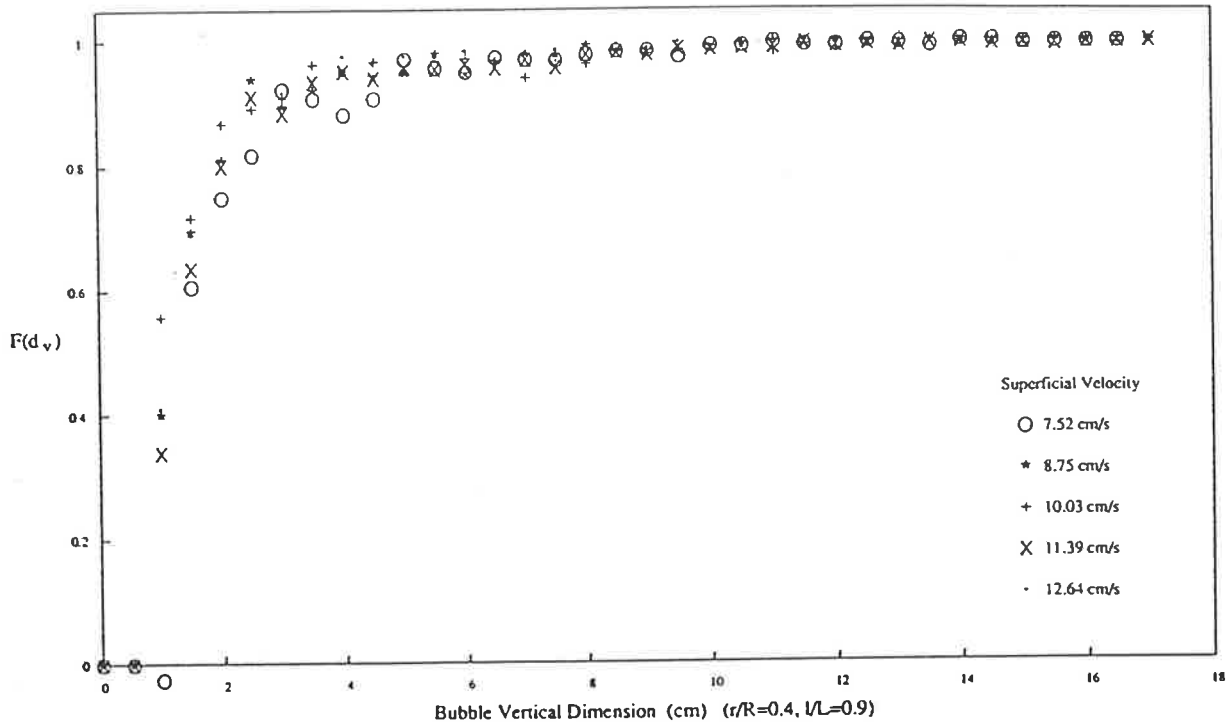

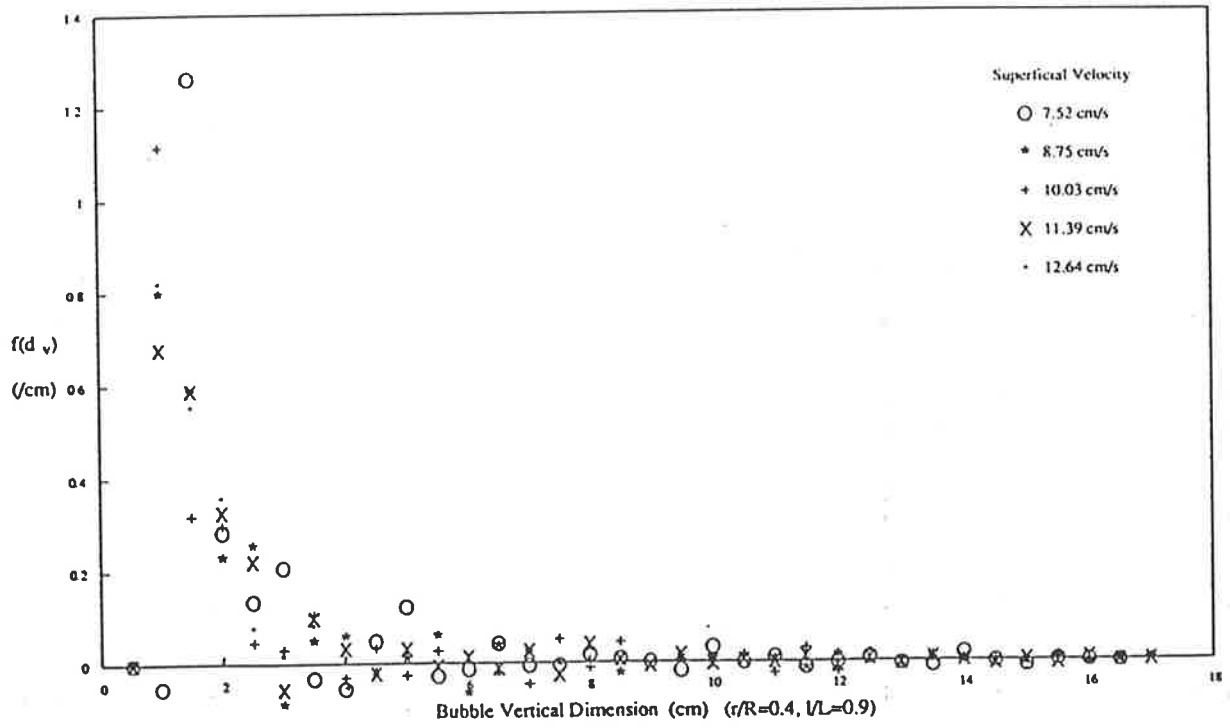

Figure 5.42 Cumulative Distribution and PDF of Bubble Vertical Dimension

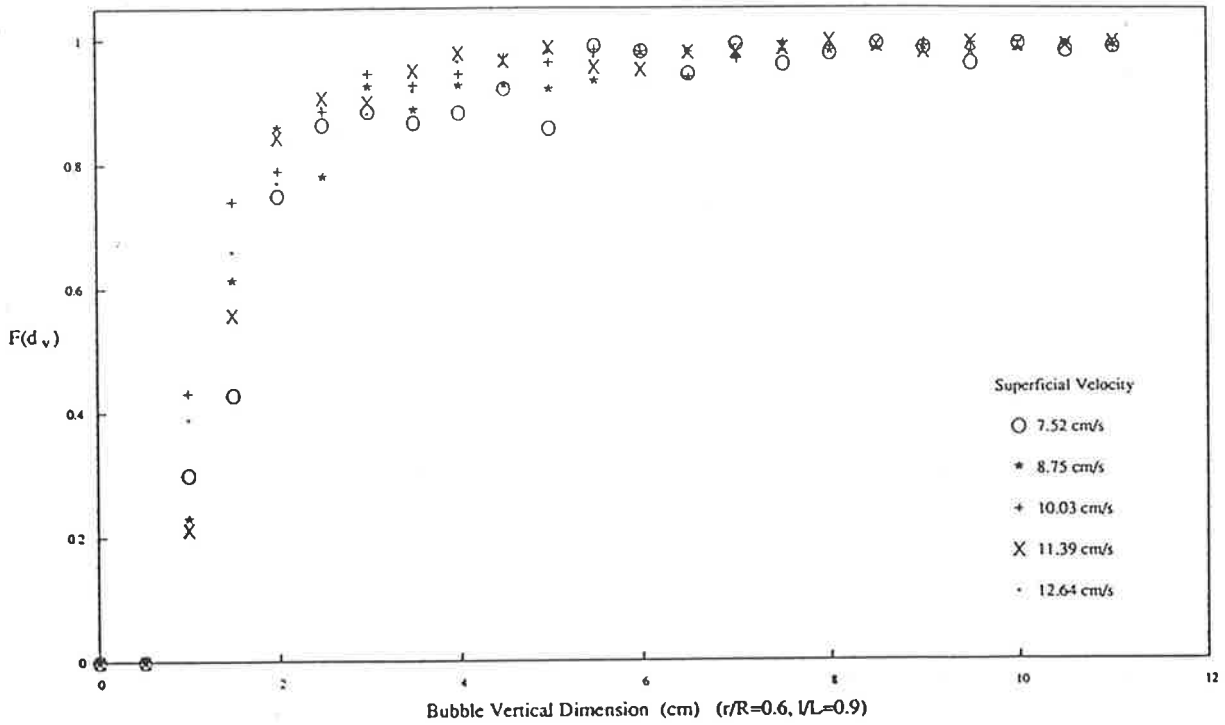

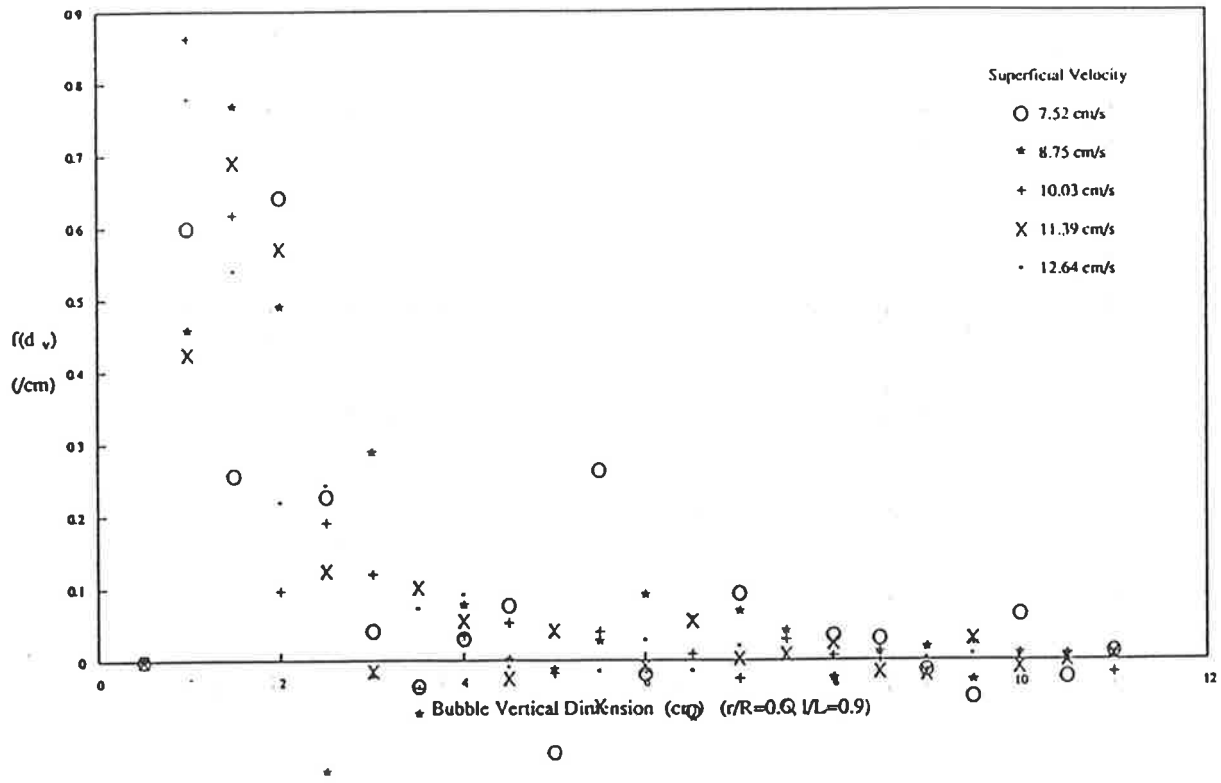

Figure 5.43 Cumulative Distribution and PDF of Bubble Vertical Dimension

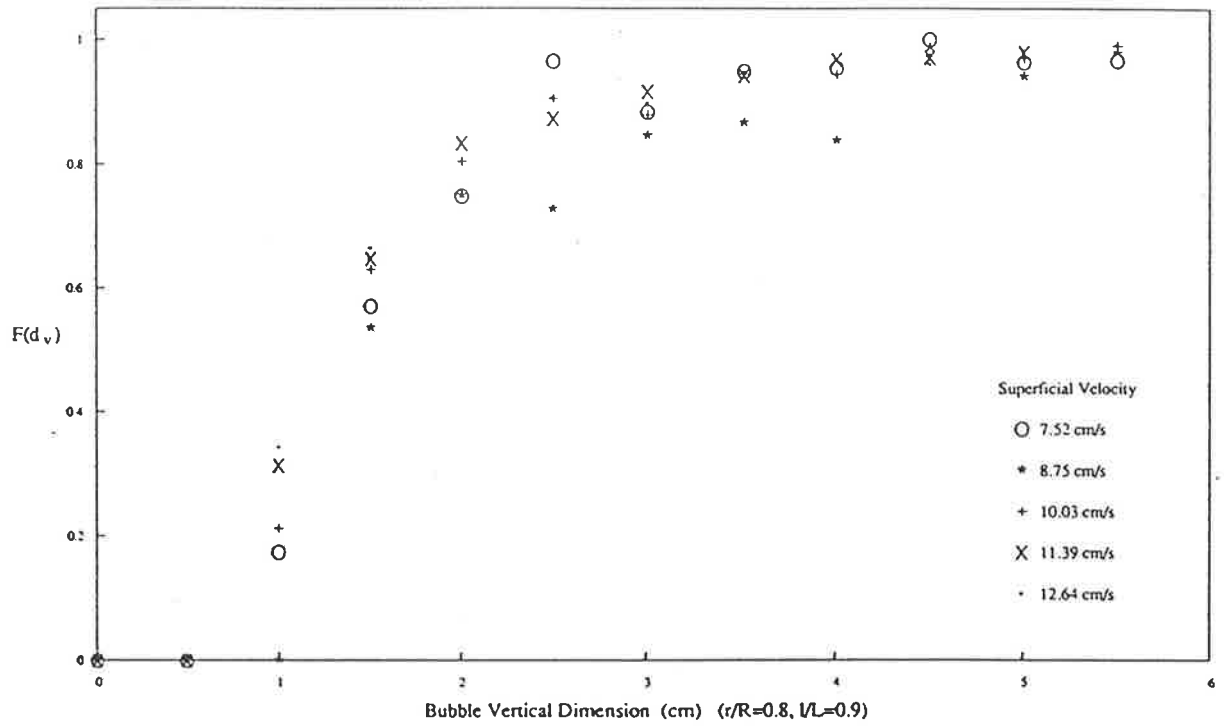

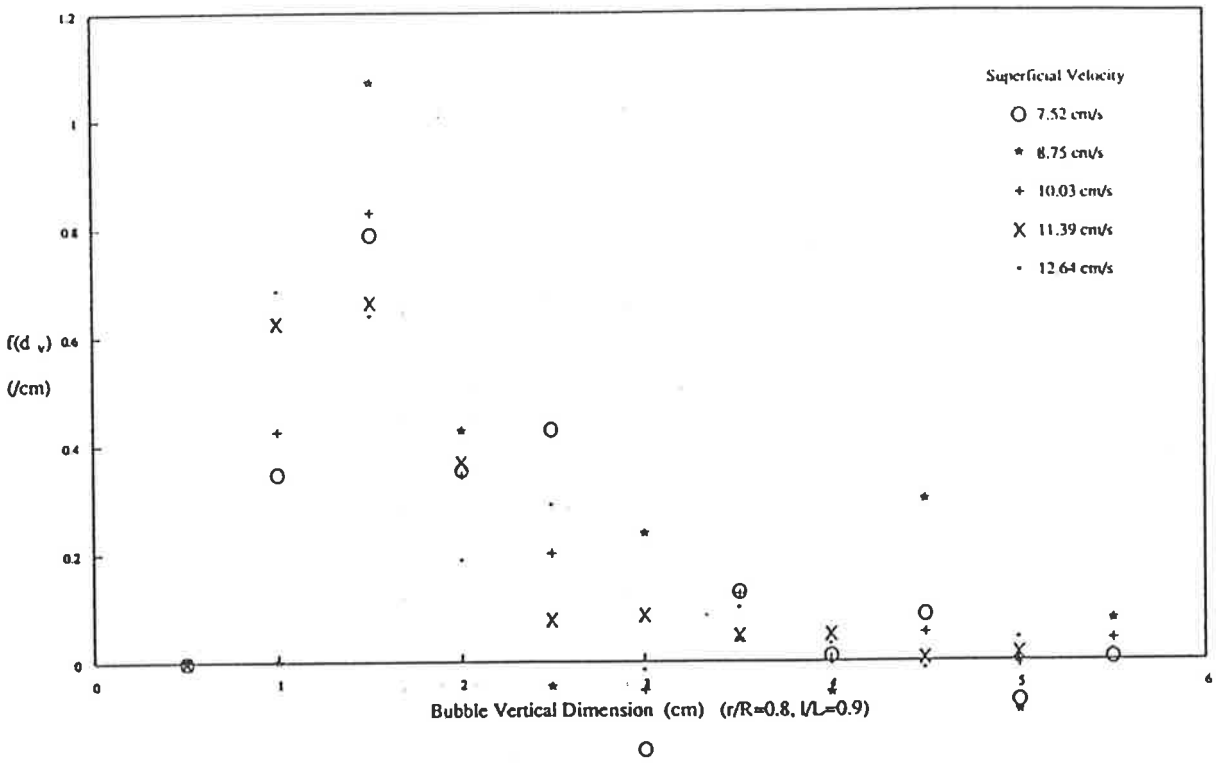

Figure 5.44 Cumulative Distribution and PDF of Bubble Vertical Dimension

5.2 Distributions of Bubble Rise Velocity

The bubble rise velocity at each probe position was also measured. Figures 5.45 to 5.88 illustrate distributions of the bubble rise velocities. As l/L increases, the bubble rise velocity increases towards the centre of the bed, as expected from observation of the distributions of bubble vertical dimensions.

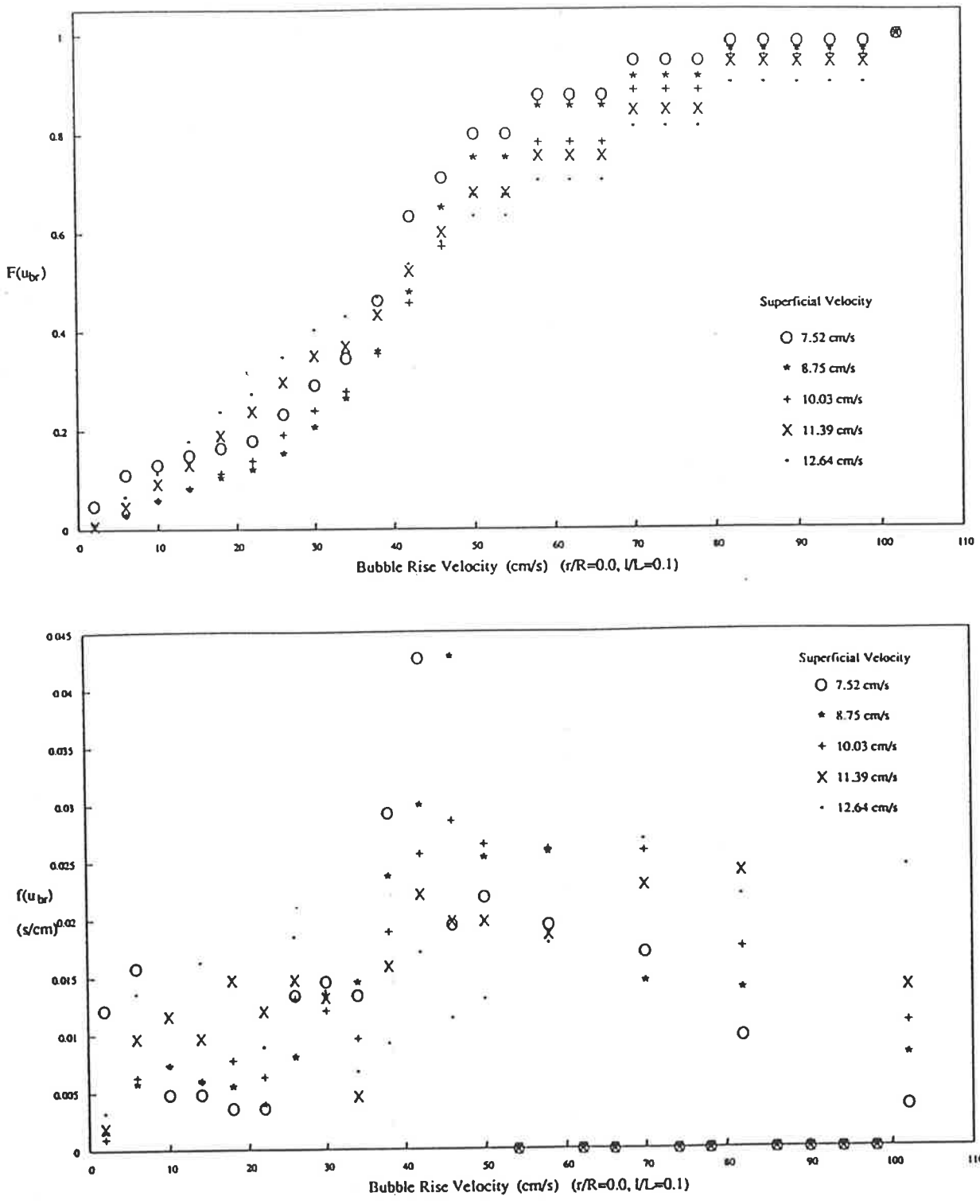

Figure 5.45 Cumulative Distribution and PDF of Bubble Rise Velocity

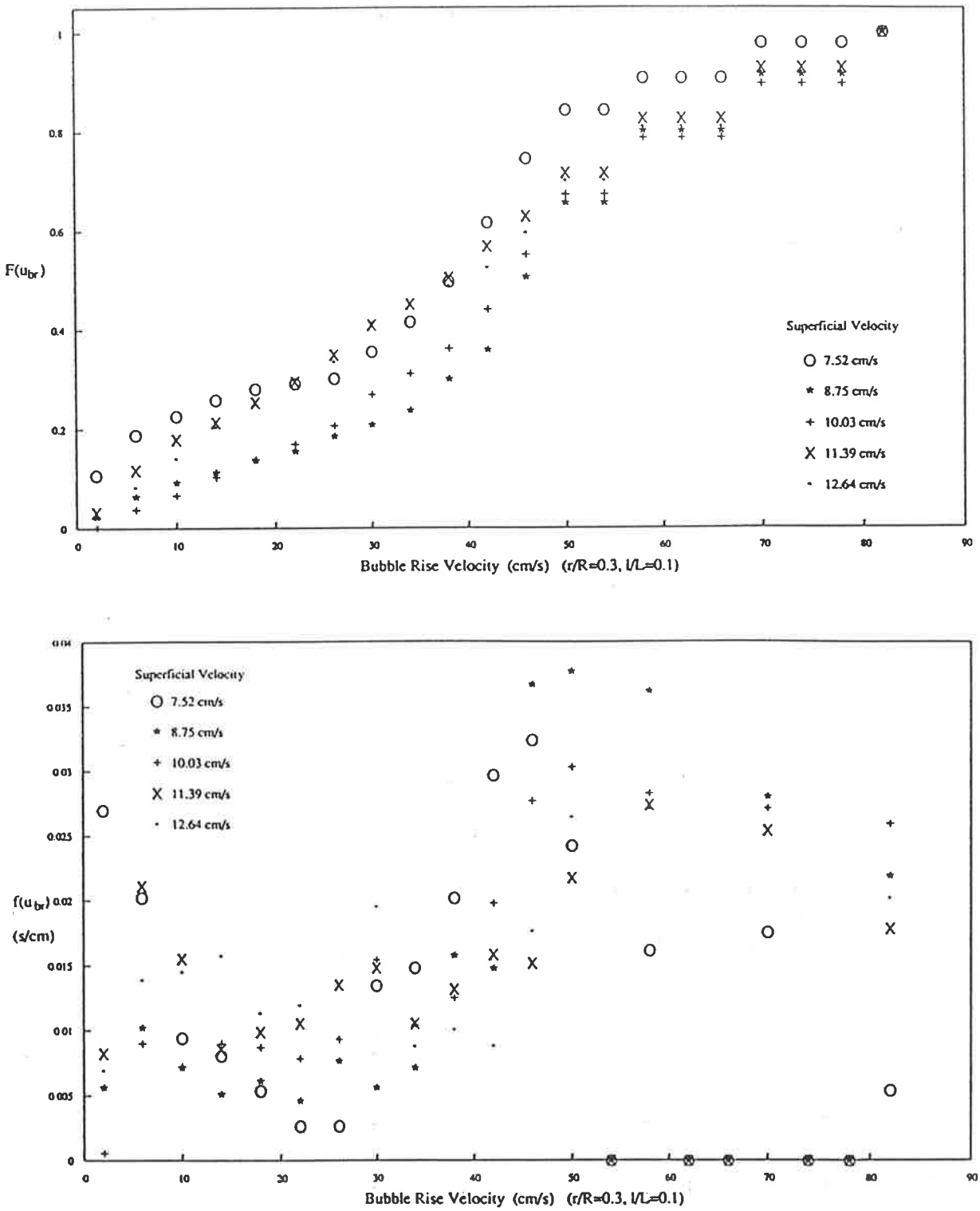

Figure 5.46 Cumulative Distribution and PDF of Bubble Rise Velocity

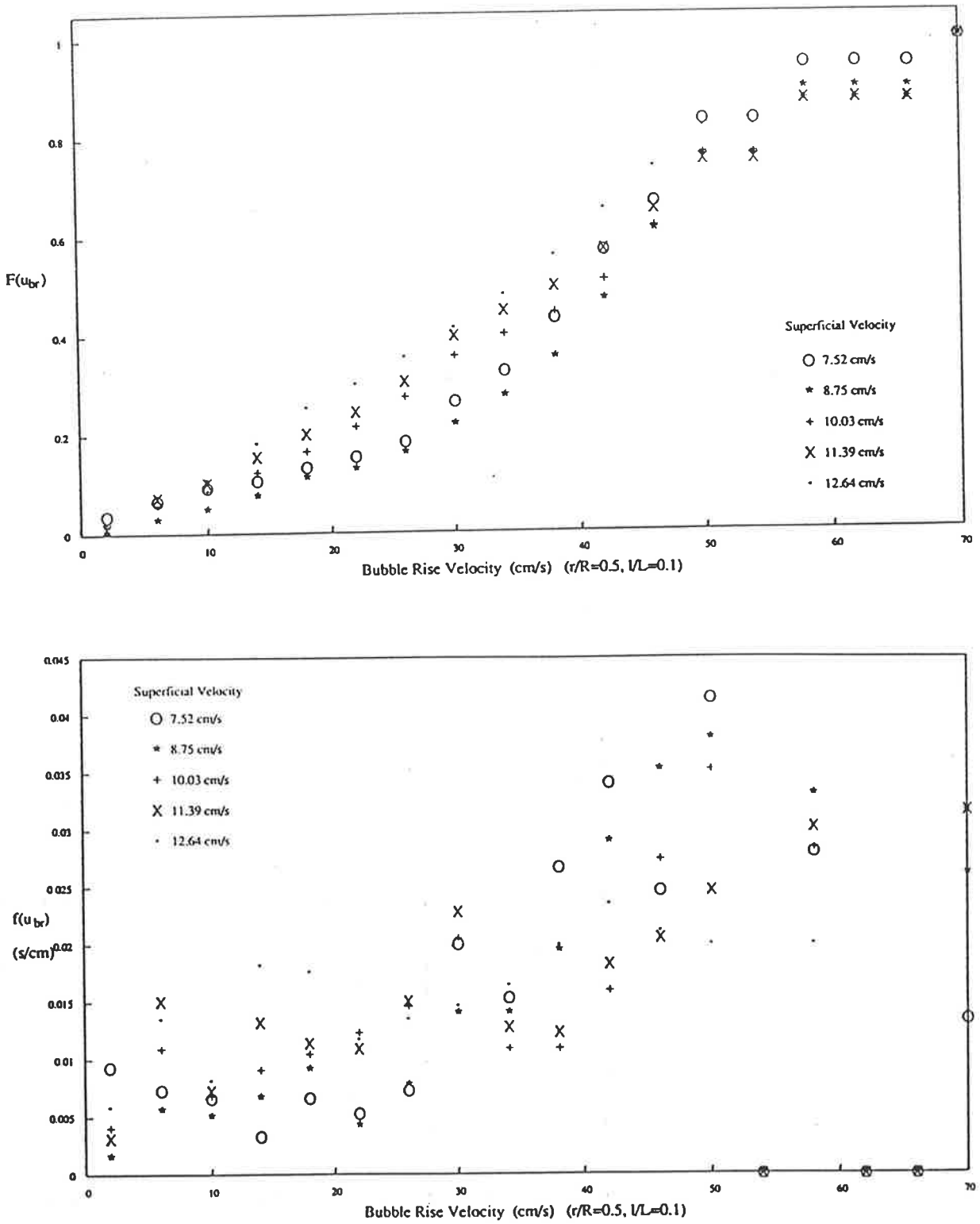

Figure 5.47 Cumulative Distribution and PDF of Bubble Rise Velocity

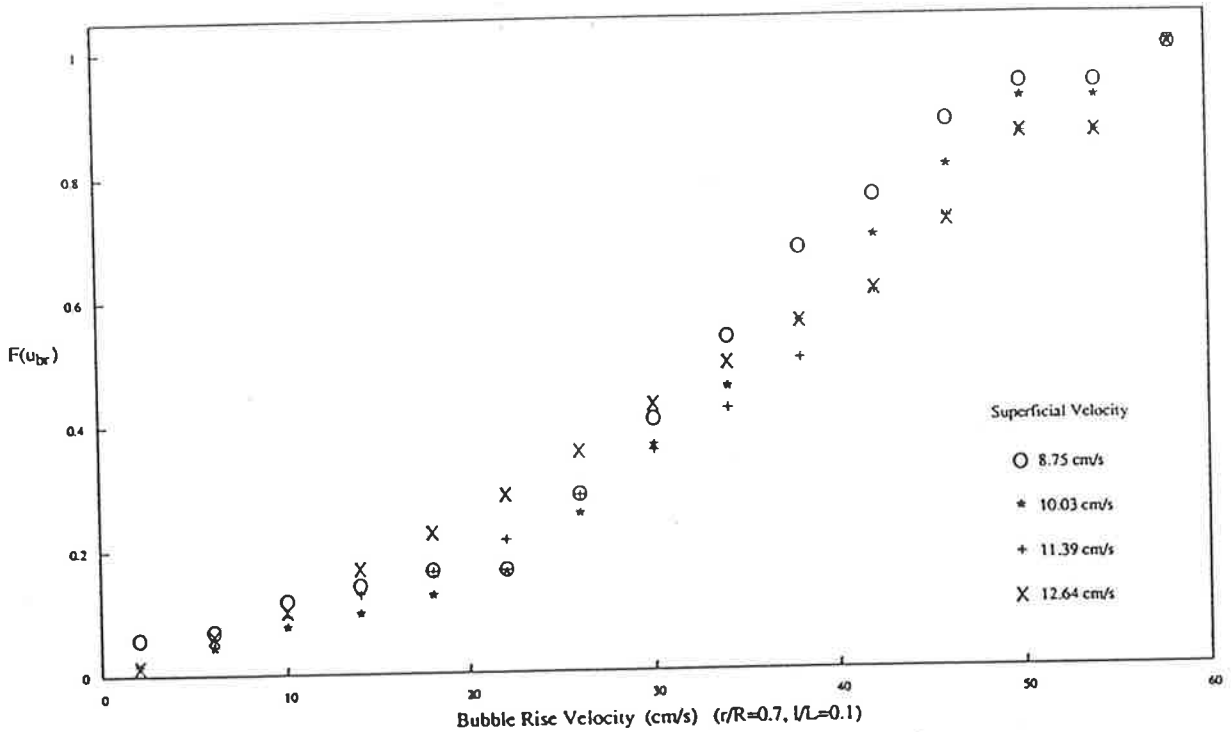

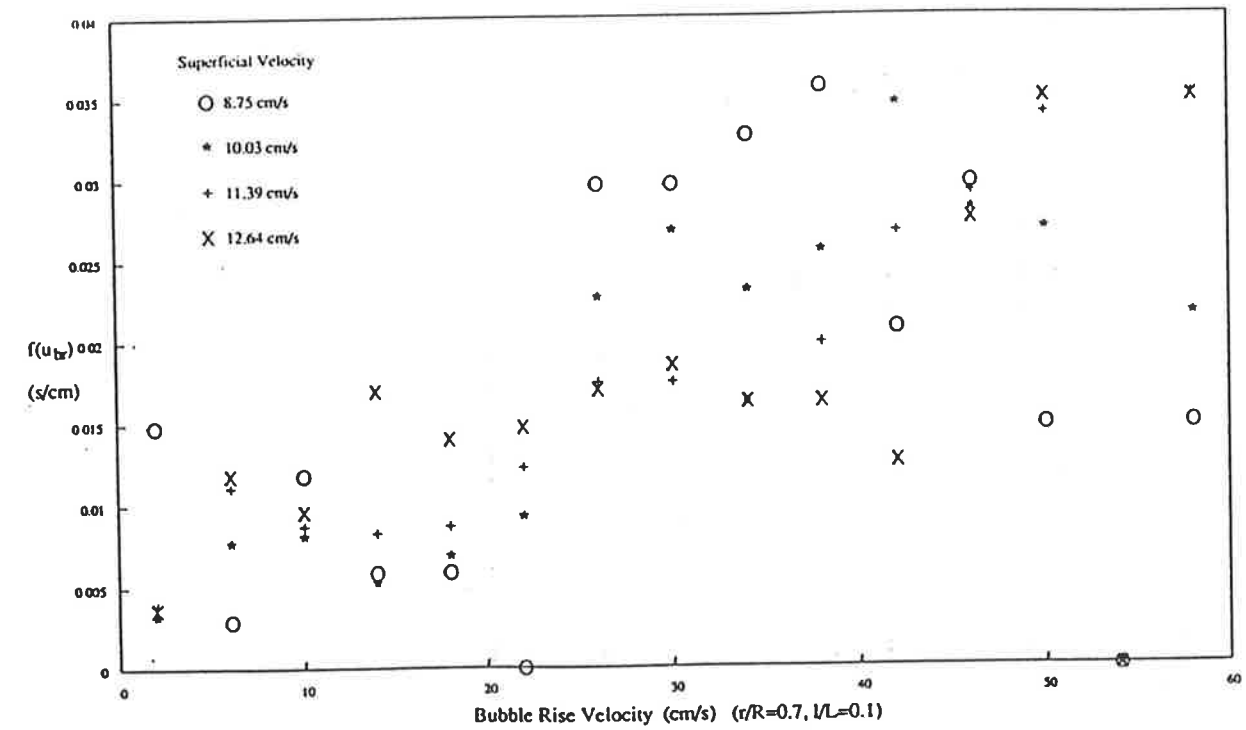

Figure 5.48 Cumulative Distribution and PDF of Bubble Rise Velocity

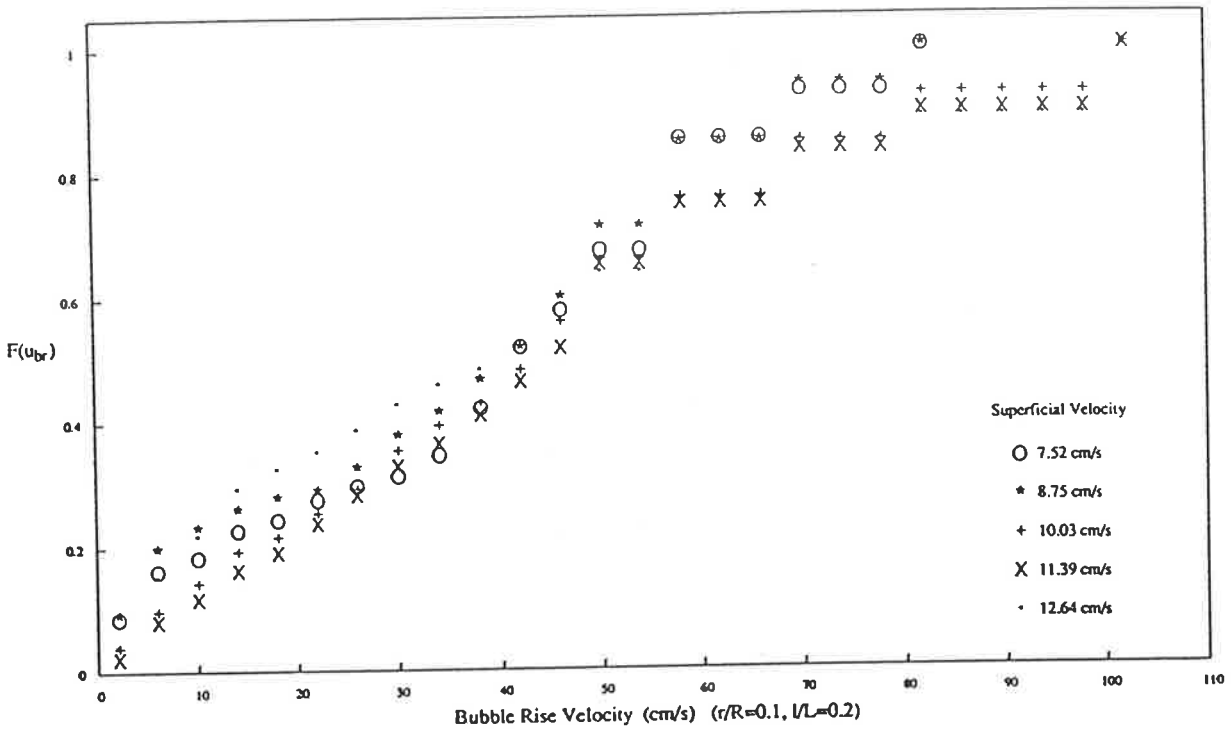

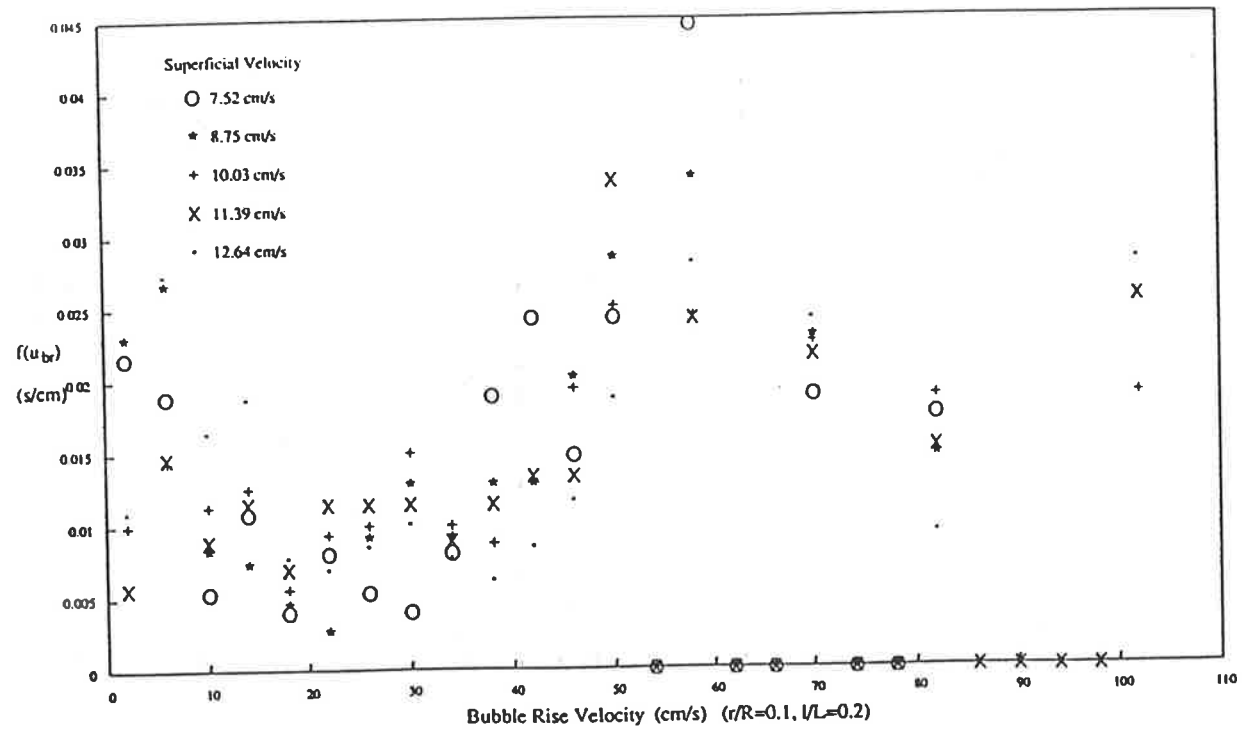

Figure 5.49 Cumulative Distribution and PDF of Bubble Rise Velocity

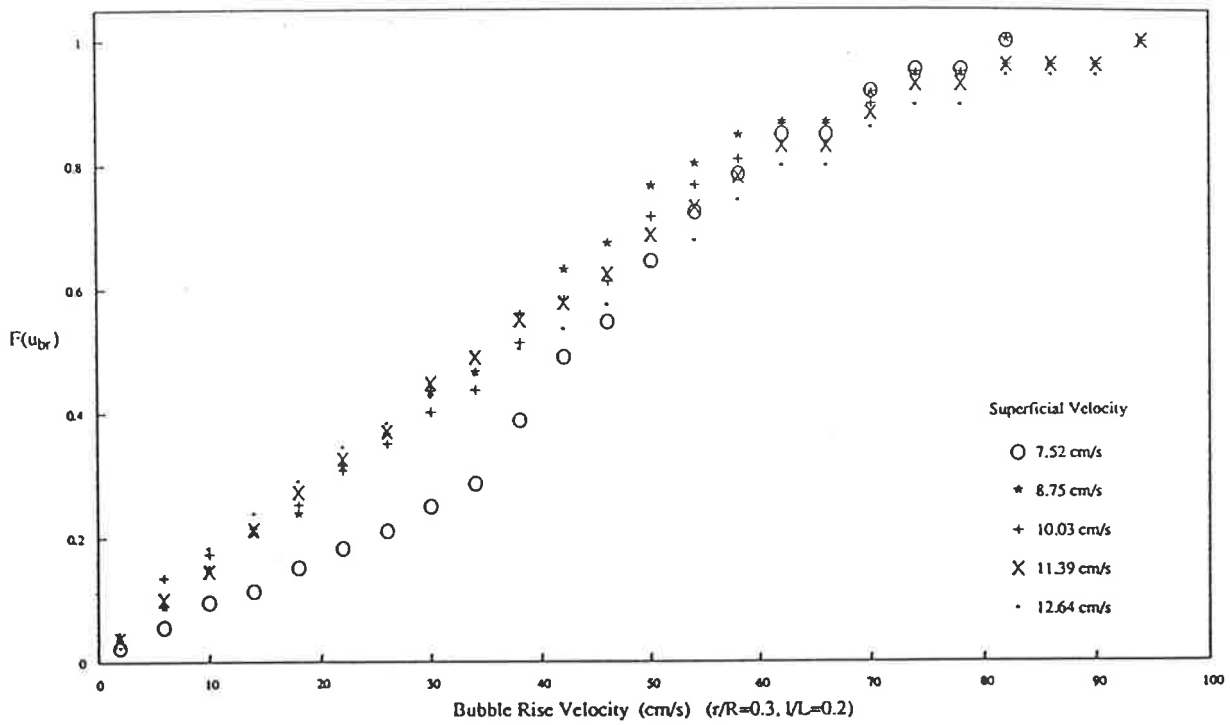

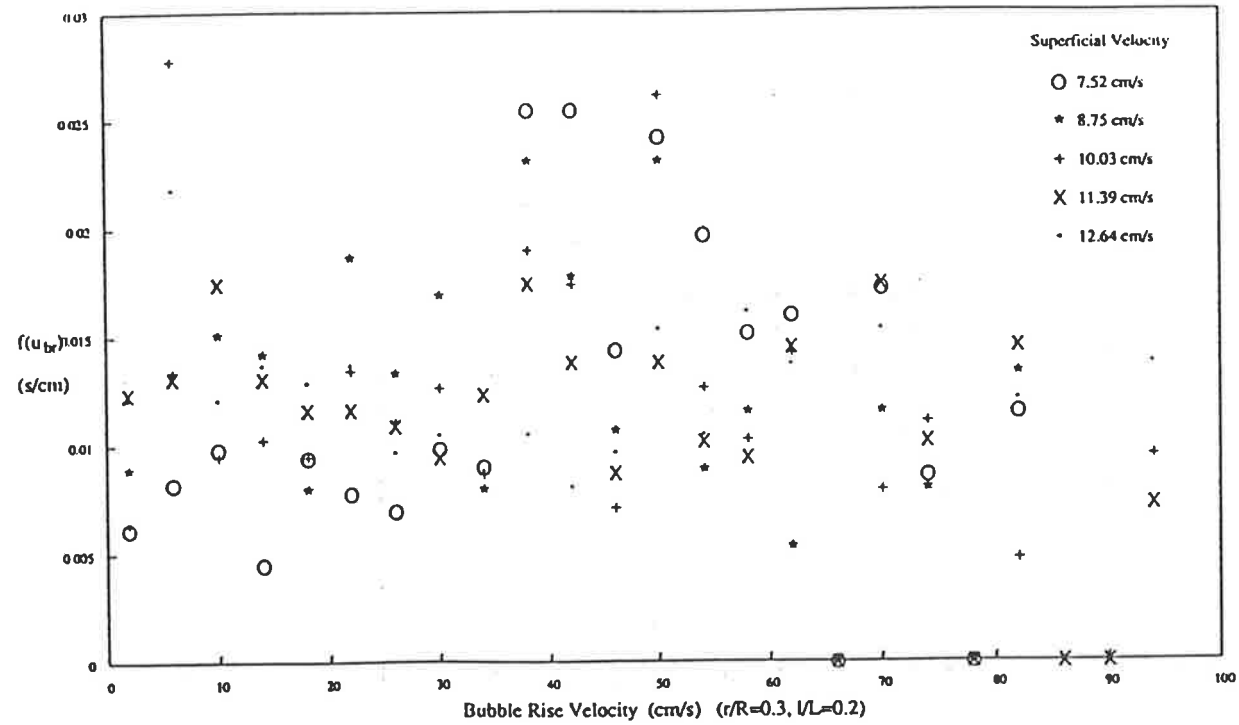

Figure 5.50 Cumulative Distribution and PDF of Bubble Rise Velocity

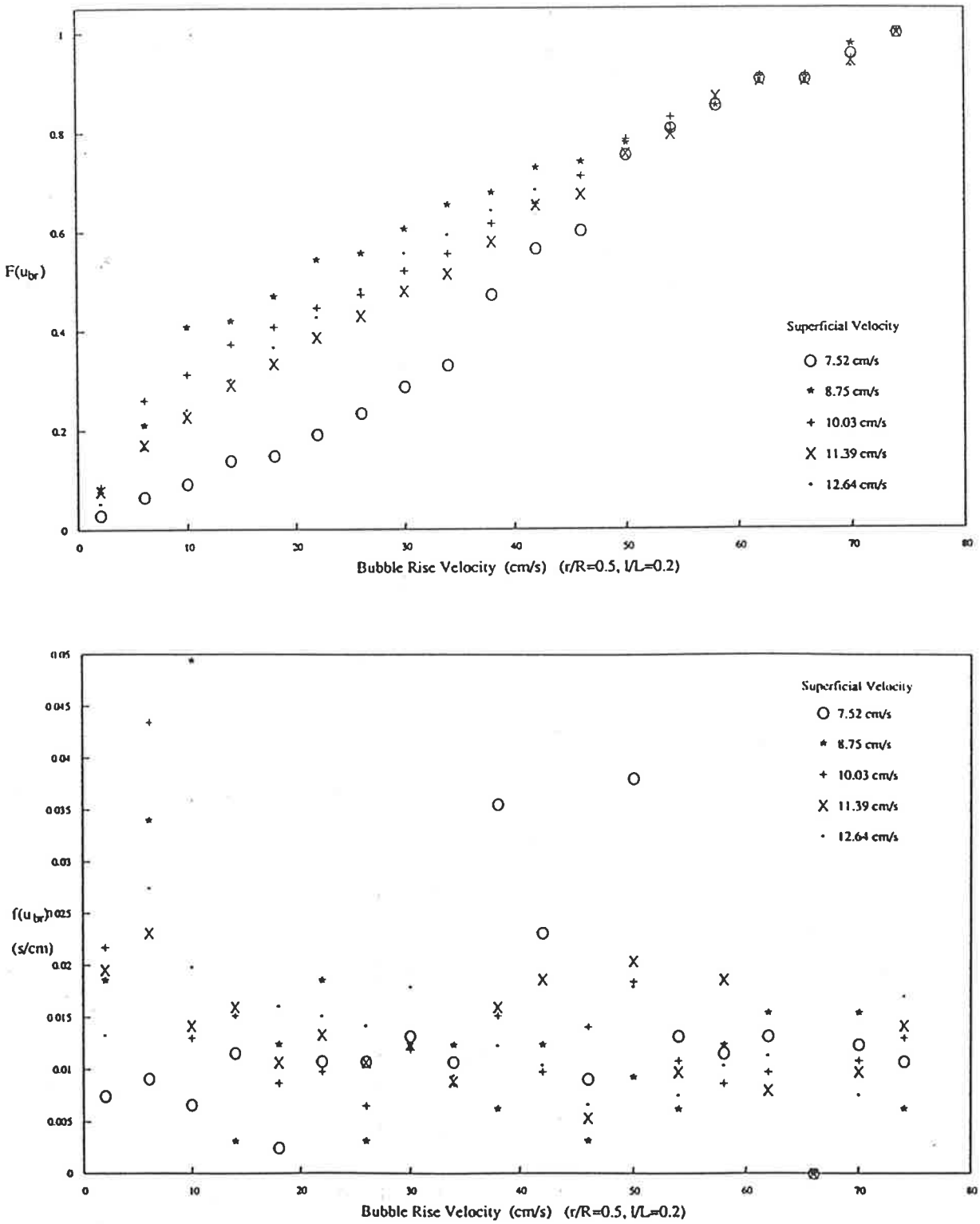

Figure 5.51 Cumulative Distribution and PDF of Bubble Rise Velocity

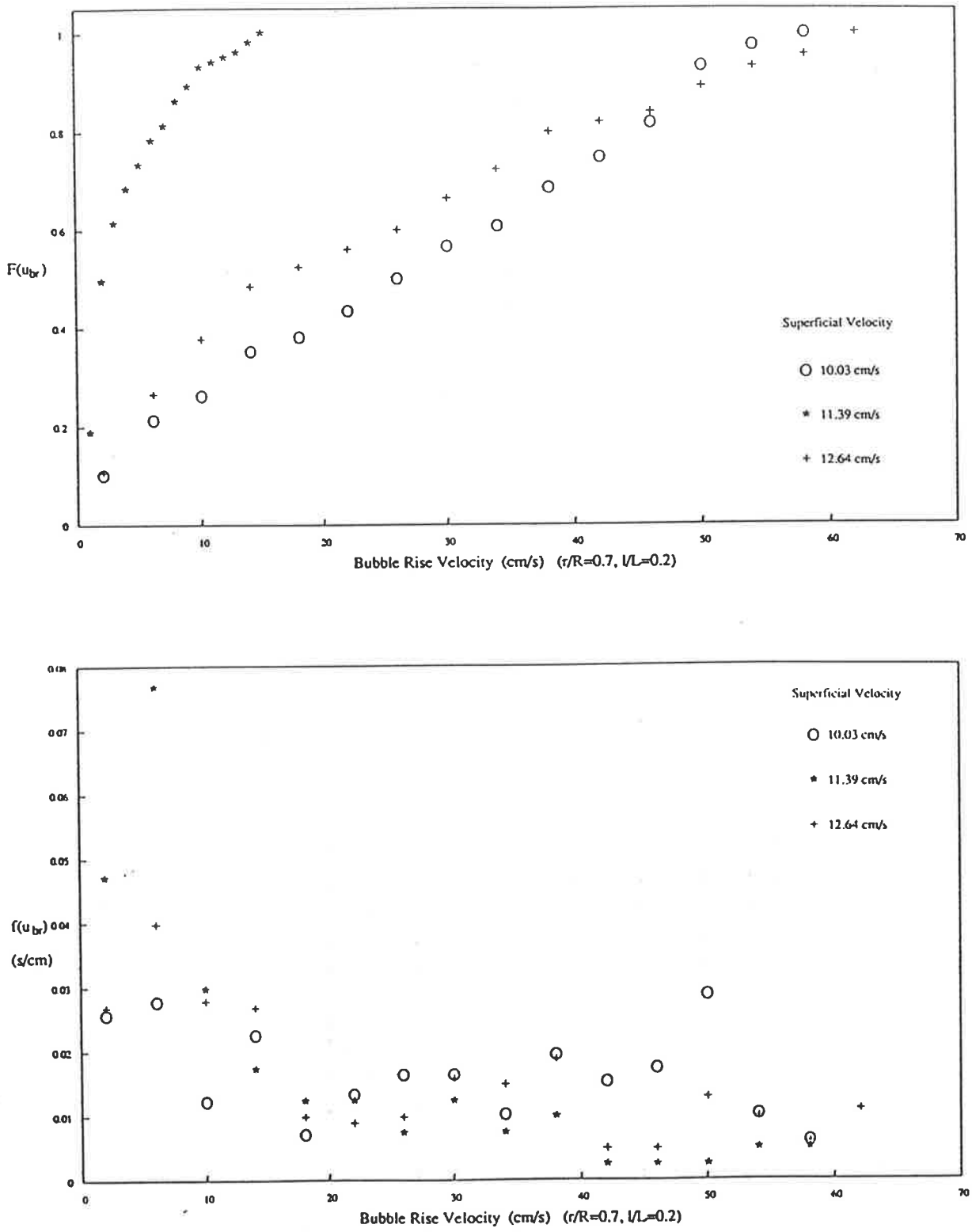

Figure 5.52 Cumulative Distribution and PDF of Bubble Rise Velocity

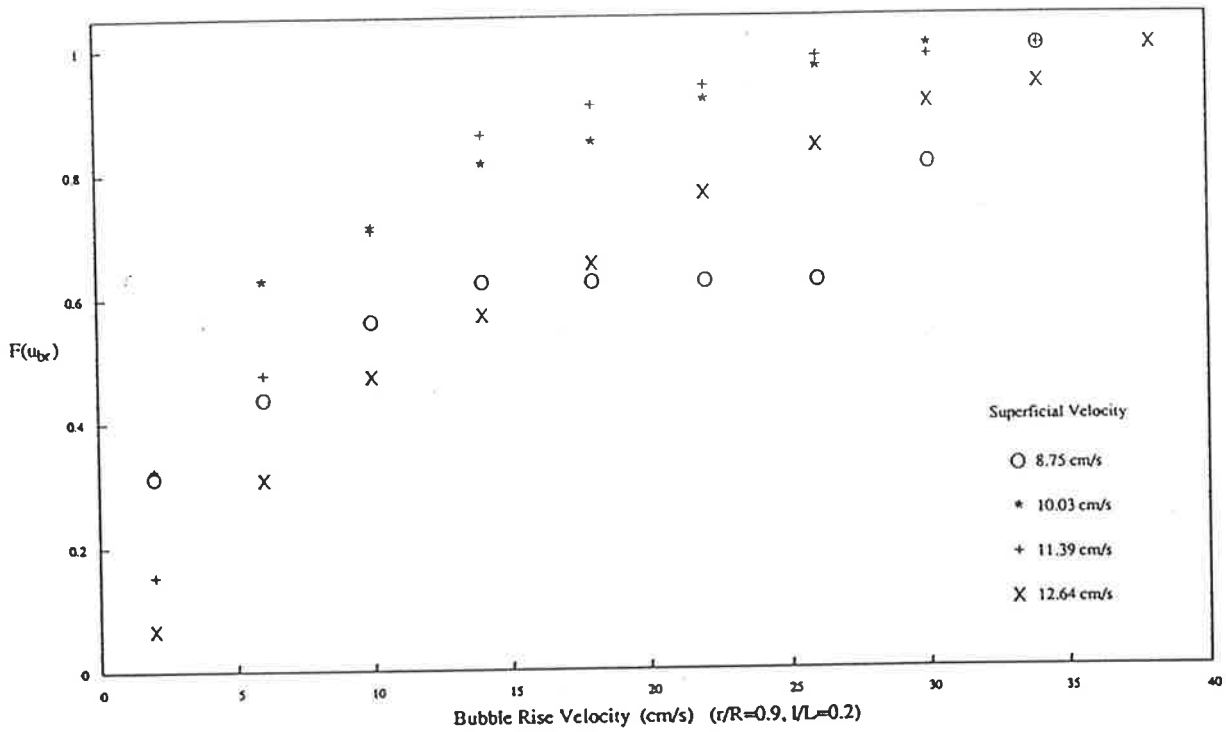

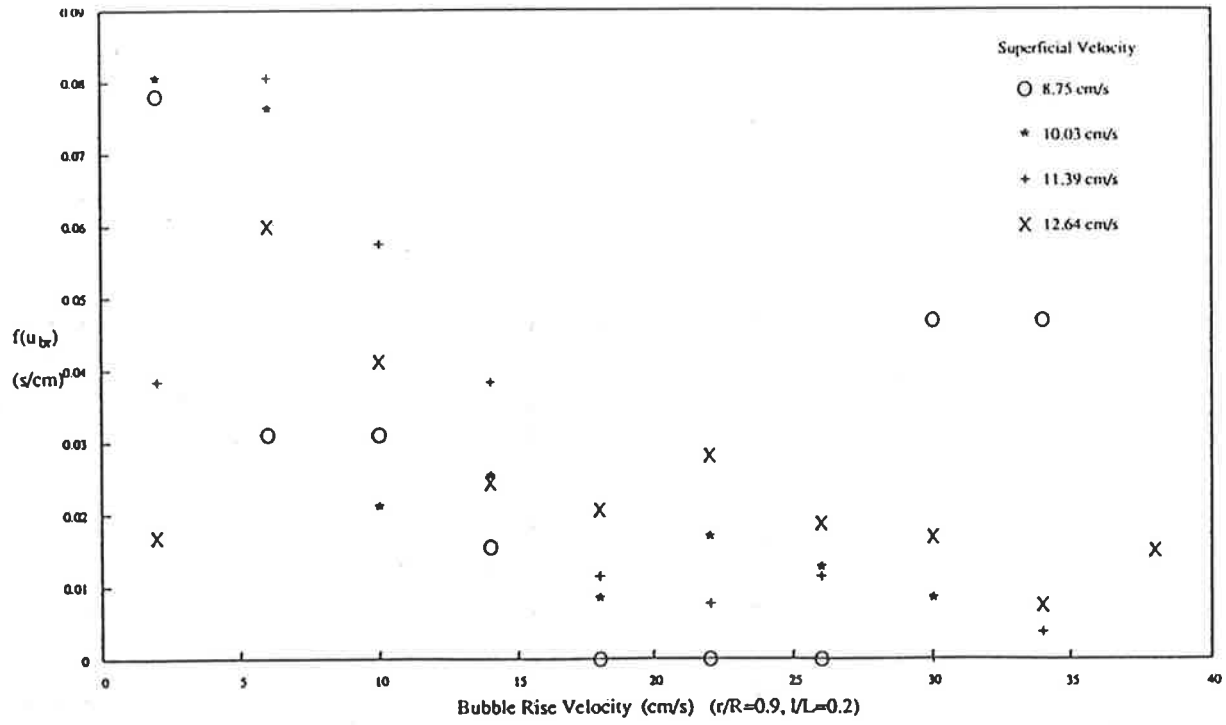

Figure 5.53 Cumulative Distribution and PDF of Bubble Rise Velocity

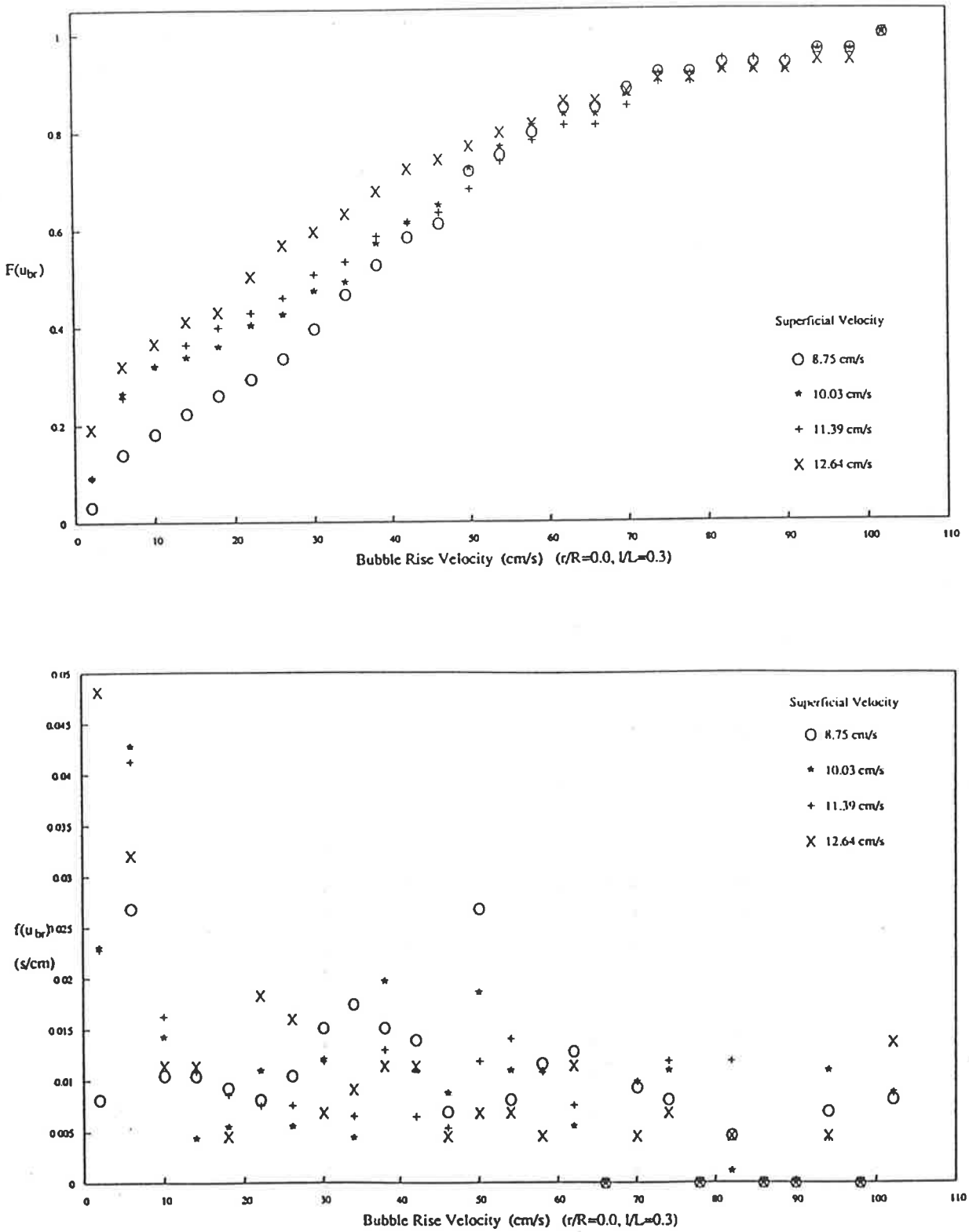

Figure 5.54 Cumulative Distribution and PDF of Bubble Rise Velocity

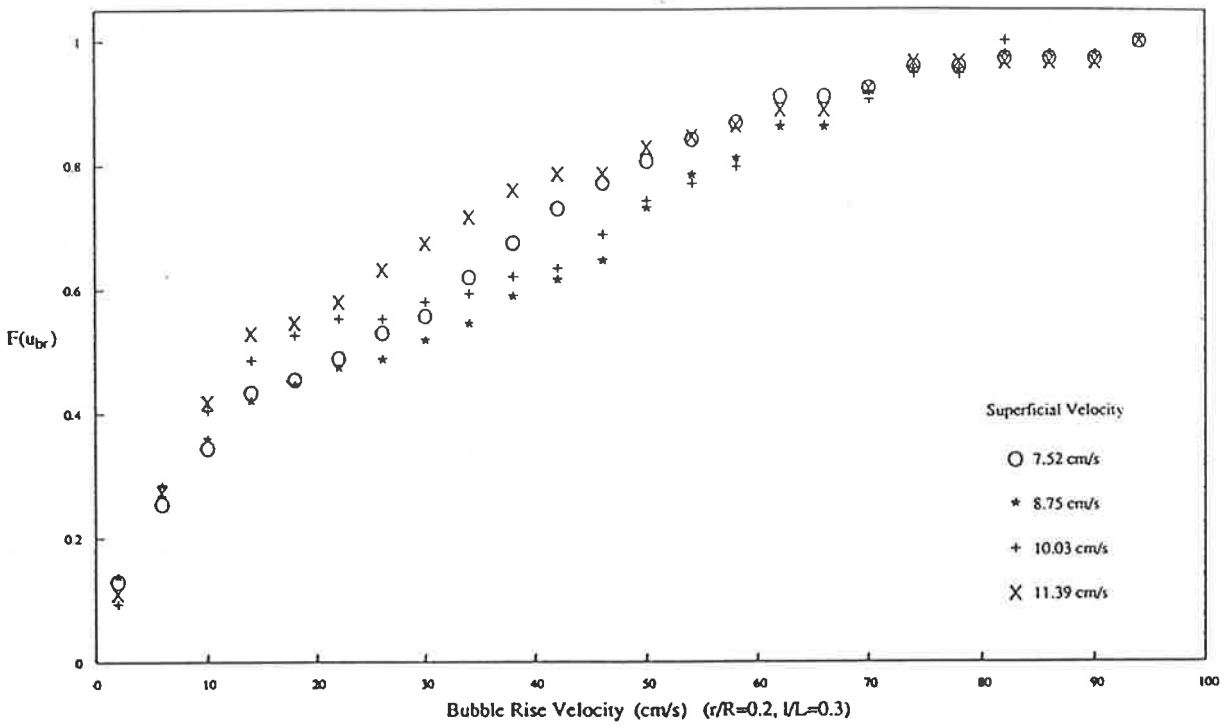

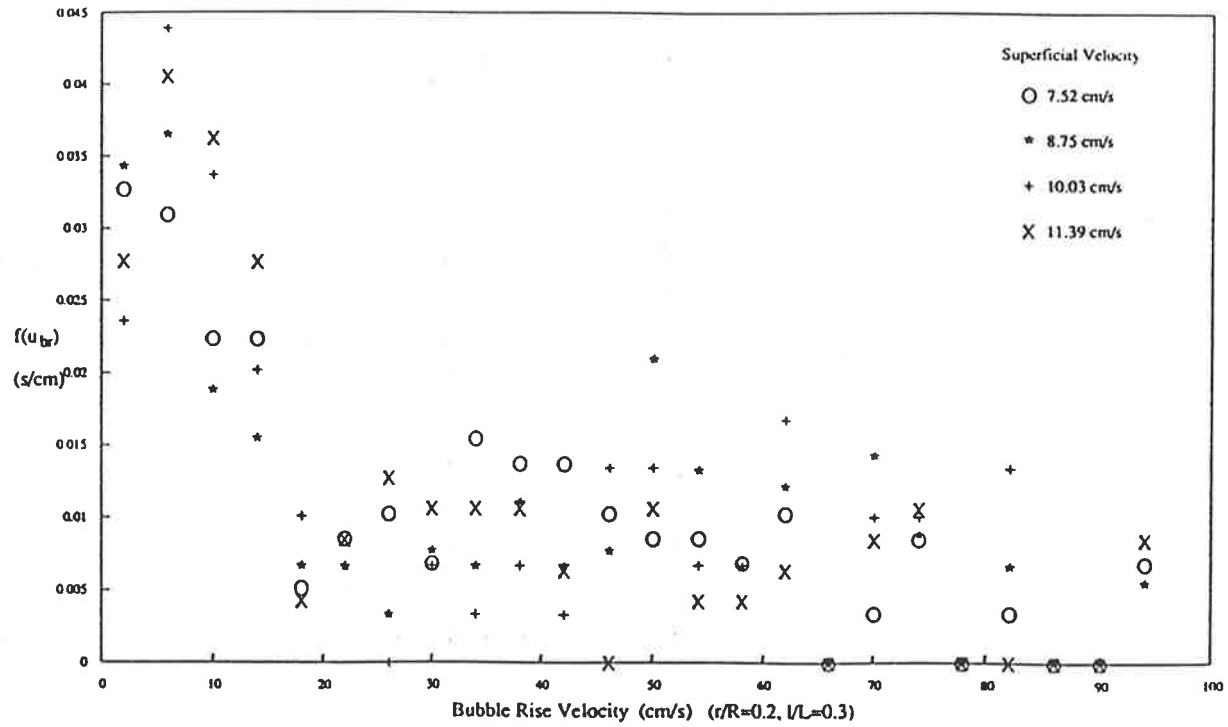

Figure 5.55 Cumulative Distribution and PDF of Bubble Rise Velocity

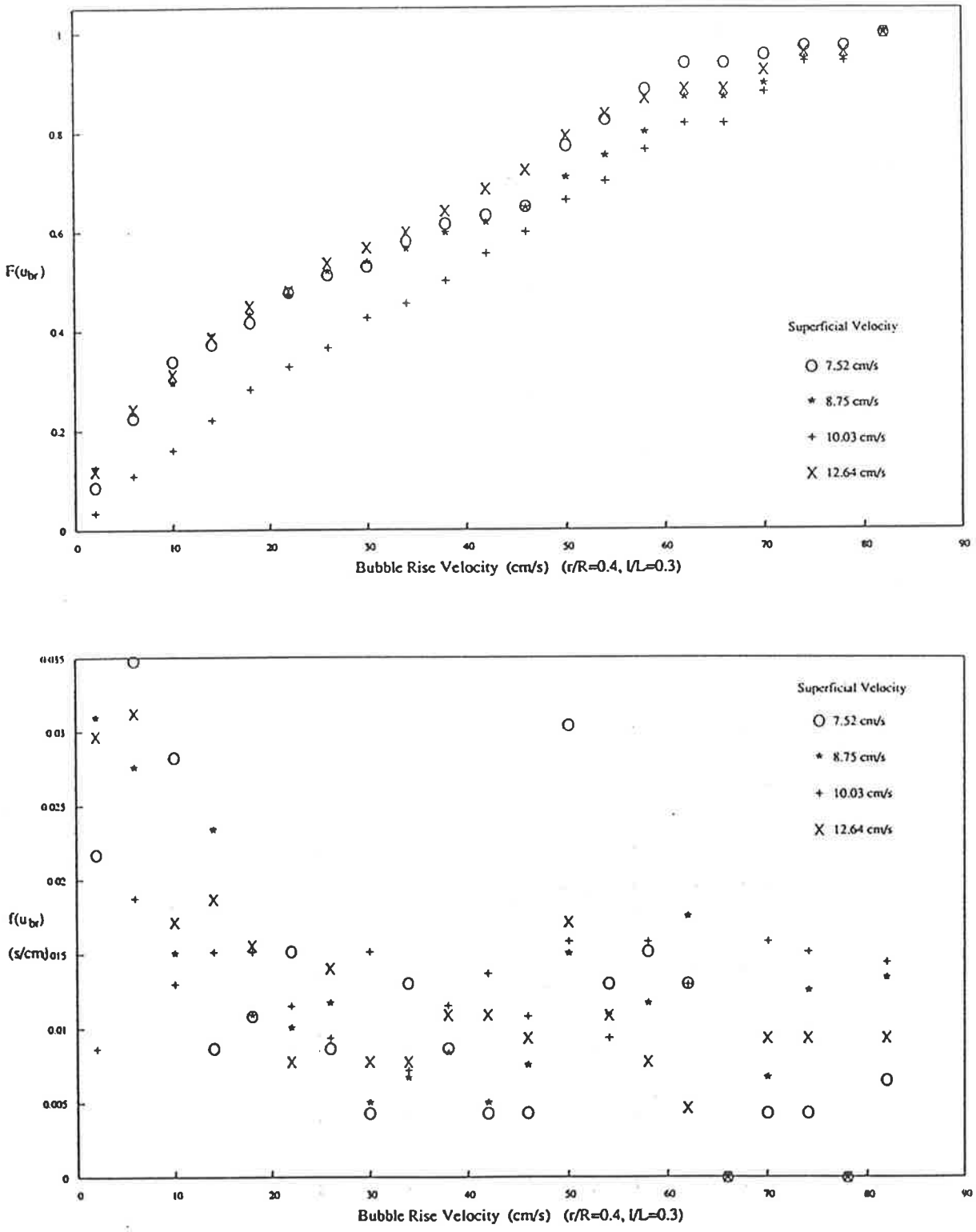

Figure 5.56 Cumulative Distribution and PDF of Bubble Rise Velocity

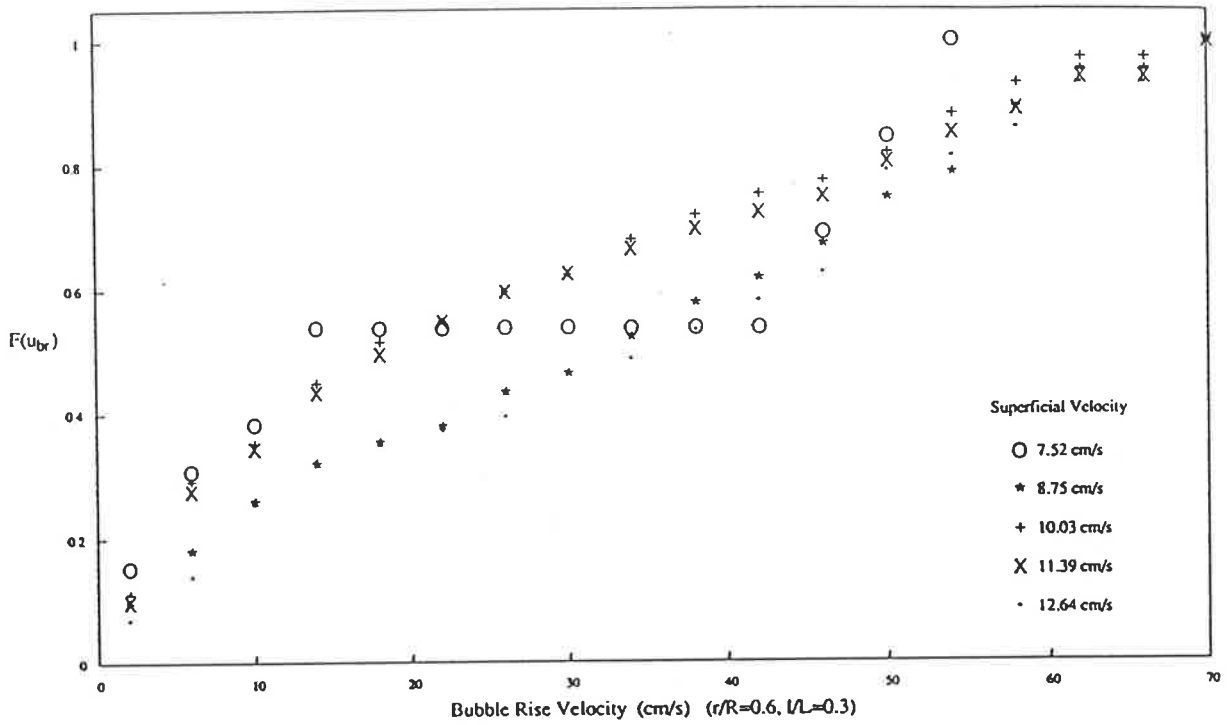

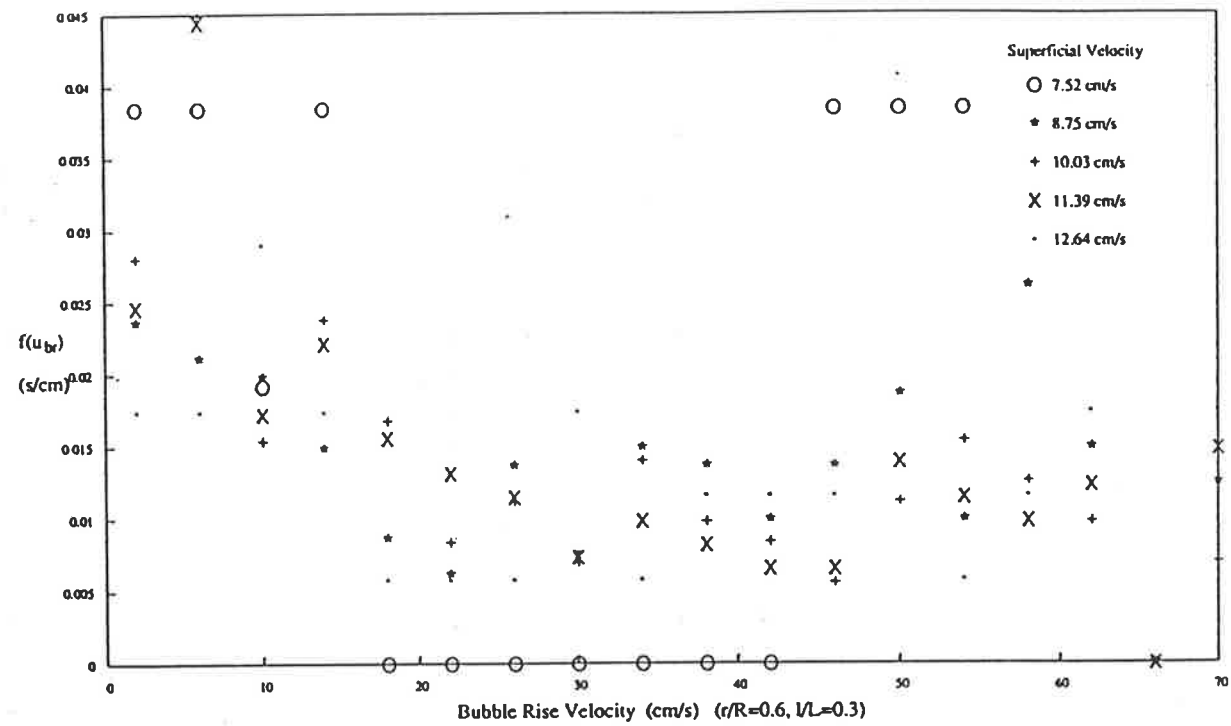

Figure 5.57 Cumulative Distribution and PDF of Bubble Rise Velocity

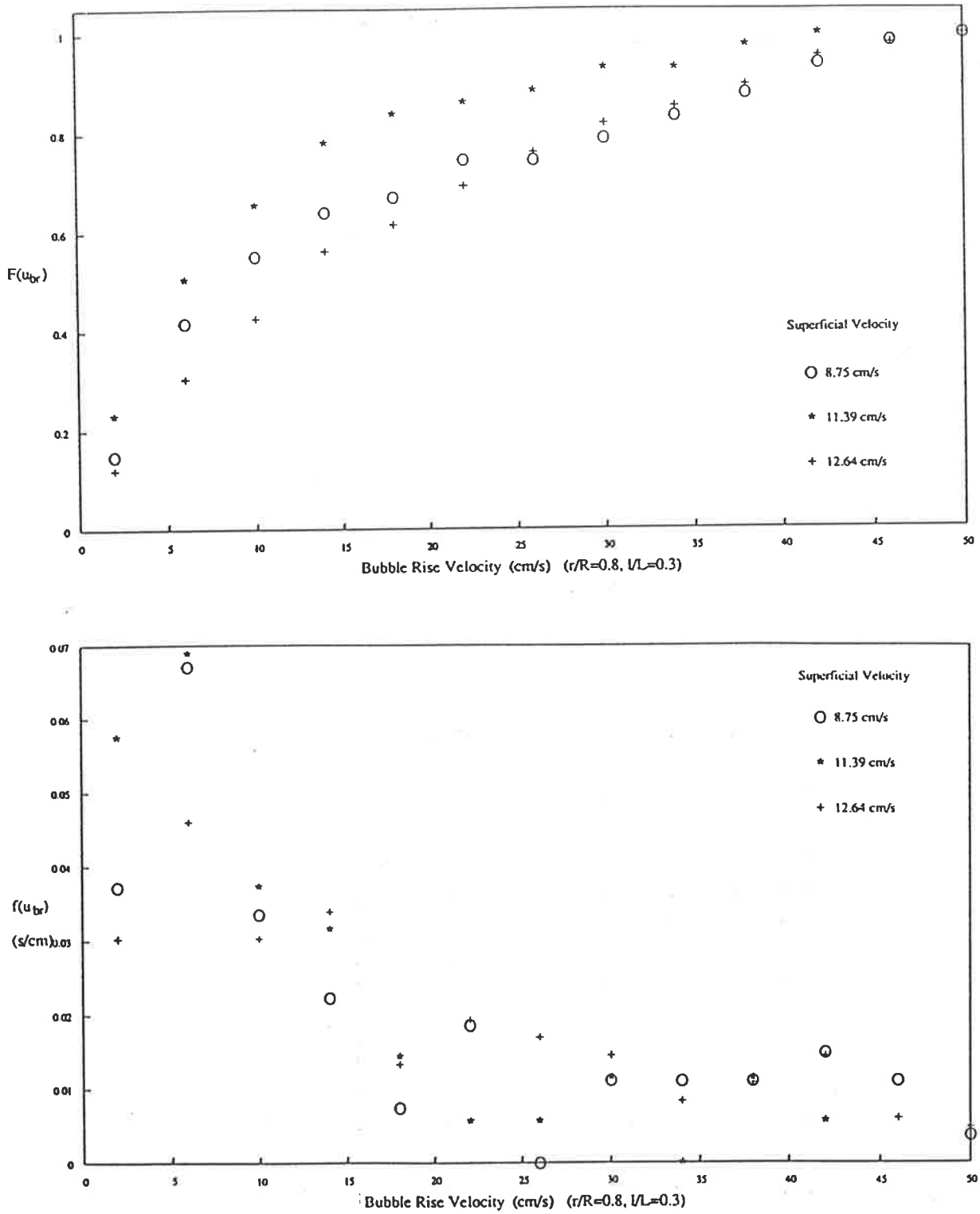

Figure 5.58 Cumulative Distribution and PDF of Bubble Rise Velocity

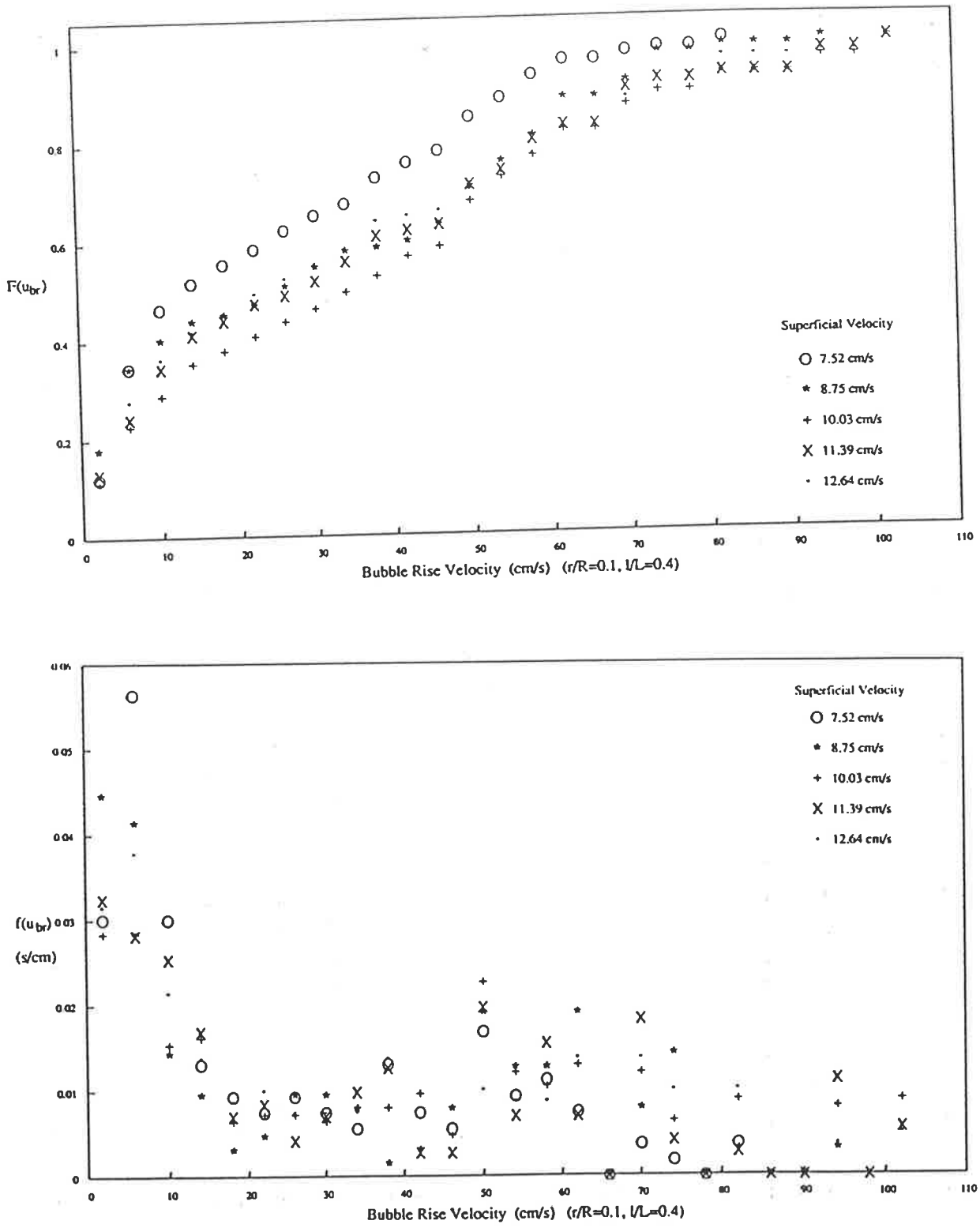

Figure 5.59 Cumulative Distribution and PDF of Bubble Rise Velocity

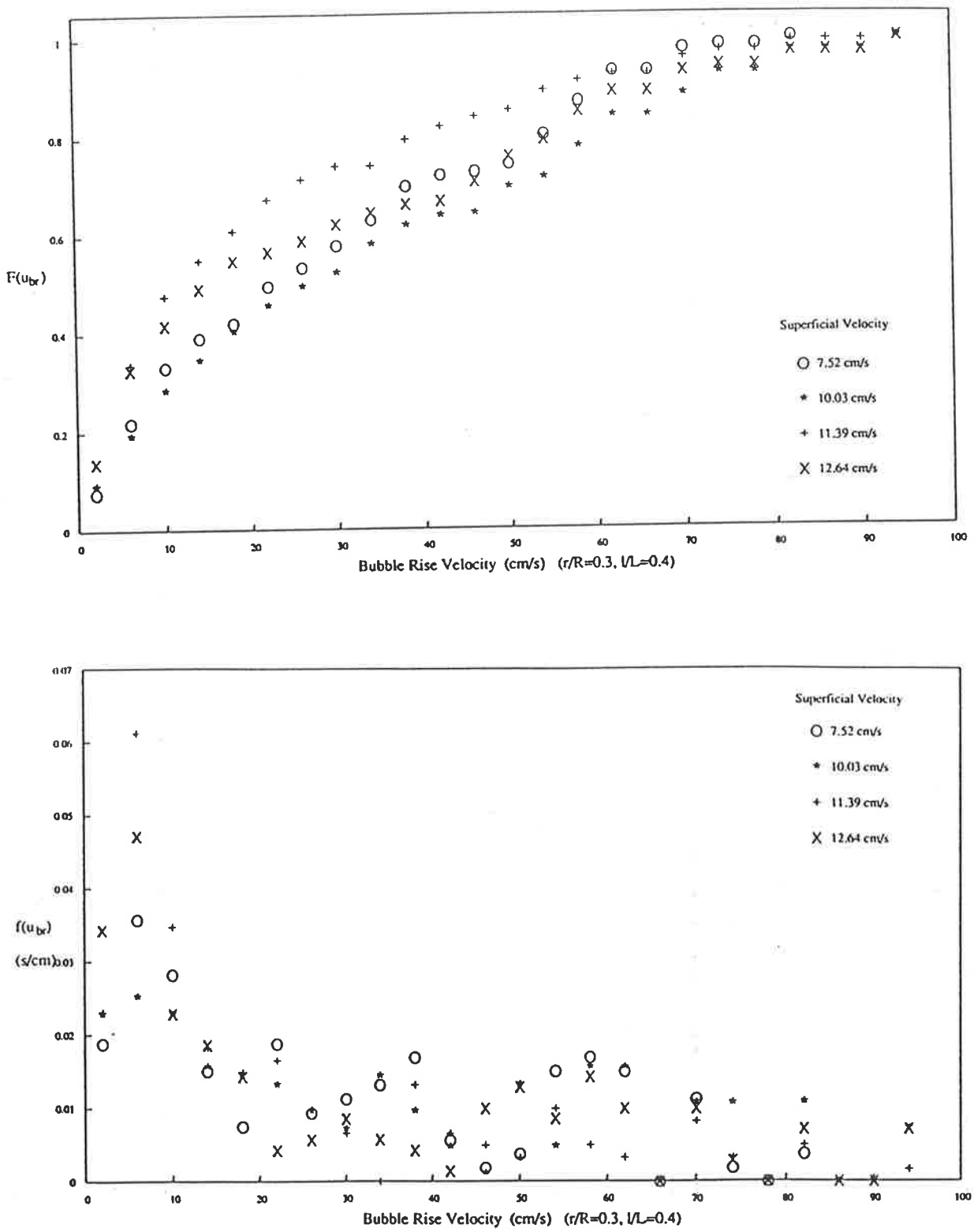

Figure 5.60 Cumulative Distribution and PDF of Bubble Rise Velocity

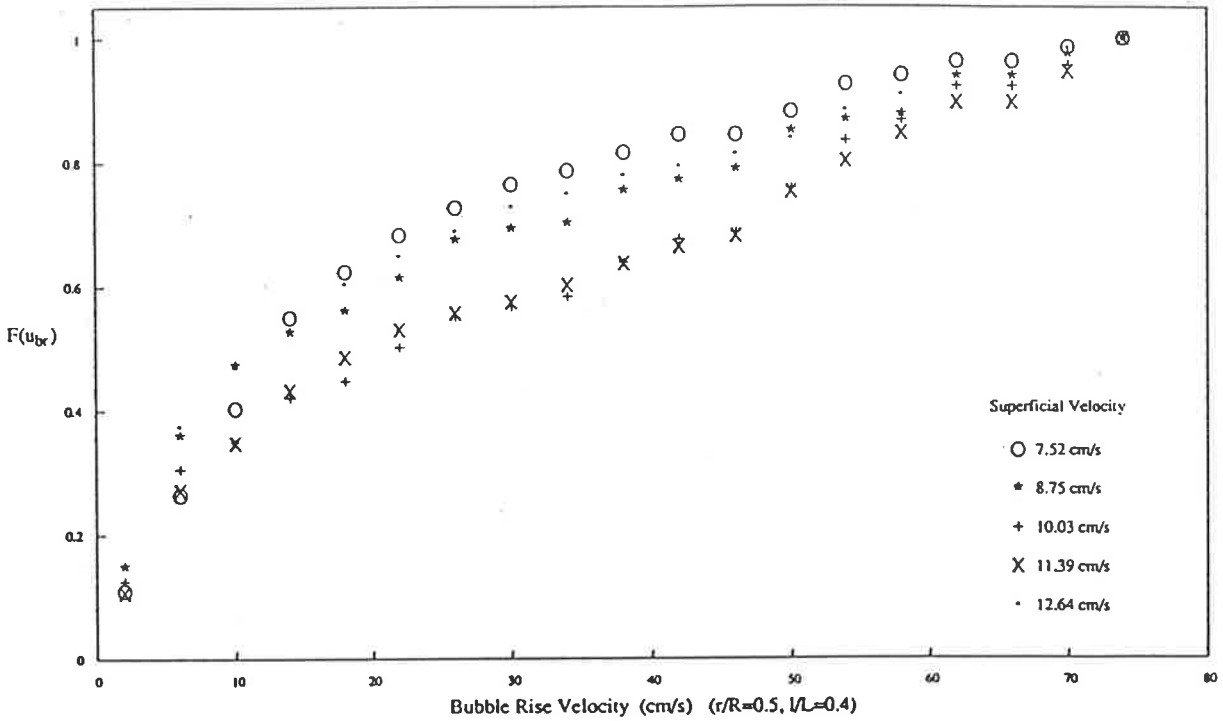

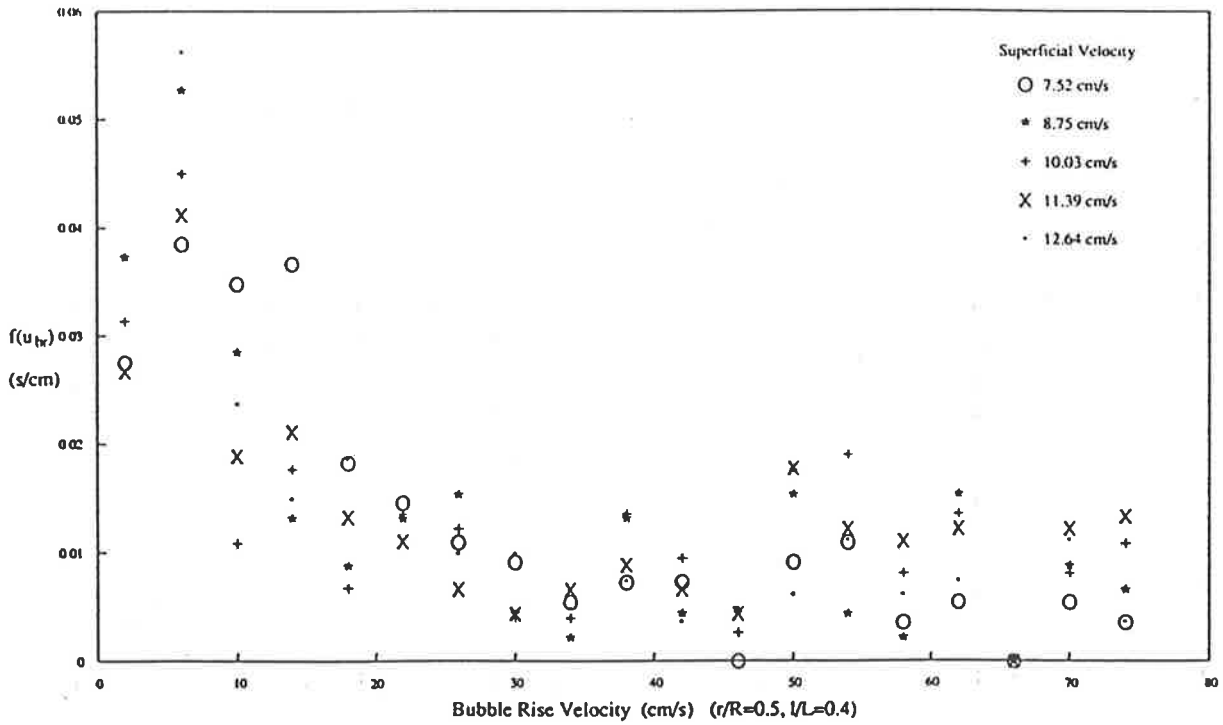

Figure 5.61 Cumulative Distribution and PDF of Bubble Rise Velocity

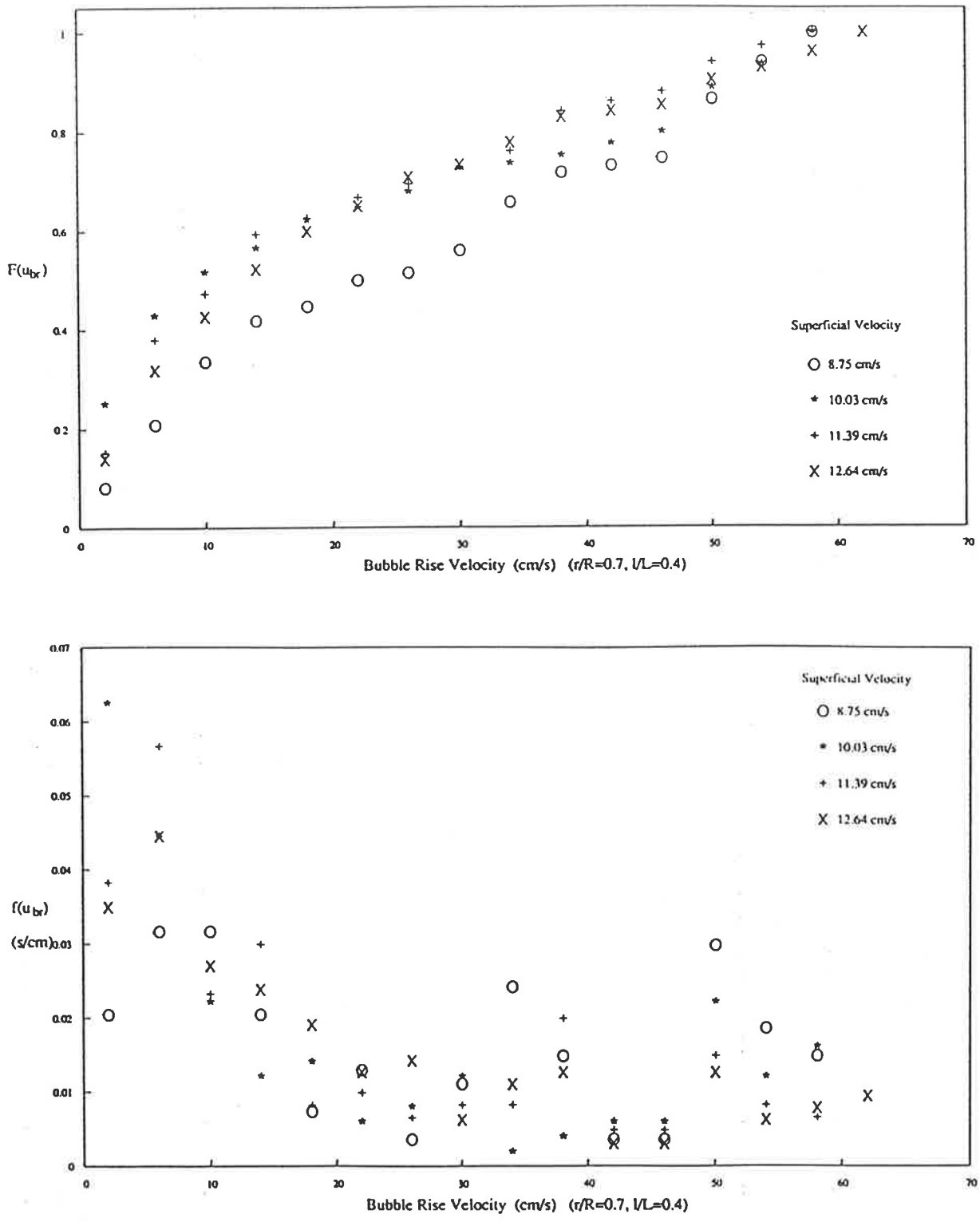

Figure 5.62 Cumulative Distribution and PDF of Bubble Rise Velocity

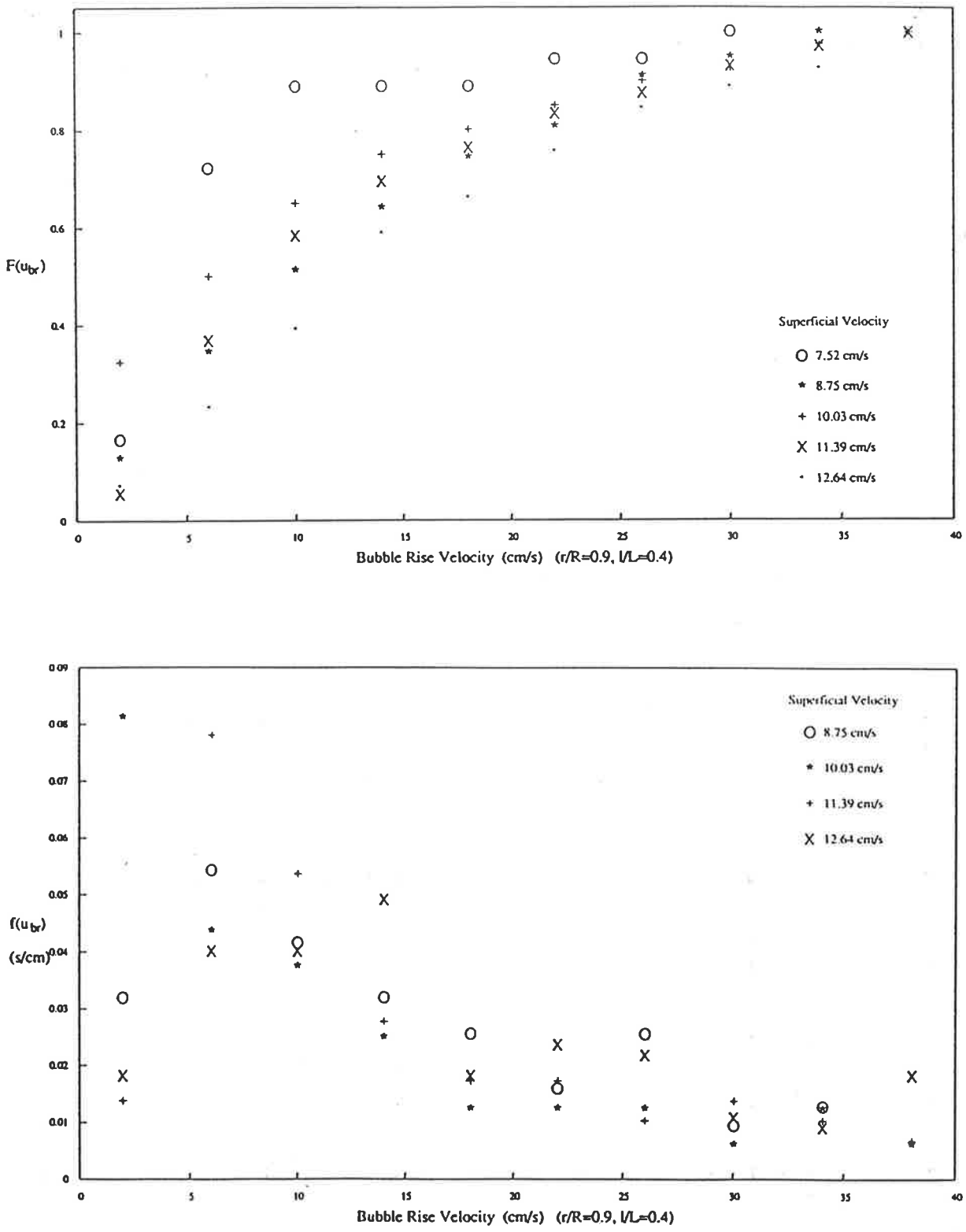

Figure 5.63 Cumulative Distribution and PDF of Bubble Rise Velocity

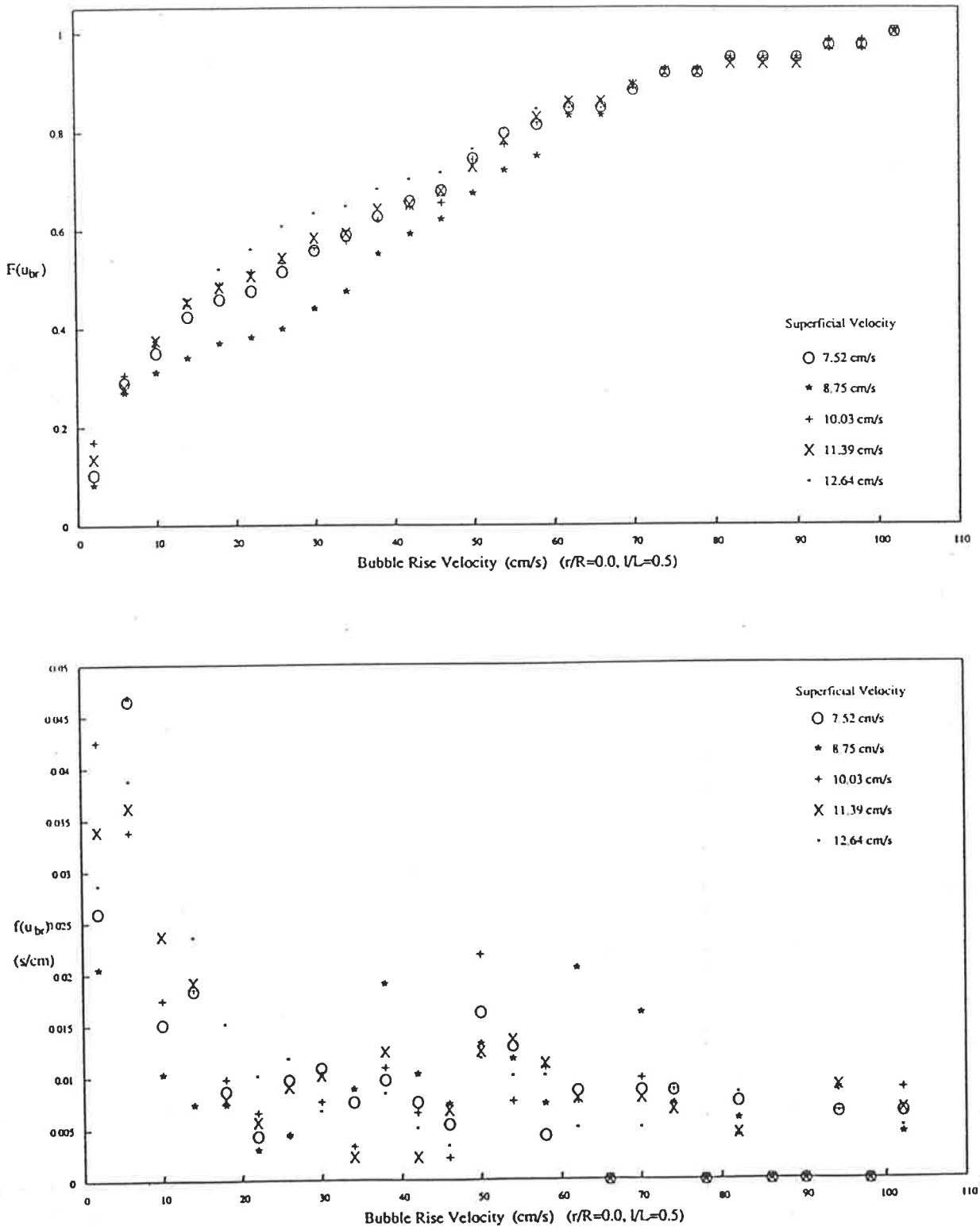

Figure 5.64 Cumulative Distribution and PDF of Bubble Rise Velocity

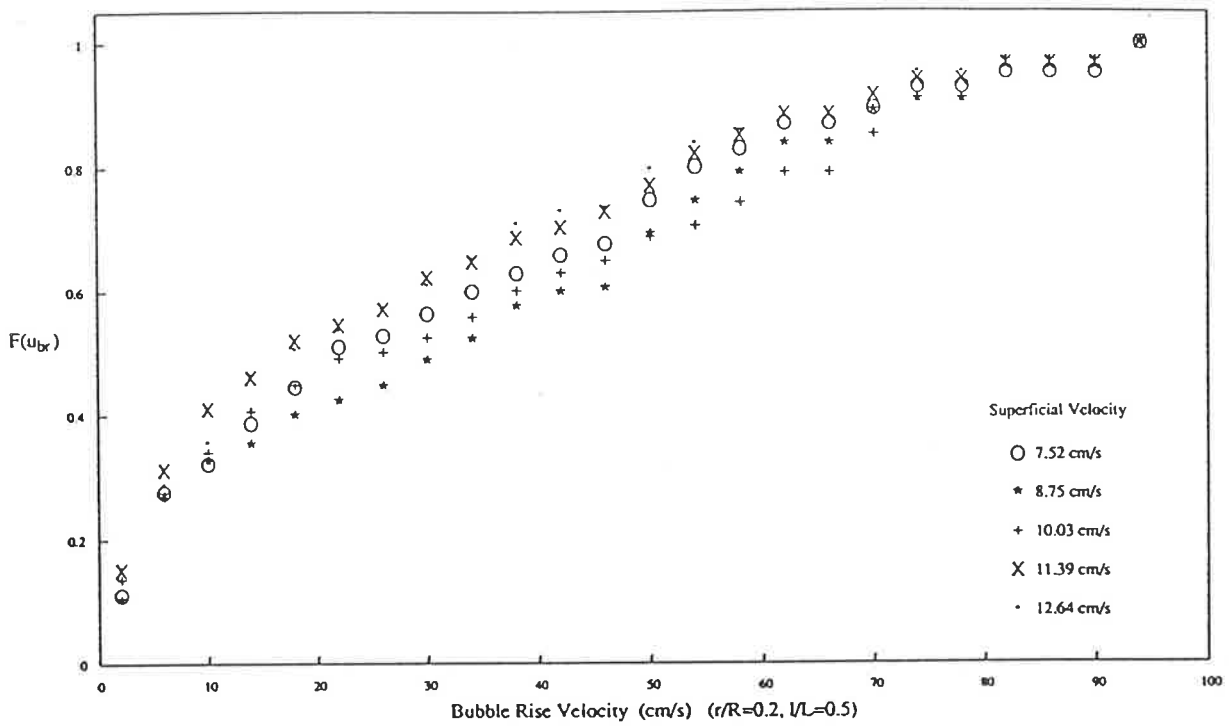

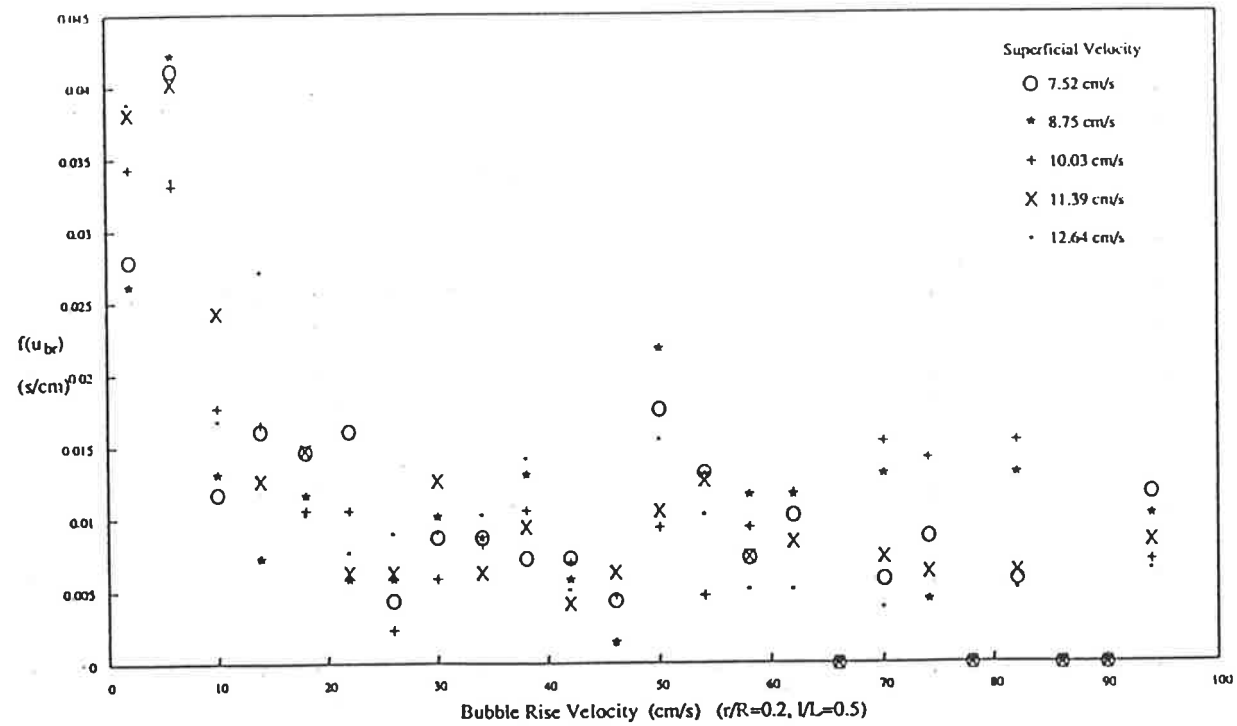

Figure 5.65 Cumulative Distribution and PDF of Bubble Rise Velocity

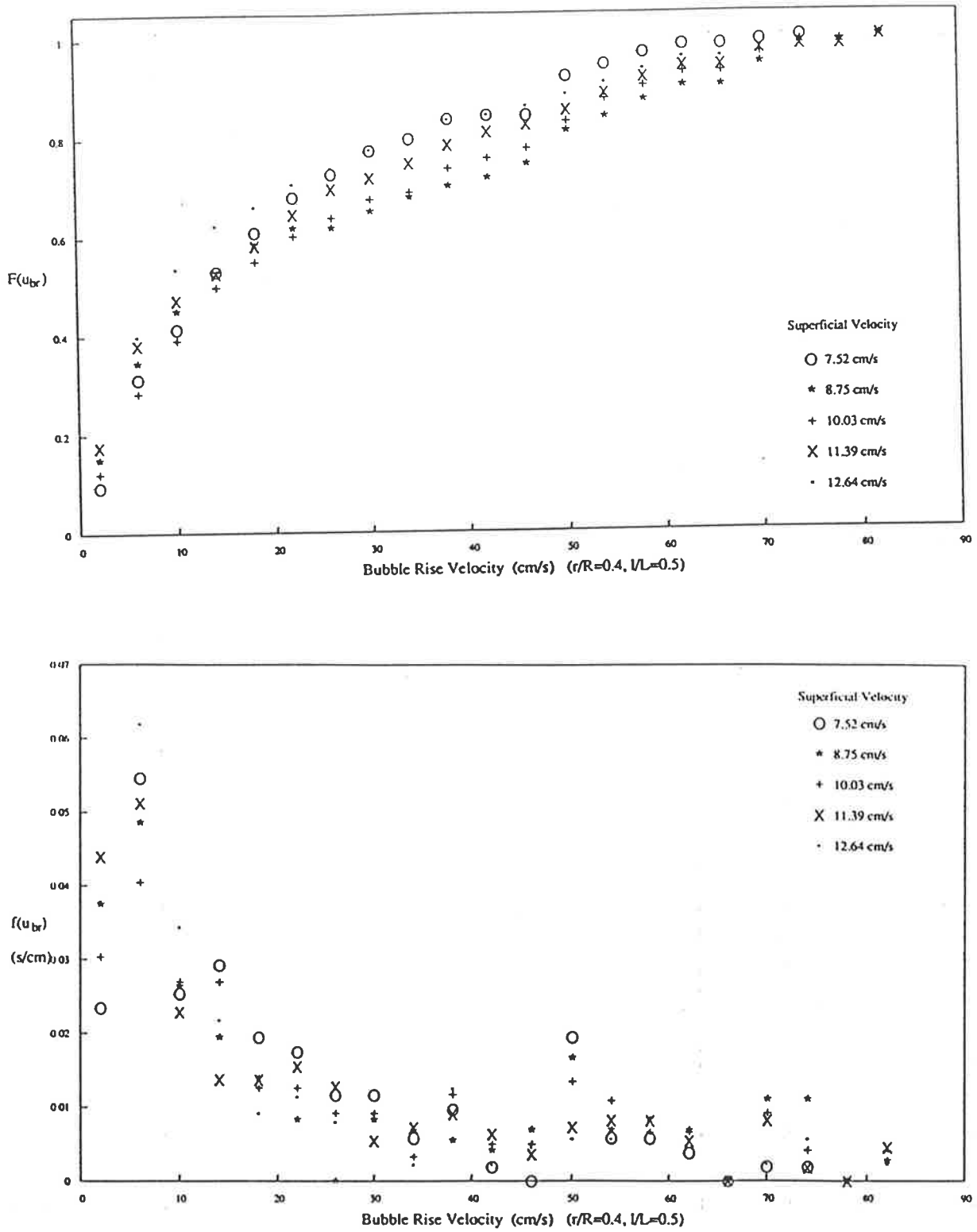

Figure 5.66 Cumulative Distribution and PDF of Bubble Rise Velocity

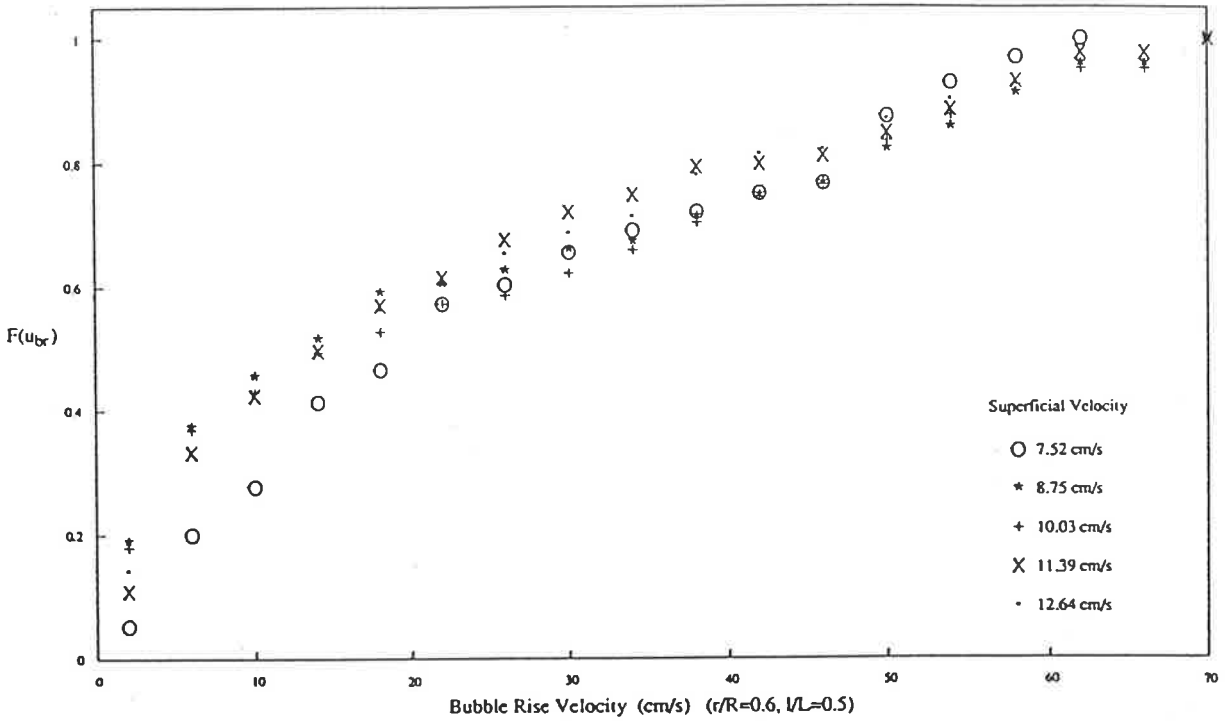

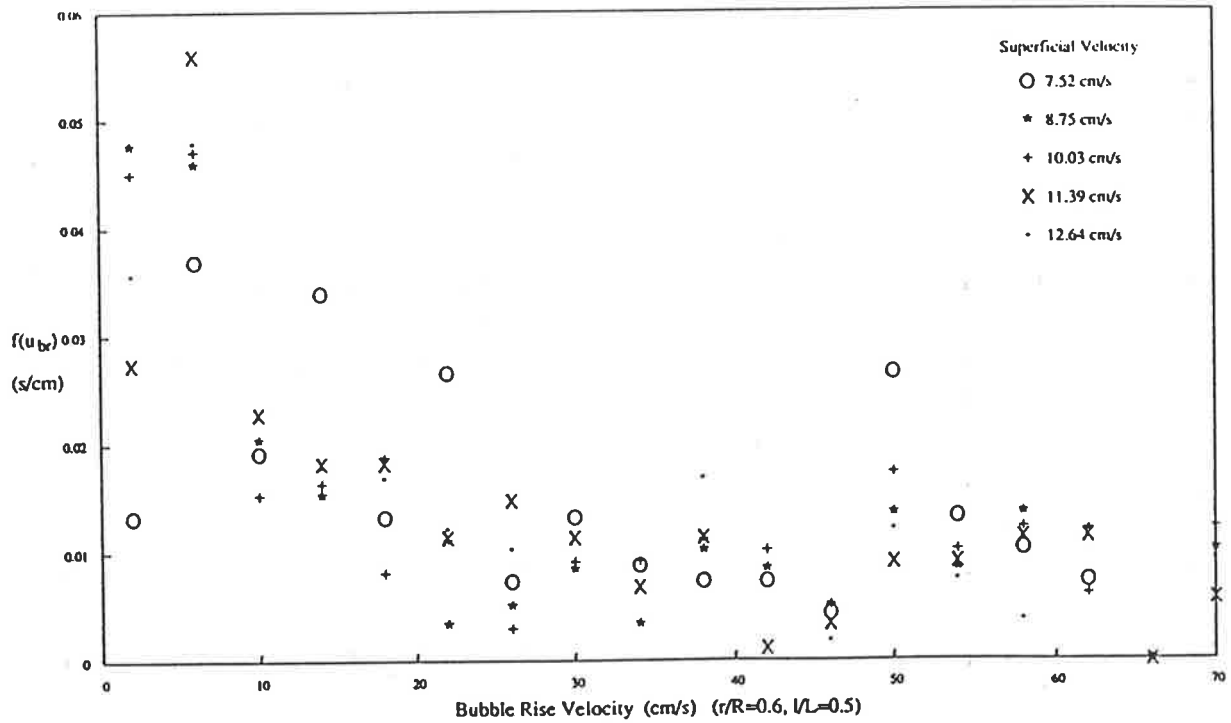

Figure 5.67 Cumulative Distribution and PDF of Bubble Rise Velocity

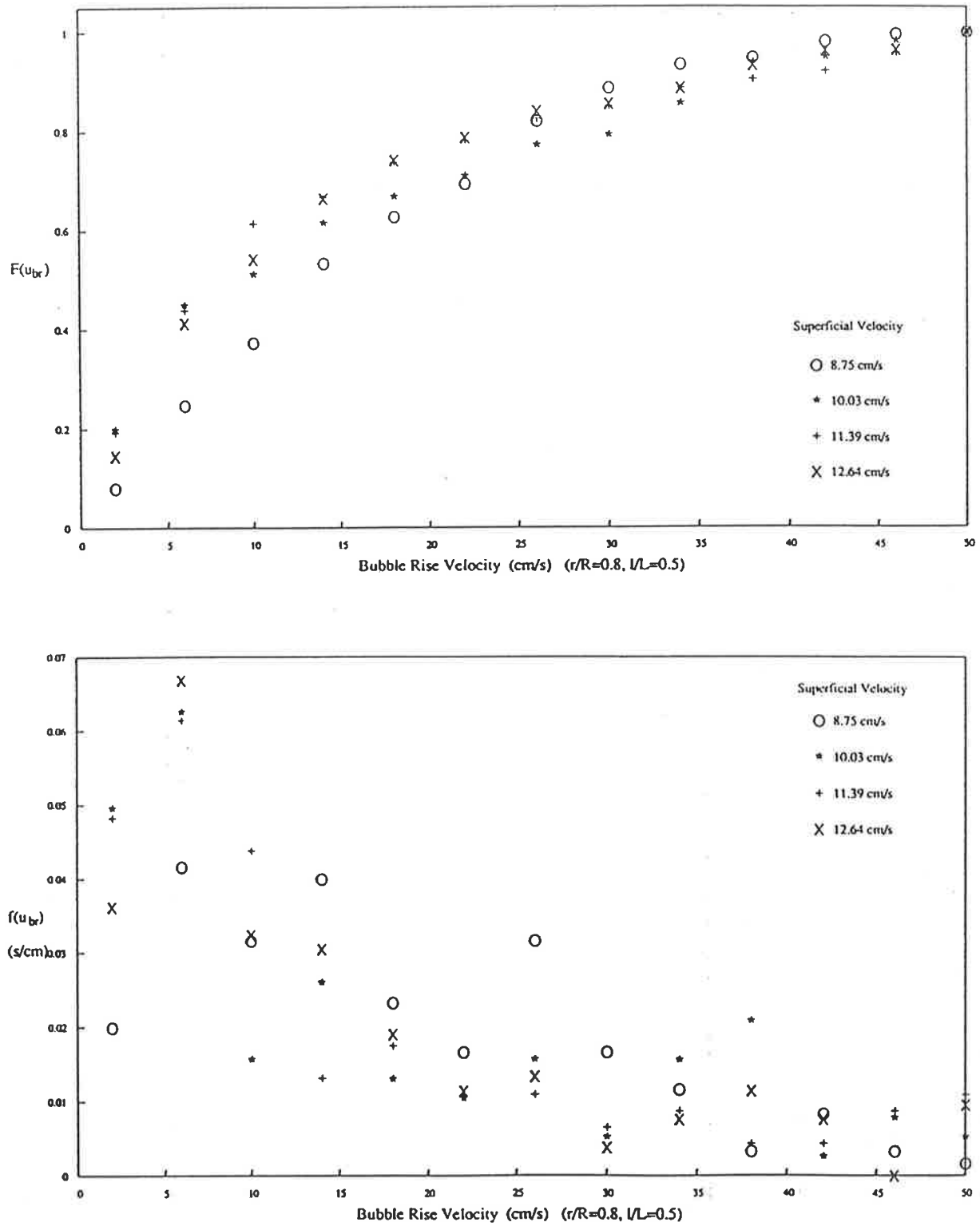

Figure 5.68 Cumulative Distribution and PDF of Bubble Rise Velocity

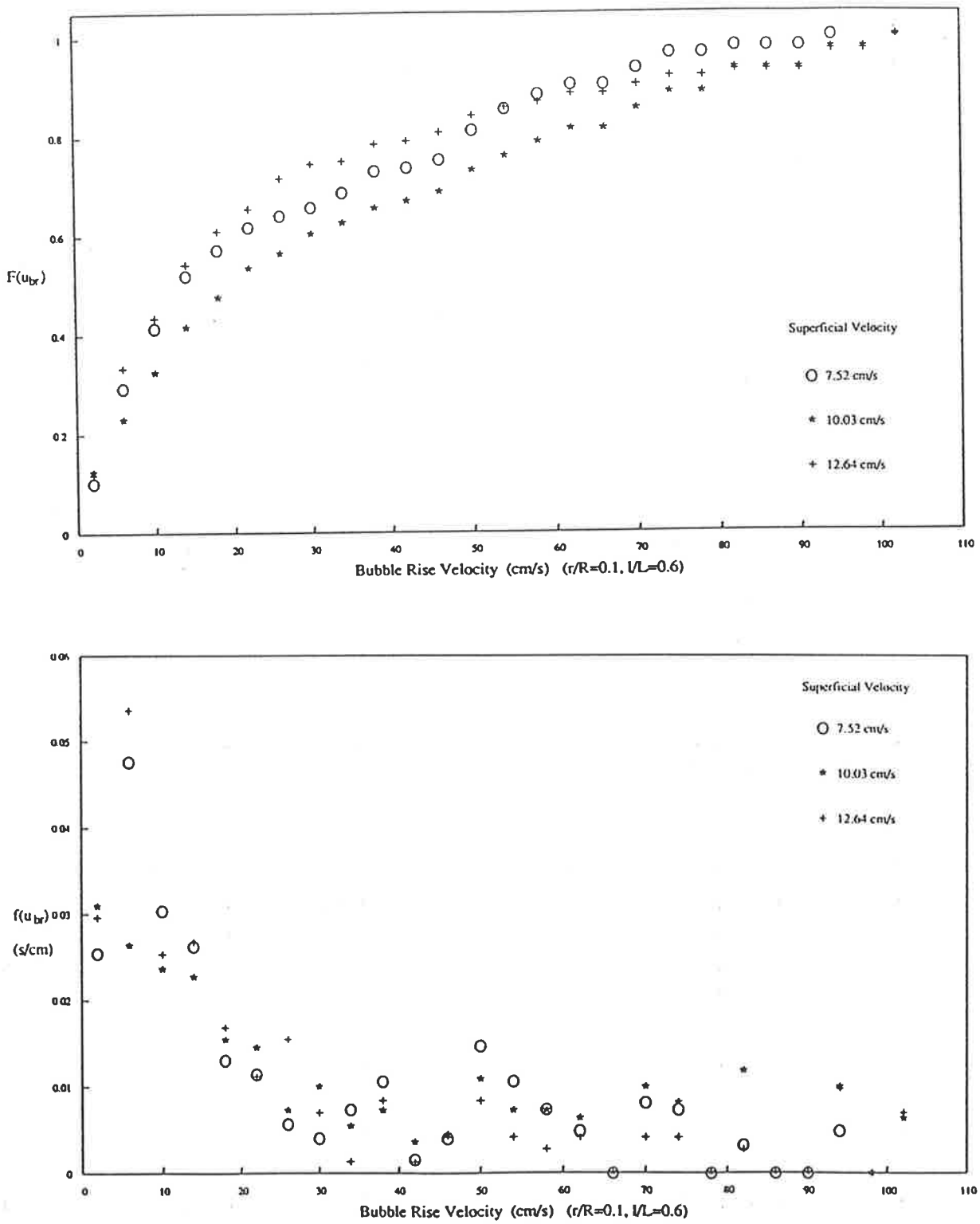

Figure 5.69 Cumulative Distribution and PDF of Bubble Rise Velocity

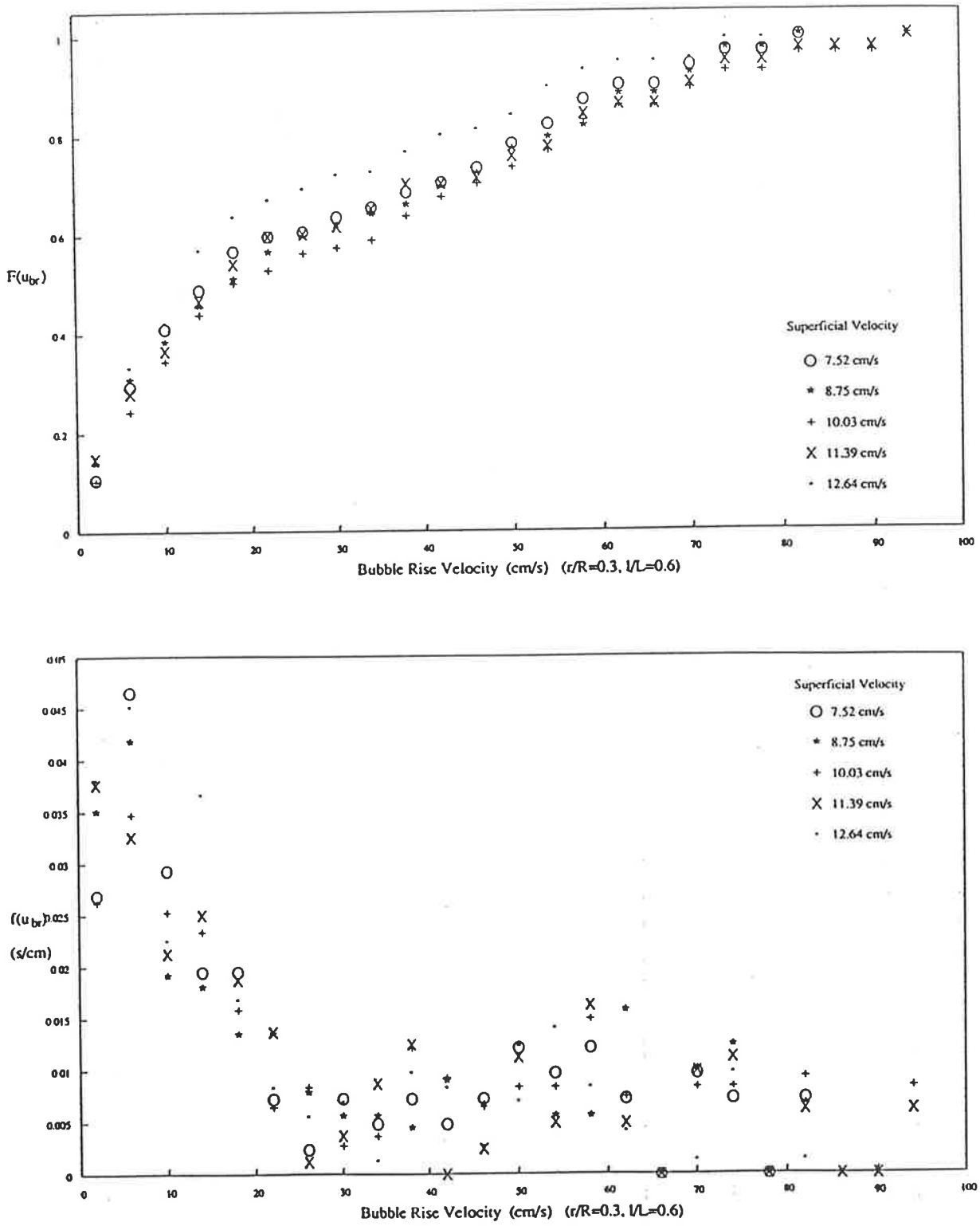

Figure 5.70 Cumulative Distribution and PDF of Bubble Rise Velocity

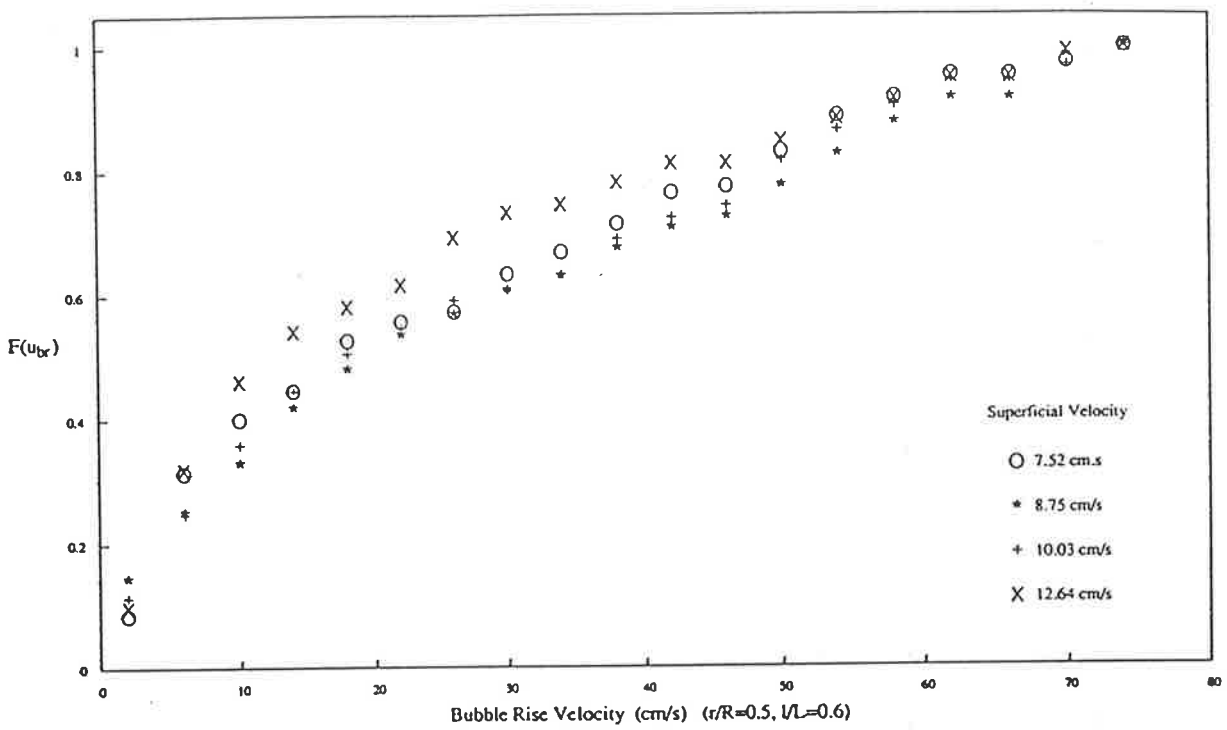

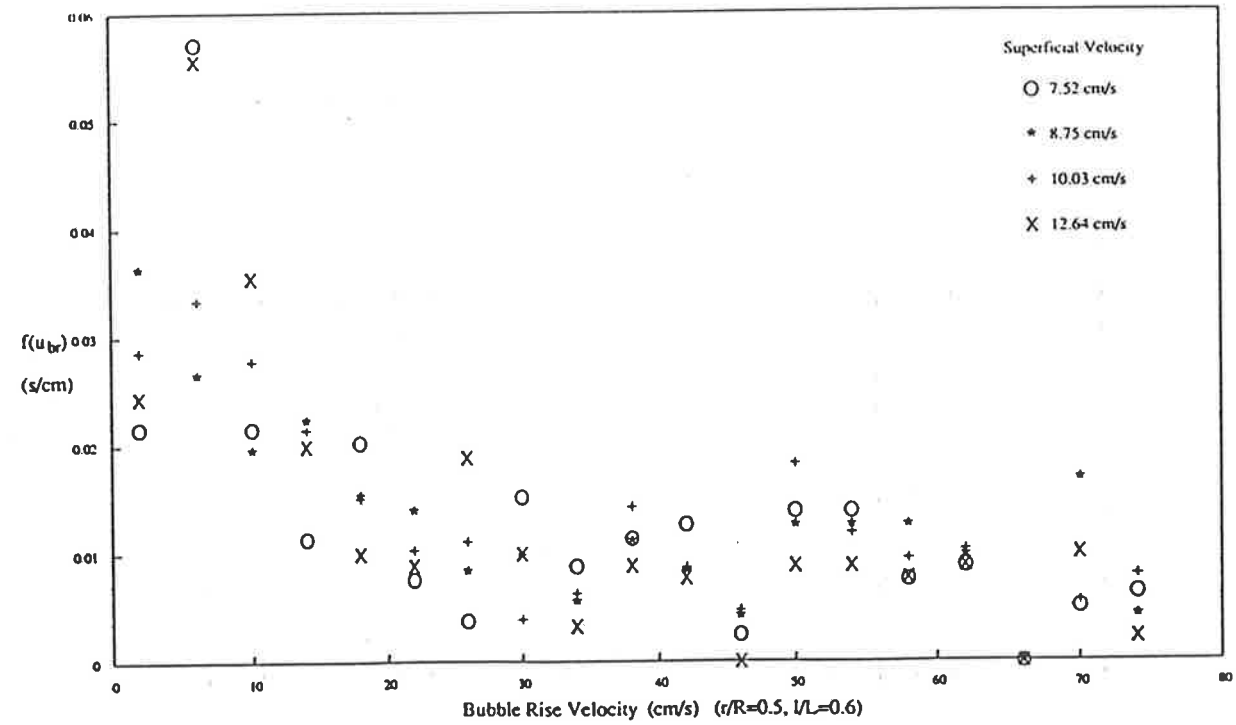

Figure 5.71 Cumulative Distribution and PDF of Bubble Rise Velocity

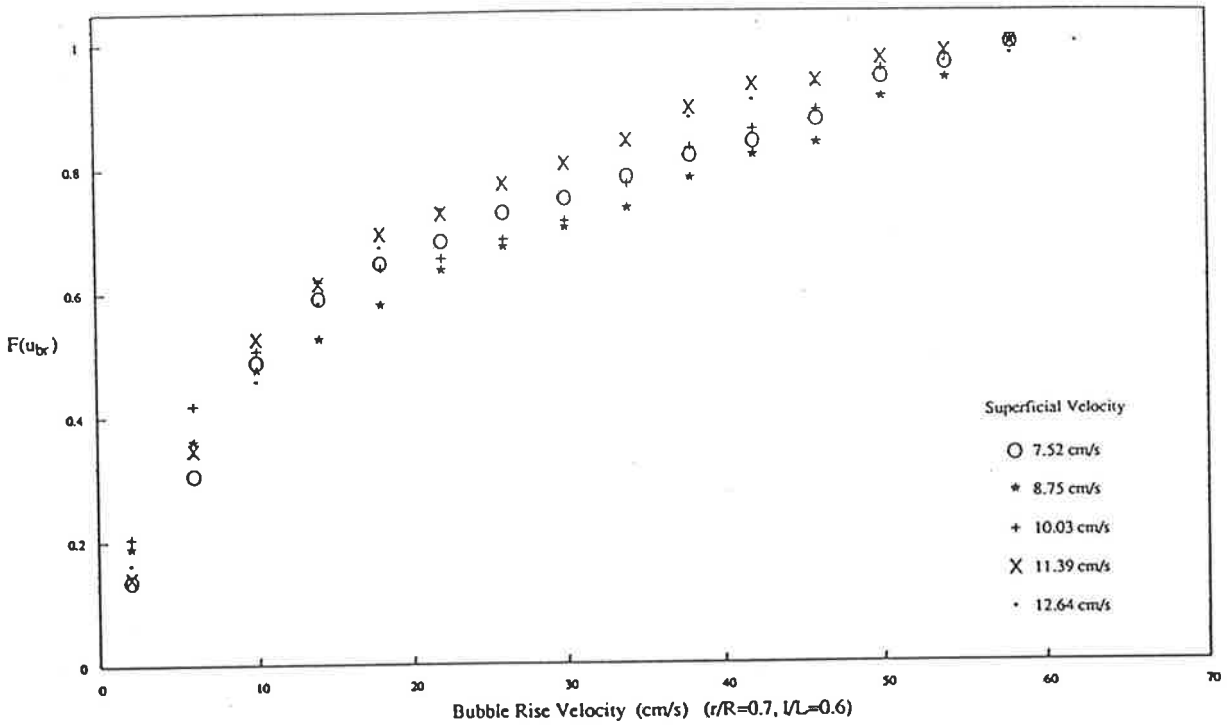

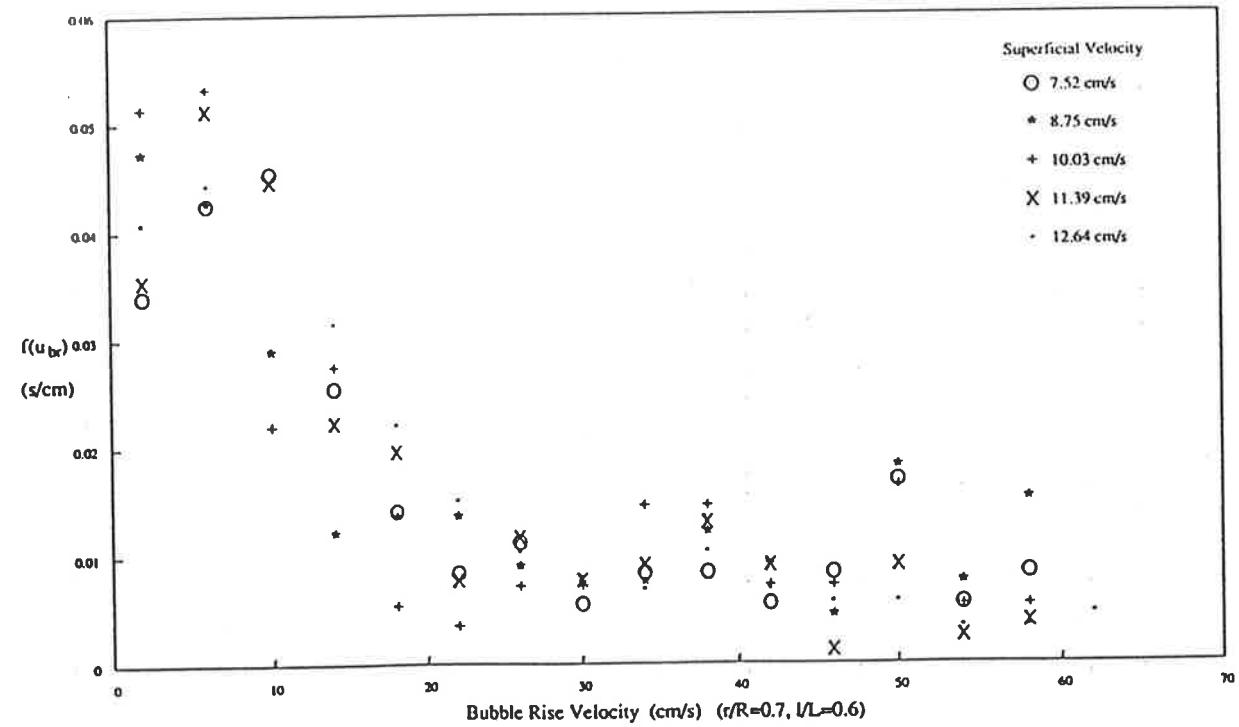

Figure 5.72 Cumulative Distribution and PDF of Bubble Rise Velocity

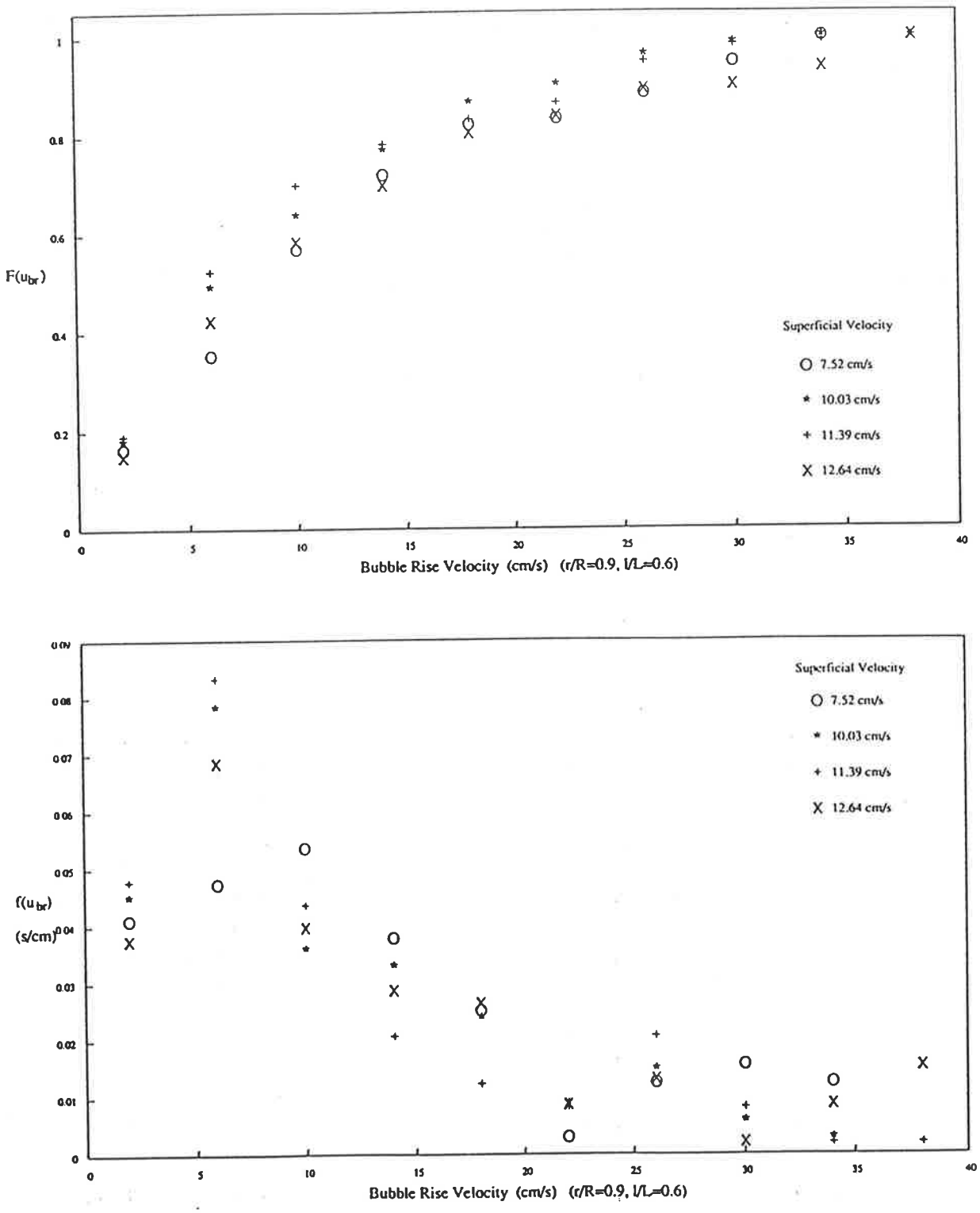

Figure 5.73 Cumulative Distribution and PDF of Bubble Rise Velocity

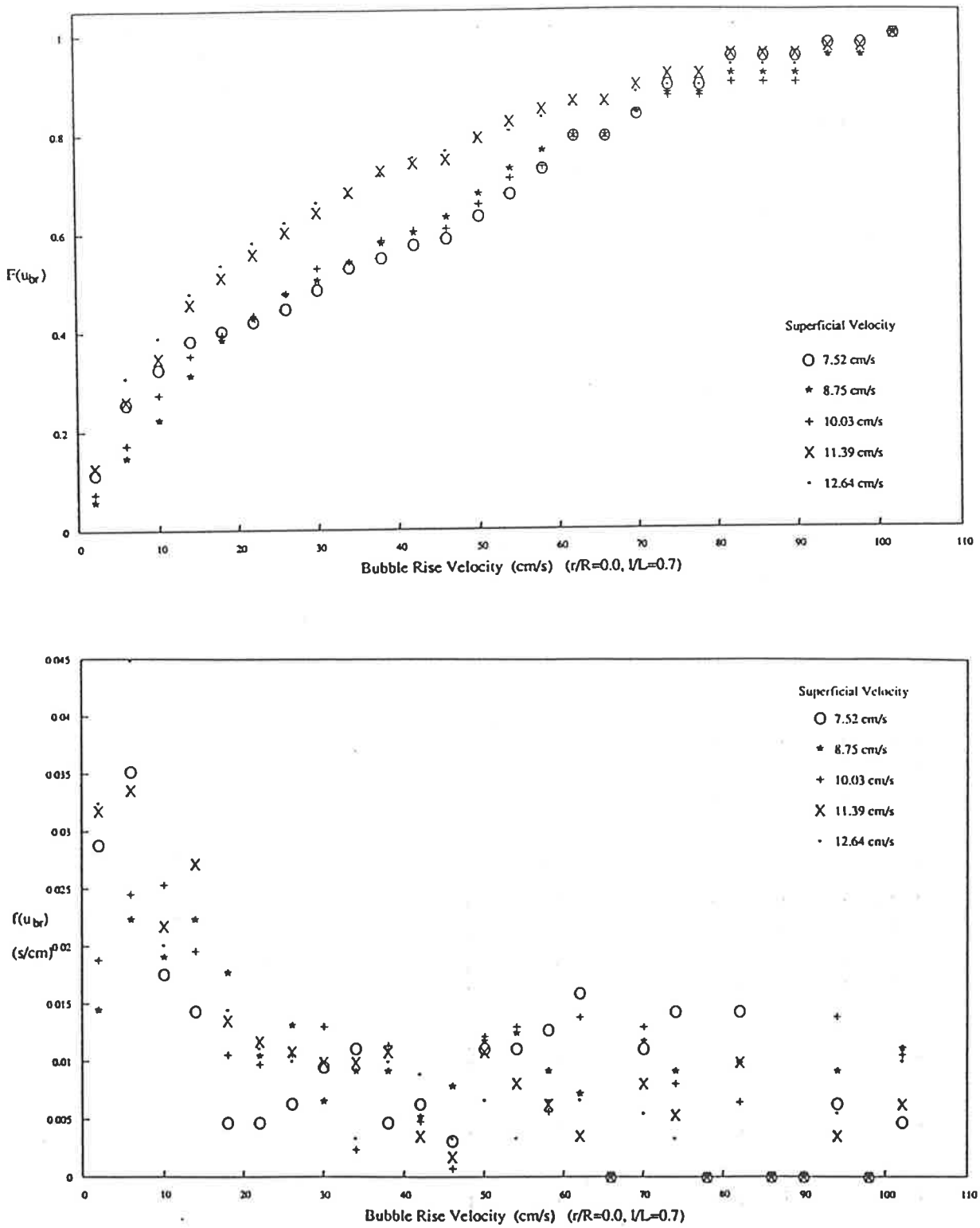

Figure 5.74 Cumulative Distribution and PDF of Bubble Rise Velocity

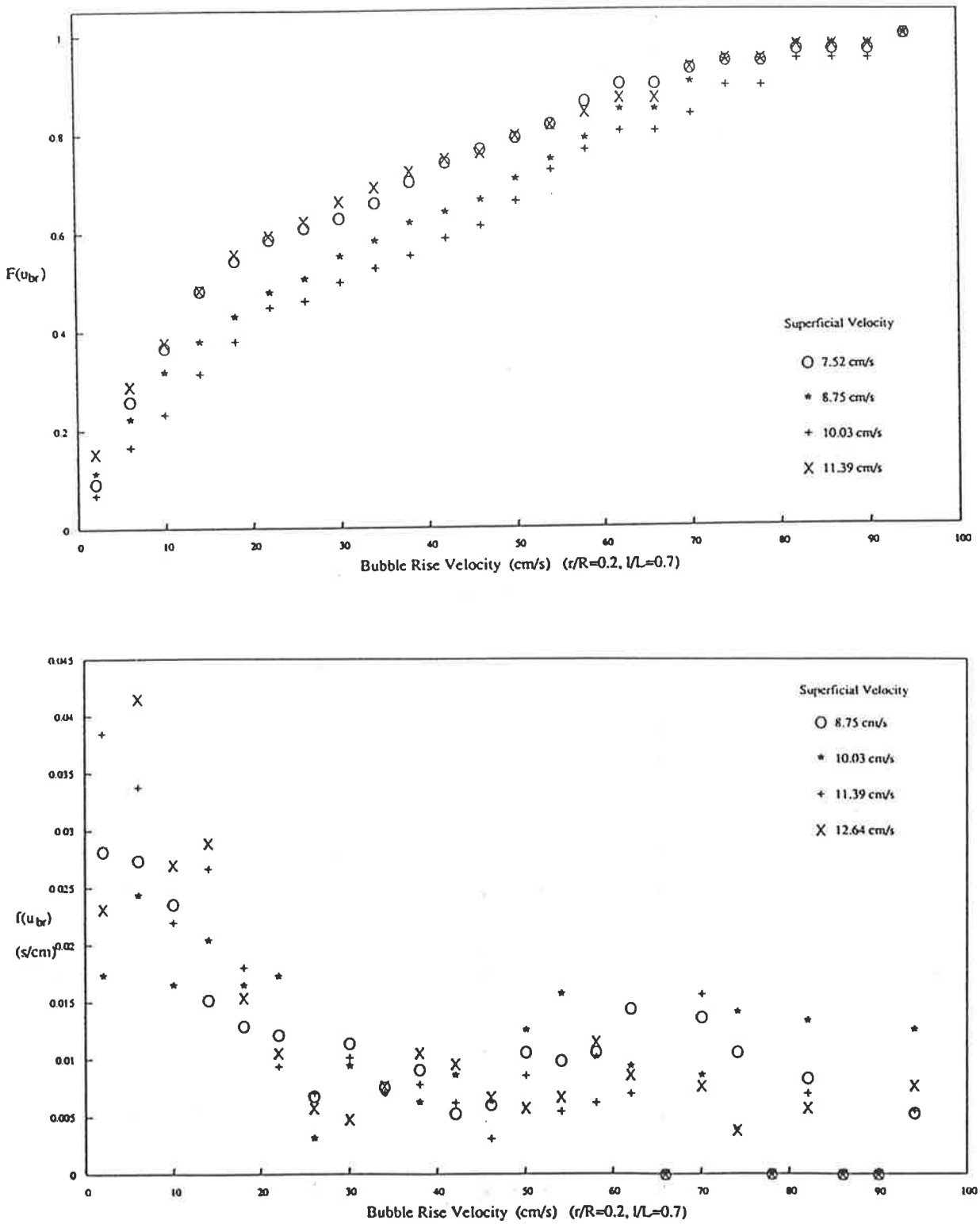

Figure 5.75 Cumulative Distribution and PDF of Bubble Rise Velocity

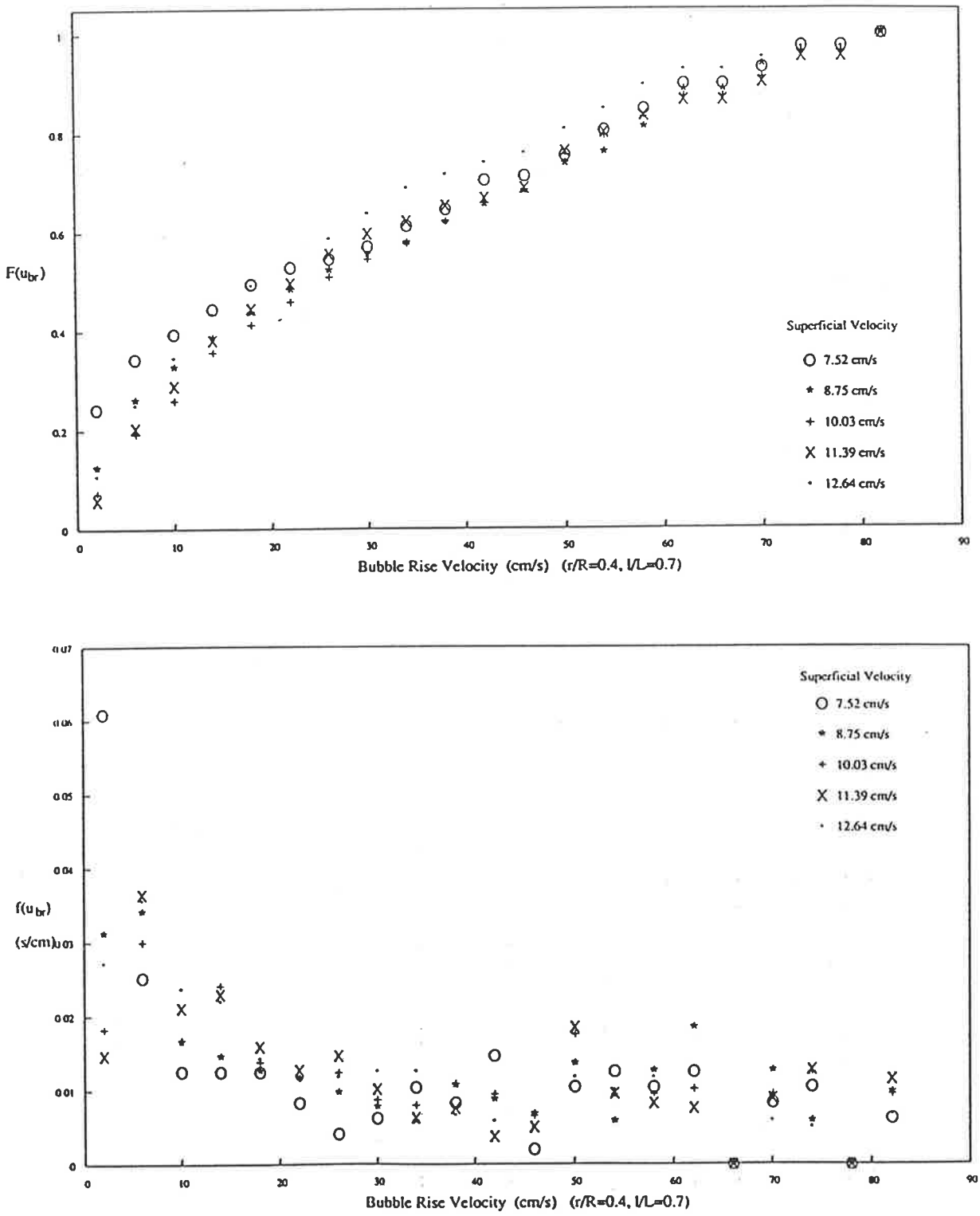

Figure 5.76 Cumulative Distribution and PDF of Bubble Rise Velocity

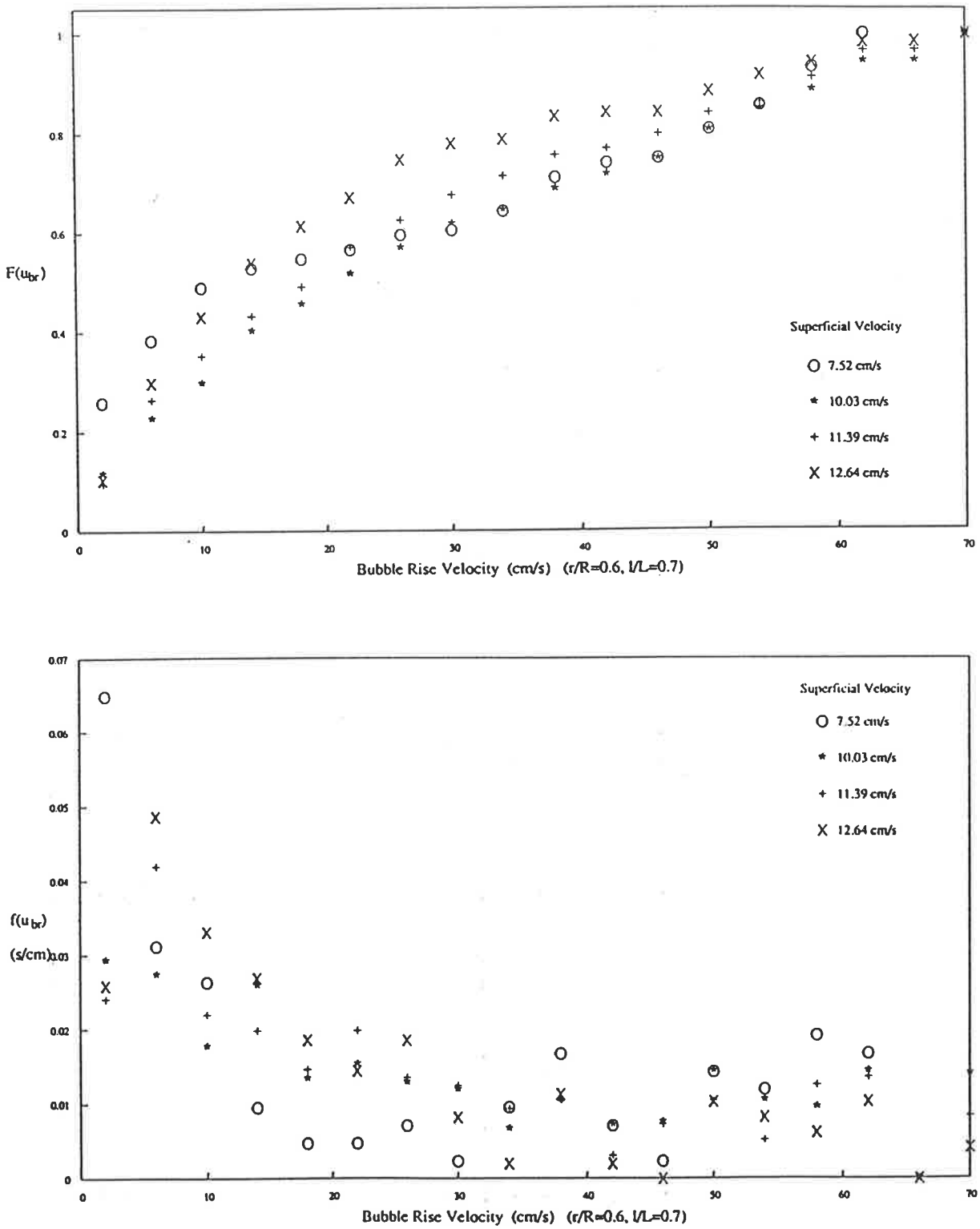

Figure 5.77 Cumulative Distribution and PDF of Bubble Rise Velocity

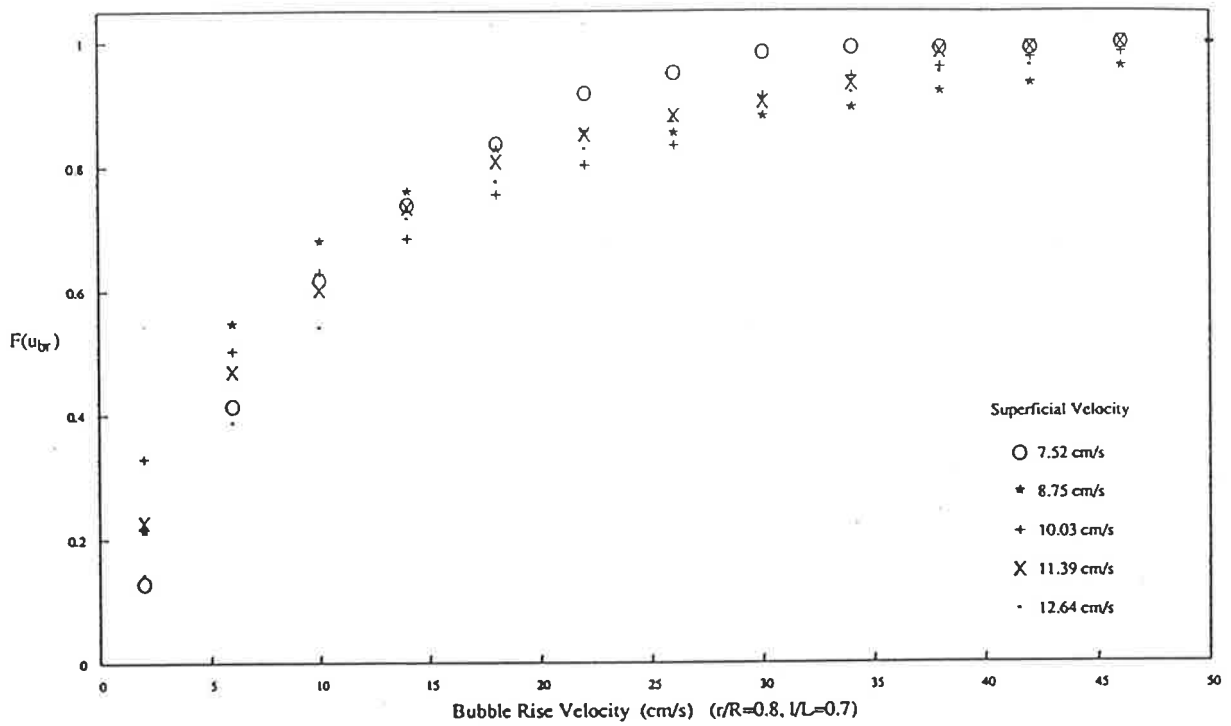

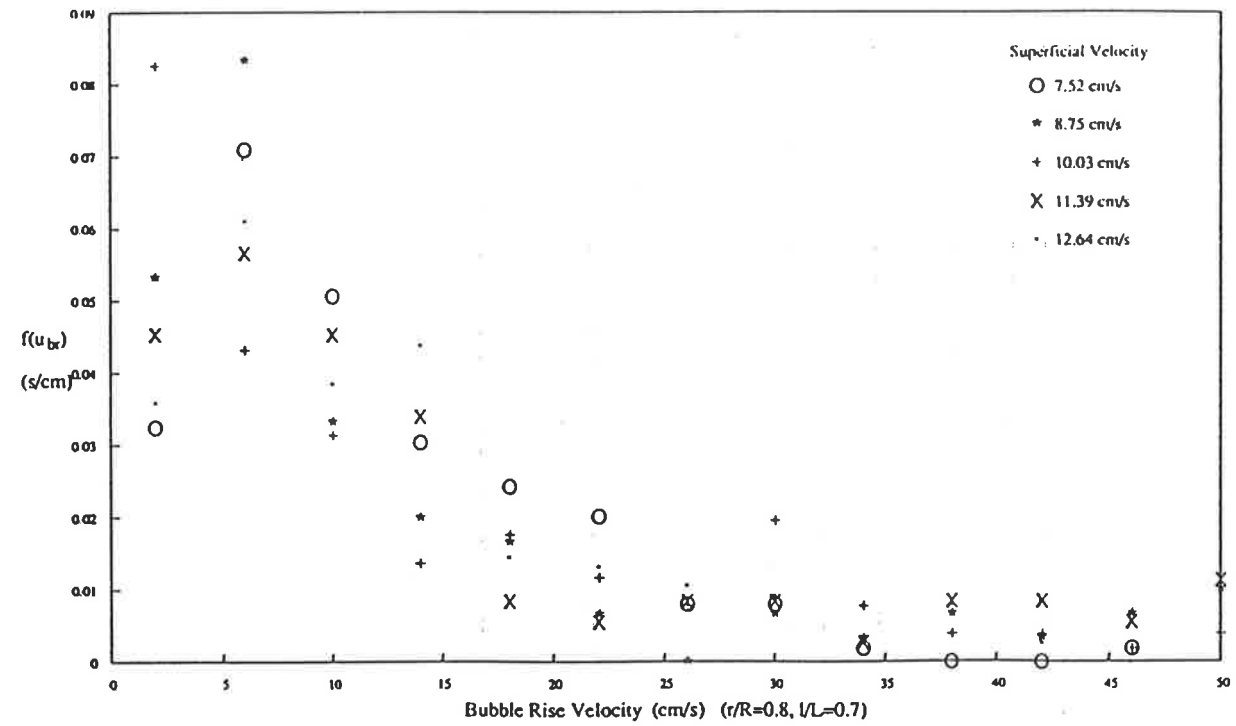

Figure 5.78 Cumulative Distribution and PDF of Bubble Rise Velocity

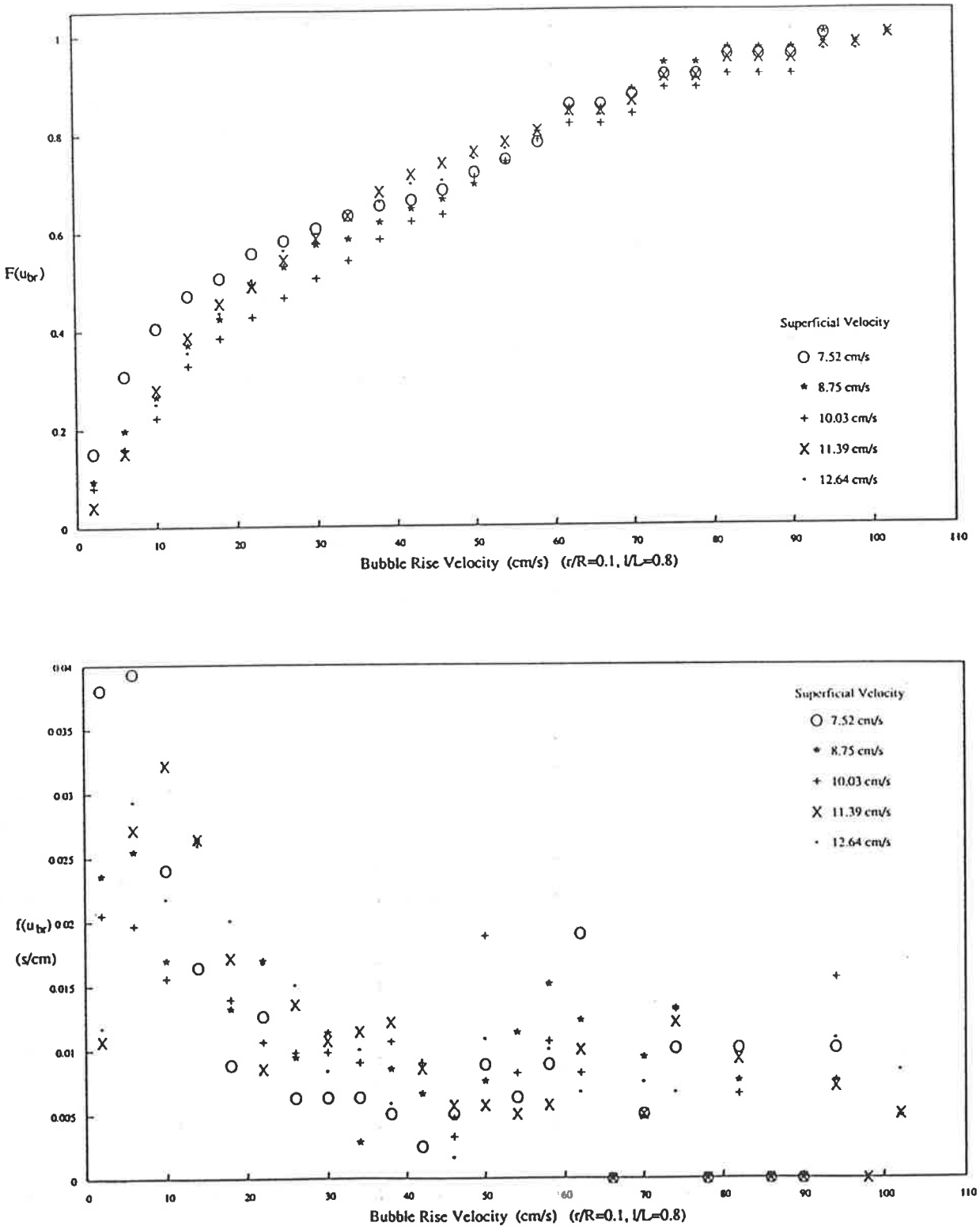

Figure 5.79 Cumulative Distribution and PDF of Bubble Rise Velocity

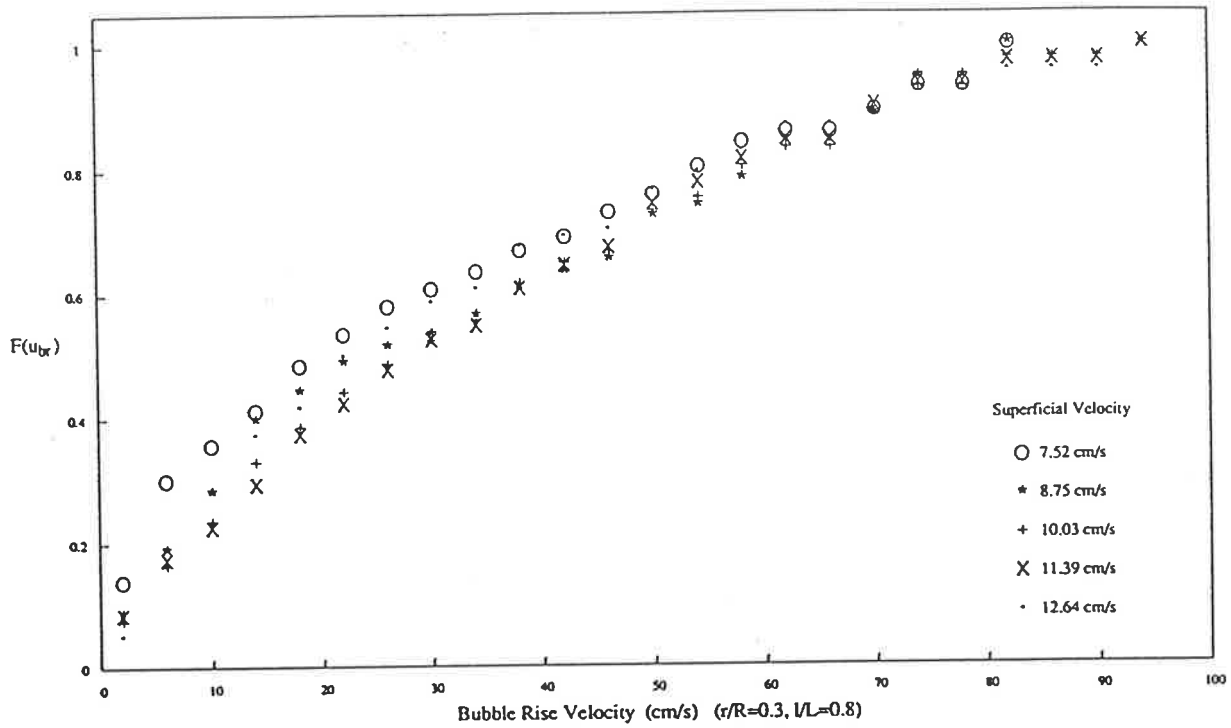

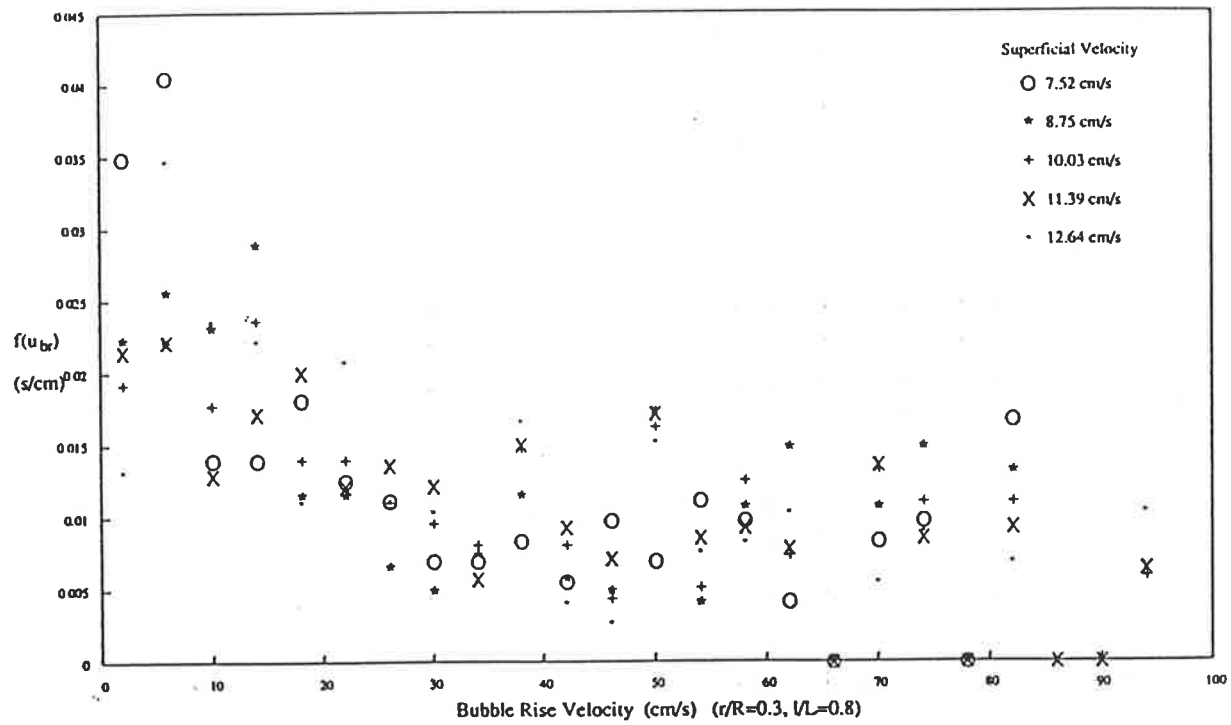

Figure 5.80 Cumulative Distribution and PDF of Bubble Rise Velocity

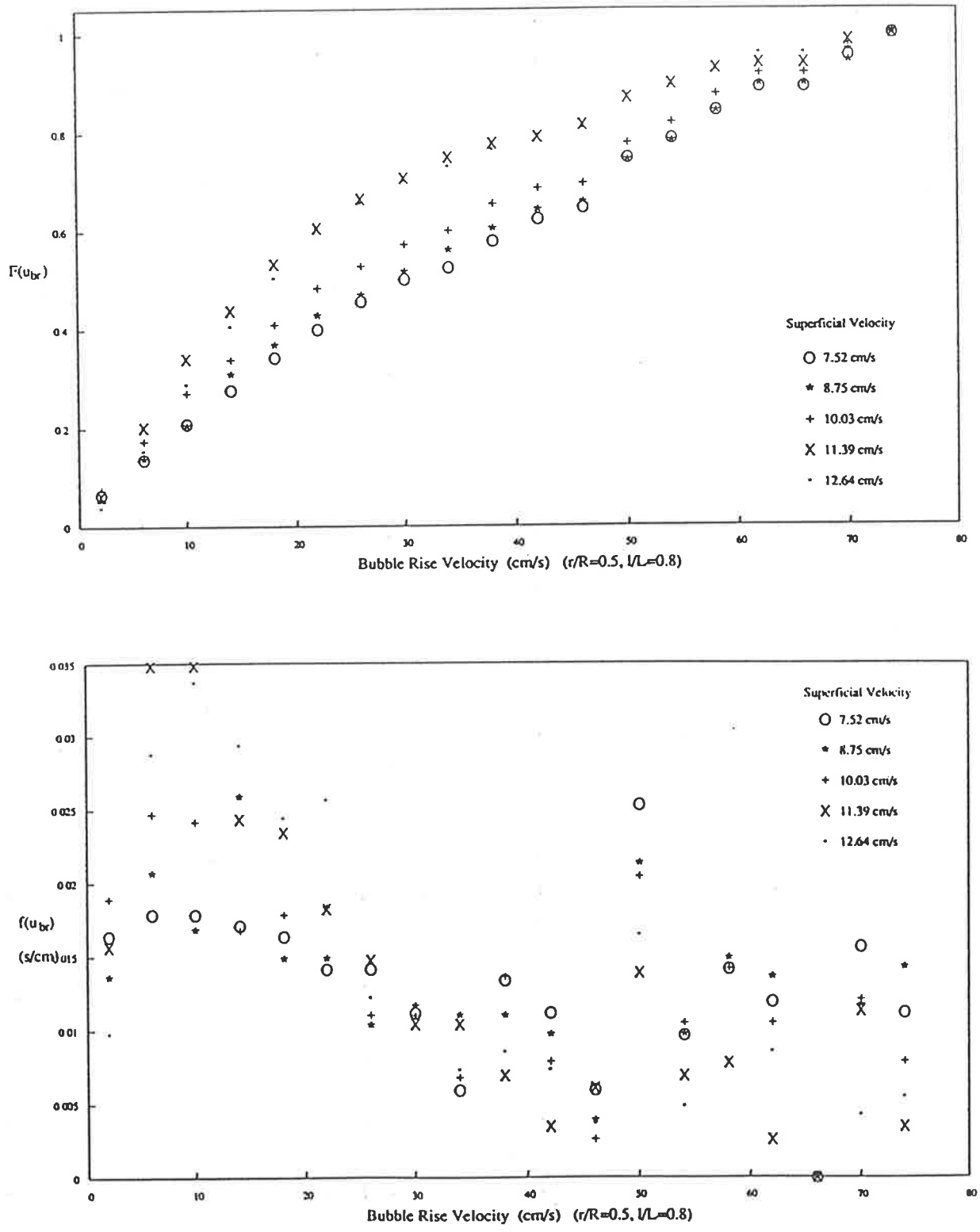

Figure 5.81 Cumulative Distribution and PDF of Bubble Rise Velocity

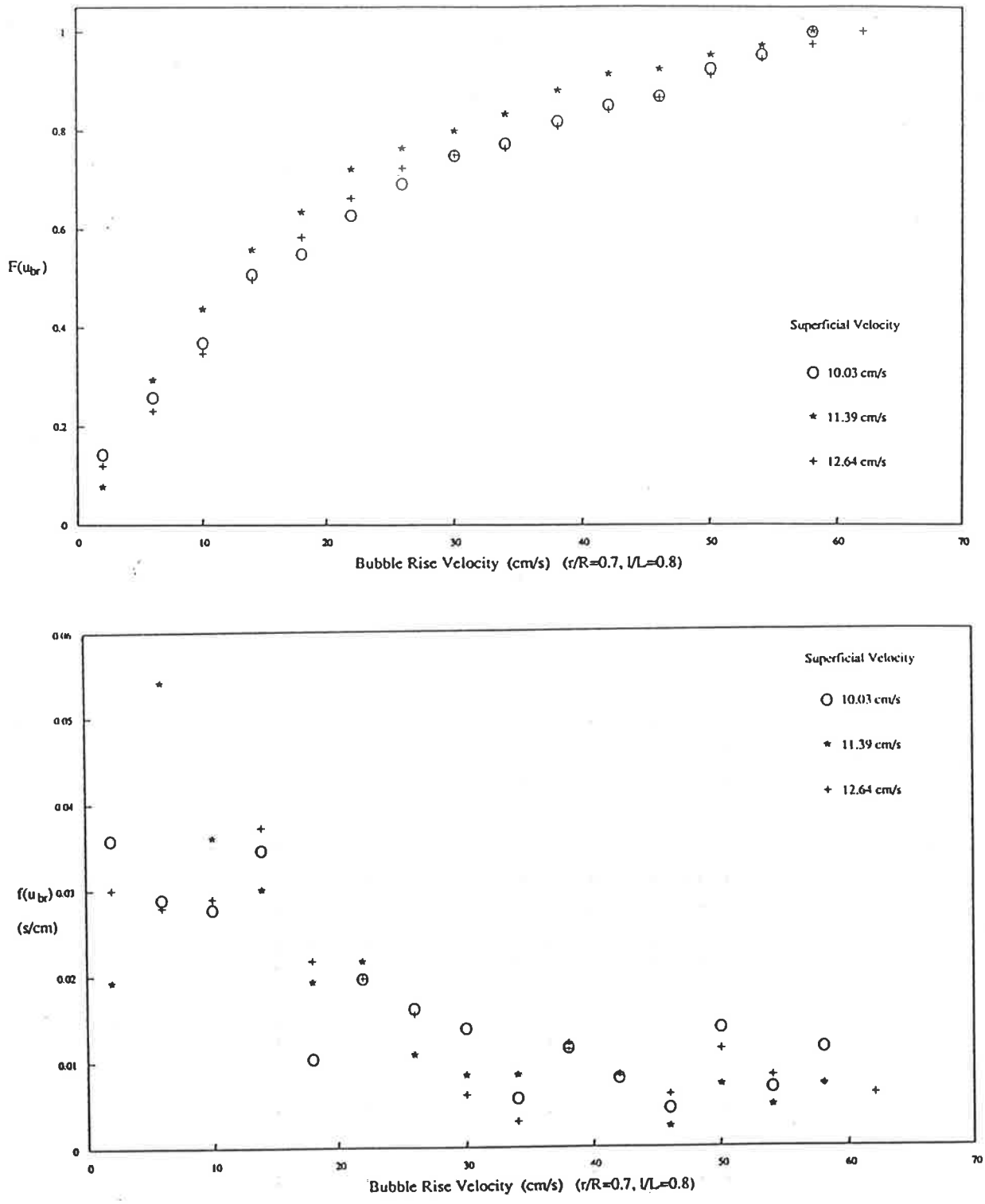

Figure 5.82 Cumulative Distribution and PDF of Bubble Rise Velocity

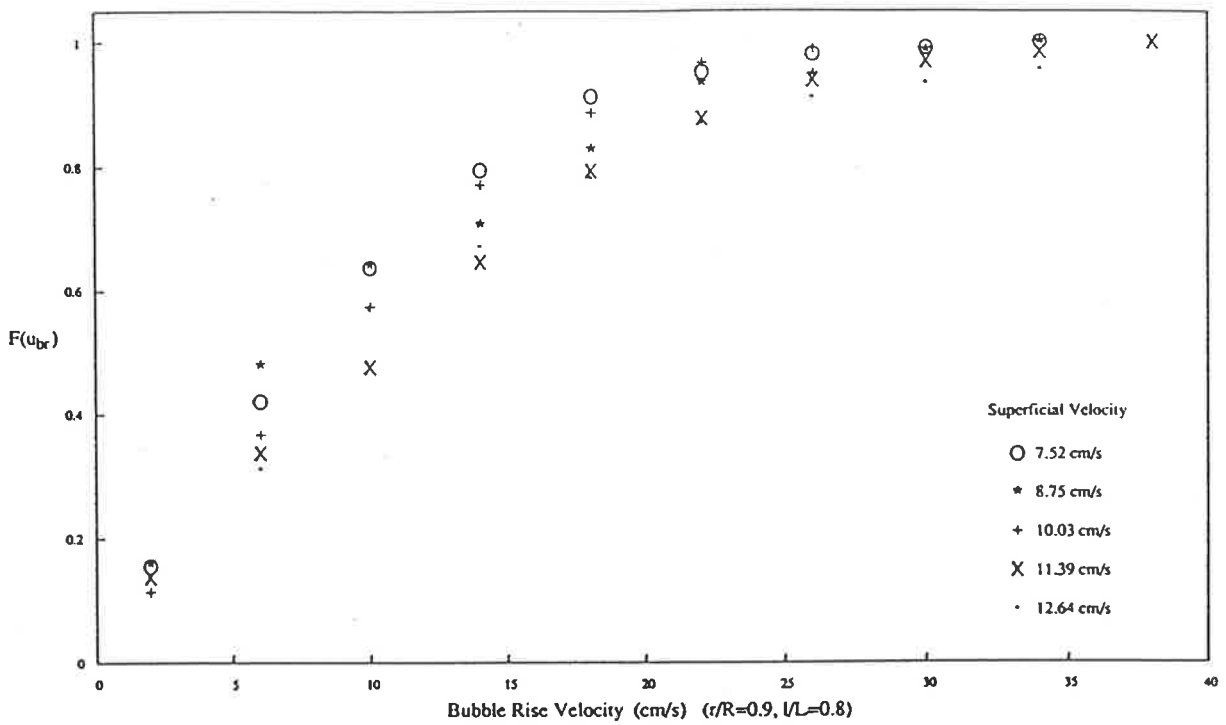

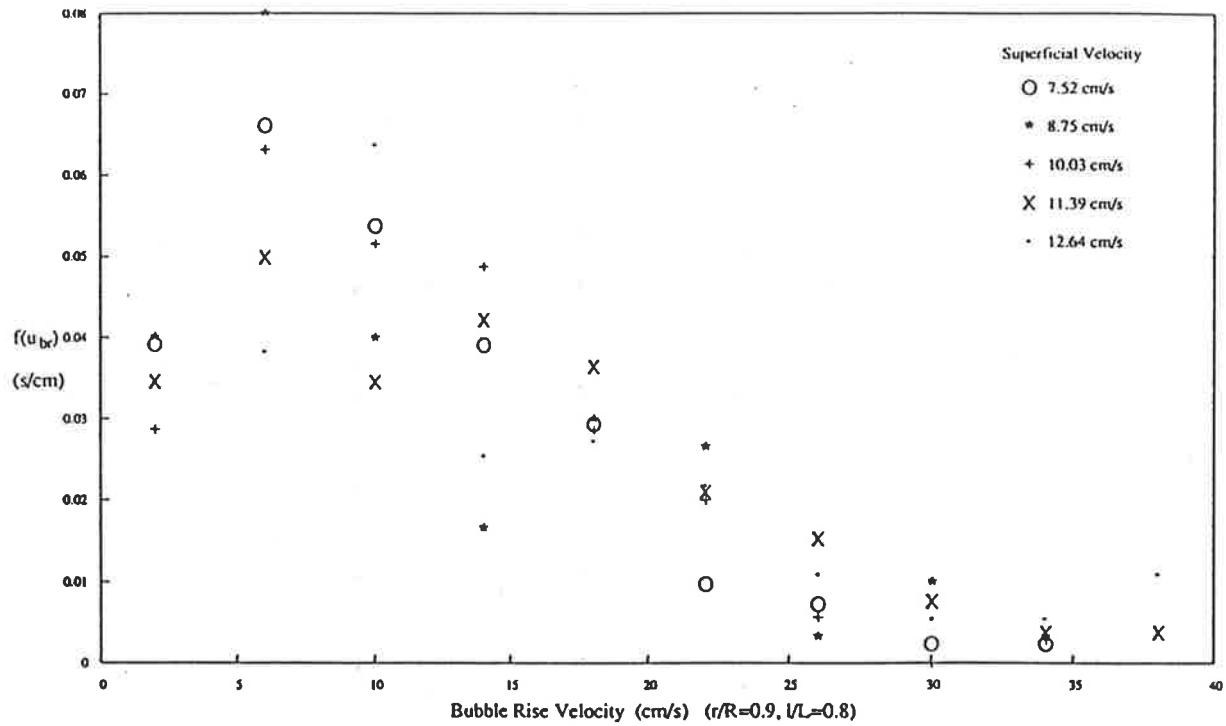

Figure 5.83 Cumulative Distribution and PDF of Bubble Rise Velocity

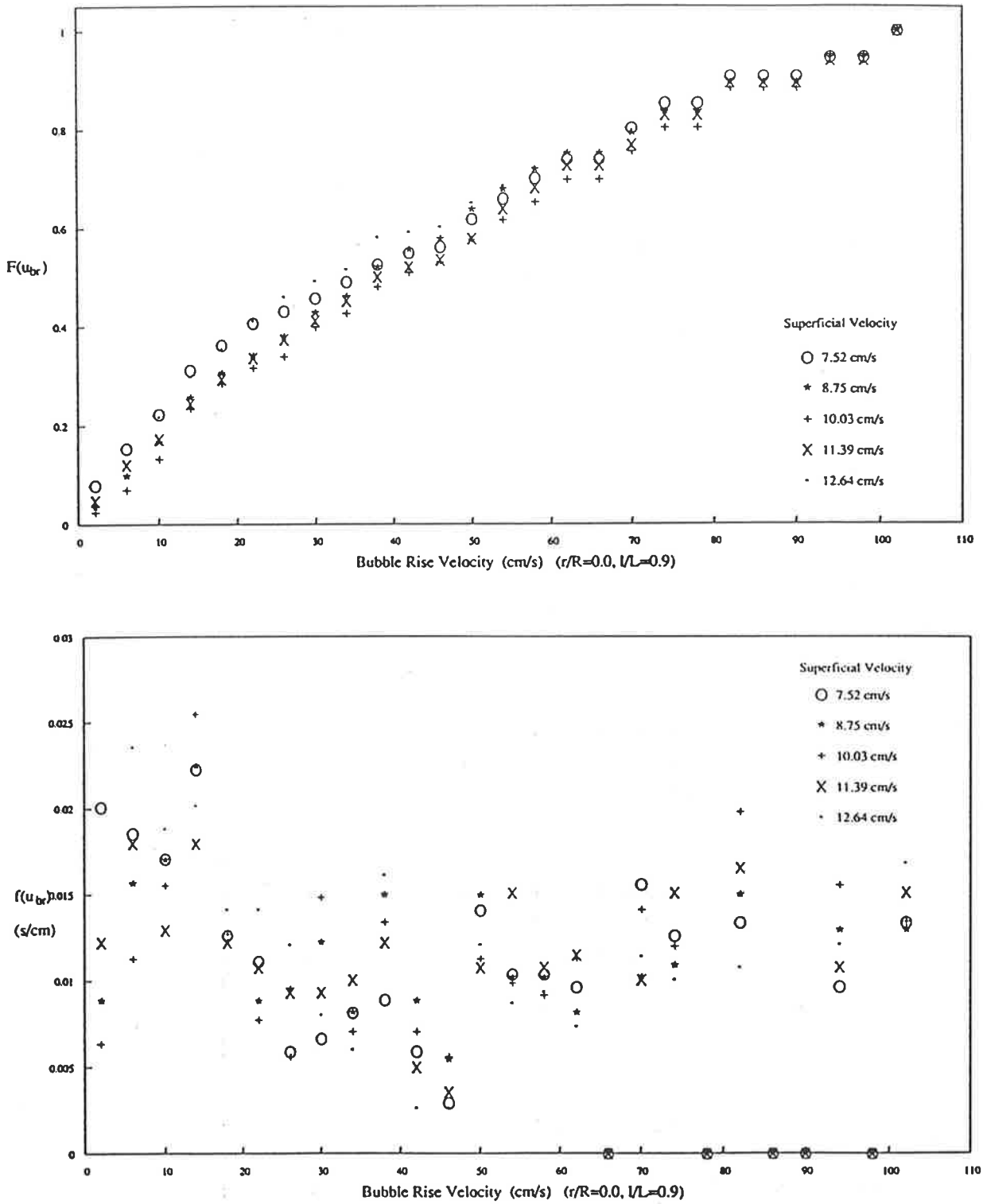

Figure 5.84 Cumulative Distribution and PDF of Bubble Rise Velocity

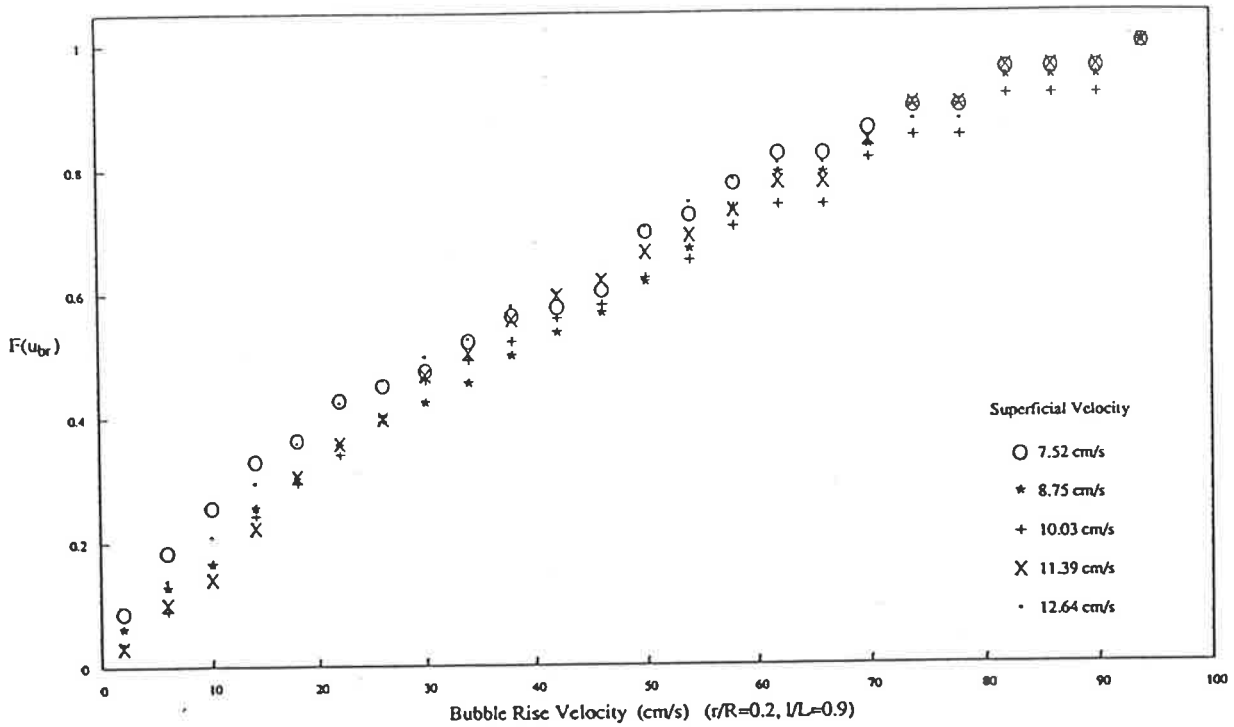

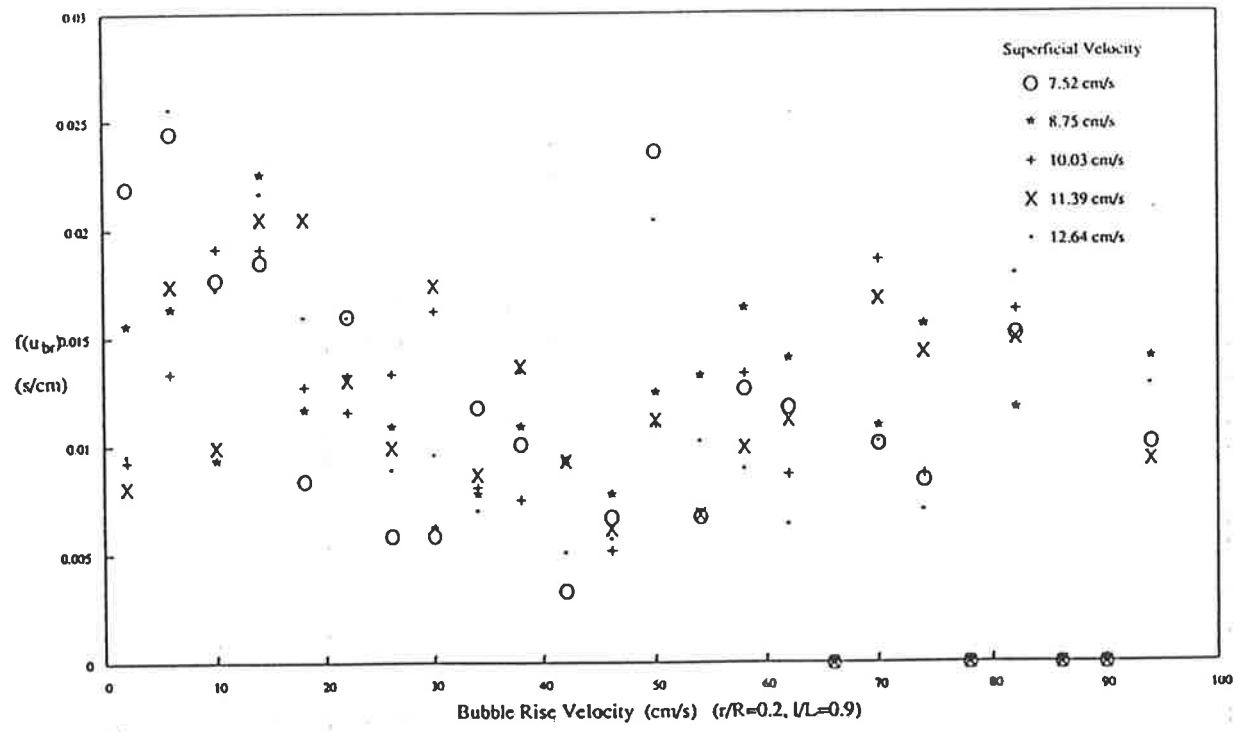

Figure 5.85 Cumulative Distribution and PDF of Bubble Rise Velocity

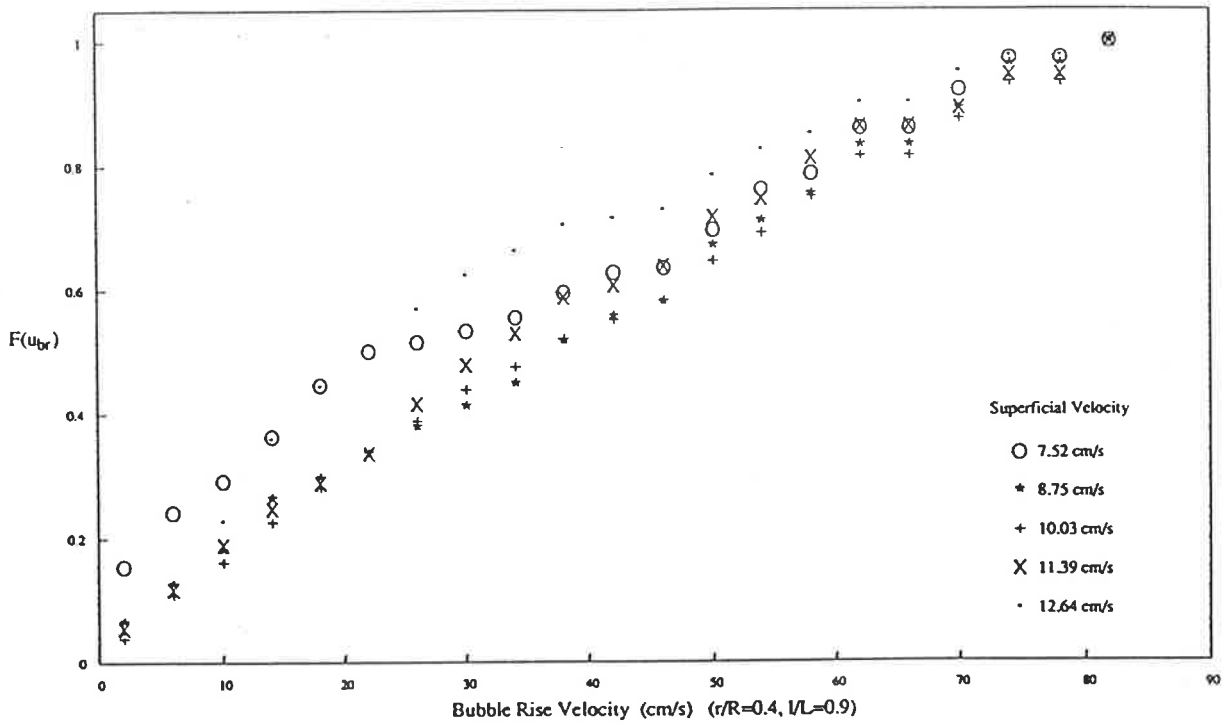

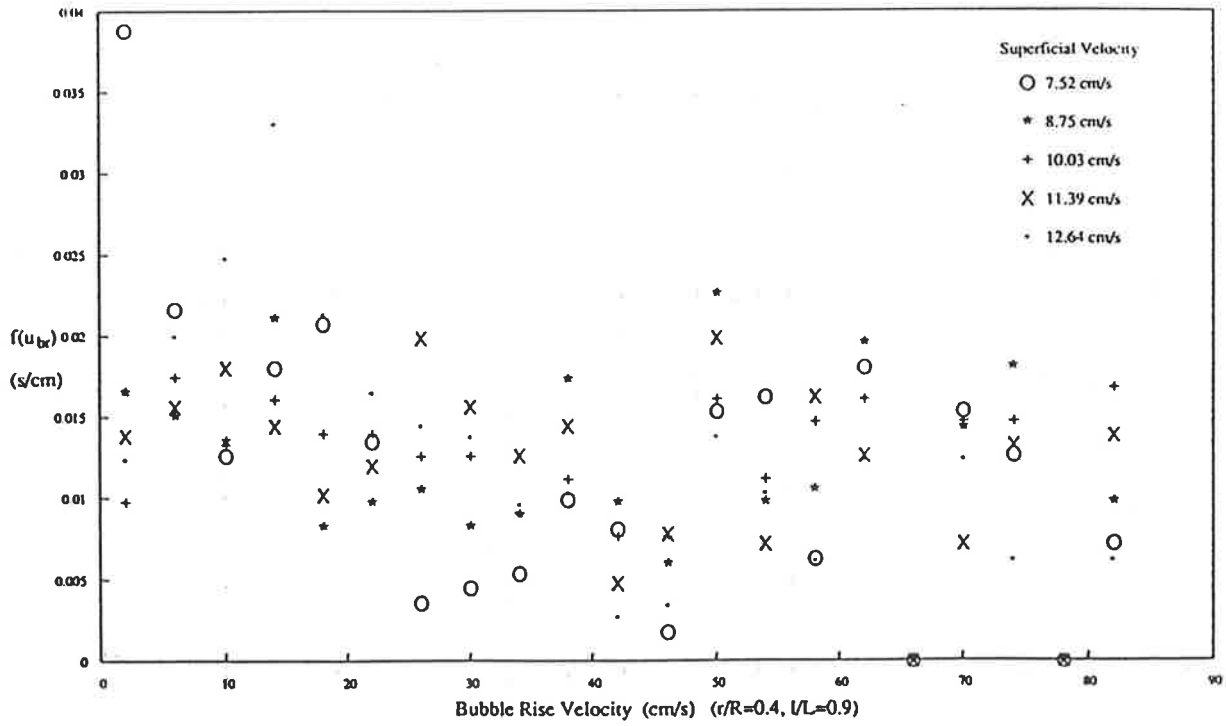

Figure 5.86 Cumulative Distribution and PDF of Bubble Rise Velocity

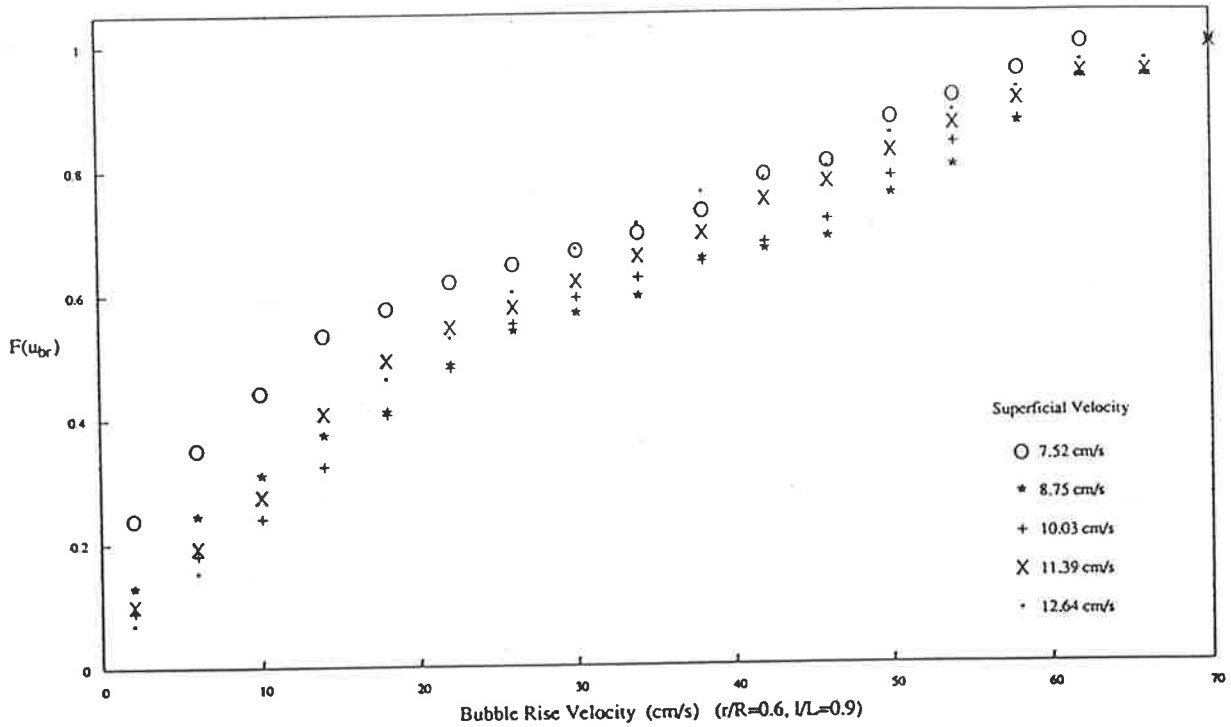

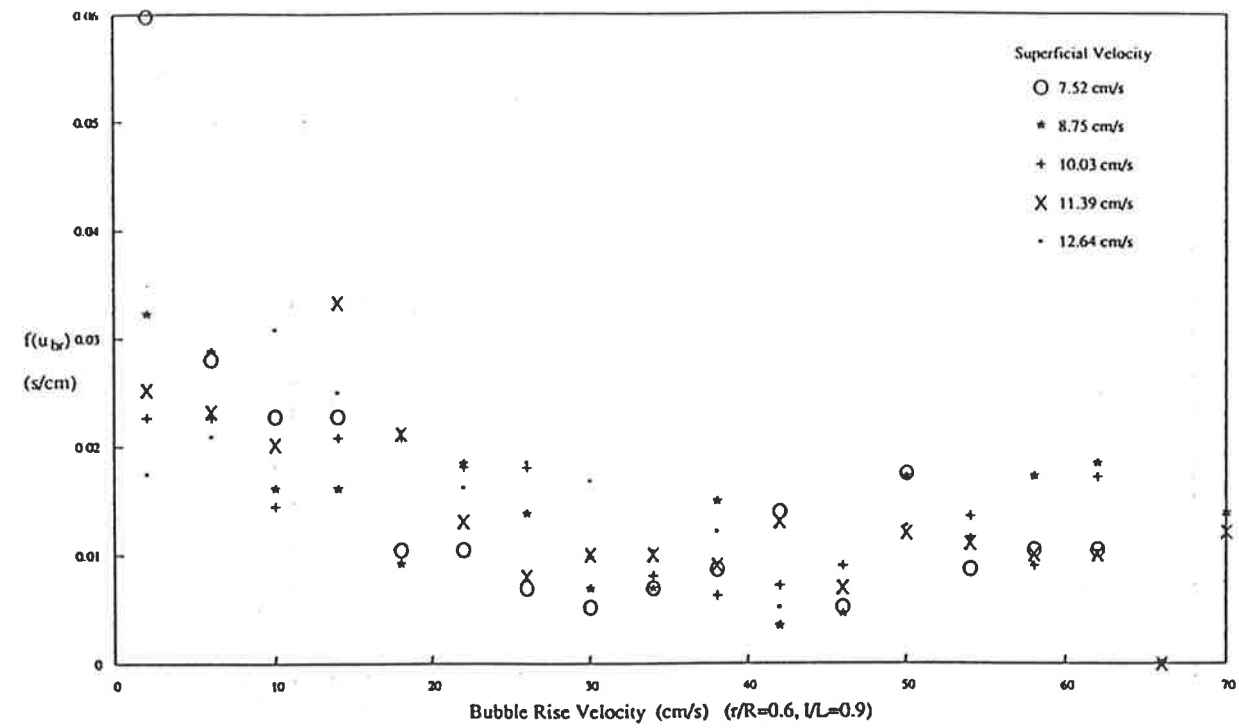

Figure 5.87 Cumulative Distribution and PDF of Bubble Rise Velocity

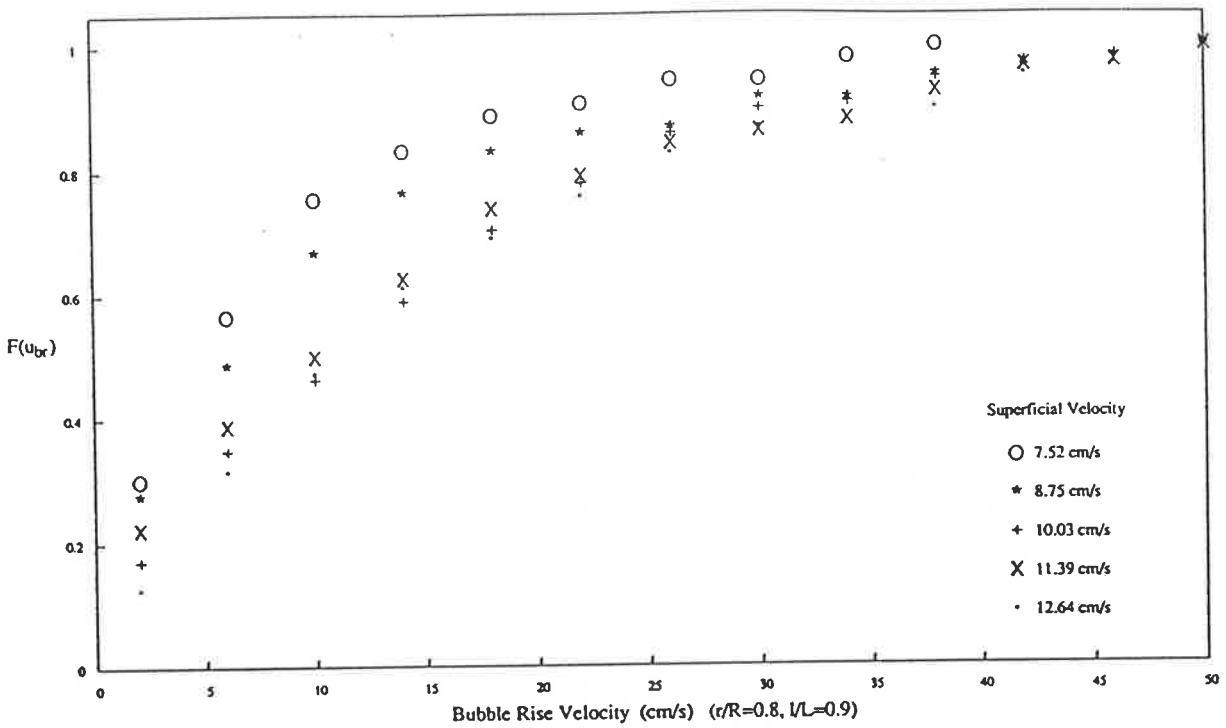

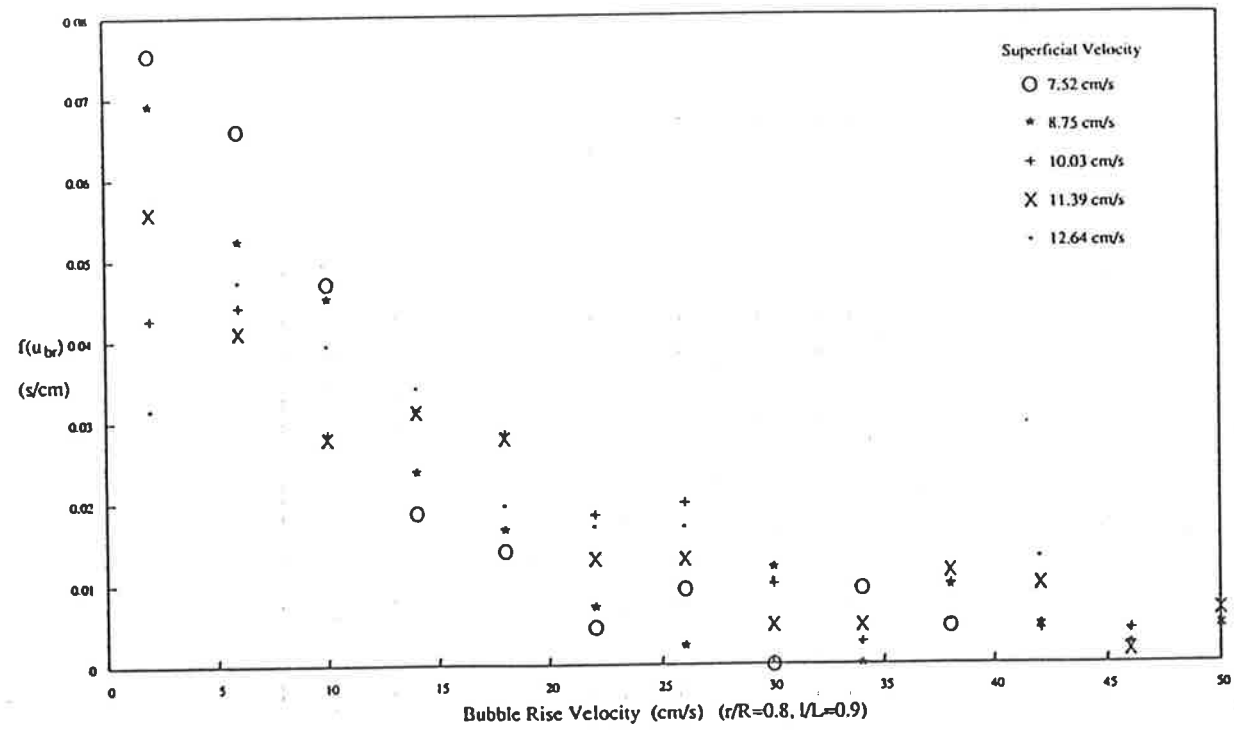

Figure 5.88 Cumulative Distribution and PDF of Bubble Rise Velocity

5.3 Replicate Experiments

Experiments were repeated at various points throughout the bed. Figures 5.89 to 5.100 detail the resulting distributions of bubble vertical dimensions and rise velocities arising from these measurements. They were conducted over an increased duration in order to test data reproducibility. All figures show good agreement between original and replicate experiments.

Figures 5.101 to 5.108 present experimental data measured at other radii, in order to test the symmetry assumption of bed characteristics. The figures represent measurements at various bed heights, radial positions and fluidizing gas velocities and are all in good agreement.

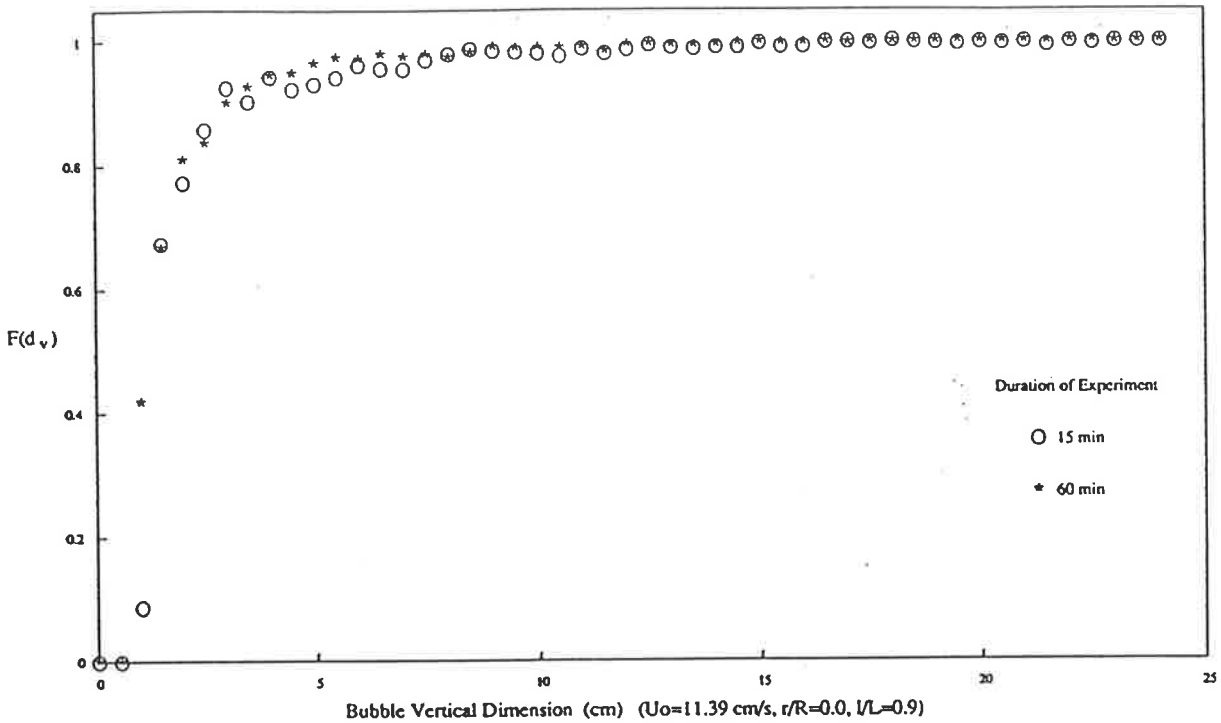

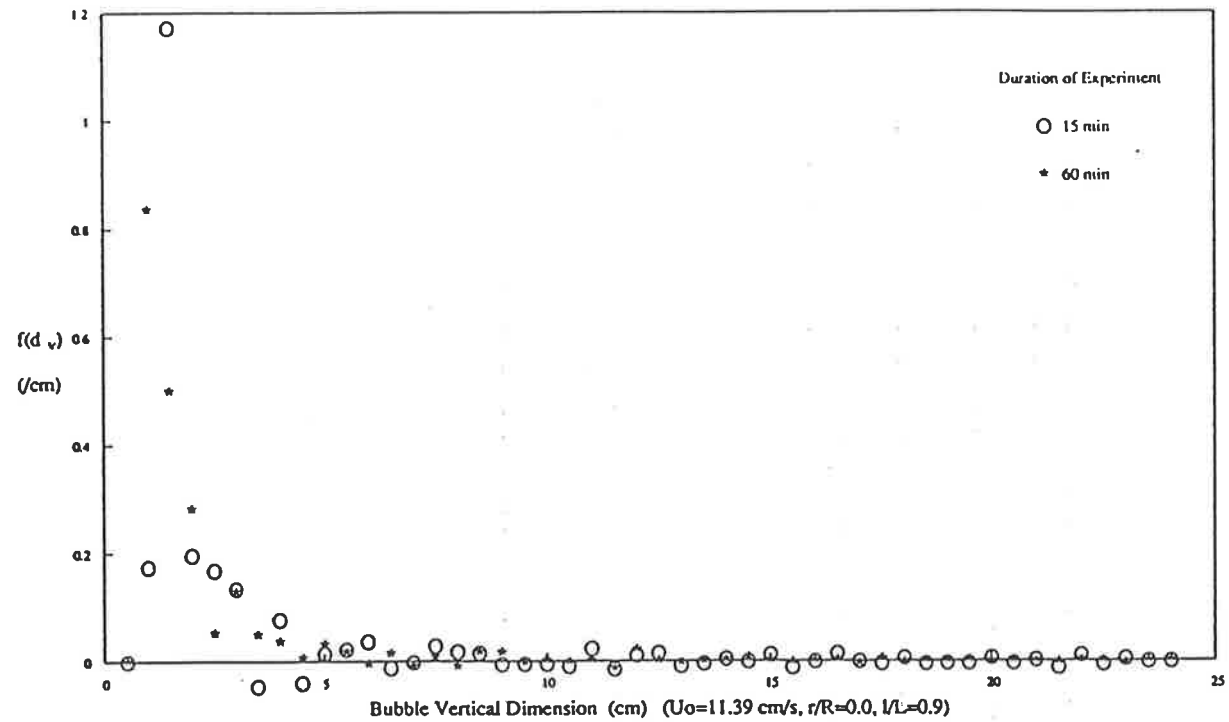

Figure 5.89 Cumulative Distribution and PDF of Bubble Vertical Dimension

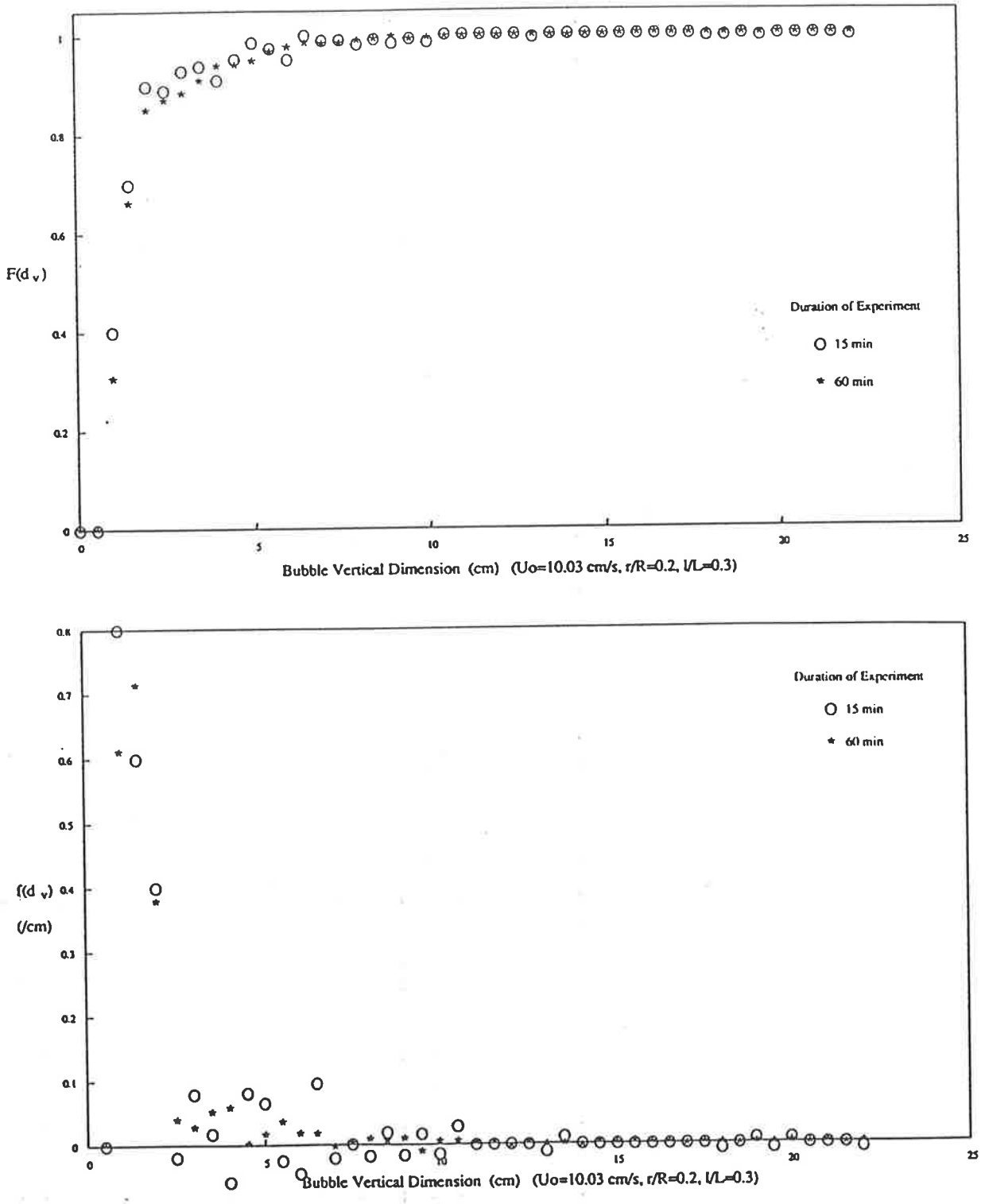

Figure 5.90 Cumulative Distribution and PDF of Bubble Vertical Dimension

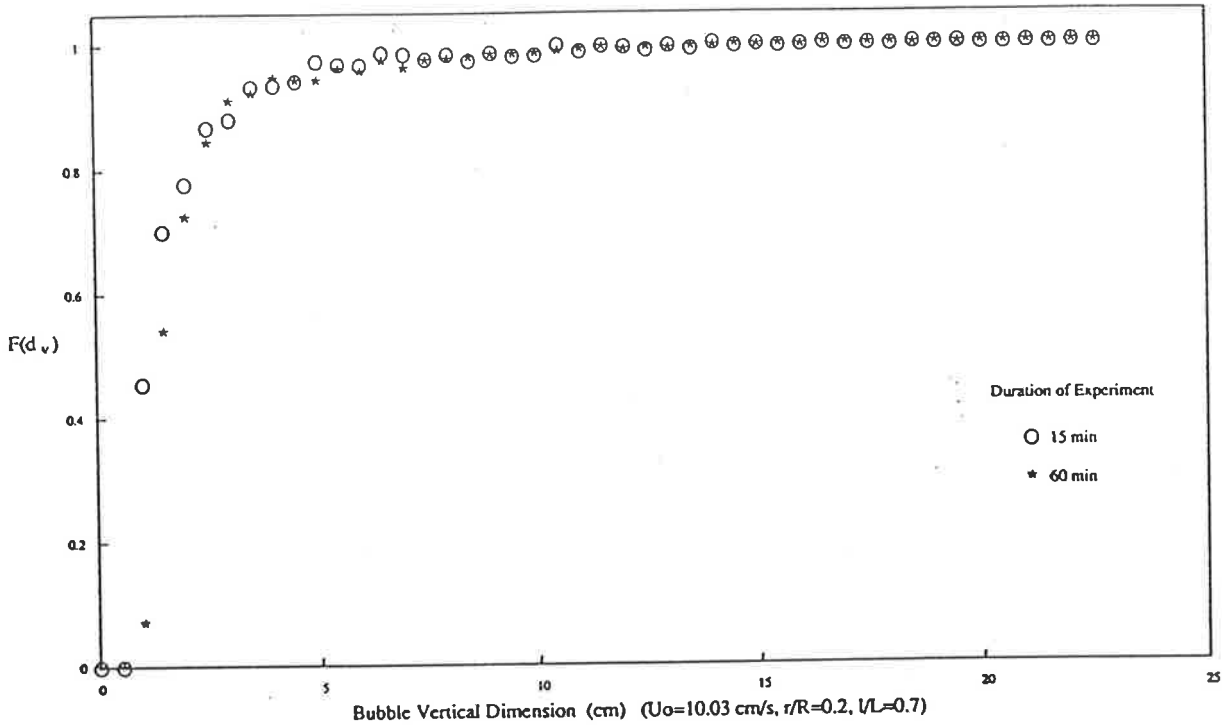

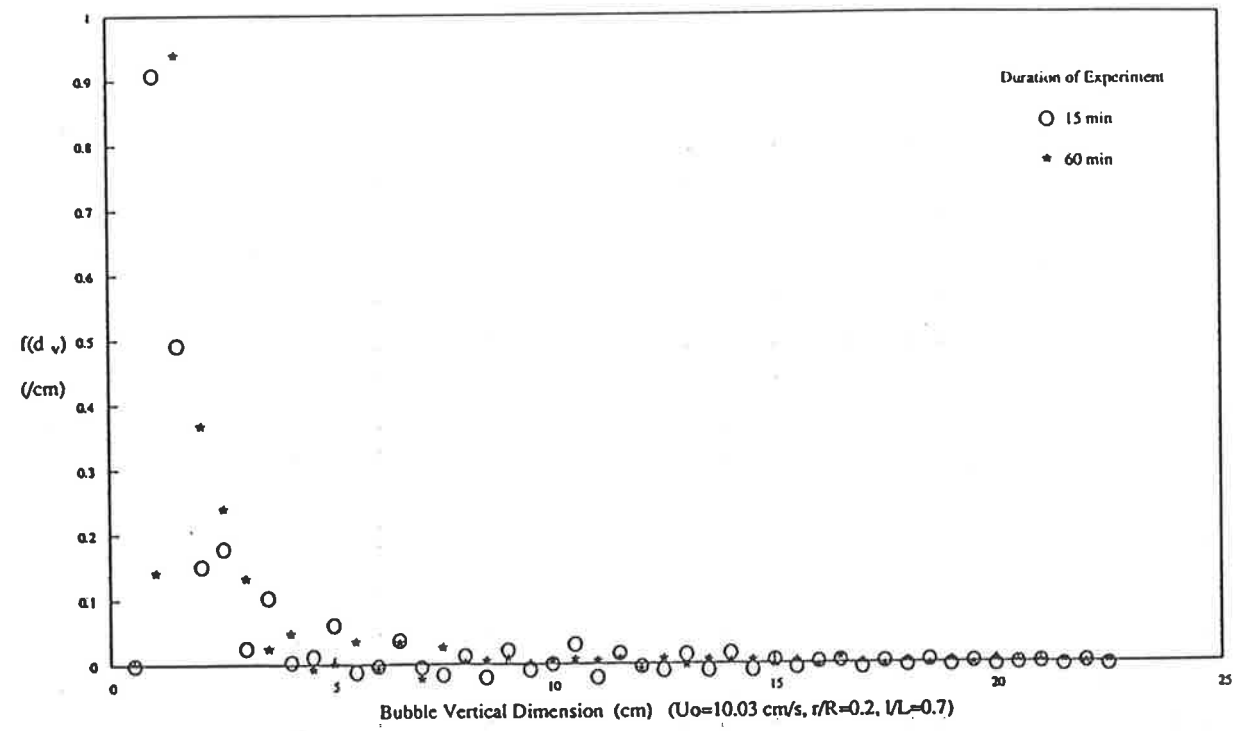

Figure 5.91 Cumulative Distribution and PDF of Bubble Vertical Dimension

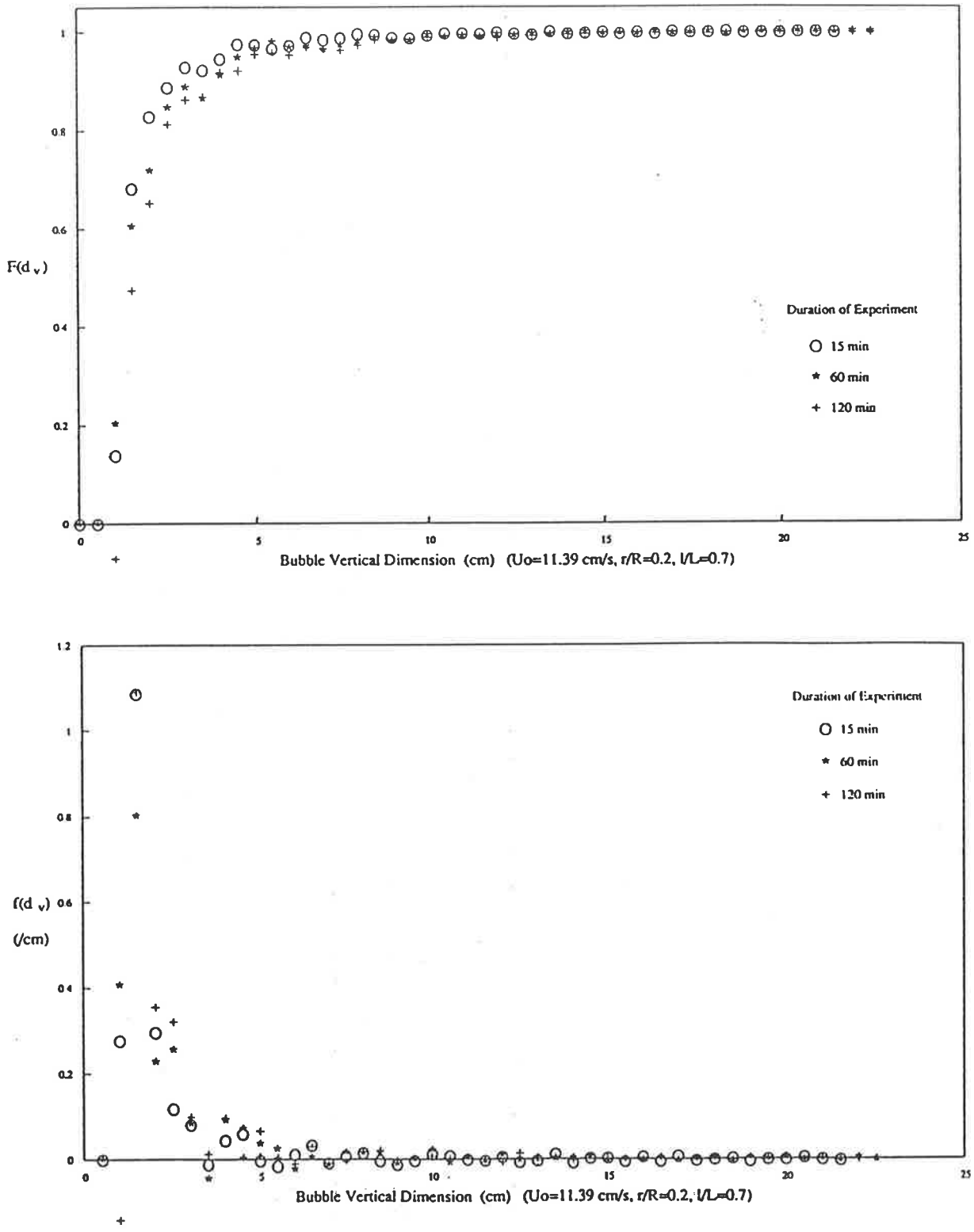

Figure 5.92 Cumulative Distribution and PDF of Bubble Vertical Dimension

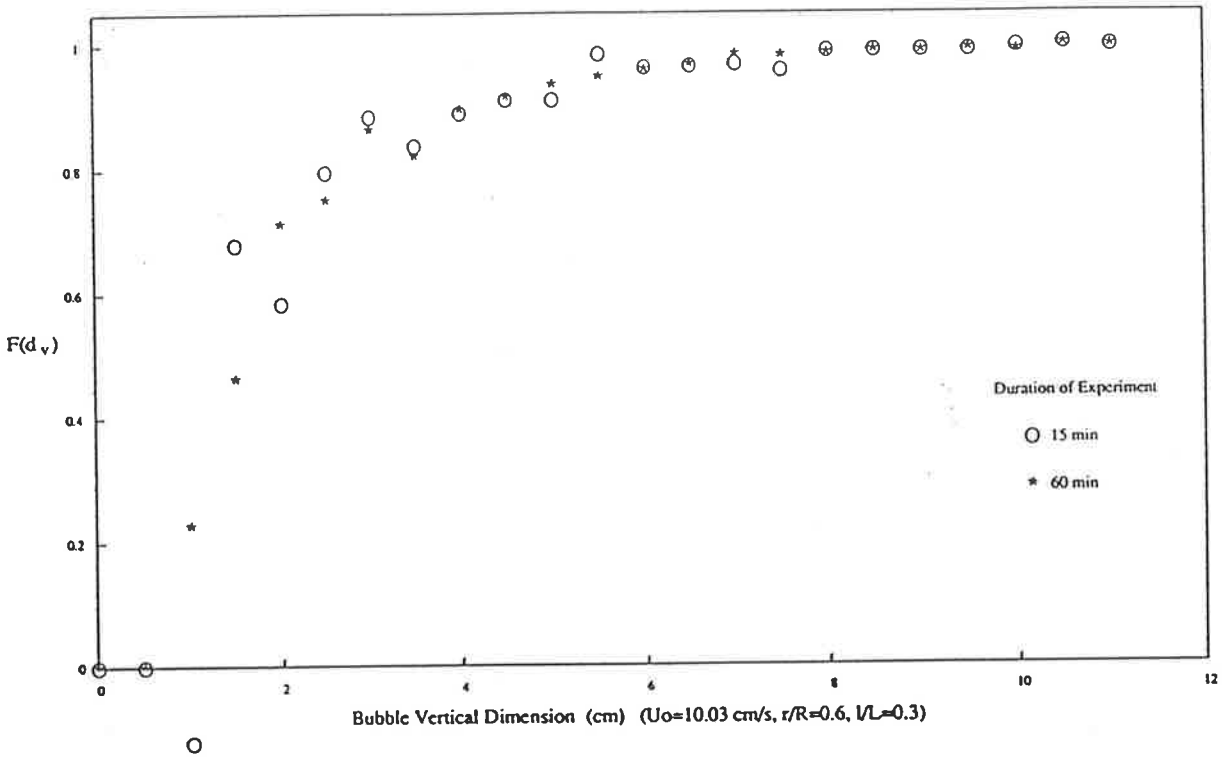

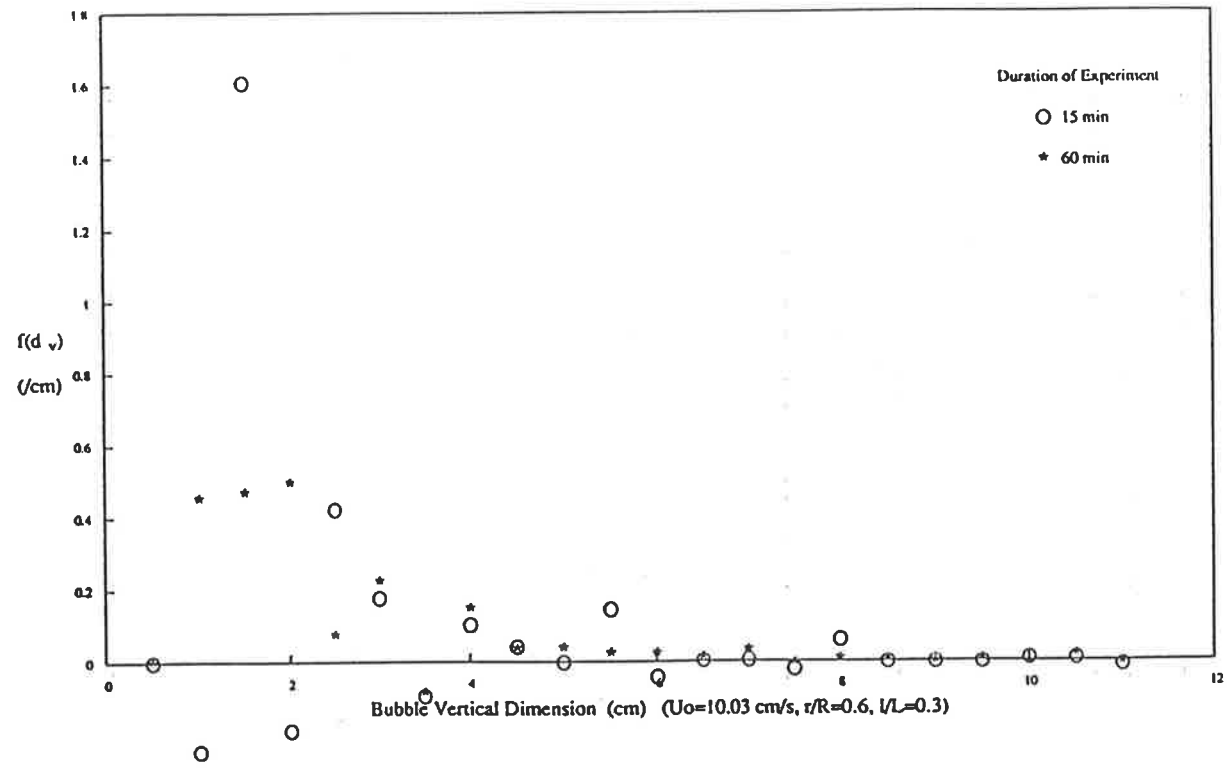

Figure 5.93 Cumulative Distribution and PDF of Bubble Vertical Dimension

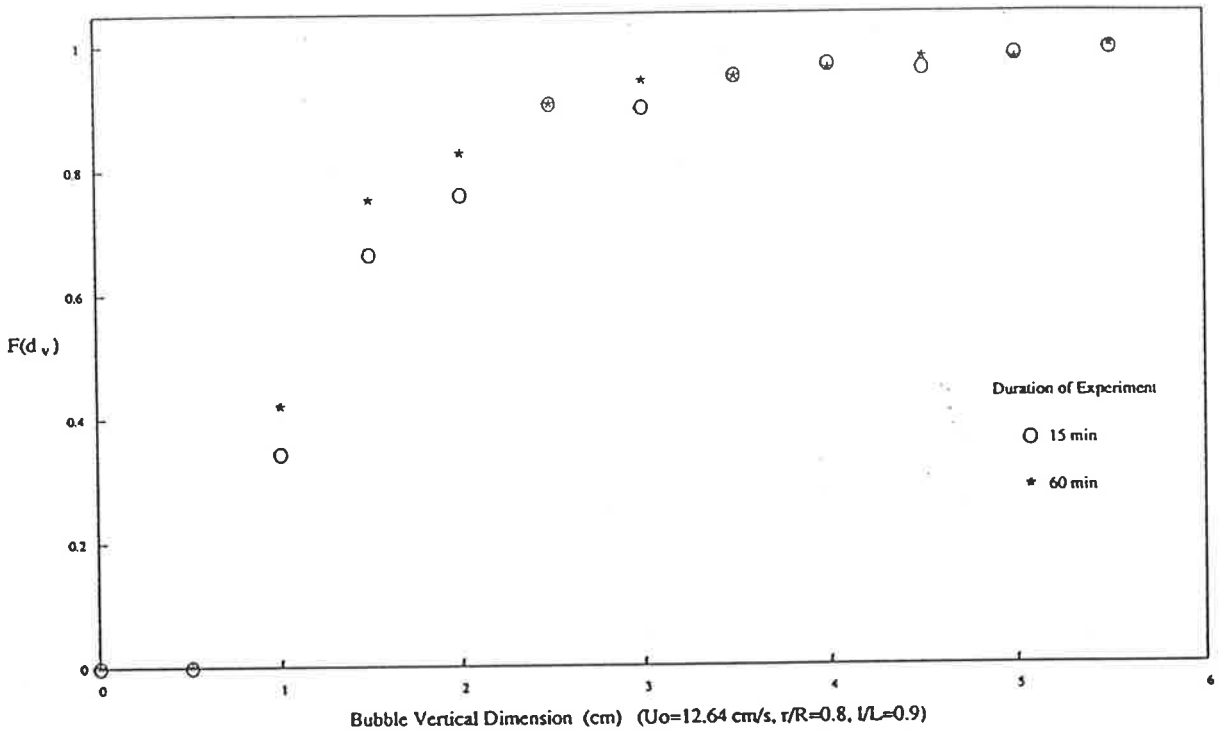

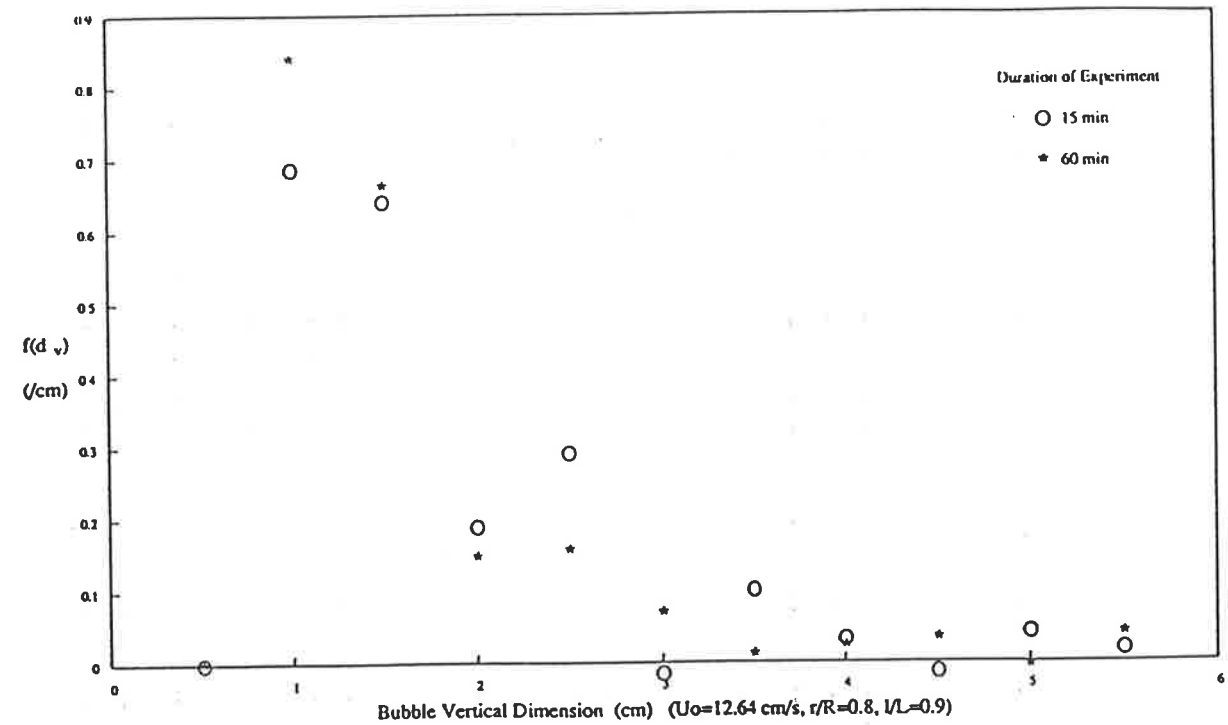

Figure 5.94 Cumulative Distribution and PDF of Bubble Vertical Dimension

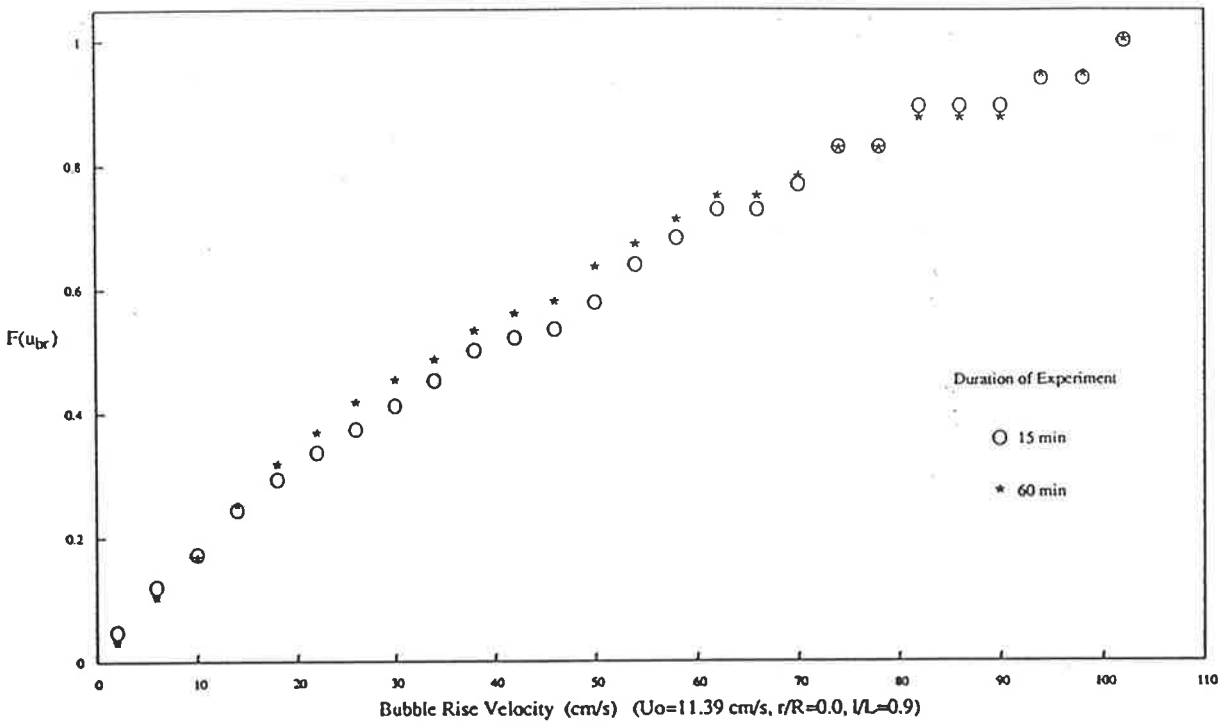

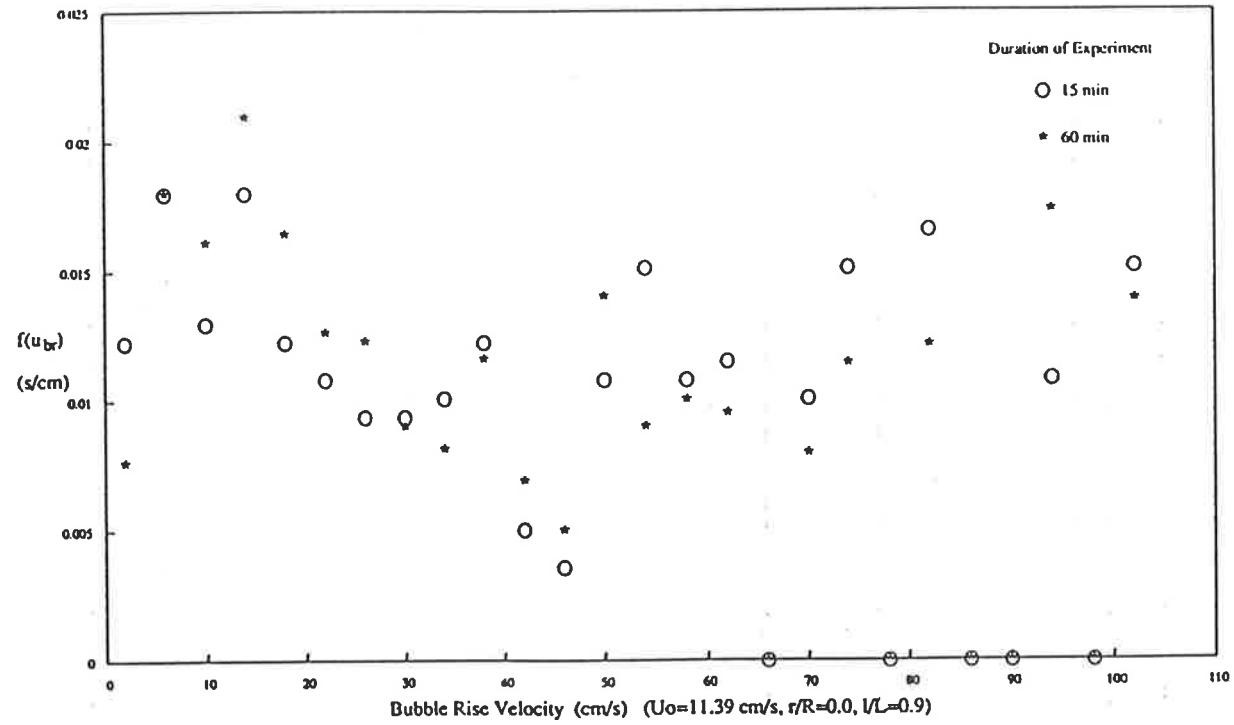

Figure 5.95 Cumulative Distribution and PDF of Bubble Rise Velocity

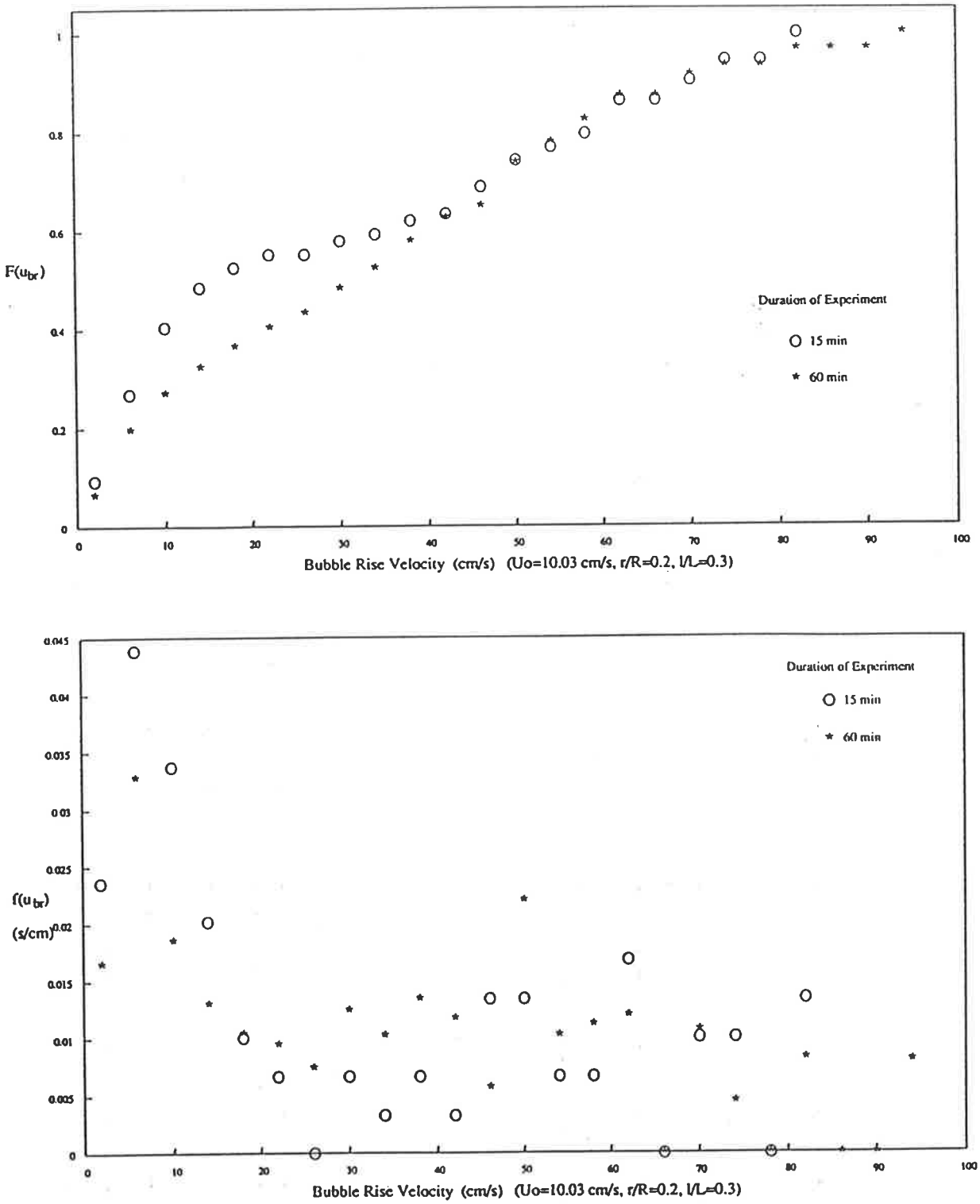

Figure 5.96 Cumulative Distribution and PDF of Bubble Rise Velocity

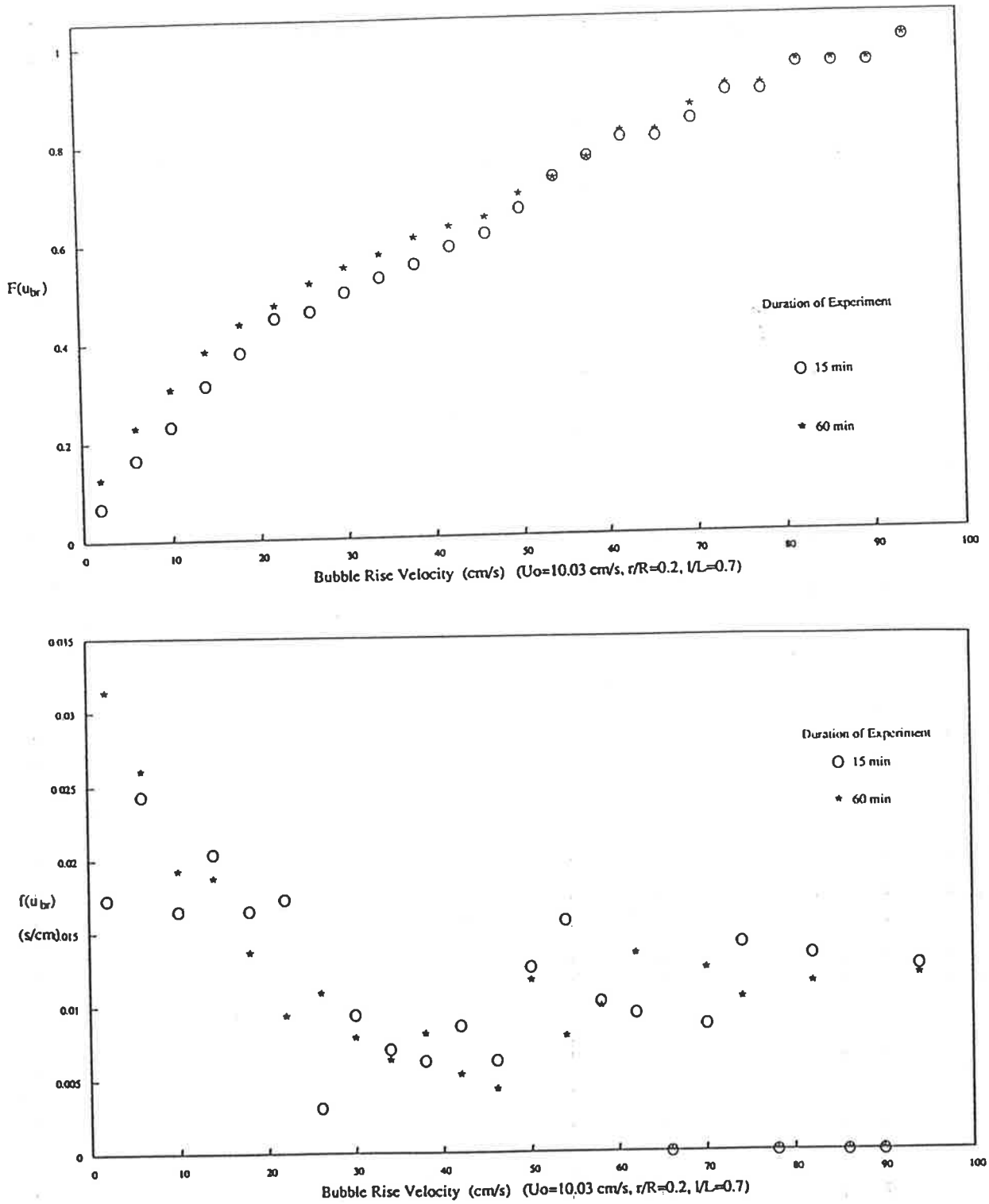

Figure 5.97 Cumulative Distribution and PDF of Bubble Rise Velocity

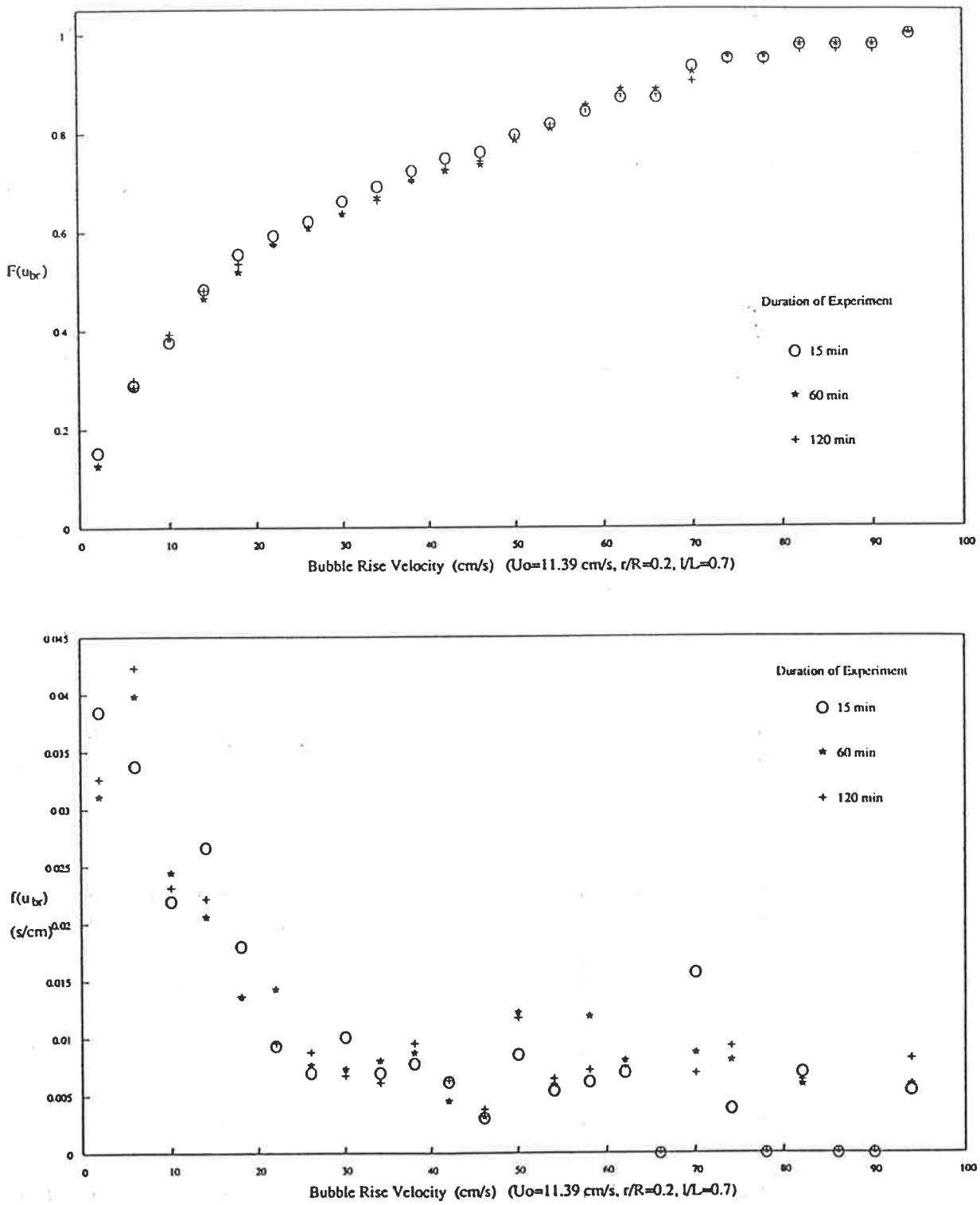

Figure 5.98 Cumulative Distribution and PDF of Bubble Rise Velocity

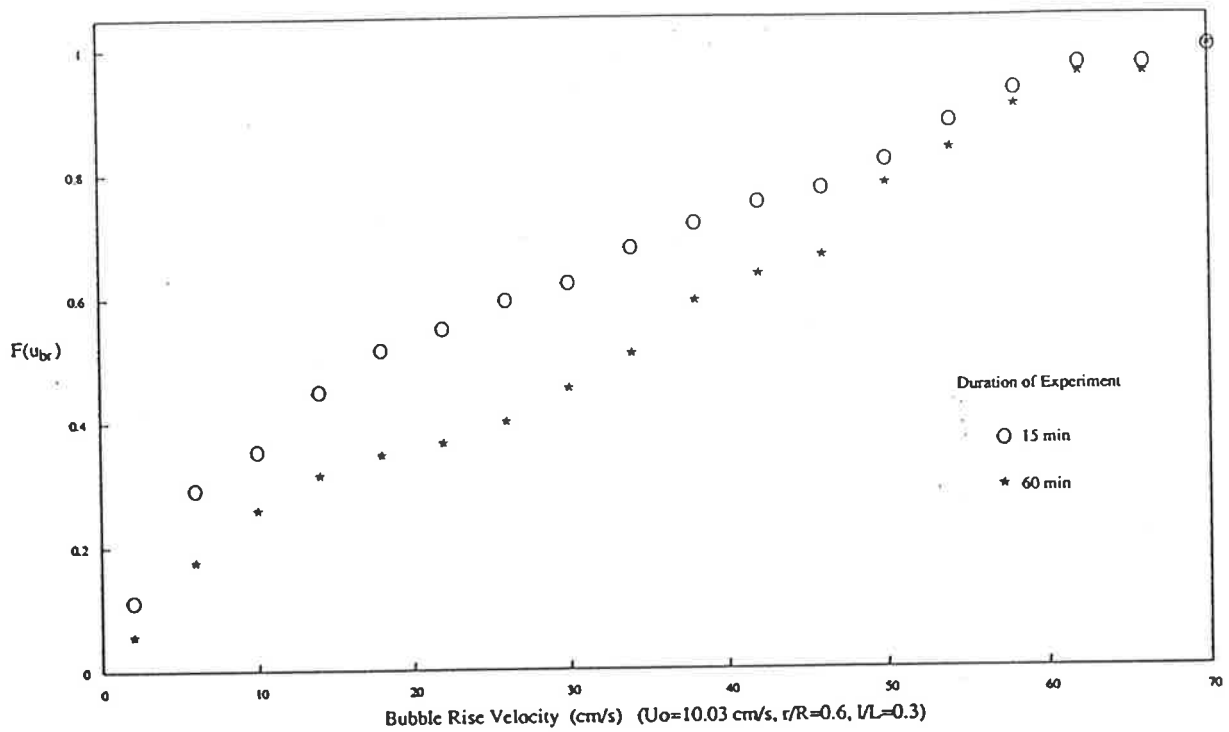

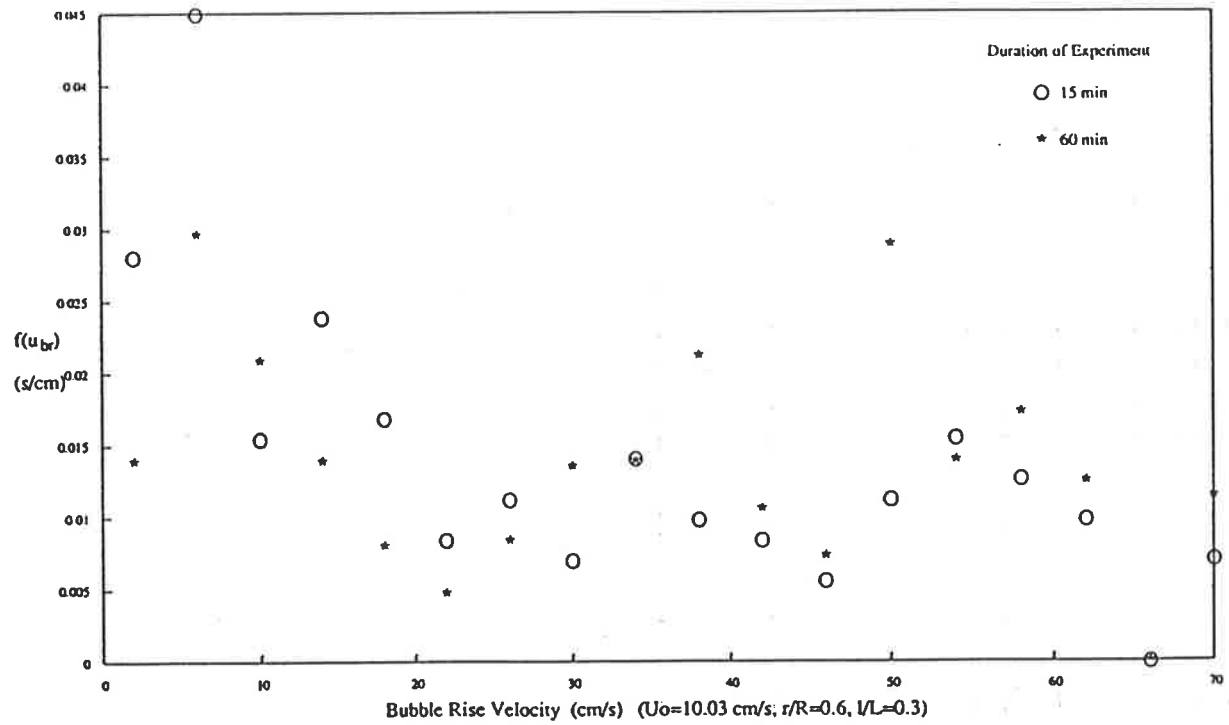

Figure 5.99 Cumulative Distribution and PDF of Bubble Rise Velocity

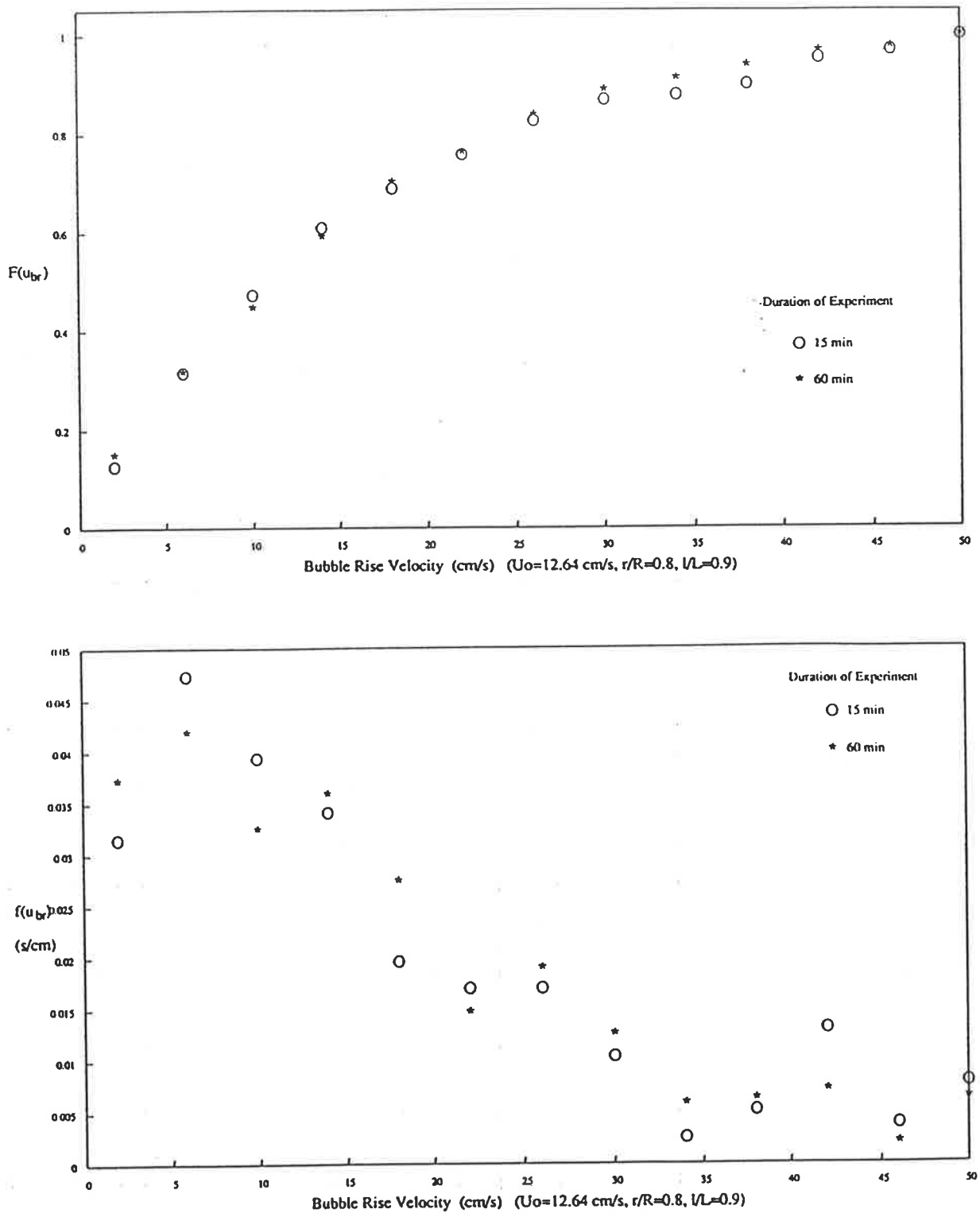

Figure 5.100 Cumulative Distribution and PDF of Bubble Rise Velocity

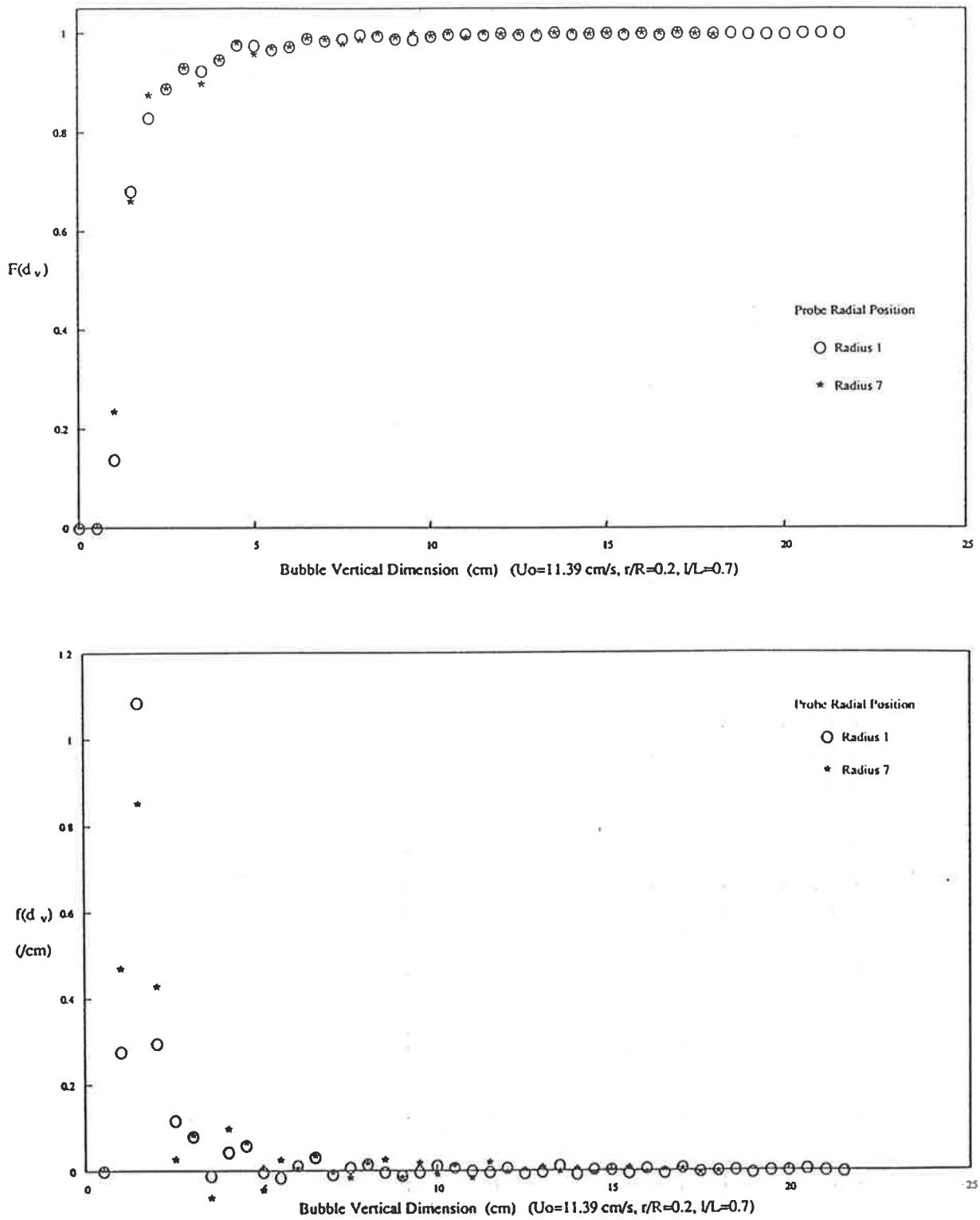

Figure 5.101 Cumulative Distribution and PDF of Bubble Vertical Dimension

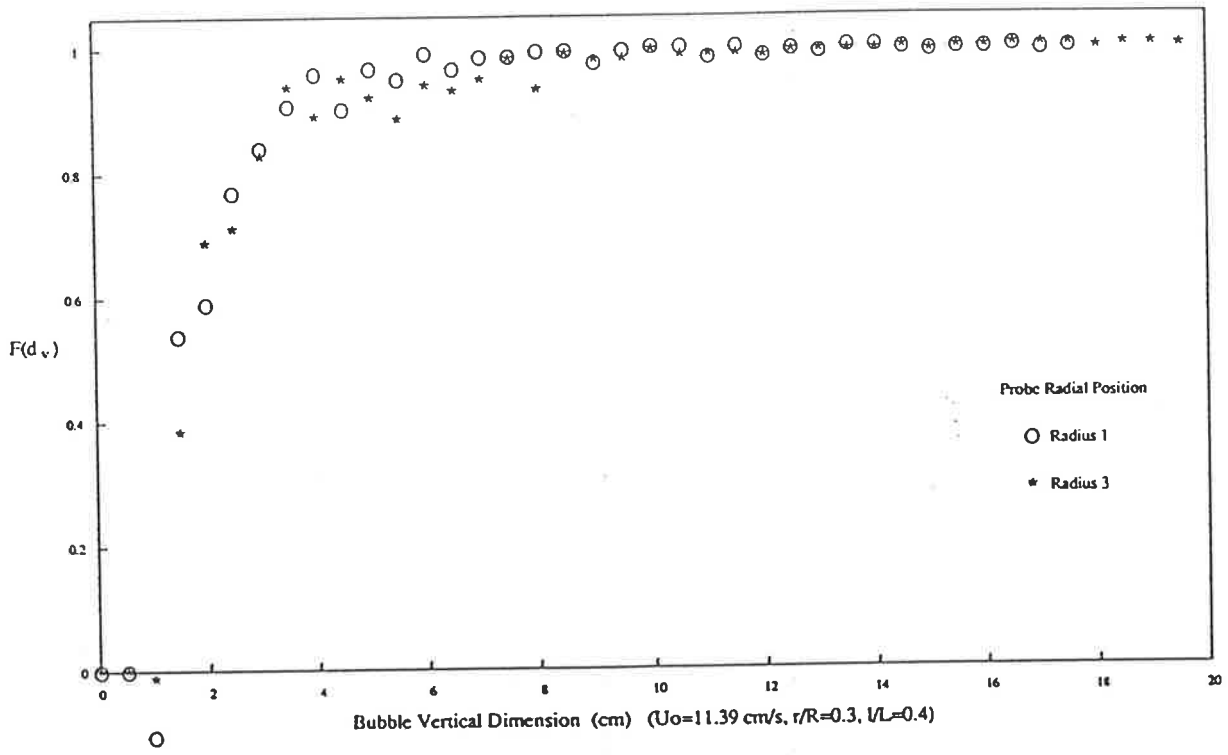

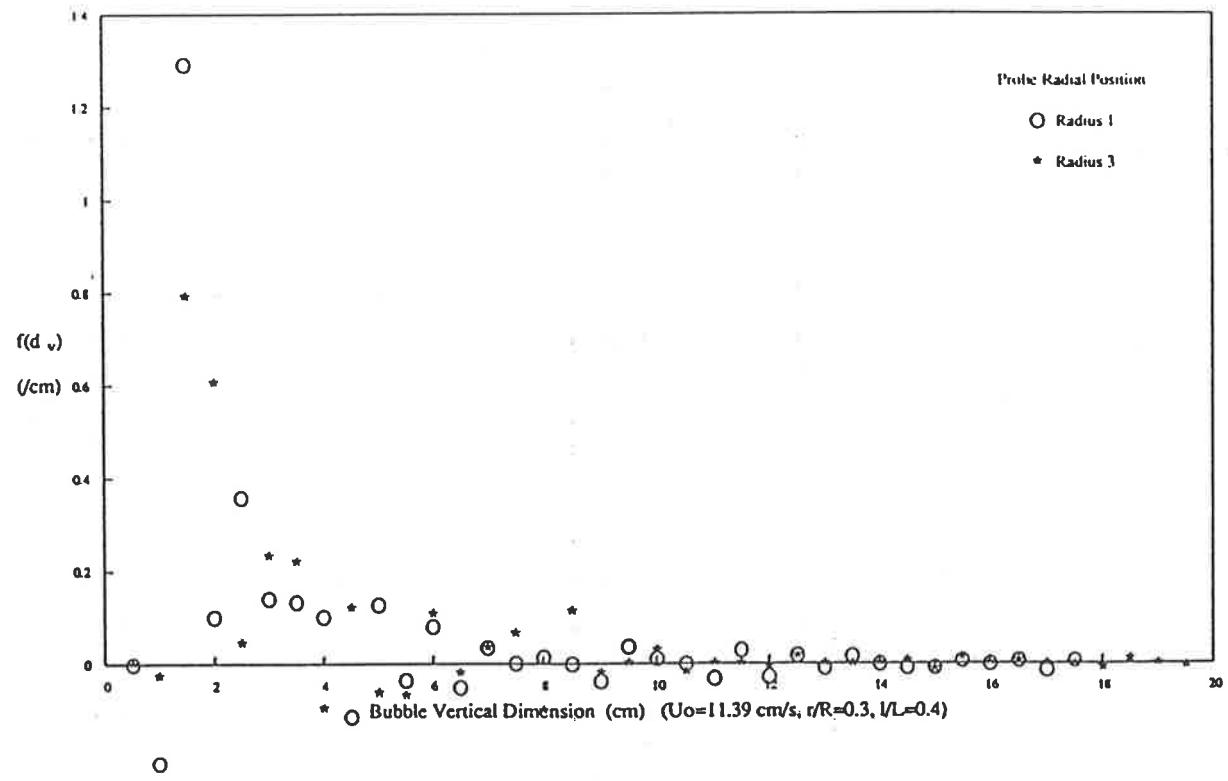

Figure 5.102 Cumulative Distribution and PDF of Bubble Vertical Dimension

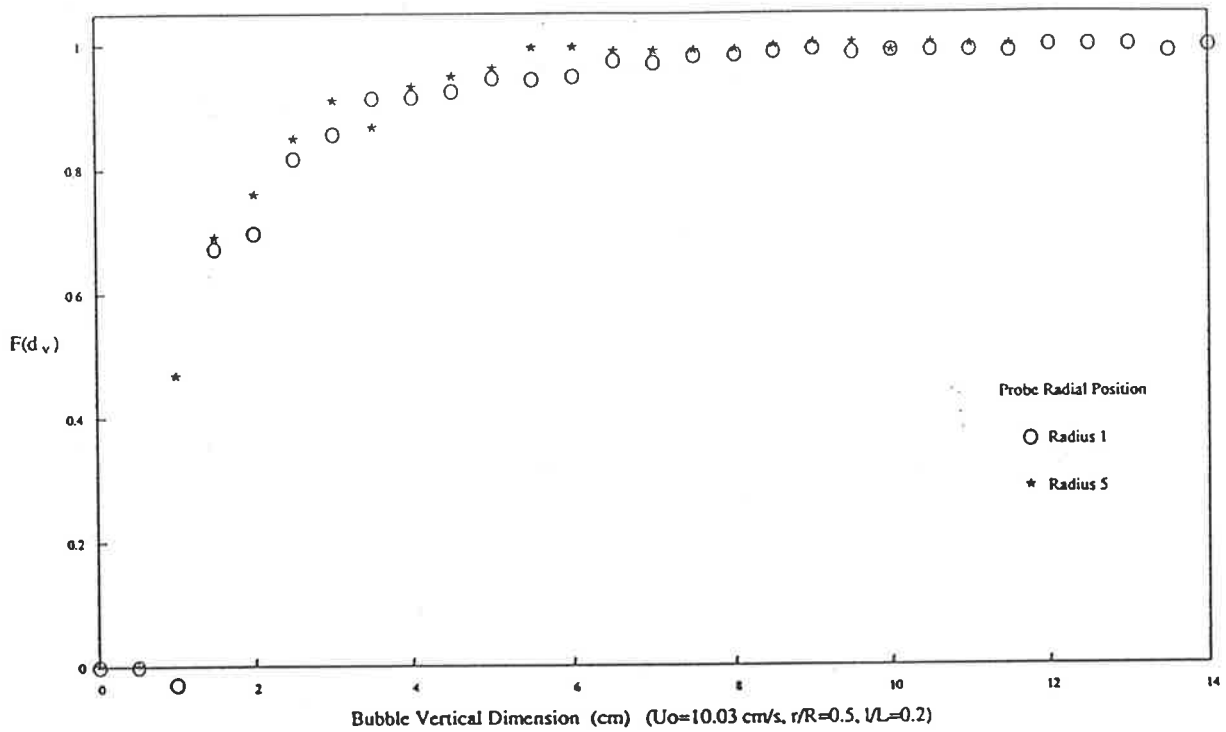

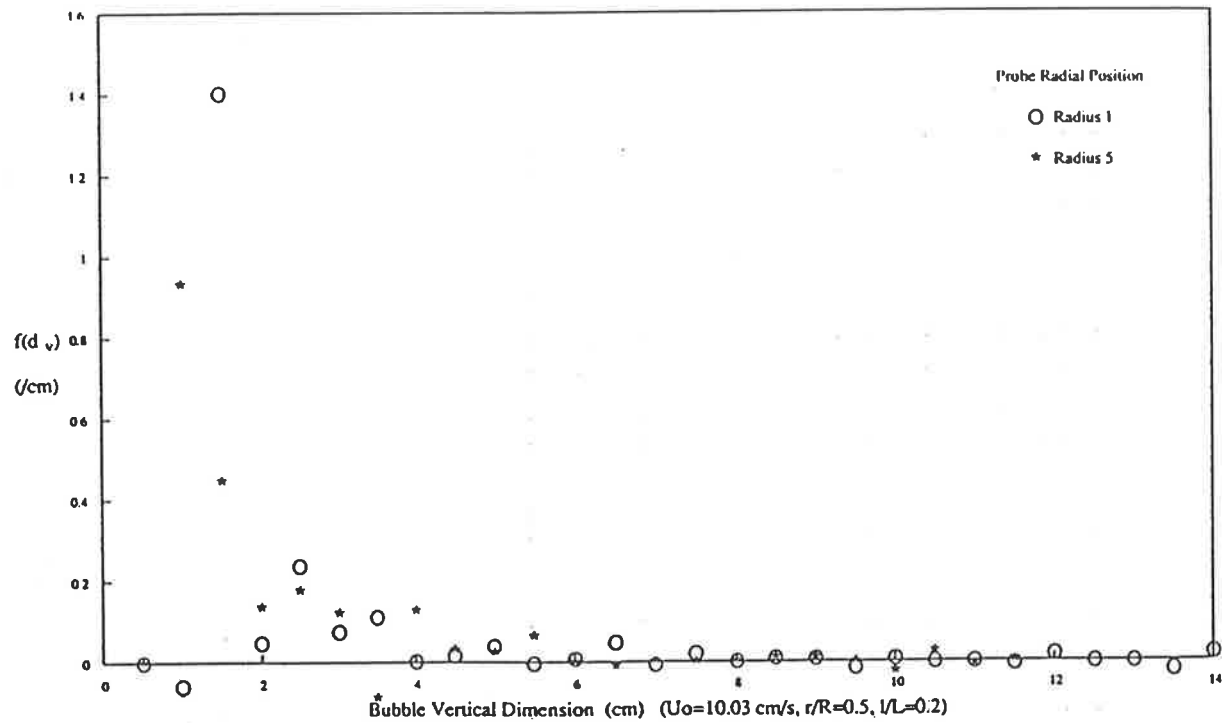

Figure 5.103 Cumulative Distribution and PDF of Bubble Vertical Dimension

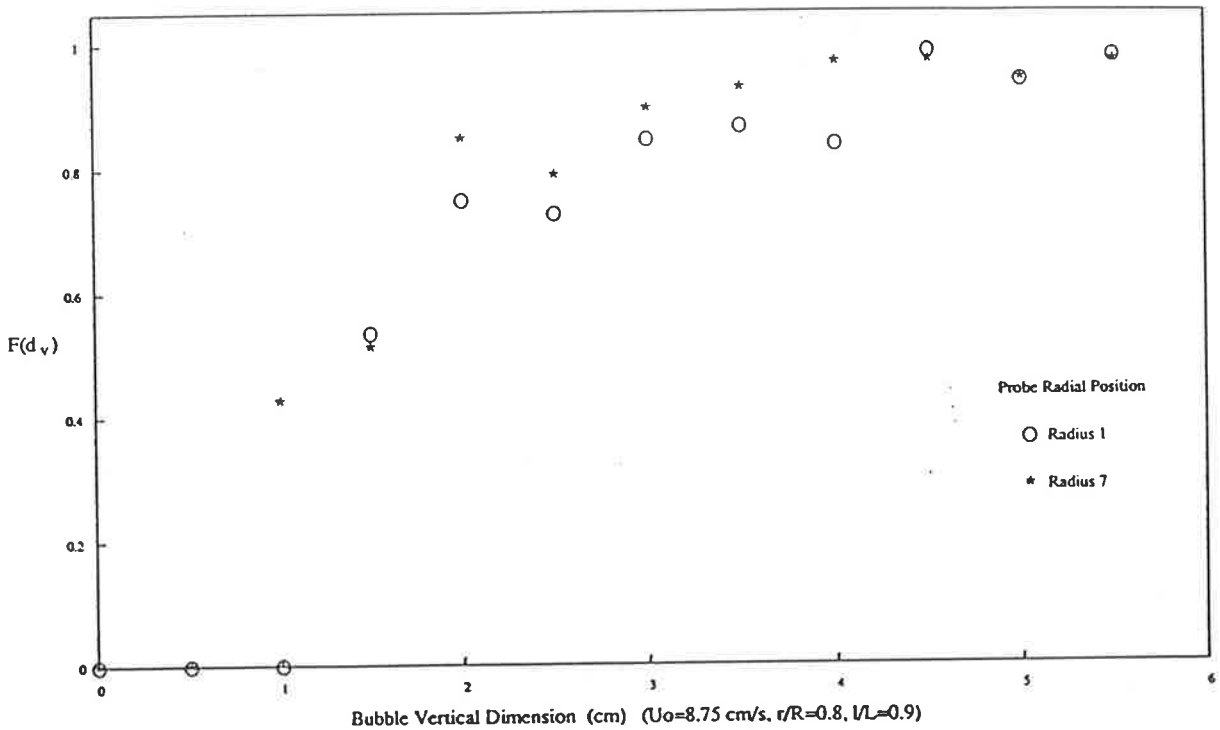

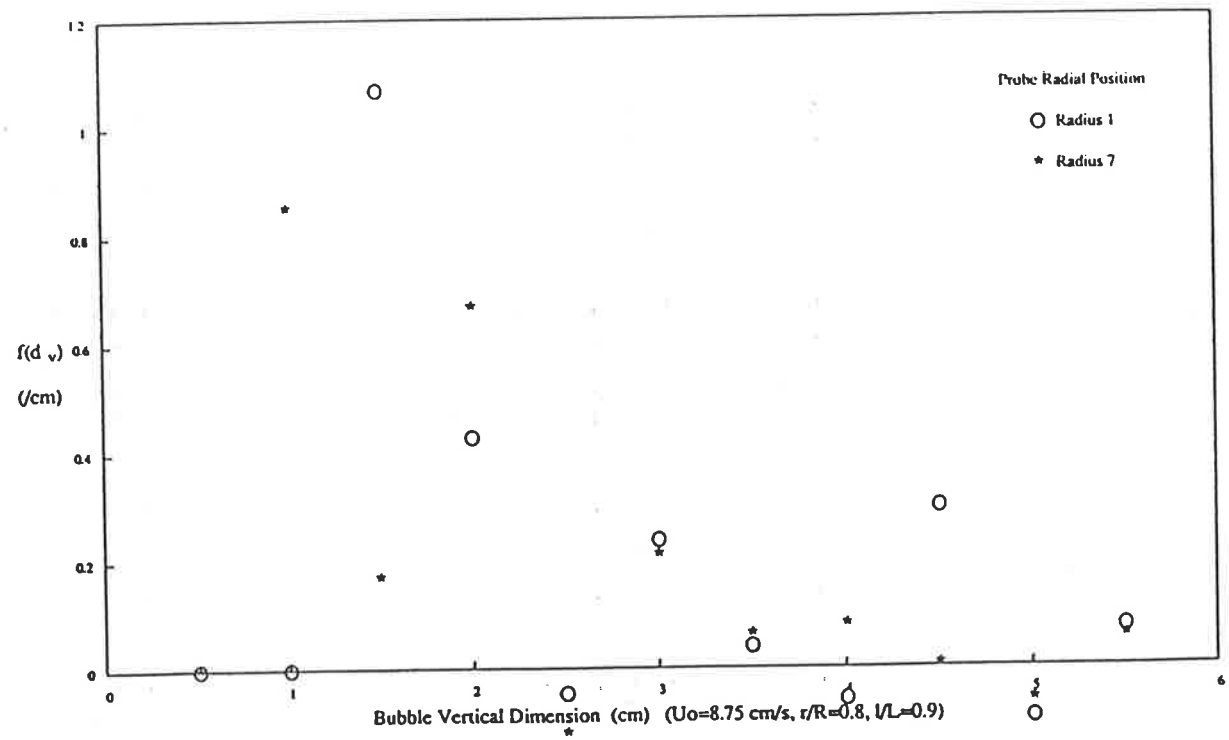

Figure 5.104 Cumulative Distribution and PDF of Bubble Vertical Dimension

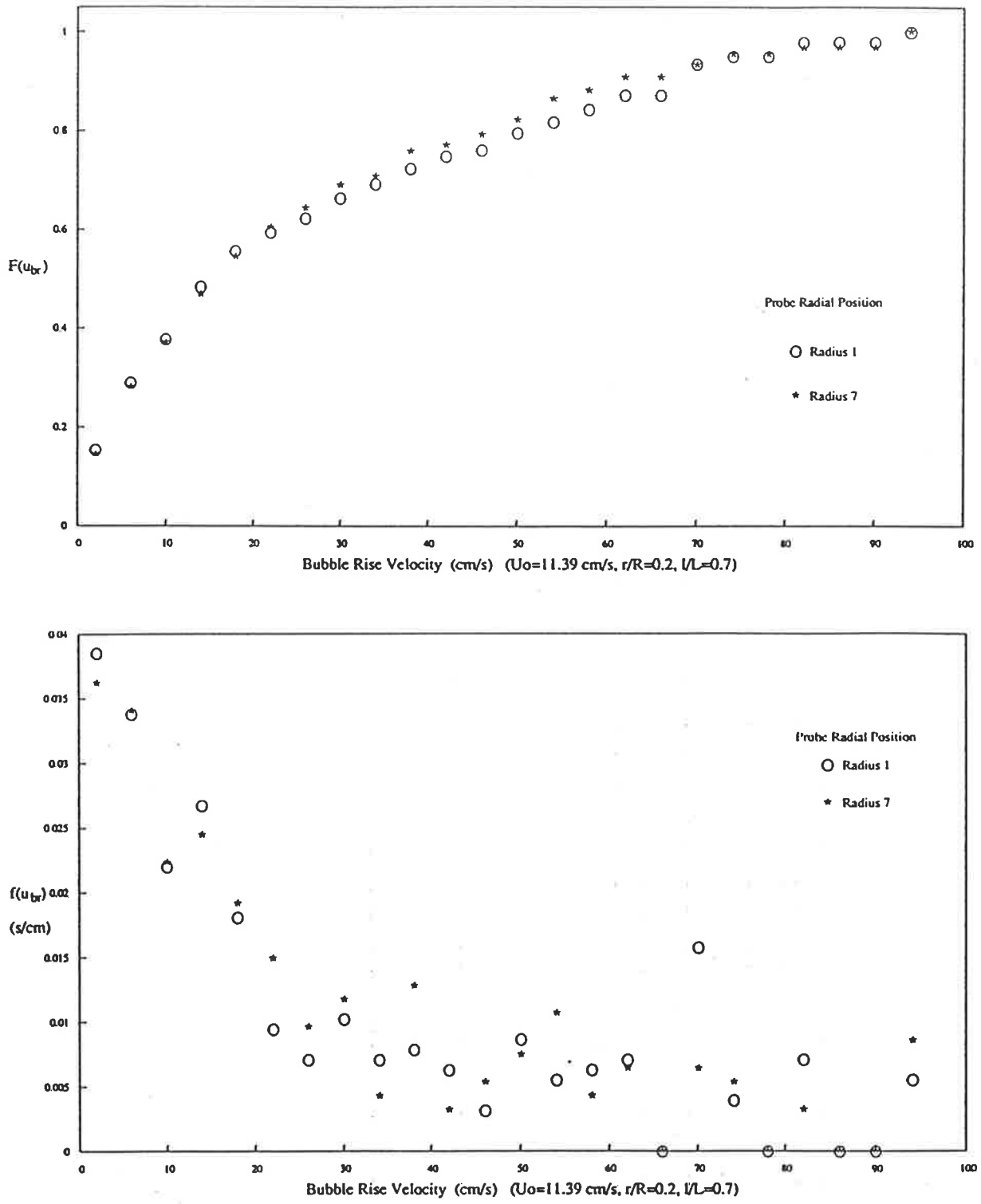

Figure 5.105 Cumulative Distribution and PDF of Bubble Rise Velocity

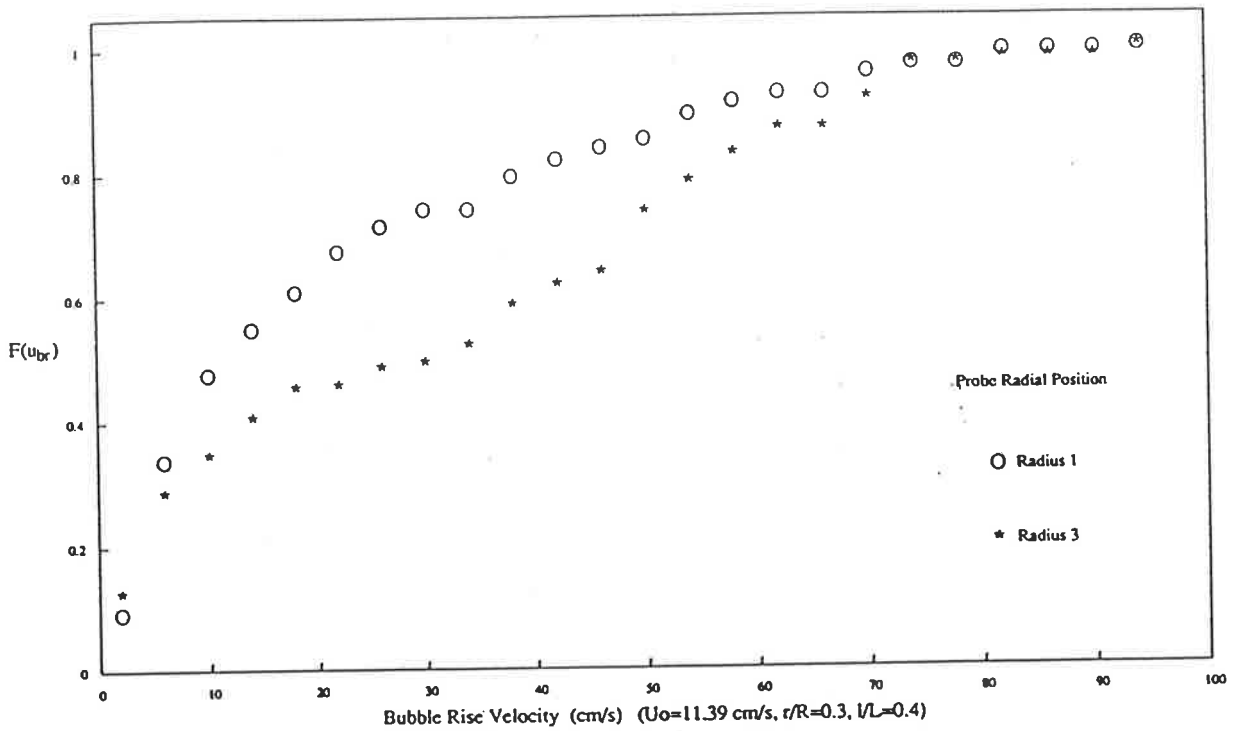

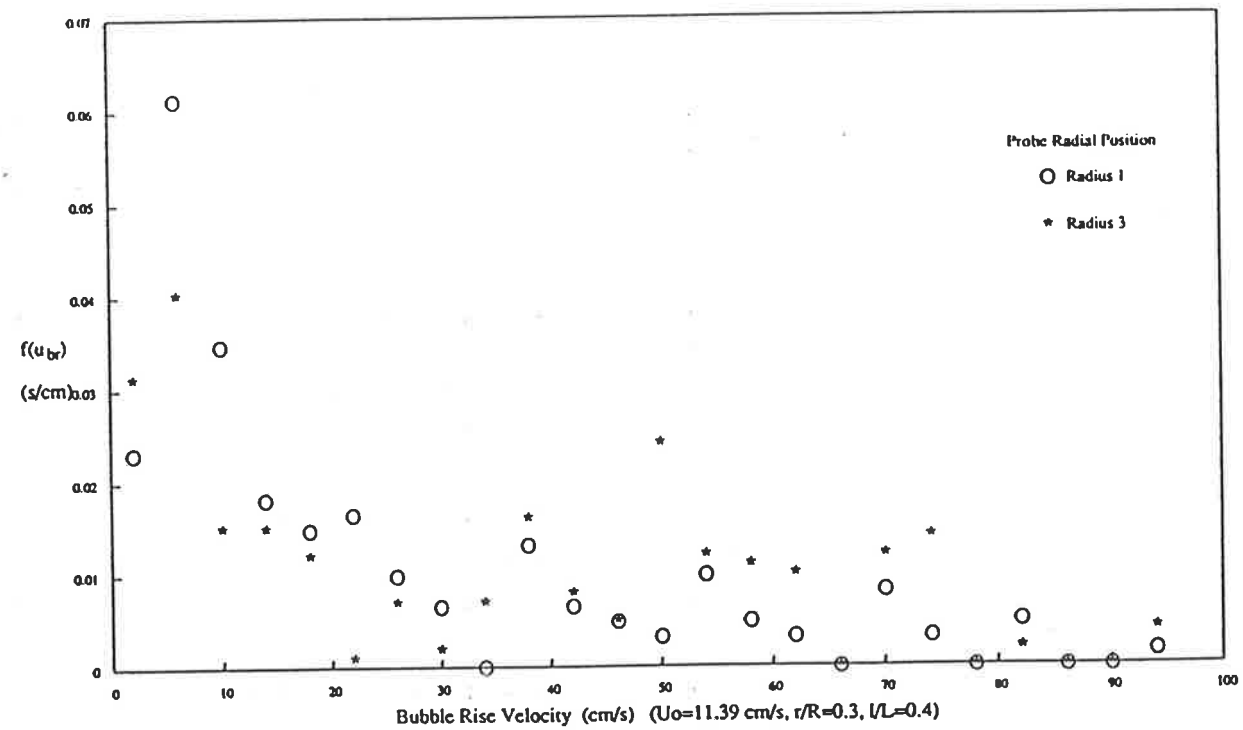

Figure 5.106 Cumulative Distribution and PDF of Bubble Rise Velocity

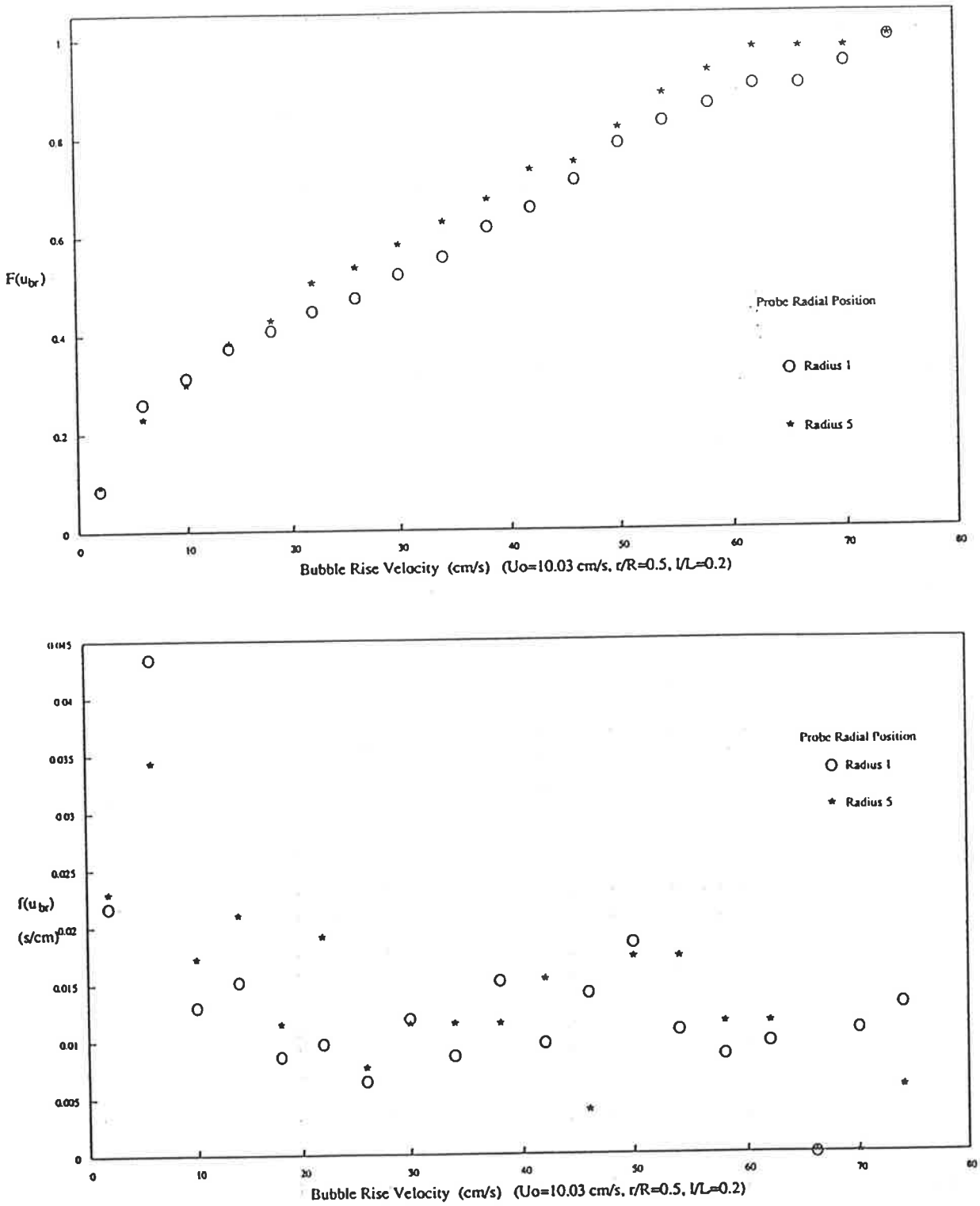

Figure 5.107 Cumulative Distribution and PDF of Bubble Rise Velocity

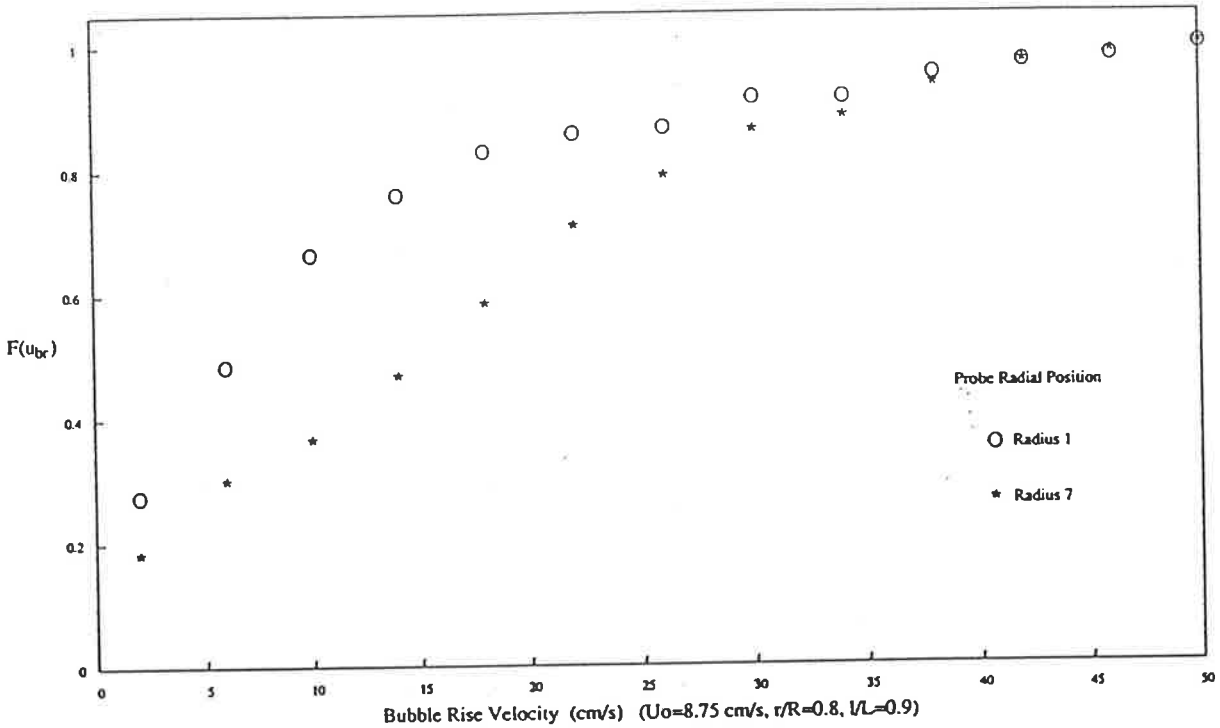

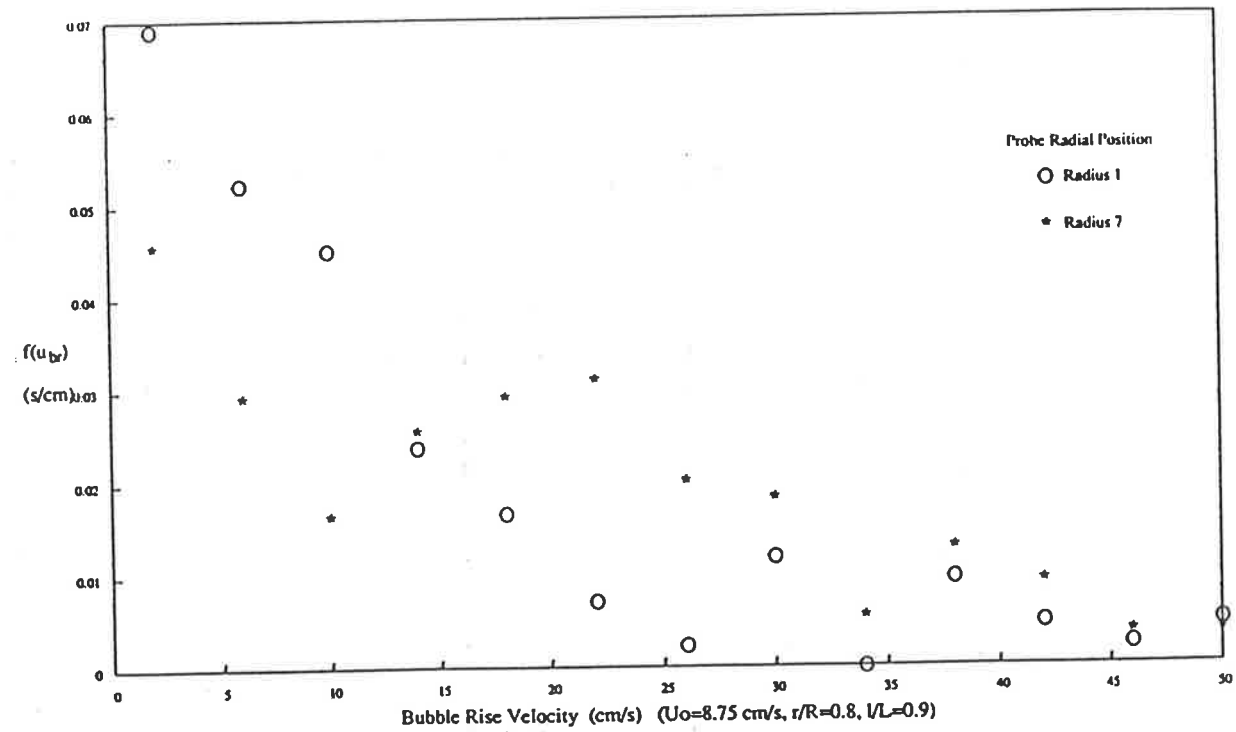

Figure 5.108 Cumulative Distribution and PDF of Bubble Rise Velocity

5.4 Overall Bed Characteristics

Overall bed characteristics can be calculated from the measured bubble parameters. The frequency of bubbles detected by the probe can be calculated from the following equation :

$$f = n/T \qquad \ldots(5.1)$$

The local bubble volume fraction is given by :

$$\varepsilon_b = f\,\bar{t}_b \qquad \ldots(5.2)$$

And the local bubble gas flow can be calculated as follows :

$$\dot{V}_b = f\,\bar{t}_b\,\overline{u}_{br} \qquad \ldots(5.3)$$

Near the distributor, the frequency of bubbles detected by the probe is higher near the wall than the centre. As *l/L* increases, the frequency increases in the centre of the bed and decreases near the wall. Figures 5.109 to 5.112 display the frequency of bubbles detected by the probe at various fluidizing gas velocities.

Figures 5.113 to 5.116 illustrate the measured local bubble volume fraction at various fluidizing gas velocities. As is the case for bubble frequency, the local bubble volume fraction is higher near the wall in the region of the distributor. As *l/L* increases, the volume fraction increases toward the centre of the bed and decreases near the wall.

At low fluidizing gas velocities, near the distributor, local bubble gas flow is higher near the wall than in the centre of the bed. Towards the top of the bed, the local bubble gas flow is greater at the centre. The distribution of local bubble gas flow becomes more uniform as fluidizing gas velocity increases. At the highest fluidizing gas velocity local bubble gas flow is uniform over the entire bed height, low near the wall and higher at the centre. Figures 5.117 to 5.120 present the variation in local bubble gas flow.

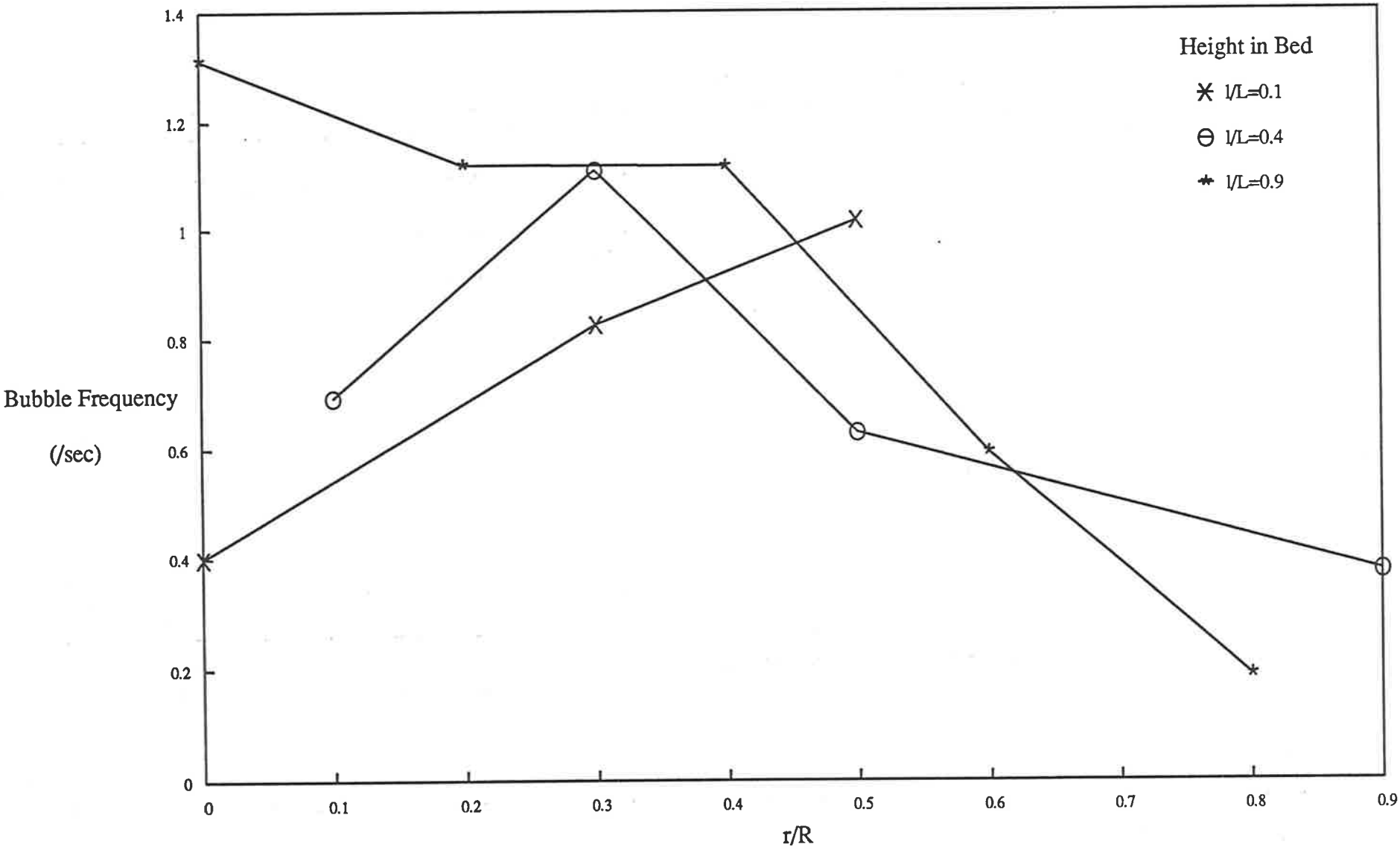

Figure 5.109 Bubble Frequency vs Radial Position (Uo=7.52 cm/s)

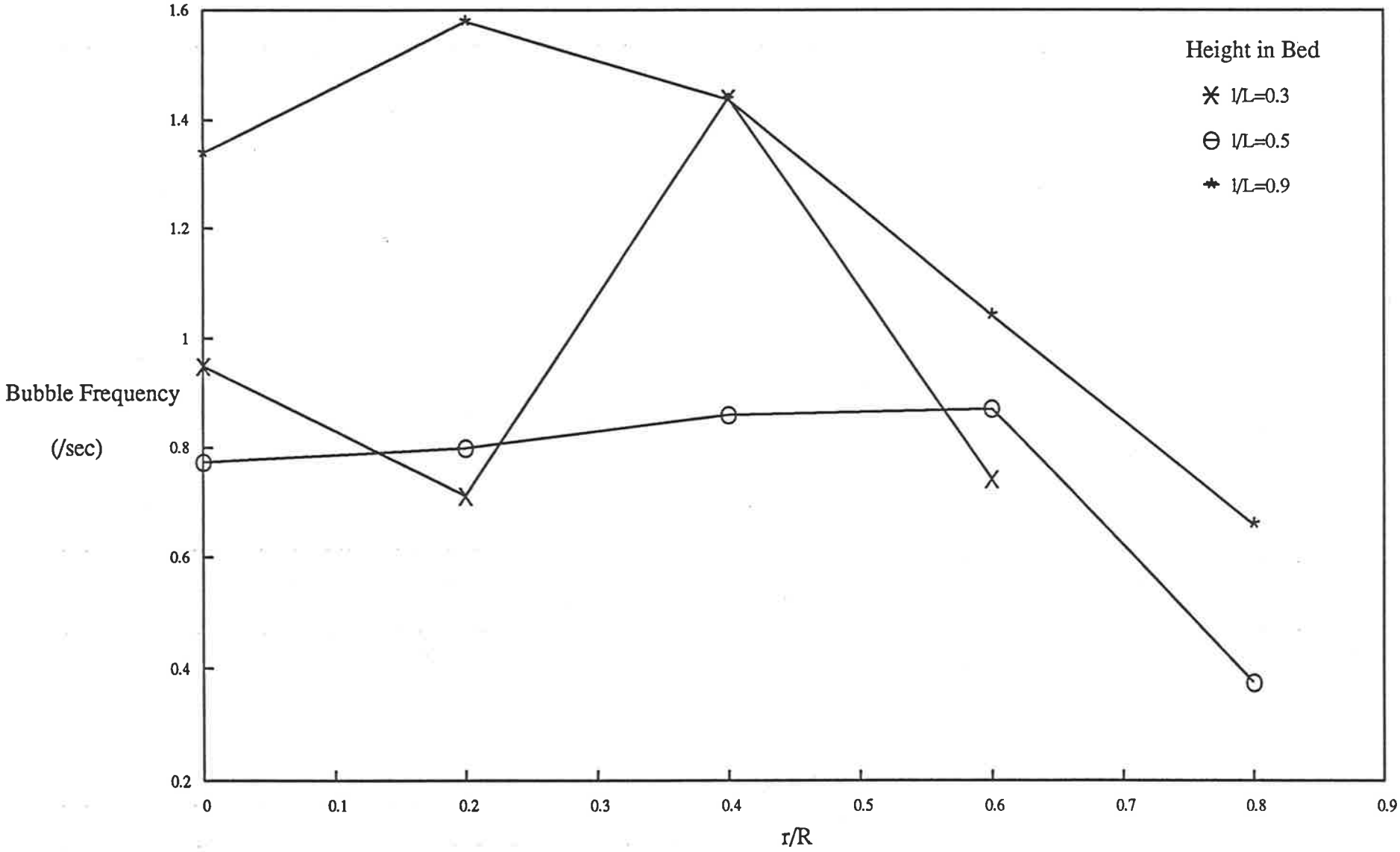

Figure 5.110 Bubble Frequency vs Radial Position (Uo=10.03 cm/s)

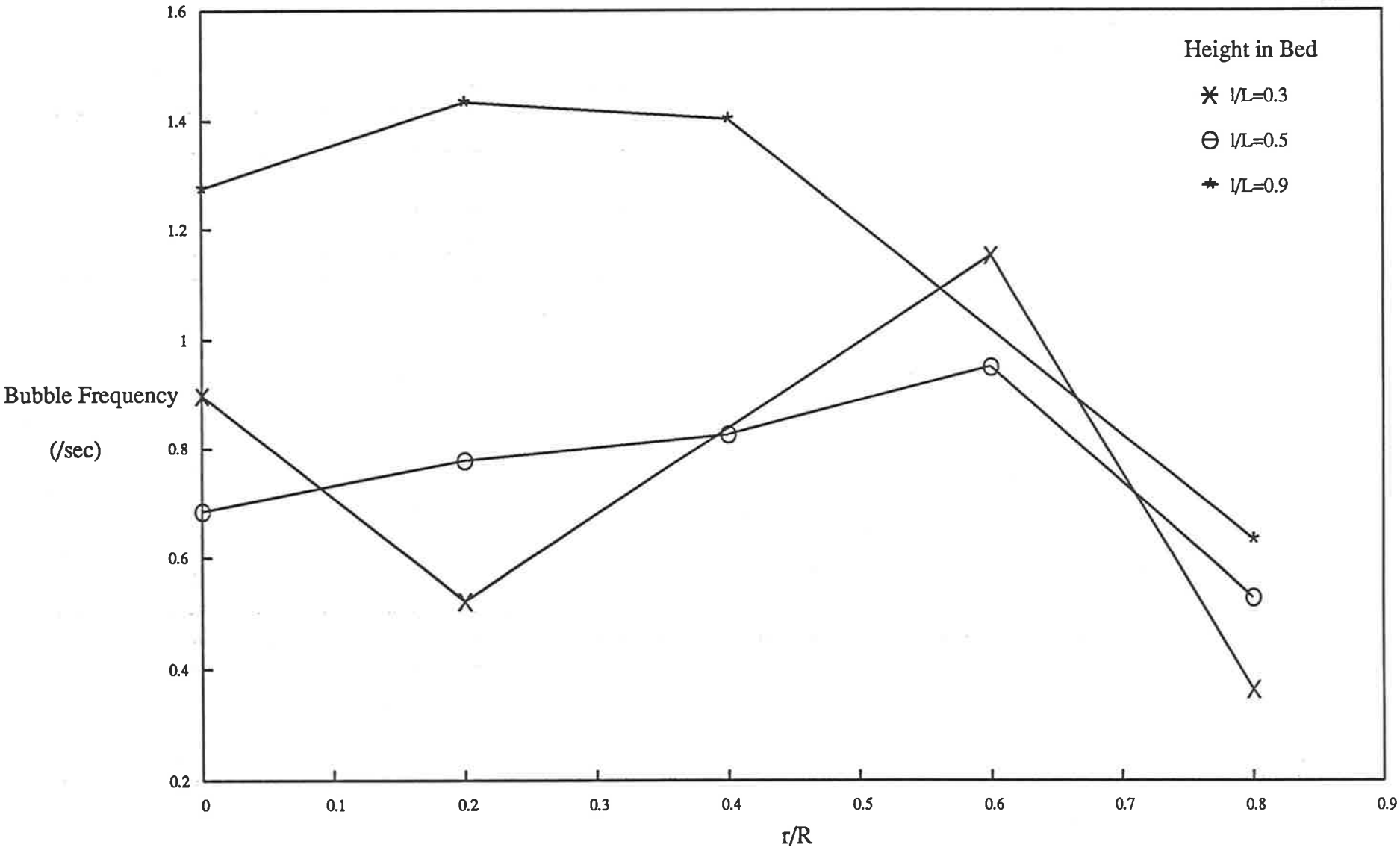

Figure 5.111 Bubble Frequency vs Radial Position (Uo=11.39 cm/s)

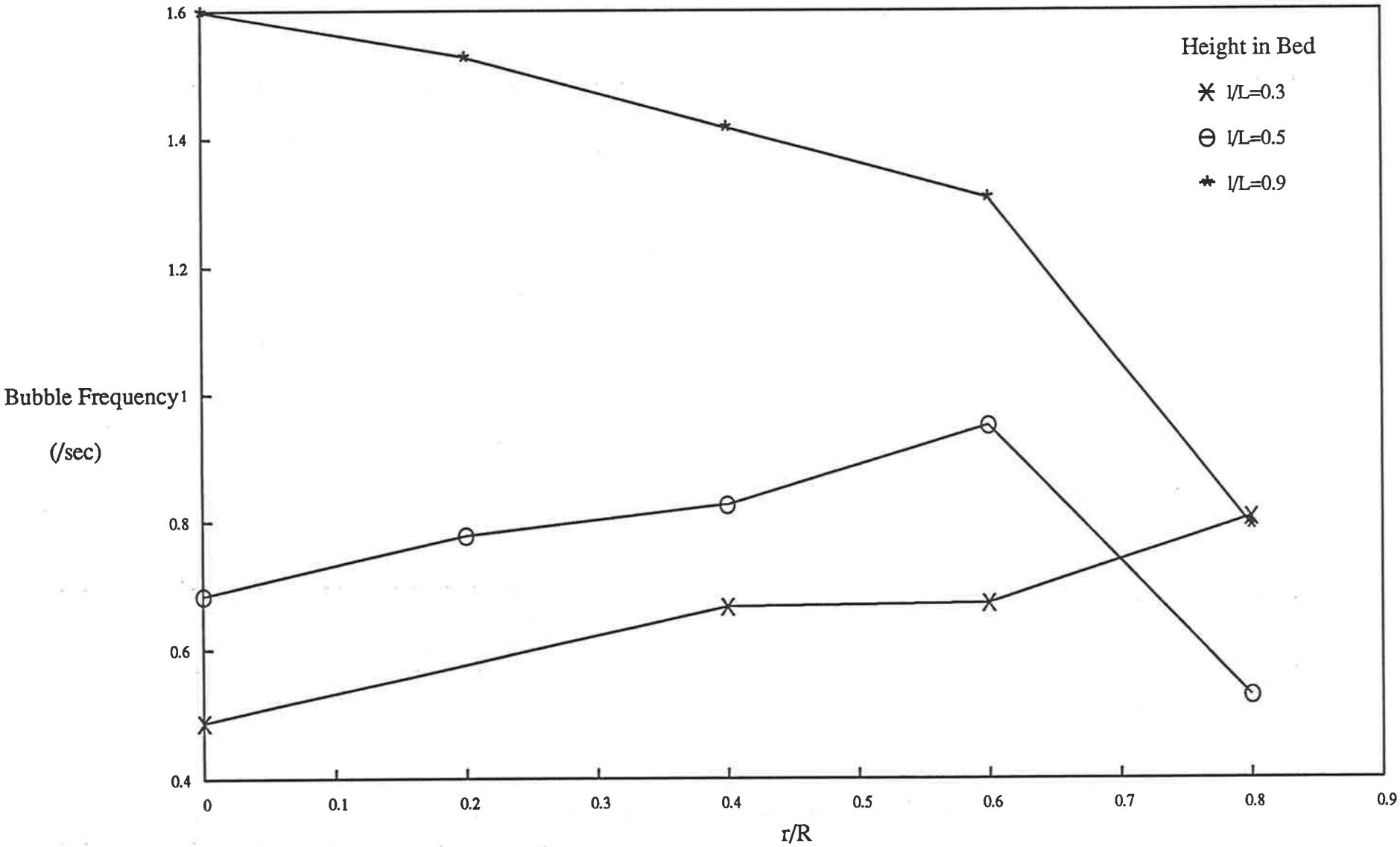

Figure 5.112 Bubble Frequency vs Radial Position (Uo=12.64 cm/s)

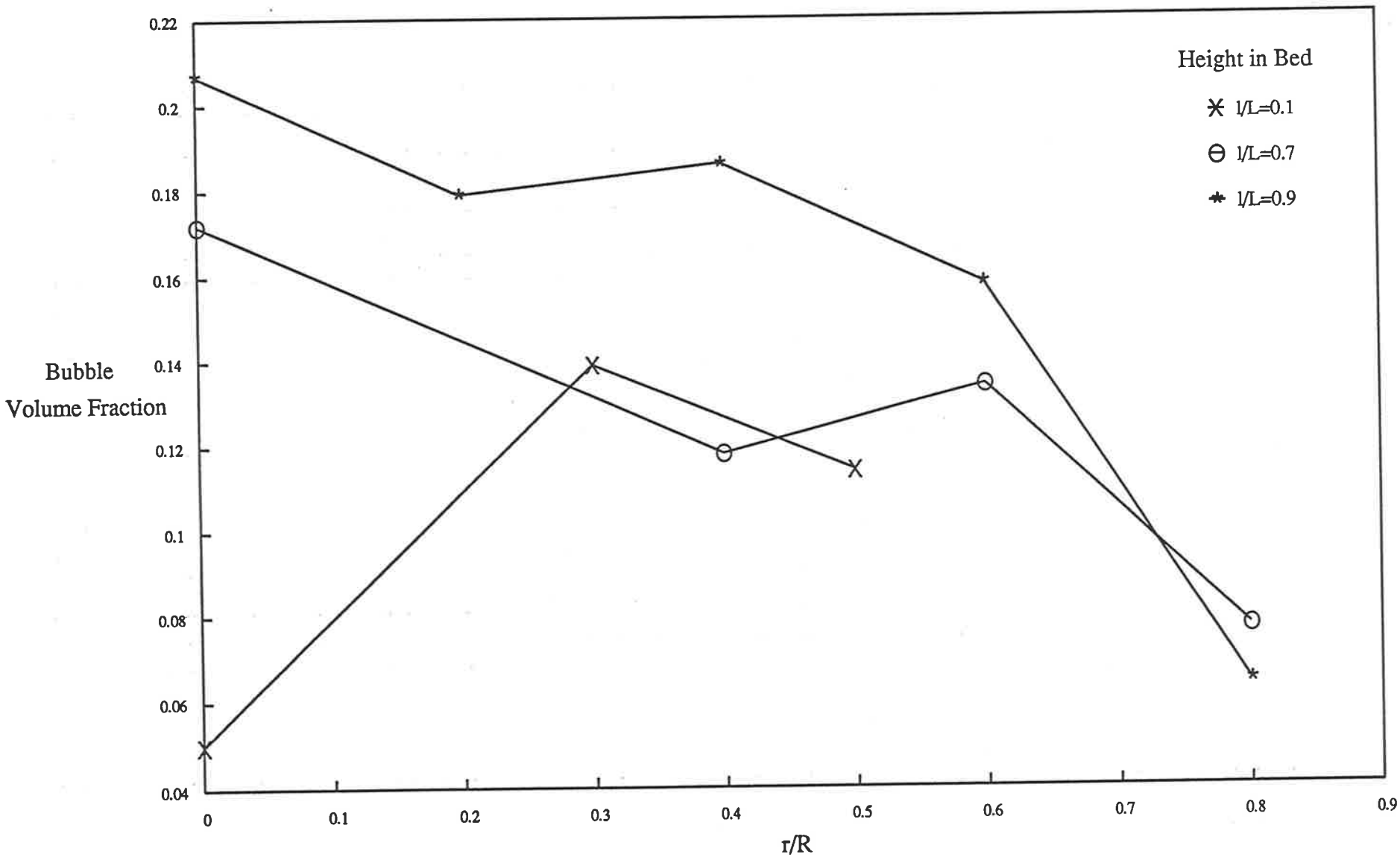

Figure 5.113 Bubble Volume Fraction vs Radial Position (Uo=7.52 cm/s)

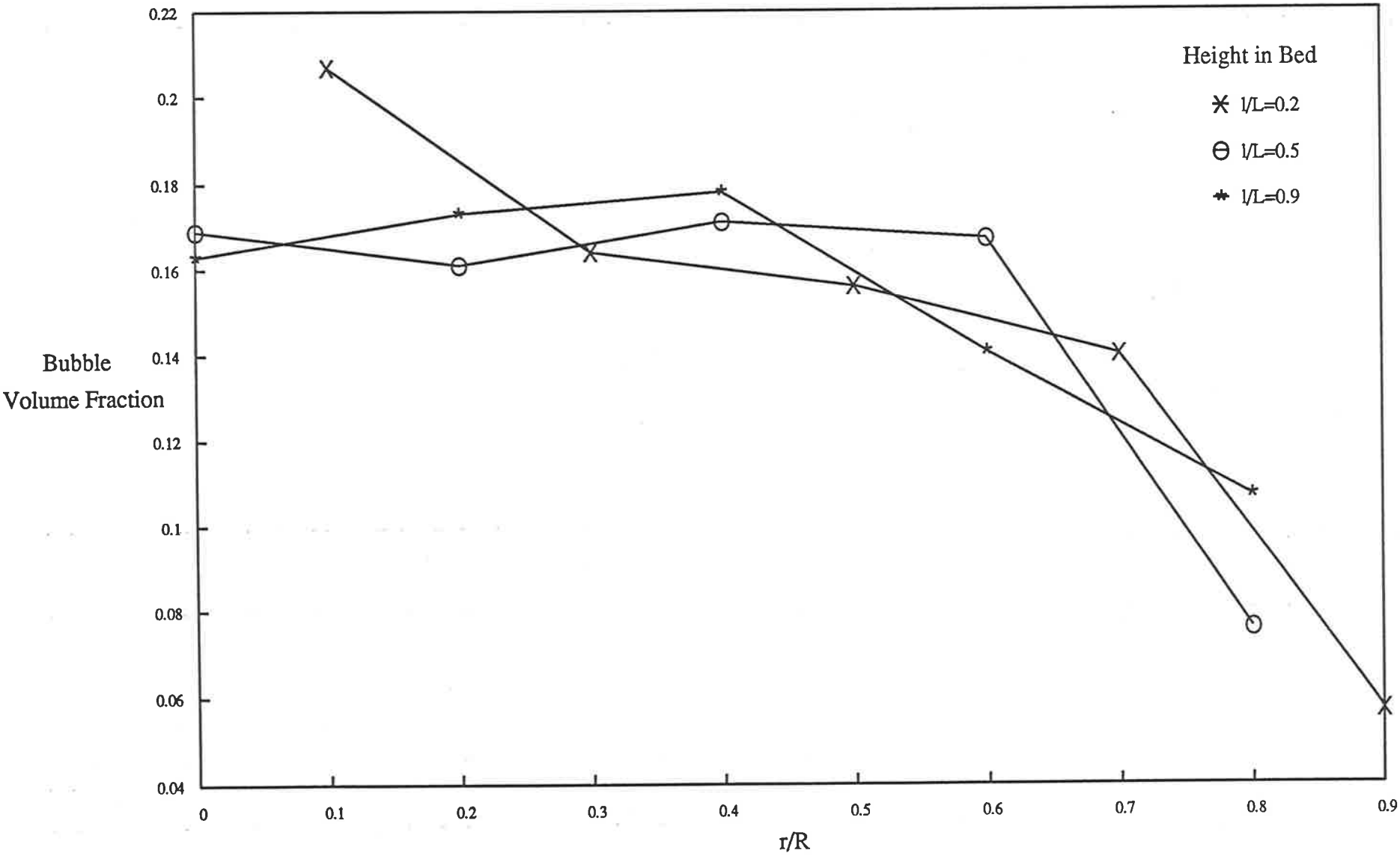

Figure 5.114 Bubble Volume Fraction vs Radial Position (Uo=10.03 cm/s)

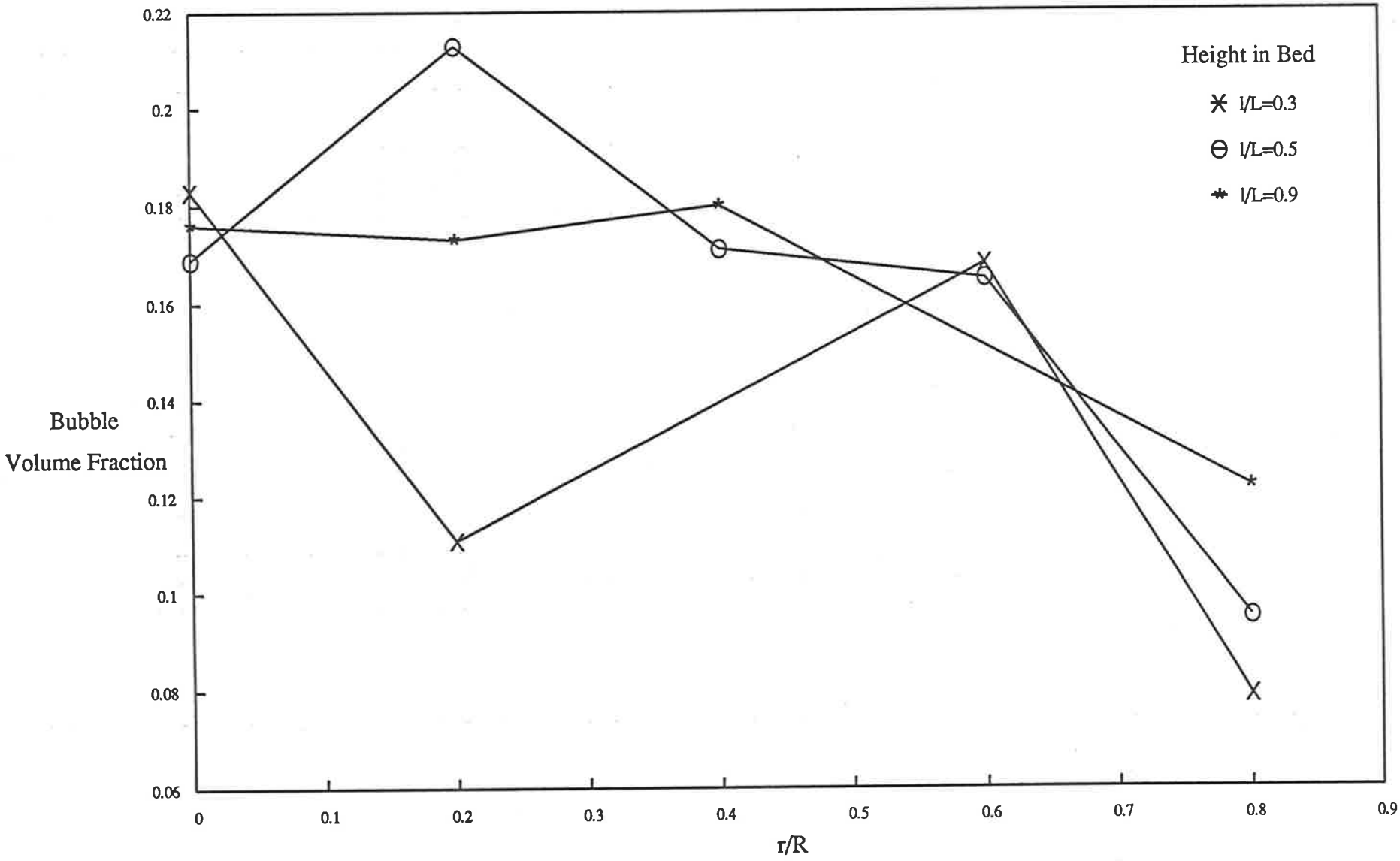

Figure 5.115 Bubble Volume Fraction vs Radial Position (Uo=11.39 cm/s)

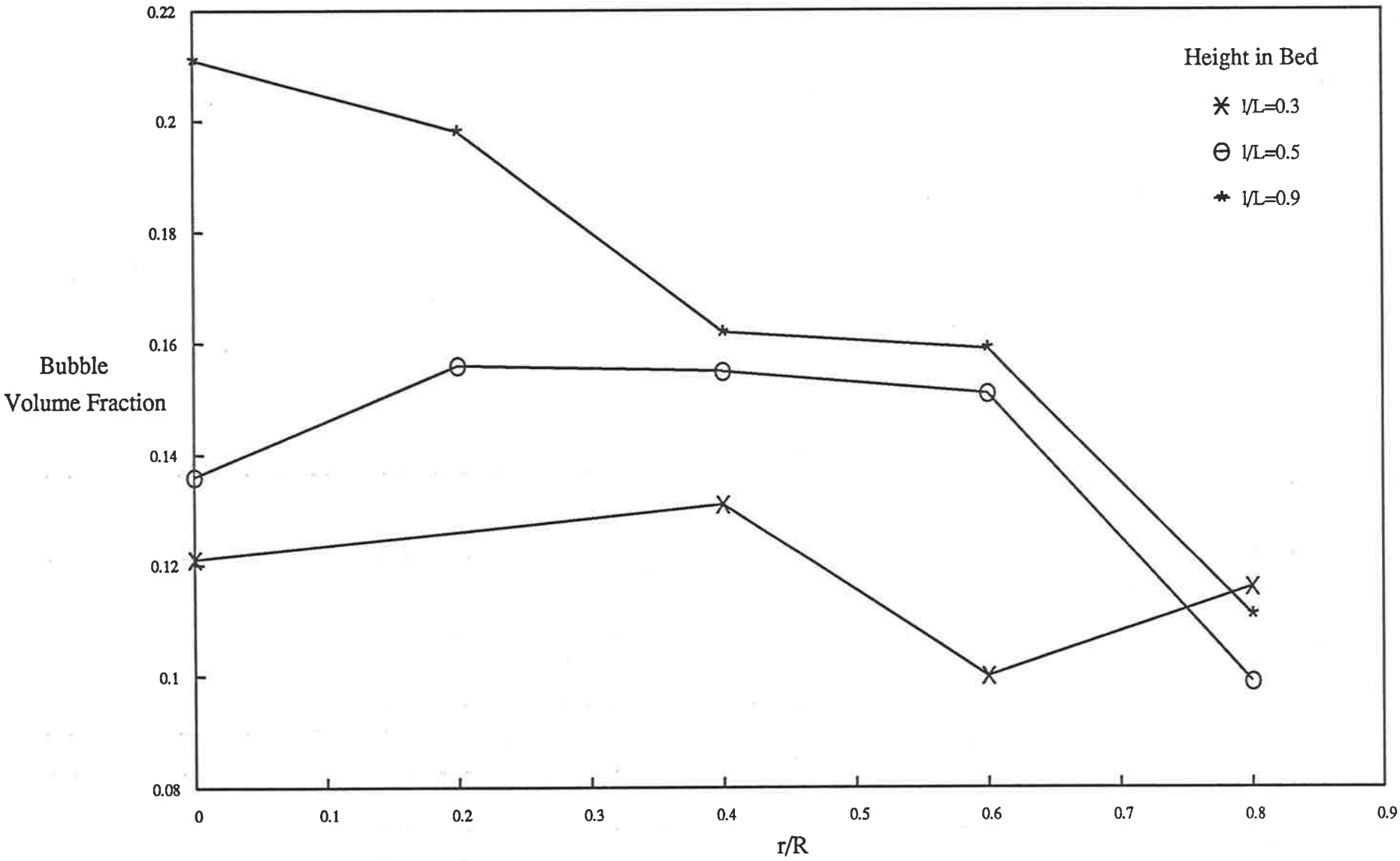

Figure 5.116 Bubble Volume Fraction vs Radial Position (Uo=12.64 cm/s)

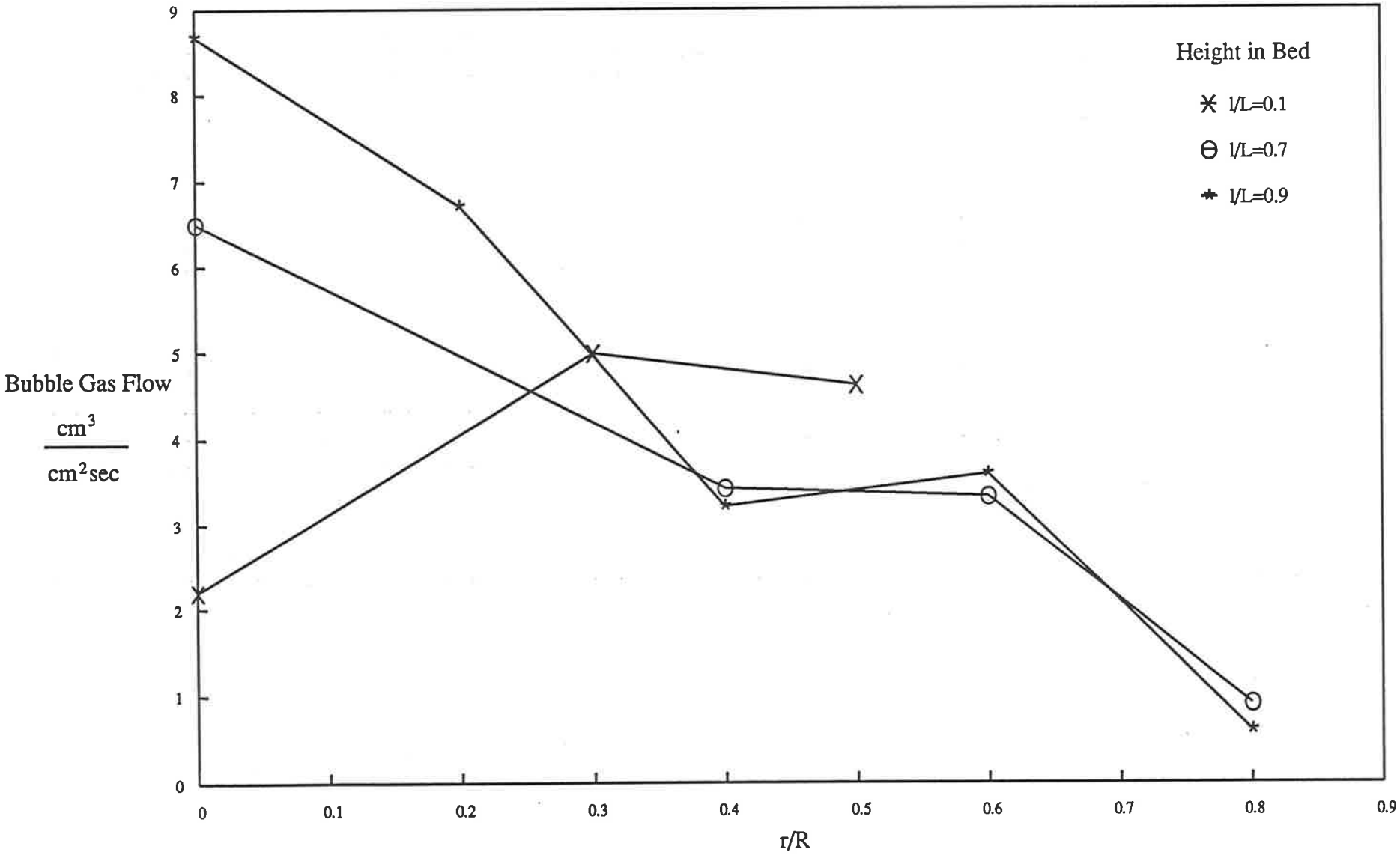

Figure 5.117 Bubble Gas Flow vs Radial Position (Uo=7.52 cm/s)

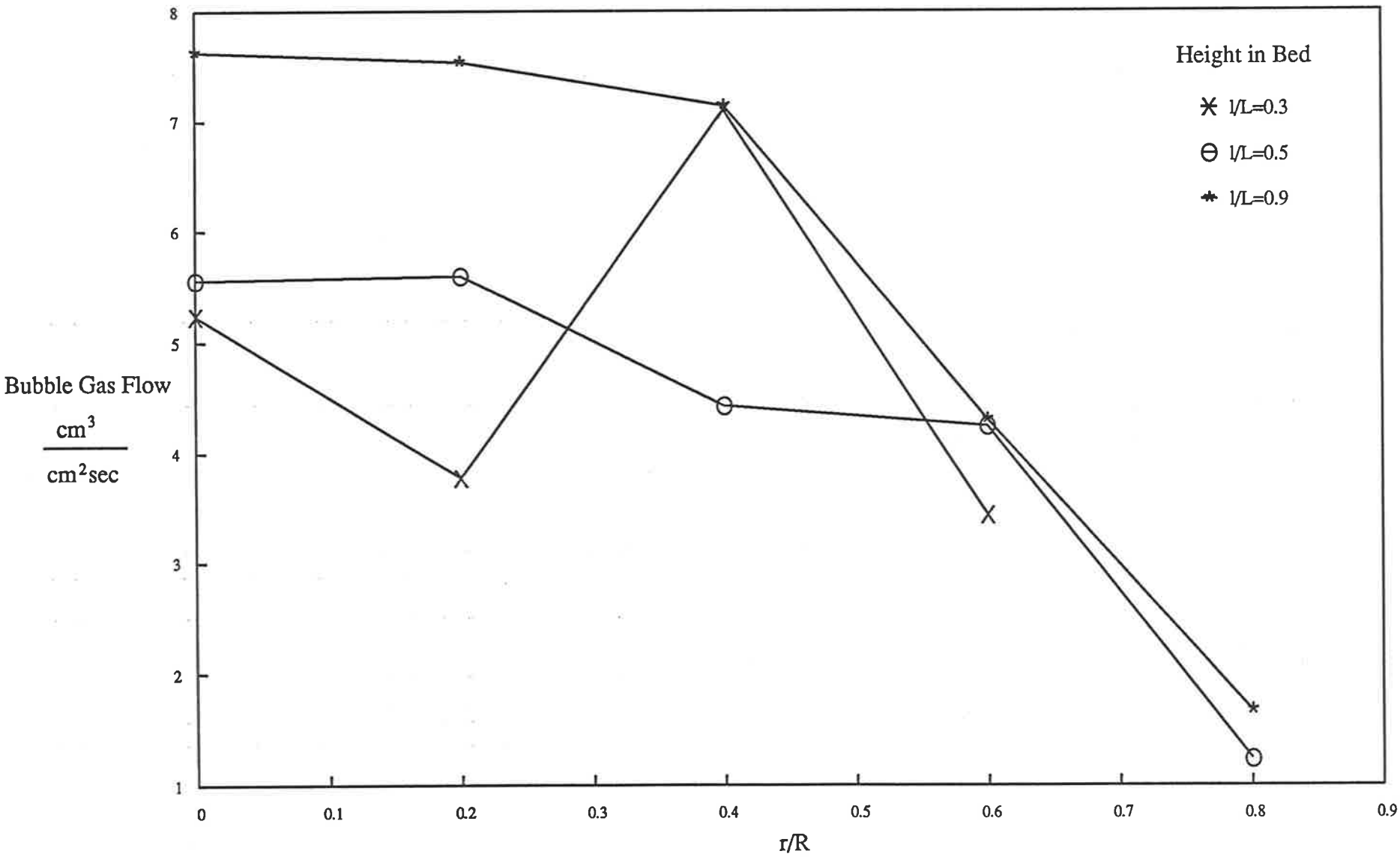

Figure 5.118 Bubble Gas Flow vs Radial Position (Uo=10.03 cm/s)

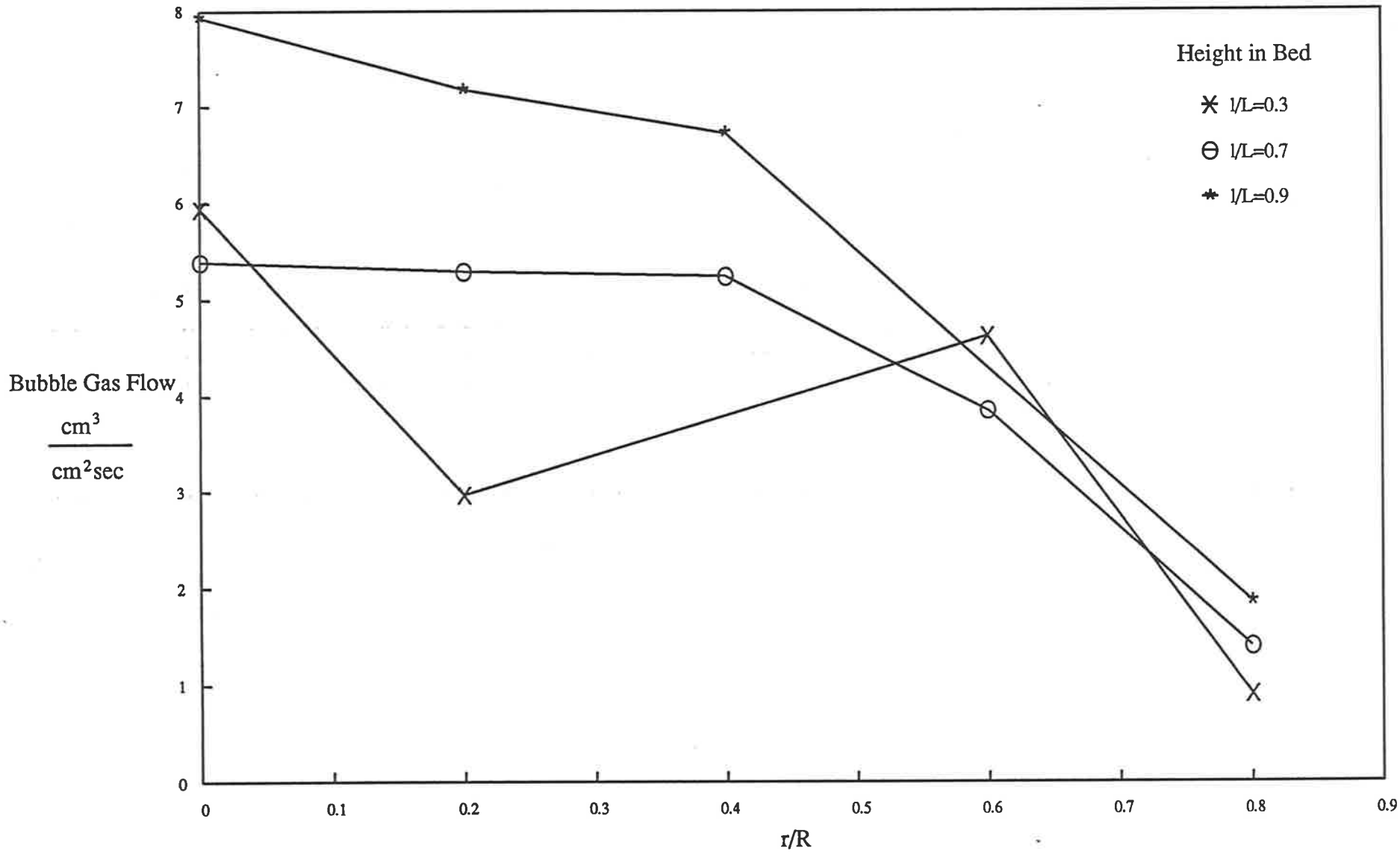

Figure 5.119 Bubble Gas Flow vs Radial Position (Uo=11.39 cm/s)

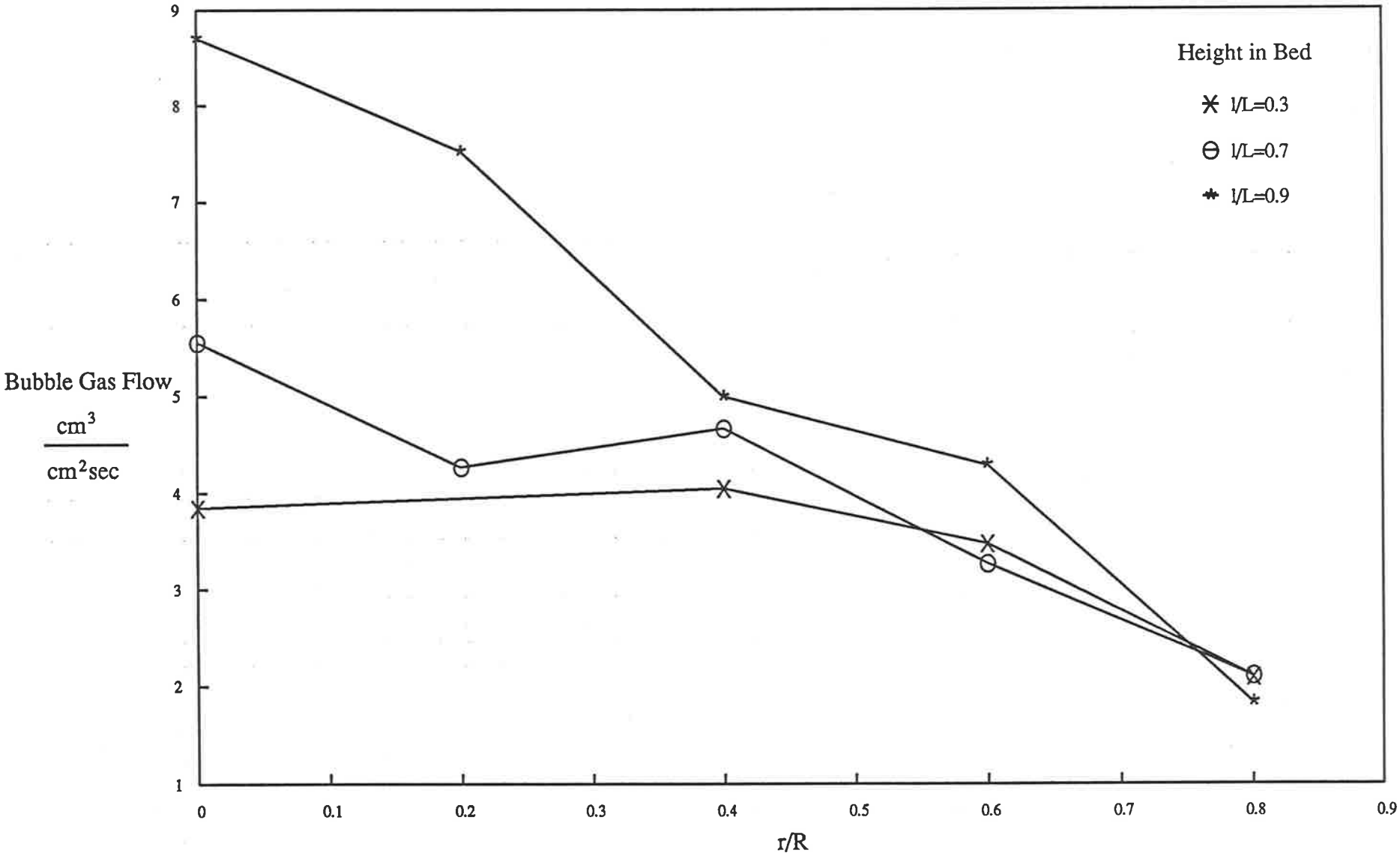

Figure 5.120 Bubble Gas Flow vs Radial Position (Uo=12.64 cm/s)

CHAPTER VI

CONCLUSIONS AND RECOMMENDATIONS

The importance of fluidization as a process technology is well documented. The studies of previous investigators present very limited quantities of measured bubble characteristics. In most instances, mean bubble characteristics are presented, whilst a convenient method of summary, these shroud the true bed hydrodynamics. This study outlines a novel method which significantly reduces the task of collecting and processing bubble characteristics. The quantity of bed hydrodynamic data presented is more extensive than any study in the previously available literature.

The capacitance probe employed in this study was modelled on previous designs but significant improvements and advances have been detailed. First, the placement of associated probe circuitry directly on top of the probe stem aided in improving the signal to noise ratio. Elimination of complex hardware previously required in this type of investigation, was a significant advance. Advanced software replaced the requirement for expensive and complex hardware. Any changes in the experimental data collection system were achieved simply and quickly by rewriting the program code rather than the detailed physical adjustments necessary in previous studies. Data collection was vastly simplified as all data acquisition functions and settings, e.g. sampling rate, experiment duration, signal amplification and filtering, were installed via the set-up menu in the data collection program. The discrimination between emulsion-phase and bubble-phase signals was achieved by real-time analysis. The data collection program processed the measured data according to the operator specified conditions. Processing options were chosen from those available in the program Process List menus. The data was then displayed

and stored for later analysis. This system proved very efficient and allowed accurate separation of the bubble and emulsion-phases. Quantities of bubble data, previously considered prohibitively large, could be collected simply and quickly and analysed immediately.

The collected bubble characteristic data was converted to cumulative distributions and probability density functions of the bubble vertical dimension and rise velocity. The quantity of data collected was formidable. Given the time constraints a limited comparison with the bubble characteristic model proposed by Agarwal (1986) was conducted. The model predictions of the probability density functions of the bubble vertical dimension were more reliable in the upper half of the fluidized bed. Closer to the distributor, the position of the peak predicted by the model deviated from that in the experimental data. The model under predicted the peak in the experimental data at the top of the bed and over predicted it near the bottom. The prediction of the cumulative distribution of the bubble vertical diameter was reasonably reliable. The experimental bubble rise velocities were evenly distributed between the maximum and minimum possible. Unfortunately, the model predictions departed significantly from the experimental data. Clearly, the model requires some modification in the light of these findings.

The variation in local bubble rise velocity was compared with that predicted from the Davidson and Harrison (1963) correlation. Good agreement with the correlation was observed. The bubble characteristic data measured by Glicksman et. al. (1987) exhibited similar behaviour to that collected in this study.

Both average and median bubble characteristics may be employed in calculations of fluidized bed performance. A comparison of median bubble characteristics, derived from correlations and experimental data, with predicted average values was undertaken. Generally, the average bubble characteristics were greater than the corresponding median (or 50% undersize) characteristics taken from the cumulative distributions. This may have been caused by the presence of a few large, fast bubbles which dominated the smaller, slower bubbles present in

the array of bubbles, leading to a distortion of the mean bubble diameter and rise velocity. There may have been a significant effect due to the presence of the smaller bubbles which was underestimated in the mean characteristics.

Figures detailing the distribution of bubble vertical dimensions and rise velocities measured in this investigation were presented. From examination, a number of conclusions could be drawn:

1) As *l/L* increased, the bubbles conglomerated and increased in size towards the centre of the bed.

2) As *l/L* increased, the bubble rise velocity increased towards the centre of the bed.

Replicate experiments were conducted at various points throughout the bed. They were conducted over an increased duration in order to test data reproducibility. All figures showed good agreement between the original and repeat experiments. Data was measured at other radii, in order to test the symmetry assumption of bed characteristics. Measurements were conducted at various bed heights, radial positions and fluidizing gas velocities and were in good agreement with those measured at radial position one.

Overall bed characteristics were calculated in order to gain additional insight into the fluidization process. Near the distributor, the frequency of bubbles detected by the probe was higher near the wall and lower in the centre. As *l/L* increased, the frequency increased in the centre of the bed and decreased near the wall. The local bubble volume fraction was higher near the wall, closer to the distributor. As *l/L* increased, the volume fraction increased toward the centre of the bed and decreased near the wall. For low fluidizing gas velocities, near the distributor, local bubble gas flow was higher near the wall and lower in the centre. Higher in the bed local bubble gas flow was greater at the centre. The distribution of local bubble gas flow became more uniform as fluidizing gas velocity increased. At the highest fluidizing gas velocity local bubble gas flow was uniform over the entire bed height, lower near the wall and higher at the centre.

Figure 6.1 illustrates the variations in bubble characteristics and overall bed hydrodynamics observed in this study.

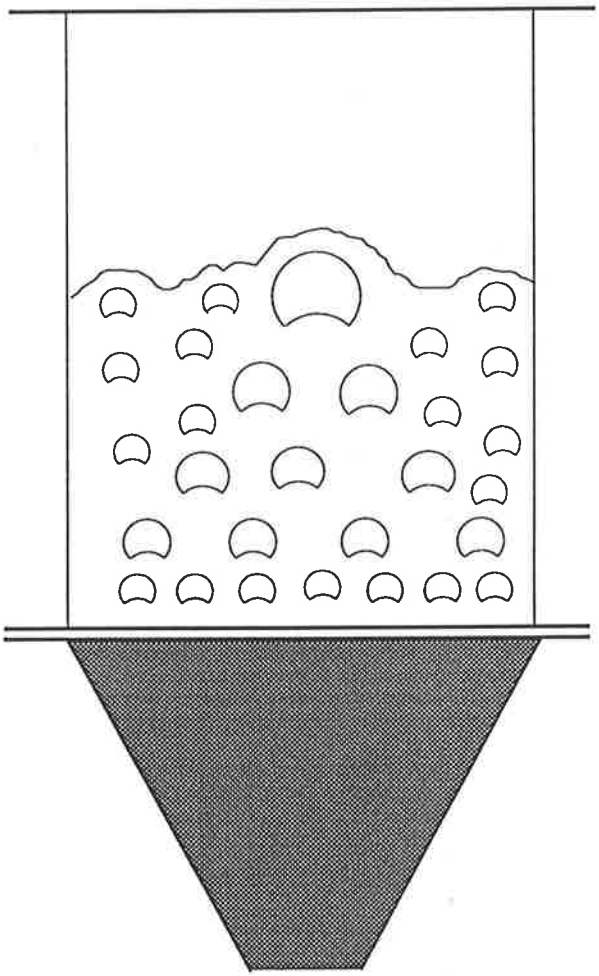

d_v , u_{br} , f , ε_b and $\dot{V}_b$ increase
towards the centre of the bed

Figure 6.1 Variations in Overall Bed Characteristics

The possible uses to which the data presented in this study may be put include :

1) The incorporation in any study linking bubble hydrodynamics with performance of fluidized bed reactors.

2) Comparison with data collected from bubble hydrodynamic studies of larger beds, for the purpose of scale-up.

3) Studies of fluidized beds of large particles are of significant interest. A comparison with data collected from such studies may be made.

The new and novel features of this study allow vast quantities of bubble characteristics to be simply and quickly gathered and analysed. Future studies in the area of bed hydrodynamics would benefit greatly from employing features developed in this investigation. Investigations of the kinetics of gas reactions, multiphase fluidization, the temperature of crude distillation, solids flow in bins and numerous others, are studies to which the current data collection software could be profitably applied with little modification. Additions to the program, such as a fast fourier transform, spline fitting or other data fitting routine would greatly improve flexibility and data utilisation.

NOMENCLATURE

a	dummy variable defined by Equation (4.3)	
a'	dummy variable defined by Equation (4.14)	
A_t	cross-sectional area of bed	cm^2
b	dummy variable defined by Equation (4.9)	
b'	dummy variable defined by Equation (4.21)	
$\overline{d}_b'$	average bubble diameter with effect of distributor taken into account	cm
$d_{b\,max}$	maximum bubble diameter	cm
d_{bo}	diameter of bubble formed at a porous plate distributor	cm
d_{br}	bubble diameter	cm
$\overline{d}_{br}$	average of bubble diameter distribution	cm
d_h	bubble equivalent horizontal dimension	cm
D_t	fluidized bed diameter	cm
d_v	bubble equivalent vertical dimension	cm
$d_{v,exp}\|_{F(d_v)=0.5}$	experimental bubble vertical dimension at $F(d_v)=0.5$	cm
$d_{br,th}\|_{F(d_{br})=0.5}$	theoretical bubble diameter at $F(d_{br})=0.5$	cm
$d_{v\,max}$	maximum bubble vertical dimension	cm
$d_{v\,min}$	minimum bubble vertical dimension	cm
f	frequency of bubbles detected by probe	sec^{-1}
$f(d_{br})$	probability density function of bubble diameter	cm^{-1}
$F(d_{br})$	cumulative distribution of bubble diameter	
$f(d_v)$	probability density function of bubble vertical dimension	cm^{-1}
$F(d_v)$	cumulative distribution of bubble vertical dimension	

$f(u_{br})$	probability density function of bubble rise velocity	s cm^{-1}
$F(u_{br})$	cumulative distribution of bubble rise velocity	
g	acceleration due to gravity	cm s^{-2}
$g(d_{v\,min})$	number density distribution of bubble pierced length at dv min	
$g(l_p)$	number density distribution of bubble pierced lengths	
i	integer	
k	adjustable parameter	
k_1	adjustable parameter	
k_2	adjustable parameter	
k_3	adjustable parameter	
l	probe tip height, measured from distributor	cm
l'	expanded bed height	cm
L	unexpanded solids height	cm
l/L	ratio of probe tip height to unexpanded solids height	
l_p	bubble pierced length	cm
m	adjustable parameter	
n	number of bubbles detected by probe over duration of experiment	
p	dummy variable	
Q_b	volumetric gas flow in bubble phase	cm^3 sec^{-1}
Q_e	volumetric gas flow in emulsion phase	cm^3 sec^{-1}
Q_t	volumetric gas through flow	cm^3 sec^{-1}
Q_{total}	total volumetric gas flow in fluidized bed	cm^3 sec^{-1}
r	probe tip radial position, measured from bed centre line	cm
R	bed radius	cm
r/R	ratio of probe tip radial position to bed radius	
s	adjustable parameter	
s_t	vertical distance between probe tips	cm
t	time	sec

T	duration of experiment	sec
t_b	bubble pierced time	sec
$\bar{t}_b$	average bubble pierced time	sec
t_r	bubble rise time	sec
$\bar{u}$	average of the velocity density function	cm s^{-1}
$\bar{u}'$	average bubble velocity with effect of distributor taken into account	cm s^{-1}
$u_{b\max}$	maximum bubble rise velocity	cm s^{-1}
u_{bo}	velocity corresponding to initial bubble diameter at distributor	cm s^{-1}
u_{br}	bubble rise velocity	cm s^{-1}
$\bar{u}_{br}$	average bubble rise velocity	cm s^{-1}
$u_{br,\exp}\|_{F(u_{br})=0.5}$	experimental bubble rise velocity at $F(u_{br})=0.5$	cm s^{-1}
$u_{br,th}\|_{F(u_{br})=0.5}$	theoretical bubble rise velocity at $F(u_{br})=0.5$	cm s^{-1}
$u_{b\infty}$	single bubble rise velocity for an isolated bubble	cm s^{-1}
u_{mf}	minimum fluidization velocity	cm s^{-1}
u_o	fluidizing gas (superficial) velocity	cm s^{-1}
$\dot{V}_b$	local bubble gas flow	$cm^3\,cm^{-2}\,sec^{-1}$
x	dummy variable defined by Equation (4.4)	
$\bar{y}$	dummy variable defined by Equation (4.2)	

Greek Symbols

ε_b	local bubble volume fraction	
ρ	density of bed particles	kg m^{-3}

BIBLIOGRAPHY

Agarwal, P. K., *Chem. Eng. Res. Des.*, **1985**, *63*, 323-337

Agarwal, P. K., *"Proceedings of the World Congress III of Chemical Engineering"*, Tokyo, Japan, **1986**, *8I-104*, 437-440

Askins, J. W., Hinds, G. P. and Kunreuther, F., *Chem. Eng. Prog.*, **1951**, *47*, 401-404

Bakker, P. J., *"Porosity Measurements in a Fluidized Bed"*, Ph. D. Thesis, TH Deflt, **1958**

Banholzer, W. F., Spiro, C. L., Kosky, P. G. and Maylotte, D. H., *Ind. Eng. Chem. Res.*, **1987**, *26*, 763-767

Bashakov, A. P., Viit, O. K., Kirakosyan, V. A., Makayev, V. K. and Filippovsky, N. F., *"Proceedings of the International Congress on Fluidization and Its Applications"*, Toulouse, France, **1973**

Bernis, A., Coeuret, F., Vergnes, F. and LeGoeff, P., *"Proceedings of the International Congress on Fluidization and Its Applications"*, Toulouse, France, **1973**

Berruti, F., Liden, A. G. and Scott, D. S., *Chem. Eng. Sci.*, **1988**, *43*, (4), 739-748

Broadhurst, T. E. and Becker, H. A., In *"Fluidization Technology"*, Davidson, J., Ed., Cambridge University Press, London, **1976**, Vol 1

Burgess, J. M. and Calderbank, P. H., *Chem. Eng. Sci.*, **1975a**, *30*, 743-750

Burgess, J. M. and Calderbank, P. H., *Chem. Eng. Sci.*, **1975b**, *30*, 1511-1518

Burns and Roe Serv. Corp., Benmol Corp. Report DE830 10792, Morgantown Energy Technology Center, US Department of Energy, **1982**

Cairns, E. J. and Prausnitz, J. M., *AIChE J*, **1960**, *6*, (4), 554-560

Chan, I. H., Sishtla, C. and Knowlton, T. M., *Powder Technol.*, **1987**, *53*, 217-235

Cheremisinoff, N. P., *Ind. Eng. Chem. Process Des. Dev.*, **1986**, *25*, 329-351

Cheremisinoff, N. P. and Cheremisinoff, P. N., *"Hydrodynamics of Gas-Solids Fluidization"*, Gulf Publishing Co., Houston, TX, **1984**

Choi, J. H., Lee, C. K., Son, J. E. and Kim, S. D., *"World Congress III of Chemical Engineering"*, Tokyo, Japan, **1986**

Choi, J. H., Son, J. E. and Kim, S. D., *Journal of Chem. Eng Japan,* **1988**, *21*, (2), 171-178

Coulaloglou, C. A. and Tavlarides, L. L., *AIChE J,* **1976**, *2,* 289-297

Davidson, J. F. and Harrison, D., *"Fluidized Particles"*, Cambridge University Press, New York, **1963**

Drahos, J., Cermák, J. and Schügerl, K., *Chem. Eng Commun.,* **1988**, *65,* 49-60

Dutta, S. and Wen, C. Y., *Can. J. Chem. Eng.,* **1979**, *57,* 115-119

Fan, L. T., Ho, T. C., Hiraoka, S. and Walawender, W. P., *AIChE J,* **1981**, *27,* (3), 388-396

Fan, L. T., Ho, T. and Walawender, W. P., *AIChE J,* **1983**, *29,* (1), 33-39

Fasching, G. E., Goff, D. R. and Maxfield, D. A., Report DOE/MC/16050-1197, NTIS, PCA03/MF A01, July **1982**, Department of Energy, Washington, DC

Fryer, C. and Potter, O. E., *"Proceedings of the International Congress on Fluidization Engineering and Its Applications"*, Toulouse, France, **1973**

Fukuda, M., Asaki, Z. and Kondo, Y., *Mem. Fac. Eng. Kyoto Univ.,* **1967**, *29,* 287-299

Geldart, D., *Powder Technol.,* **1970/71**, *4,* 41-55

Geldart, D. and Kelsey, J. R., *Powder Technol.,* **1972**, *6,* 45-60

Glicksman, L. R., Lord, W. K. and Sakagami, M., *Chem. Eng. Sci.,* **1987**, *42,* (3), 479-491

Goosens, W. R. A. and Hellinckx, L., *"Proceedings of the International Congress on Fluidization and Its Applications"*, Toulouse, France, **1973**

Gunn, D. J. and Al-Doori, H. H., *Int. J. Multiphase Flow,* **1985**, *11,* (4), 535-551

Hager, W. R. and Thompson, W. J., *AIChE Symp. Ser.,* **1973**, *69,* (68), 128

Haines, A. K., King, R. P. and Woodburn, E. T., *AIChE J,* **1972**, *18,* (3), 591-599

Harrison, D. and Leung, L. S., *"Proc. Symp. on Interaction between Fluids and Particles, Inst. Chem. Engrs."*, 127, June, **1962**

Hayakawa, T., Graham, W. and Osberg, G. L., *Can. J Chem. Eng.*, **1964**, *42*, 99-103

Hilligardt, K. and Werther, J., *"World Congress III of Chem. Eng."*, Tokyo, Japan, **1986**

Hiraki, I., Kunii, D. and Levenspiel, O., *Powder Technol.*, **1968/69**, *2*, 247-252

Homsy, G. M., Report DOE/PC/30244-T3, NTIS, PC A02/MF A01, Sept. **1981**, Department of Energy, Washington, DC

Ishida, M., Shirai, T. and Nishiwaki, A., *Powder Technol.*, **1980**, *27*, 1-6

Johnson, D. S. L., Ph. D. Thesis, Univ. Edin., **1970**,

Judd, M. and Dixon, P., *AIChE Symp. Ser.*, **1978**, *74*, (38), 176

Kai, T., Shirakawa, Y., Takahashi, T. and Furusaki, S., *Powder Technol.*, **1987**, *51*, 267-271

Kilkis, B., DeGeyter, F. M. and Ginoux, J. J., *"Proceedings of the International Congress on Fluidization and Its Applications"*, Toulouse, France, **1973**

Krautkramer, J. and Krautkramer, H., *"Ultrasonic Testing of Materials"*, Springer-Verlag, Berlin, Germany, **1983**

Kunii, D., Yoshida, K. and Hiraki, J., *"Proceedings of the International Symposium on Fluidization"*, Netherland's University Press, Eindhoven, Amsterdam, **1967**

Kunii, D. and Levenspiel, O., *"Fluidization Engineering"*, R. E. Kreiger Publishing Co., Huntington, NY, **1977**

Lanneau, K. P., *Trans. Inst. Chem. Eng.*, **1960**, *38*, 125-142

Lockett, M. J. and Safekourdi, A. A., *AIChE J*, **1977**, *23*, (3), 395-398

Lowry, G. and Barrett, D., *"AIE National Conference"*, Newcastle, Australia, **1979**

Lowry, G. and Barrett, D., *"Eighth National Chemical Engineering Conference"*, Melbourne, Australia, **1980**

Matsui, I., Kojima, T., Kunii, D. and Furusawa, T., *Ind. Eng. Chem. Res.*, **1987**, *26*, 95-100

Maylotte, D. H., Lamby, E. J., Kosky, P. G. and Peters, R. L. St., *"Proceedings of the 41st Ironmaking Conference 41"*, AIME, Pittsburg, PA, **1982**

Miwa, K., Mori, S., Kato, T. and Muchi, I., *Intl. Chem. Eng.*, **1972**, *12*, (1), 187

Morse, R. D. and Ballou, C. O., *Chem. Eng. Prog.*, **1951**, *47*, 199-211

Muramoto, T., Nakajima, M., Morooka, S. and Matsuyama, H., *Chem. Eng. Commun.*, **1985**, *35*, 193-201

Nicklin, D. J., *Chem. Eng. Sci.*, **1962a**, *17*, 693

Nicklin, D. J., Wilkes, J. O. and Davidson J. F., *Trans. Inst. Chem. Eng.*, **1962b**, *40*, 61

Ohki, K., Walawender, P. A. and Fan L. T., *Powder Technol.*, **1977**, *18*, 171-178

Ohki, K. and Shirai, T., In *"Fluidization Technology"*, Keairns, D. L., Ed., Cambridge University Press, London, **1978**, Vol 1

Orcutt, J. C. and Carpenter, B. H., *Chem. Eng. Sci.*, **1971**, *26*, 1049

Otake, T., Tone, S., Kawashima, M. and Shibata, T., *Journal of Chem. Eng. Japan*, **1975**, *8*, (5), 388-392

Park, W. H., Kang, W. K., Capes, C. E. and Osberg, G. L., *Chem. Eng. Sci.*, **1969**, *24*, 851-865

Patrose, B. and Caram, H. S., *AIChE J*, **1982**, *28*, (4), 604-609

Put, M., Francesconi, A. and Goosens, W., *"Proceedings of the International Congress on Fluidization and Its Applications"*, Toulouse, France, **1973**

Rowe, P. N., In *"Fluidization"*, Davidson, J. F. and Harrison, D., Eds., Academic Press, London and New York, **1971**

Rowe, P. N. and Masson, H., *Chem. Eng. Sci.*, **1980**, *35*, 1443-1447

Rowe, P. N. and Masson, H., *Trans. Inst. Chem. Eng.*, **1981**, *59*, 178

Rowe, P. N. and Matsumo, R., *Chem. Eng. Sci.*, **1971**, *26*, 923

Rowe, P. N. and Partridge, B., *Trans. Inst. Chem. Eng.*, **1965**, *43*, T157

Schmalfeld, J., Diss., University of Karlsruhe, **1973**

Sung, J. S. and Burgess, J. M., *Powder Technol.*, **1987**, *49*, 165-175

Taylor, P. A., Lorenz, M. M. and Sweet, M. R., *"Proceedings of the International Congress on Fluidization and Its Applications"*, Toulouse, France, **1973**

Tomita, M. and Adachi, T., *Journal of Chem. Eng. Japan,* **1973**, *6,* (2), 196-201

Tone, S., Seko, H., Maruyama, H. and Otake, T., *Journal of Chem. Eng. Japan,* **1974**, *7,* (1), 44-51

Upson, P. C. and Pyle, D. L., *"Proceedings of the International Congress on Fluidization and Its Applications"*, Toulouse, France, **1973**

Valenzuela, J. A. and Glicksman, L. R., *Powder Technol.,* **1984**, *38,* 63-72

Weimer, A. W., Gyure, D. C. and Clough, D. E., *Powder Technol.,* **1985**, *44,* 179-194

Wen, C. Y., Krishnan, R., Khosravi, R. and Dutta, S., In *"Fluidization"*, Davidson, J. F., Ed., Cambridge University Press, London, **1978**, Vol 32

Werther, J., *Trans. Inst. Chem. Eng.,* **1974a**, *52,* 149-159

Werther, J., *AIChE Symp. Ser.*, **1974b**, *70,* (141), 53-62

Werther, J., *Powder Technol.*, **1976**, *15,* 155-167

Werther, J., *Int. J. Multiphase Flow,* **1977**, *3,* 367-381

Werther, J., In *"Fluidization Technology"*, Keairns, D. L., Ed., Cambridge University Press, London, **1978a**, Vol 1

Werther, J., In *"Proceedings of the 2nd Engineering Foundation Conference on Fluidization"*, Davidson, J. F. and Keairns, D. L., (Eds.), Cambridge University Press, London, **1978b**

Werther, J. and Molerus, O., *Int. J. Multiphase Flow,* **1973a**, *1,* 103-122

Werther, J. and Molerus, O., *Int. J. Multiphase Flow,* **1973b**, *1,* 123-138

Whitehead, A. B., Gartside, G. and Dent, D. G., *Chem. Eng. Prog.,* **1970**, *1,* 175-190

Yamazaki, M., Fukuta, K. and Tokumoto, J., *"World Congress III of Chemical Engineering"*, Tokyo, Japan, **1986**

Yang, J. S., Liu, Y. A. and Squires, A. M., *Powder Technol.,* **1987**, *49,* 177-187

Yasui, G. and Johanson, L. N., *AIChE J,* **1958**, *4,* 446

Yong, J., Zhiqing, Y., Zhang, L. and Zhanwen, W., In *"Fluidization"*, Grace J. R. and Matsen, J. M., Eds., Plenum Press, New York, **1980**

Yosef, B., Ginio, O., Mahlab, D. and Weitz A., *J Appl. Phys.*, **1975**, *46*, (2), 738-740

Yoshida, K. and Kunii, D., *Journal of Chem. Eng. Japan*, **1968**, *1*, (1), 11-16

Yoshida, K., Nakajima, K., Hamatami, N. and Shimizu, F., *"Fluidization"*, Cambridge University Press, London, **1978a**, Vol 13

Yoshida, K., Nakajima, K., Hamatami, N. and Shimizu, F., *"Proceedings of the Engineering Foundation Conference, 2nd, Trinity College, Cambridge, England"*, Cambridge University Press, April 2-6, **1978b**

Yutani, N., Fan, L. T. and Ho, T. C., *Can. J. Chem. Eng.*, **1983a**, *61*, 121-125

Yutani, N., Ho, T. C., Fan, L. T., Walawender, W. P. and Song, J. C., *Chem. Eng. Sci.*, **1983b**, *38*, (4), 575-582

Yutani, N., Ototake, N. and Fan, L. T., *Powder Technol.*, **1986**, *48*, 31-38

Zhang, X. R., Homsy, G. M. and Ropchan, W. T., *Int J. Multiphase Flow*, **1987**, *13*, (5), 649-660

APPENDICES

Appendix A

Derivation of Bubble Diameter formed at the Distributor

There are three components of gas flow in a fluidized bed ; gas flow in the dense phase, gas flow in the bubble phase and gas through flow. The continuity equation can be expressed as :

$$Q_{total} = Q_e + Q_b + Q_t \qquad \ldots(A.1)$$

where

$$Q_{total} = A_t u_o \qquad \ldots(A.2)$$

$$Q_e = A_t (1 - \varepsilon_b) k_1 u_{mf} \qquad \ldots(A.3)$$

$$Q_b = A_t \varepsilon_b u_{br} \qquad \ldots(A.4)$$

$$Q_t = A_t \varepsilon_b k_1 k_2 u_{mf} \qquad \ldots(A.5)$$

Thus

$$\begin{aligned} Q_b &= Q_{total} - Q_e - Q_t \\ &= A_t u_o - A_t (1 - \varepsilon_b) k_1 u_{mf} - A_t \varepsilon_b k_1 k_2 u_{mf} \end{aligned} \qquad \ldots(A.6)$$

Assuming the Davidson model for an isolated bubble (Davidson and Harrison (1963)) :

$$k_1 = 1 \quad \text{and} \quad k_2 = 3$$

Thus

$$Q_b = A_t[u_o - (1-\varepsilon_b)u_{mf} - \varepsilon_b 3u_{mf}]$$

$$= A_t[u_o - u_{mf} + \varepsilon_b u_{mf} - 3\varepsilon_b u_{mf}]$$

$$= A_t[u_o - u_{mf}(1+2\varepsilon_b)] \qquad \ldots(A.7)$$

Now

$$Q_b = A_t \varepsilon_b u_{br}$$

hence

$$A_t \varepsilon_b u_{br} = A_t[u_o - u_{mf}(1+2\varepsilon_b)]$$

$$\Rightarrow \varepsilon_b u_{br} = u_o - u_{mf}(1+2\varepsilon_b)$$

$$\Rightarrow \varepsilon_b u_{br} + 2\varepsilon_b u_{mf} = u_o - u_{mf}$$

$$\Rightarrow \varepsilon_b(u_{br} + 2u_{mf}) = u_o - u_{mf}$$

$$\Rightarrow \varepsilon_b = \frac{u_o - u_{mf}}{u_{br} + 2u_{mf}}$$

$$u_{br} = u_{bo} = u_o - u_{mf} + 22.26\sqrt{d_{bo}} \qquad \ldots(A.8)$$

Thus

$$\varepsilon_b = \frac{u_o - u_{mf}}{u_o - u_{mf} + 22.26\sqrt{d_{bo}} + 2u_{mf}} \qquad \ldots(A.9)$$

Now Miwa et. al. (1972) proposed that the diameter of a bubble formed at the distributor is given by the expression :

$$d_{bo} = 0.00376[u_o - u_{mf}]^2 \qquad \ldots(A.10)$$

We replace $u_o - u_{mf}$ in the Miwa equation by $u_o - (1 + 2\varepsilon_b)u_{mf}$ to obtain :

$$d_{bo} = 0.00376[u_o - (1 + 2\varepsilon_b)u_{mf}]^2 \qquad \ldots(A.11)$$

Equations (A.9) and (A.11) are solved by trial and error to obtain the bubble diameter formed at the distributor.

Appendix B

Computer Programs

This program converts the measured bubble pierced times and rise times into the bubble pierced length and rise velocity. It further calculates the probability density function and the cumulative distribution of the bubble pierced length and rise velocity. The PDF of the bubble pierced length is converted to a number density distribution and from this the cumulative distribution and PDF of the bubble vertical dimension is calculated, as outlined by Werther (1974a). Overall bed characteristics are also calculated.

```
program ublpave;

uses turbo3,crt;
type real=extended;

var
 ber,enr,minr,cbr,dlrawr,dtrawr,dlmod,dveln,lpmin,dbv,dbvd,
 fn,dlpm,slp,svel,sdlmod,avelp,avevel,qdlpmin,qdv,
 avetb,dtmod,vel,lp,dvel,dlp,pdvel,dvelp,rr,dvmin,
 dlpq,rate,totaltime,qdlp,bubfreq,ndlp,uo,umf,dt,lpleast,
 bvolfrac,bgasflow,cuslp,cusvel,ndvel,lpmax,ubmax,
 eny,bey,cby,miny,dlrawy,dtrawy,dtraw,dlraw:real;
 nf,i,j,nbr,nby,k,totalnbr,
 s,r,n,m,p,q,nmax,mmax,sumvinc,
 svinc,sumlinc,slinc,a,b,c,d,e,
 preframe,linesdone:integer;
 vtest,ltest,avetest:boolean;
 vinc:array[0..2100] of real;
 linc:array[0..2000] of real;
 s50,f50,g50,h50,i50:string[50];
 q2txt_file,q2dtdltxt_file,q2dtpdftxt_file,
 q2dlpdftxt_file,q2qdvtxt_file:text;
 ans,nans:char;

procedure init;
begin
nmax:=0;
mmax:=0;
for r:=1 to 2100 do
  begin
  vinc[r]:=0;
  end;
for s:=1 to 2000 do
  begin
  linc[s]:=0;
  end;
end;

procedure freq;

begin
vtest:=false;
ltest:=false;
n:=0;
m:=0;
repeat
```

```
n:=n+1;
dveln:=dvel*n;
if vel<dveln then
 begin
 vinc[n]:=vinc[n]+1;
 vtest:=true;
 if n>nmax then
   begin
   nmax:=n;
   end;
 end;
until vtest=true;
repeat
m:=m+1;
dlpm:=dlp*m;
if lp<dlpm then
 begin
 linc[m]:=linc[m]+1;
 ltest:=true;
 if m>mmax then
   begin
   mmax:=m;
   end;
 end;
until ltest=true;
end;


procedure pdf;

begin
lpmin:=1000;
cusvel:=0;
cuslp:=0;
sumlinc:=0;
sumvinc:=0;
writeln(q2dtpdftxt_file,'  ubr  ','  f(ubr)  ','  F(ubr)  ',' n  vinc(n)  ','  ndubr');
for p:=1 to nmax do
  begin
  dvelp:=(dvel*p)-(dvel/2);
  pdvel:=(vinc[p]/totalnbr)/dvel;
  ndvel:=vinc[p]/totalnbr;
  cusvel:=cusvel+ndvel;
  svinc:=round(vinc[p]);
  sumvinc:=sumvinc+svinc;
  writeln(q2dtpdftxt_file,dvelp:10:6,pdvel:10:6,cusvel:10:6,p:5,vinc[p]:5:0,ndvel:10:6);
  end;
writeln(q2dtpdftxt_file,'total vel records (# bubbles) =',sumvinc:5);
writeln(q2dlpdftxt_file,'  lpr  ','  f(lpr)  ','  F(lpr)  ',' n  linc(n)  ','  ndlpr');
for q:=1 to mmax do
  begin
  dlpq:=(dlp*q)-(dlp/2);
  qdlp:=(linc[q]/totalnbr)/dlp;
  ndlp:=linc[q]/totalnbr;
  if qdlp>0 then          {pdf lp may be zero}
    begin
    if (dlpq<lpmin) and (dlpq>=0.4{  =dvmin}) then
      begin
      lpmin:=dlpq;
      qdlpmin:=qdlp;
      end;
    end;
  cuslp:=cuslp+ndlp;
  slinc:=round(linc[q]);
  sumlinc:=sumlinc+slinc;
  writeln(q2dlpdftxt_file,dlpq:10:6,qdlp:10:6,cuslp:10:6,q:5,linc[q]:5:0,ndlp:10:6);
  end;
writeln(q2dlpdftxt_file,'total lp records (# bubbles) =',sumlinc:5);
```

```
close(q2dtpdftxt_file);
close(q2dlpdftxt_file);
end;

procedure qzerodv;
begin
writeln(q2qdvtxt_file,' dv"-ddv"/2',' dv" ',' dv ',' Qodv');
assign(q2dlpdftxt_file,h50);
reset(q2dlpdftxt_file);
readln(q2dlpdftxt_file);
for q:=1 to mmax do
  begin
  readln(q2dlpdftxt_file,dlpq,qdlp);
  {include shape factor ie. /0.8}
  if dlpq>=lpmin then
    begin
    qdv:=1-((qdlp/qdlpmin)*(lpmin/dlpq));
    end
  else
    begin
    qdv:=0;
    writeln('qdv=0');
    end;
dbv:=dlpq/0.8;
dbvd:=(dbv-dlp/1.6);
{  dv"-ddv"/2 = dbv-dlp/0.8/2}
writeln(q2qdvtxt_file,dbvd:10:6,dbv:10:6,dlpq:10:6,qdv:10:6);
end;
close(q2qdvtxt_file);
end;

procedure convert;
begin
svel:=0;
slp:=0;
sdlmod:=0;
totalnbr:=0;
preframe:=0;
linesdone:=0;
writeln('Enter number of frames to be processed');
writeln('and rate of data collection.');
readln(nf,rate);
writeln('Enter uo, r/R (from centre), umf and dt in cgs units.');
readln(uo,rr,umf,dt);
writeln('Enter range over which to calculate velocity pdf (min=0.2 cm/s)');
readln(dvel);
writeln('Enter range over which to calculate pierced length pdf (min=0.01 cm)');
readln(dlp);
writeln(q2dtdltxt_file,' lp ',' ub ',' tb ');
for i:=1 to nf do
  begin
  readln(q2txt_file,nbr,nby);
  for j:=1 to nbr do
    begin
    avetest:=false;
    readln(q2txt_file,ber,enr,minr,cbr,dlrawr,dtrawr);
    if dtrawr>0 then     {else do nothing}
      begin
      if (nbr>=nby) and (j<=nby) then
        begin
        e:=nbr-1;
        for a:=1 to e do
          readln(q2txt_file);
        b:=nby-j;
        for c:=0 to b do
          begin
```

```
            readln(q2txt_file,bey,eny,miny,cby,dlrawy,dtrawy);
            if avetest=false then
              begin
              if (-dtrawy=dtrawr) then
                begin
                dlraw:=(dlrawr+dlrawy)/2;
                dtraw:=dtrawr;
                avetest:=true;
                end;
              end;
            end;
          end;
        if avetest=false then
          begin
          dlraw:=dlrawr;
          dtraw:=dtrawr;
          end;
        dlmod:=2*dlraw/rate;
        dtmod:=dtraw/rate;
        vel:=0.406/dtmod;
        lp:=vel*dlmod;
        lpmax:=dt*(1-rr);
        ubmax:=(uo-umf)+22.26*sqrt(lpmax);
        {if ub<=max and lp<=max then do the following else skip data}
        if (vel<=ubmax) and (lp<=lpmax) then
          begin
          totalnbr:=totalnbr+1;
          svel:=svel+vel;
          slp:=slp+lp;
          sdlmod:=sdlmod+dlmod;
          writeln(q2dtdltxt_file,lp:10:6,vel:10:6,dlmod:10:6);
          freq;
          end;
        end;
      linesdone:=1+j+preframe;
      reset(q2txt_file);
      for d:=1 to linesdone do
        readln(q2txt_file);
      end;
    for k:=1 to nby do
      readln(q2txt_file);
    preframe:=1+nby+nbr+preframe;
    end;
avevel:=svel/totalnbr;
avelp:=slp/totalnbr;
avetb:=sdlmod/totalnbr;
fn:=nf;
totaltime:=(fn*16384)/rate;    {#frames.#spans.#samples/span.#channels}
                               {rate/channel}
bubfreq:=totalnbr/totaltime;
bvolfrac:=bubfreq*avetb;
bgasflow:=bubfreq*avetb*avevel;
pdf;
qzerodv;
writeln(q2dtdltxt_file,'# frames =',nf,'  rate =',rate:10:6);
writeln(q2dtdltxt_file,'total number of bubbles');
writeln(q2dtdltxt_file,'in this series =',totalnbr);
writeln(q2dtdltxt_file,'uo =',uo:10:6,'cm/s');
writeln(q2dtdltxt_file,'umf =',umf:10:6,'cm/s');
writeln(q2dtdltxt_file,'dt =',dt:10:6,'cm');
writeln(q2dtdltxt_file,'lpmax =',lpmax:10:6);
writeln(q2dtdltxt_file,'ubmax =',ubmax:10:6);
writeln(q2dtdltxt_file,'ave bubble ub =',avevel:10:6);
writeln(q2dtdltxt_file,'ave pierced length =',avelp:10:6);
writeln(q2dtdltxt_file,'ave bubble pierced time (tb ave)=',avetb:10:6);
writeln(q2dtdltxt_file,'total time of experiment =',totaltime:10:6);
writeln(q2dtdltxt_file,'bubble frequency =',bubfreq:10:6);
writeln(q2dtdltxt_file,'bubble volume fraction =',bvolfrac:10:6);
writeln(q2dtdltxt_file,'bubble gas flow =',bgasflow:10:6);
```

```
writeln(q2dtdltxt_file,'dvmin =0.4 cm');
writeln(q2dtdltxt_file,'min lp =',lpmin:10:6);
writeln(q2dtdltxt_file,'pdf(lpmin) =',qdlpmin:10:6);
close(q2dtdltxt_file);
end;

procedure sd;

begin
  sound(2100);
  delay(200);
  nosound;
  delay(100);
  sound(2100);
  delay(200);
  nosound;
end;



begin
clrscr;
writeln('This program calculates bubble velocity, pierced length,');
writeln('pdf and cumulative of bubbles from the output text files');
writeln('of experiments collected using q2.');
writeln('This program uses cgs units.');
repeat
write('Do a calculation? (y/n)');
 ans:=readkey;writeln;
 if ans in['y','Y'] then
 begin
   writeln('Enter file that contains data from q2.');
   write('[Filename.txt]:');
   readln(s50);
   assign(q2txt_file,s50);
   reset(q2txt_file);
   writeln('Enter name of file to store velocity and lp data in:');
   readln(f50);
   assign(q2dtdltxt_file,f50);
   rewrite(q2dtdltxt_file);
   writeln('Enter name of file to store velocity pdf data in:');
   readln(g50);
   assign(q2dtpdftxt_file,g50);
   rewrite(q2dtpdftxt_file);
   writeln('Enter name of file to store lp pdf data in:');
   readln(h50);
   assign(q2dlpdftxt_file,h50);
   rewrite(q2dlpdftxt_file);
   writeln('Enter name of file to store F"(dv) data in:');
   readln(i50);
   assign(q2qdvtxt_file,i50);
   rewrite(q2qdvtxt_file);
   init;
   convert;
   sd;
   writeln('ALL DONE !');
   close(q2txt_file);
 end
 else if ans in['n','N'] then
 begin
   write('Are you sure you want to quit? (y/n)');
   nans:=readkey;writeln;
    if nans in['y','Y'] then
    begin
    writeln('Goodbye until next time!');
    end
    else
    ans:='y';
```

```
  end
  else
    begin
    writeln('Answer yes or no.');
    ans:='y';
  end;
until not (ans in['y','Y']);
end.
```

This program predicts the cumulative distribution and probability density function of the bubble diameter from the model proposed by Agarwal (1986).

```
program dvdboad;

uses turbo3,crt;
type real=extended;

var
 s,k3,uo,umf,dt,zuf,rh,rr,z,r,dbo,ubo,dbx,
 dbd,a,x,gmp,gmm,ingma,kk,ll,av,faci,pa,
 insum,ptb,pta,dbmax,ubmax,dv,yt,divd,
 pt1,pt2,pt3,pt4,pt5,pt6,pt7,pt8,pt9,pt10,
 pdf,vb,fdv,ingmb,b,sum,ingmamin,ingmam,
 gm,p1,p2,p3,p4,dbrbar,deltadv,deltan,deltao,
 deltad:real;
 p,m,d,w,i,mv,j:integer;
 f50:string[50];
 q2dvpdftxt_file:text;
 ans,nans:char;
 etest,dtest:boolean;


 function power(k,l:real):real;
 begin
 if l=0 then
   begin
   power:=1;
   end
 else if l<0 then
   begin
   if k=0 then
     begin
     power:=0;
     end
   else if k<0 then
     begin
     if frac(l)=0 then
       begin
       if odd(trunc(l)) then
         begin
         power:=-exp(l*ln(abs(k)));
         end
       else
         begin
         power:=exp(l*ln(abs(k)));
         end;
       end
     else if frac(l)<>0 then
       begin
       writeln('Power not possible: -k**fraction.');
       power:=0;
       end;
     end
   else if k>0 then
     begin
     power:=exp(l*ln(k));
     end;
   end
 else if l>0 then
   begin
   if k=0 then
     begin
     power:=0;
     end
   else if k<0 then
     begin
     if frac(l)=0 then
```

```
        begin
        if odd(trunc(l)) then
          begin
          power:=-exp(l*ln(abs(k)));
          end
        else
          begin
          power:=exp(l*ln(abs(k)));
          end;
        end
      else if frac(l)<>0 then
        begin
        writeln('Power not possible: -k**fraction.');
        power:=0;
        end;
      end
    else if k>0 then
      begin
      power:=exp(l*ln(k));
      end;
    end;
  end;


  function factorial(p:integer):real;

  begin
  if p=0 then
    begin
    b:=1;
    end
  else
    b:=1;
    for d:=1 to p do
    begin
    b:=b*d;
    end;
  factorial:=b;
  end;


  function ingamma(mv:integer;av:real):real;

  begin
  insum:=0;
  for i:=0 to mv-1 do
    begin
    faci:=factorial(i);
    pa:=power(av,i);
    divd:=pa/faci;
    insum:=insum+divd;
    end;
  ptb:=1-(exp(-av)*insum);
  pta:=factorial(mv-1)*ptb;
  ingamma:=pta;
  end;

procedure input;

begin
writeln('Enter superficial velocity, min fluidisation vel.,');
writeln('bed diameter, height of unfluidised bed and k,m,s.');
readln(uo,umf,dt,zuf,k3,m,s);
writeln('Enter position in bed that pdf of Dv is to be generated,');
writeln('give ratio of height above distributor and');
writeln('FROM CENTRE OF BED (NB: r/R=0).');
readln(rh,rr);
end;
```

```
procedure consts;
begin
dtest:=false;
deltao:=0;
z:=zuf*rh;        {no ajustment for z as zo=0 for a porous plate}
r:=(dt/2)*rr;
dbmax:=dt*(1-rr);
ubmax:=(uo-umf)+(22.26*sqrt(dbmax));
repeat
  dbo:=0.00376*sqr(uo-((1+(2*deltao))*umf));
  deltan:=(uo-umf)/(uo-umf+(22.26*sqrt(dbo))+(2*umf));
  deltad:=Abs(deltan-deltao);
  if deltad<0.0001 then
    dtest:=true;
  deltao:=deltan;
until (dtest=true);
ubo:=(uo-umf)+(22.26*sqrt(dbo));
dbd:=dbo+((k3/(11.13*m))*power(z,s)*sqrt(dbo))+(sqr(k3/22.26)*sqr(power(z,s))/(m*(m-1)));
x:=(sqrt(dbd-(dbo/m)))-(sqrt(((m-1)*dbo)/m));
gmp:=factorial(m);
gmm:=factorial(m-2);
gm:=factorial(m-1);
a:=(sqrt(gmp/gmm)*x)/((sqrt(dt)*sqrt(1-rr))-sqrt(dbo));
ingma:=ingamma(m+1,a);
ingmamin:=ingamma(m-1,a);
ingmam:=ingamma(m,a);
p1:=sqr(x)*(gmp/gmm)*((gmm-ingmamin)/(gmp-ingma))+dbo;
p2:=2*x*(sqrt(dbo*(gmp/gmm)));
p3:=((gm-ingmam)/(gmp-ingma));
p4:=p2*p3;
dbrbar:=p1+p4;
end;

procedure fd;
begin
etest:=false;
sum:=0;
j:=0;
writeln(q2dvpdftxt_file,' dbr  ',' f(dbr)  ',' F(dbr)  ',' sum nd');
deltadv:=(dbmax-dbo)/100;
repeat
  j:=j+1;
  dv:=j*deltadv;    {from dbo adjusted to dbmax}
  if dv>dbo then
    begin
    yt:=sqrt(dv)-sqrt(dbo);
    pt1:=gmp/gmm;
    pt2:=(m+1)/2;
    pt3:=0.5*power(pt1,pt2);
    pt4:=power(x,m+1);
    pt5:=exp(-(sqrt(gmp/gmm)*(x/yt)));
    pt6:=pt4*pt5;
    pt7:=power(yt,m+2)*sqrt(dv);
    pt8:=gmp-ingma;
    pt9:=pt7*pt8;
    pt10:=pt6/pt9;
    pdf:=pt3*pt10;
    sum:=sum+(pdf*deltadv);
    vb:=(sqrt(gmp/gmm)*x)/(sqrt(dv)-sqrt(dbo));
    ingmb:=ingamma(m+1,vb);
    fdv:=(gmp-ingmb)/(gmp-ingma);
    writeln(q2dvpdftxt_file,(dv-(deltadv/2)):10:6,pdf:10:6,fdv:10:6,sum:10:6);
    if dv>dbmax-deltadv then
      etest:=true;
    if  fdv>1 then
      etest:=true;
```

```
    end;
until (etest=true);
end;


procedure output;
begin
writeln(q2dvpdftxt_file,'uo=',uo:10:6);
writeln(q2dvpdftxt_file,'umf=',umf:10:6);
writeln(q2dvpdftxt_file,'dt=',dt:10:6);
writeln(q2dvpdftxt_file,'zuf=',zuf:10:6);
writeln(q2dvpdftxt_file,'rh=',rh:10:6);
writeln(q2dvpdftxt_file,'rr=',rr:10:6);
writeln(q2dvpdftxt_file,'z=',z:10:6);
writeln(q2dvpdftxt_file,'r=',r:10:6);
writeln(q2dvpdftxt_file,'dbmax=',dbmax:10:6);
writeln(q2dvpdftxt_file,'dbo (dbo adjusted) =',dbo:10:6);
writeln(q2dvpdftxt_file,'ubmax=',ubmax:10:6);
writeln(q2dvpdftxt_file,'ubo=',ubo:10:6);
writeln(q2dvpdftxt_file,'dbrbar=',dbrbar:10:6);
writeln(q2dvpdftxt_file,'k3,m,s=',k3:3,m:3,s:5:3);
end;

procedure sd;
begin
  sound(2100);
  delay(200);
  nosound;
  delay(100);
  sound(2100);
  delay(200);
  nosound;
end;



begin
clrscr;
writeln('This program calculates the pdf and cumulative of the');
writeln('vertical dimension of bubbles from the Agarwal equation.');
writeln('This program uses cgs units throughout.');
writeln('This program uses the adjusted Miwa dbo correlation.');
repeat
write('Do a calculation? (y/n)');
 ans:=readkey;writeln;
 if ans in['y','Y'] then
 begin
   writeln('Enter name of file to put data in:');
   readln(f50);
   assign(q2dvpdftxt_file,f50);
   rewrite(q2dvpdftxt_file);
   input;
   consts;
   fd;
   output;
   sd;
   writeln('ALL DONE !');
   close(q2dvpdftxt_file);
 end
 else if ans in['n','N'] then
 begin
   write('Are you sure you want to quit? (y/n)');
   nans:=readkey;writeln;
    if nans in['y','Y'] then
    begin
    writeln('Goodbye until next time!');
    end
```

```
    else
    ans:='y';
  end
  else
   begin
   writeln('Answer yes or no.');
   ans:='y';
  end;
until not (ans in['y','Y']);
end.
```

This program predicts the cumulative distribution and probability density function of the bubble rise velocity from equations derived from consideration of the model proposed by Agarwal (1986).

```
program vr;

uses turbo3,crt;
type real=extended;

var
 s,k3,uo,umf,dt,zuf,rh,rr,z,r,dbo,ubo,dbx,
 dbd,a,gmp,gmm,ingma,av,faci,pa,
 insum,ptb,pta,dbmax,ubmax,dvr,yt,divd,
 pt1,pt2,pt3,pt4,pt5,pt6,pt7,pt8,pt9,
 pdf,vb,fvr,ingmb,b,sum,ingmamin,ingmam,
 gm,p1,p2,p3,p4,ubbard,ubbar,deltavr,deltan,deltao,
 deltad:real;
 p,m,d,w,i,mv,j:integer;
 f50:string[50];
 q2dvpdftxt_file:text;
 ans,nans:char;
 etest,dtest:boolean;


 function power(k,l:real):real;
 begin
 if l=0 then
   begin
   power:=1;
   end
 else if l<0 then
   begin
   if k=0 then
     begin
     power:=0;
     end
   else if k<0 then
     begin
     if frac(l)=0 then
       begin
       if odd(trunc(l)) then
         begin
         power:=-exp(l*ln(abs(k)));
         end
       else
         begin
         power:=exp(l*ln(abs(k)));
         end;
       end
     else if frac(l)<>0 then
       begin
       writeln('Power not possible: -k**fraction.');
       power:=0;
       end;
     end
   else if k>0 then
     begin
     power:=exp(l*ln(k));
     end;
   end
 else if l>0 then
   begin
   if k=0 then
     begin
     power:=0;
     end
   else if k<0 then
     begin
     if frac(l)=0 then
```

```
        begin
        if odd(trunc(l)) then
          begin
          power:=-exp(l*ln(abs(k)));
          end
        else
          begin
          power:=exp(l*ln(abs(k)));
          end;
        end
      else if frac(l)<>0 then
        begin
        writeln('Power not possible: -k**fraction.');
        power:=0;
        end;
      end
    else if k>0 then
      begin
      power:=exp(l*ln(k));
      end;
    end;
  end;


  function factorial(p:integer):real;
  begin
  if p=0 then
    begin
    b:=1;
    end
  else
    b:=1;
    for d:=1 to p do
    begin
    b:=b*d;
    end;
  factorial:=b;
  end;


  function ingamma(mv:integer;av:real):real;
  begin
  insum:=0;
  for i:=0 to mv-1 do
    begin
    faci:=factorial(i);
    pa:=power(av,i);
    divd:=pa/faci;
    insum:=insum+divd;
    end;
  ptb:=1-(exp(-av)*insum);
  pta:=factorial(mv-1)*ptb;
  ingamma:=pta;
  end;

procedure input;
begin
writeln('Enter superficial velocity, min fluidisation vel.,');
writeln('bed diameter, height of unfluidised bed and k, m, s.');
readln(uo,umf,dt,zuf,k3,m,s);
writeln('Enter position in bed that pdf of ubr is to be generated,');
writeln('give ratio of height above distributor and');
writeln('FROM CENTRE OF BED (NB: r/R=0).');
readln(rh,rr);
end;
```

```
procedure consts;
begin
dtest:=false;
deltao:=0;
z:=zuf*rh;        {no adjustment for z as zo=0 for a porous plate}
r:=(dt/2)*rr;
dbmax:=dt*(1-rr);
ubmax:=(uo-umf)+(22.26*sqrt(dbmax));
repeat
  dbo:=0.00376*sqr(uo-((1+(2*deltao))*umf));
  deltan:=(uo-umf)/(uo-umf+(22.26*sqrt(dbo))+(2*umf));
  deltad:=Abs(deltan-deltao);
  if deltad<0.0001 then
    dtest:=true;
  deltao:=deltan;
until (dtest=true);
ubo:=(uo-umf)+(22.26*sqrt(dbo));
ubbar:=(k3/m)*power(z,s);
ubbard:=ubbar+ubo;
gmp:=factorial(m);
gmm:=factorial(m-2);
gm:=factorial(m-1);
a:=(m*(ubbard-ubo))/(ubmax-ubo);
ingma:=ingamma(m+1,a);
ingmamin:=ingamma(m-1,a);
ingmam:=ingamma(m,a);
end;

procedure fu;
begin
etest:=false;
sum:=0;
j:=0;
writeln(q2dvpdftxt_file,' ubr ',' f(ubr) ',' F(ubr) ',' sum nd');
deltavr:=(ubmax-ubo)/100;
repeat
  j:=j+1;
  dvr:=j*deltavr;    {from ubo to ubmax}
  if dvr>ubo then
    begin
    pt1:=power(m,m+1);
    pt2:=ubbard-ubo;
    pt3:=power(pt2,m+1);
    pt4:=dvr-ubo;
    pt5:=power(pt4,m+2);
    pt6:=(pt1*pt3)/pt5;
    pt7:=exp(-(m*(pt2/pt4)));
    pt8:=gmp-ingma;
    pt9:=(pt6*pt7)/pt8;
    pdf:=pt9;
    sum:=sum+(pdf*deltavr);
    vb:=(m*(ubbard-ubo))/(dvr-ubo);
    ingmb:=ingamma(m+1,vb);
    fvr:=(gmp-ingmb)/(gmp-ingma);
    writeln(q2dvpdftxt_file,(dvr-(deltavr/2)):10:6,pdf:10:6,fvr:10:6,sum:10:6);
    if dvr>ubmax-deltavr then
      etest:=true;
    if  fvr>1 then
      etest:=true;
    end;
until (etest=true);
end;

procedure output;
```

```
begin
writeln(q2dvpdftxt_file,'uo=',uo:10:6);
writeln(q2dvpdftxt_file,'umf=',umf:10:6);
writeln(q2dvpdftxt_file,'dt=',dt:10:6);
writeln(q2dvpdftxt_file,'zuf=',zuf:10:6);
writeln(q2dvpdftxt_file,'rh=',rh:10:6);
writeln(q2dvpdftxt_file,'rr=',rr:10:6);
writeln(q2dvpdftxt_file,'z=',z:10:6);
writeln(q2dvpdftxt_file,'r=',r:10:6);
writeln(q2dvpdftxt_file,'dbo (dbo adjusted) =',dbo:10:6);
writeln(q2dvpdftxt_file,'ubo=',ubo:10:6);
writeln(q2dvpdftxt_file,'dbmax=',dbmax:10:6);
writeln(q2dvpdftxt_file,'ubmax=',ubmax:10:6);
writeln(q2dvpdftxt_file,'ubbard=',ubbard:10:6);
end;

procedure sd;
begin
  sound(2100);
  delay(200);
  nosound;
  delay(200);
  sound(2100);
  delay(200);
  nosound;
end;



begin
clrscr;
writeln('This program calculates the pdf and cumulative');
writeln('of bubbles from the Agarwal equation.');
writeln('This program uses cgs units throughout.');
writeln('This program uses the adjusted Miwa dbo correlation.');
repeat
write('Do a calculation? (y/n)');
 ans:=readkey;writeln;
 if ans in['y','Y'] then
 begin
   writeln('Enter name of file to put data in:');
   readln(f50);
   assign(q2dvpdftxt_file,f50);
   rewrite(q2dvpdftxt_file);
   input;
   consts;
   fu;
   output;
   sd;
   writeln('ALL DONE !');
   close(q2dvpdftxt_file);
 end
 else if ans in['n','N'] then
 begin
   write('Are you sure you want to quit? (y/n)');
   nans:=readkey;writeln;
    if nans in['y','Y'] then
    begin
    writeln('Goodbye until next time!');
    end
    else
    ans:='y';
 end
 else
  begin
  writeln('Answer yes or no.');
  ans:='y';
```

```
 end;
until not (ans in['y','Y']);
end.
```